UNIVERSITY OF ADELAIDE LIBRARY
11.8.95

NEURAL MECHANISMS OF ANAESTHESIA

Ahmad Hashemi-Sakhtsari

Thesis submitted for the degree of

Doctor of Philosophy

in

Faculty of Science

The University of Adelaide

Department of Physiology December 1994

Corrigenda

page 72 add N.B. all computer-collected responses presented in Chapters 5,6,7 and 8 are amplified 50,000 times, i.e. 1V= 20 μV in all Figures.

page 86 line 7, animals should read 'animal'

page 110 line 4, Chamrlin should read 'Chamberlin'

page 114 line 15, mammilary should read 'mamillary'

page 126 line 6, greater that should read 'greater than'

page 130, 5.4, line 3, after brain slices. insert "CCh was applied in the range 10-500 μM, the latter having the most pronounced effect"

page 158, 5.10, page 2, line 4, conotoxin, Co^{2+} and Cd^{2+} should read 'conotoxin and Cd^{2+}'

page 184 Table 6.1, TEA should read 'TEA and CCh'

page 205, paragraph 2, It can be concluded should read 'It perhaps may be concluded'

In Chapter 8, all section subheadings should read 'Effects of baclofen on the response of .....'

page 266, paragraph 2, line 7, experiments on baclofen mediation should read 'experiments on the effects of baclofen upon'

page 268, paragraph 2, line 1, show $BaCl_2$-induced actions..... should read 'show effects of baclofen on $BaCl_2$-induced.....'

page 269, line 11, baclofen mediated tests, should read 'baclofen-interaction tests'

page 271, paragraph 2, line 6, of baclofen mediation of, should read 'of baclofen effects on'

page 363 Ref. Harrison and Simmonds, Quantatative should read 'Quantitative'

CONTENTS

TABLE OF CONTENTS ii

ABSTRACT ix

DECLARATION xi

ACKNOWLEDGEMENTS xii

PUBLICATIONS xiv

RECEPTOR MECHANISMS – DEFINITION OF SOME COMMON TERMS xv

CHAPTER 1 – INTRODUCTION 1

1.1 GENERAL ANAESTHESIA 1

1.1.1 Definition of General Anaesthesia 1

1.1.2 A Brief History of Anaesthesia 3

1.1.3 Sites of Action of Anaesthesia 4

1.1.4 Mechanisms of Anaesthesia 6

1.1.5 Stereoselectivity of Anaesthetic Agents 11

1.2 POTASSIUM CHANNELS 13

1.2.1 An Introduction to Potassium Channels 13

1.2.2 Voltage-Activated K^+ Currents 15

1.2.2.1 Delayed (outward) rectifier current ($I_{K(V)}$) 15

1.2.2.2 Fast transient current ($I_{K(A)}$) 15

1.2.2.3 Rapid delayed current ($I_{K(Vr)}$) 15

1.2.2.4 Slow delayed current ($I_{K(Vs)}$) 16

1.2.2.5 Muscarinic-inactivated current ($I_{K(M)}$) 16

1.2.2.6 Inward (anomalous) rectifier current ($I_{K(IR)}$) ... 16

1.2.2.7 Calcium-activated K^+ currents 16

1.2.3 Ligand-Activated K^+ Currents 17

1.2.4 Other K^+-Specific Channels 17

1.3 GABA PHARMACOLOGY 18

1.3.1 History of GABA 18

1.3.1.1 History of $GABA_B$-receptors 19

1.3.2 An Introduction to GABA-Receptors 20

1.3.2.1 $GABA_A$-receptors 20

1.3.2.2 $GABA_B$-receptors 22

1.3.2.3 GABA-autoreceptors 23

1.3.3 GABA-Receptor Distribution 23

1.3.4 GABA-Receptors and Excitatory Transmission 24

1.3.5 $GABA_B$-Receptor Electrophysiology 25

1.3.5.1 $GABA_B$-receptors and Ca^{2+} channels 25

1.3.5.2 $GABA_B$-receptors and K^+ channels 26

1.3.6 Absence Epilepsy 27

1.4 ANAESTHESIA AND EXCITATORY OR INHIBITORY TRANSMISSION 28

1.5 ANAESTHESIA AND GABA-RECEPTORS 31

1.5.1 Effects of Anaesthetics on $GABA_A$-Receptor Channel Kinetics 34

1.6 ROLES OF ION CHANNELS, TRANSMITTER RELEASE AND SECOND MESSENGERS IN ANAESTHESIA 35

1.6.1 Anaesthesia and Na^+ Channels 35

1.6.2 Anaesthesia and K^+ Channels 36

1.6.2.1 A novel neuronal K^+ current 37

1.6.3 Anaesthesia and Metabotropic Receptors 37

1.6.4 Anaesthesia and Ca^{2+} Channels 38

1.6.5 Anaesthesia and Transmitter Release 39

1.6.6 Anaesthesia and Second Messengers 40

CHAPTER 2 – SPONTANEOUS EPILEPTIFORM DISCHARGES 42

2.1 ROLE OF NON-NMDA GLUTAMATE RECEPTORS IN EPILEPTOGENESIS 48

2.1.1 Kainic Acid 49

2.2 ROLES OF CALCIUM CHANNELS AND NEUROTRANSMITTER RELEASE IN EPILEPTOGENESIS 50

2.3 ROLE OF POTASSIUM CHANNELS IN EPILEPTOGENESIS 51

2.4 ROLE OF CYCLIC AMP IN EPILEPTOGENESIS 52

CHAPTER 3 – RECORDING FROM BRAIN SLICES 54

3.1 COMPUTER-BASED ELECTROPHYSIOLOGICAL DATA ACQUISITION AND ANALYSIS 54

3.2 POPULATION DISCHARGE (EXTRACELLULAR FIELD POTENTIAL) RECORDING 57

3.3 A GREASE-GAP RECORDING MODEL 58

3.3.1 Experimental Procedures 58

3.3.2 An Introduction to ASYST Version 2.1 65

3.3.3 Metrabyte DASH-16F Board 67

3.3.4 Interface Circuit Box 68

3.3.4.1 Instrumentation amplifiers 69

3.3.4.2 Earthing and power supply arrangements for the interface box 70

CHAPTER 4 – EVOKED POTENTIAL RECORDING FROM RABBIT BRAIN 73

4.1 AN INTRODUCTION TO WHOLE-ANIMAL DATA ACQUISITION AND PROCESSING SYSTEM 73

4.1.1 Analogue Stimulator Output 76

4.1.2 Analogue-to-Digital External trigger Input 76

4.1.3 Digitimer 77

4.1.4 Gated Pulse Generator 78

4.1.5 Isolated Stimulator 78

4.1.6 Stimulating Electrodes 79

4.1.7 Recording Electrodes 80

4.1.8 Amplifier and Filter 82

4.1.9 Baseline Stabiliser 83

4.1.10 Data Acquisition and Analysis Software 84

4.2 EVOKED POTENTIAL RECORDING FROM STRUCTURES IN RABBIT BRAIN 85

4.2.1 General Anaesthesia 86

4.3 EXPERIMENTAL PROCEDURE 92

4.3.1 Perfusion and Sectioning 95

4.4 RESULTS AND DISCUSSION 96

CHAPTER 5 – EFFECTS OF POTASSIUM CHANNEL BLOCKERS ON EPILEPTIFORM DISCHARGES RECORDED FROM RAT NEOCORTICAL SLICES IN VITRO 110

5.1 SPONTANEOUS DISCHARGES WITH AFTER-ACTIVITY 113

5.2 EFFECTS OF NMDA ON SPONTANEOUS DISCHARGES 116

5.3 EFFECTS OF TEA ON SPONTANEOUS DISCHARGES 119

5.3.1 Phase-Plane Plot Study 127

5.4 EFFECTS OF CCh ON SPONTANEOUS DISCHARGES 130

5.5 EFFECTS OF CsCl ON SPONTANEOUS DISCHARGES 135

5.6 EFFECTS OF 4-AP ON SPONTANEOUS DISCHARGES 140

5.7 EFFECTS OF $BaCl_2$ ON SPONTANEOUS DISCHARGES 146

5.8 EFFECTS OF $SrCl_2$ ON SPONTANEOUS DISCHARGES 154

5.9 EFFECTS OF $CoCl_2$ ON SPONTANEOUS DISCHARGES 156

5.10 EFFECTS OF REDUCING EXTERNAL Ca^{2+} ON SPONTANEOUS DISCHARGES 158

5.11 EFFECTS OF CAFFEINE ON SPONTANEOUS DISCHARGES 161

5.12 BASELINE POTENTIAL SHIFT 164

5.13 EFFECTS OF TEMPERATURE ON NEOCORTICAL SLICE ACTIVITY 165

CHAPTER 6 – POWER SPECTRUM ANALYSIS OF DISCHARGES WITH AFTER-ACTIVITY RECORDED FROM RAT NEOCORTICAL SLICES IN VITRO 167

6.1 INTRODUCTION 167

6.2 FOURIER TRANSFORM AS A CLASSICAL SPECTRAL ANALYSIS METHOD 169

6.3 MODERN SPECTRAL ANALYSIS TECHNIQUES 171

6.3.1 Non-Parametric Methods 174

6.3.2 Parametric Methods 174

6.3.2.1 Yule-Walker method 176

6.4 RESULTS AND DISCUSSION 179

6.5 CONCLUSIONS 200

CHAPTER 7 – EFFECTS OF $GABA_A$- AND $GABA_B$-RECEPTOR AGONISTS AND ANTAGONISTS ON SPONTANEOUS EPILEPTIFORM DISCHARGES RECORDED FROM NEOCORTICAL SLICES IN VITRO 201

7.1 EFFECTS OF GABA AND 3-AMINOPROPYLSULPHONIC ACID ON SPONTANEOUS NEOCORTICAL DISCHARGES 202

7.1.1 Muscimol, THIP, and Propofol as Notable $GABA_A$-Receptor Agonists 211

7.2 EFFECTS OF BICUCULLINE METHIODIDE ON SPONTANEOUS NEOCORTICAL DISCHARGES 212

7.3 EFFECTS OF BACLOFEN AS A $GABA_B$-RECEPTOR AGONIST ON SPONTANEOUS NEOCORTICAL DISCHARGES 219

7.4 EFFECTS OF A MIXTURE OF BACLOFEN AND 3-APS ON SPONTANEOUS NEOCORTICAL DISCHARGES 233

7.5 INVESTIGATION OF THE VALIDITY OF THE EQUATION BMI + GABA = BACLOFEN + BMI 236

7.5.1 Effects of GABA on Spontaneous Neocortical Discharges in the Presence of DABA 240

7.6 EFFECTS OF 4-AMINOBUTYLPHOSPHONIC ACID ON SPONTANEOUS NEOCORTICAL DISCHARGES 252

CHAPTER 8 - INTERACTION STUDIES BETWEEN BACLOFEN AND POTASSIUM CHANNEL BLOCKERS 259

8.1 EFFECTS OF BACLOFEN ON THE RESPONSE OF A NEOCORTICAL SLICE TO TEA 260

8.2 EFFECTS OF BACLOFEN ON THE RESPONSE OF A NEOCORTICAL SLICE TO CCh 262

8.3 EFFECTS OF BACLOFEN ON THE RESPONSE OF A NEOCORTICAL SLICE TO CsCl 264

8.4 EFFECTS OF BACLOFEN ON THE RESPONSE OF A NEOCORTICAL SLICE TO 4-AP 266

8.5 EFFECTS OF BACLOFEN ON THE RESPONSE OF NEOCORTICAL SLICES TO $BaCl_2$ 268

SUMMARY AND CONCLUSIONS 272

APPENDIX A.3.1 - A Method for Chloriding Silver Electrodes 273

APPENDIX A.3.2 - Temperature Controller 274

APPENDIX A.3.3 - Low-pass and Notch Filters 275

APPENDIX A.3.4 - Instrumentation Amplifiers and Direct Channel Connections to the DASH-16F Board 276

APPENDIX A.3.5 - An Instrumentation Amplifier AD625 Circuit Arrangement in the Interface Box 277

APPENDIX A.3.6 - Voltage Regulators and Low Level Ground Line..... 278

APPENDIX A.3.7 - Brain Slice Data Acquisition and Analysis Programme 279

APPENDIX A.4.1 - Stimulus Trigger Output 314

APPENDIX A.4.2 - Trigger Circuit 315

APPENDIX A.4.3 - Baseline Stabiliser 316

APPENDIX A.4.4 - Evoked Potential Data Acquisition and Analysis Programme 317

REFERENCES 350

ABSTRACT

Despite almost a century of research, the mechanisms of anaesthesia remains obscure. Stereoselectivity of anaesthetic agents supports interaction of anaesthetic agents with cellular protein targets rather than an indiscriminate perturbation of the lipid bilayer as was previously proposed. In general, at neural level anaesthesia is produced by reducing excitation or enhancing inhibition. In the 1990s, the hypothesis that anaesthetics in large part produce their pharmacological actions at specific loci on the $GABA_A$-receptor complex has become most favoured. In this thesis, possible neural mechanisms of action of general Anaesthesia are introduced.

Preliminary evoked potential recordings from the brain of anaesthetised rabbits are presented, before proceeding to report *in vitro* studies of a slice preparation from rat brain using a grease-gap recording model which allows detailed investigations in a relatively undisturbed, but controlled environment. Cellular excitatory mechanisms leading to spontaneous epileptiform discharges in the neocortical slices in a Mg^{2+}-free artificial cerebro-spinal medium are discussed.

Potassium channels control cell excitability and its firing properties. The study of effects of various classical potassium channel blockers on spontaneous discharges from neocortical slices has revealed that, as well as causing tissue excitability, each agent has definite signatory effects on individual discharges. Modern spectral analysis of the

after-activity of responses enabled numerical values for frequency and power density of control, and discharges in the presence of each potassium channel blocker to be obtained.

4-Aminobutyric acid (GABA) is the major inhibitory neurotransmitter in the central nervous system, its actions being mediated through both $GABA_A$- and $GABA_B$-receptors. The effects of $GABA_A$- and $GABA_B$-receptor agonists and antagonists on spontaneous discharges in the slice model are presented and discussed. These studies suggest that agents acting on GABA receptors can intensely modulate neuronal activity, providing a conceivable basis for the actions of both analgesic and anaesthetic agents.

Finally interaction studies between baclofen, a $GABA_B$-receptor agonist, and various potassium channel blockers identifies baclofen as a potent agent in diminishing or abolishing spontaneous discharges. These studies show that, with the exception of Ba^{2+}, baclofen is capable of suppressing the hyperexcitability induced by potassium channel blockers.

DECLARATION

This work contains no material which has been accepted for the award of any other degree or diploma in any university or other tertiary institution and, to the best of my knowledge and belief, contains no material previously published or written by another person, except where due reference has been made in the text.

I give consent to this copy of my thesis, when deposited in the University Library, being available for loan and photocopying.

SINGED: DATE: 29th December, 1994

ACKNOWLEDGMENTS

During this study, I was a recipient of an Australian Postgraduate Research Award from 31 March 1991 until 31 March 1994, and a Special University of Adelaide Postgraduate Research Award from 1 April 1994 until 30 September 1994.

I am most grateful to Dr David Kerr, my principal supervisor, for his ample guidance, encouragement, and support throughout the project, and during the writing of this thesis. Dr Kerr always managed to explain difficult concepts in a simple language. Having extensive experience and insight, Dr Kerr advised me in ways that enabled me to make the best use of my time. I am also indebted to Dr Jennifer Ong who patiently demonstrated the preparation and use of the cortical slices.

I am also grateful to Associate Professor Allan Bretag, my second supervisor, who has always been pleasant, encouraging and supportive.

I would like to sincerely thank Dr Abdesselam Bouzerdoum from the Department of Electrical and Electronic Engineering of this University, and his final year project students: David Flower, Douglas Jinu, Andrew Lin and Shiuwen Wong, who developed theories and software for performing spectral analysis which were applied in chapter 6 of this thesis.

I wish to gratefully acknowledge Mr Dennis Pfeiffer, the manager of the Medical School Electronics workshop, who

participated in the design and development of all electronic instrumentation circuits used in this project.

I owe much gratitude to members of the Graduate Studies Branch of the University of Adelaide, especially Professor Ian Davey, the former Dean of Graduate Studies, without whom this thesis may have never been produced.

Finally, I appreciate the strong support of my wife Catherine, and dedicate this thesis to her and our two children, Darioush and Sussan.

PUBLICATIONS

Hashemi-Sakhtsari, A. and Dennis, B.J. (1991) A temperature controller for maintaining viable brain slices, Proceedings of the Australian physiological and Pharmacological Society, 22(1): 12P.

Hashemi-Sakhtsari, A., Pfeiffer, D.G. and Dennis, B.J. (1992) ASYST software based acquisition, analysis and display of evoked potentials, Proceedings of the Australian Neuroscience Society, 3: 142.

Hashemi-Sakhtsari, A., Flower, D.G., Bouzerdoum, A. and Kerr, D.I.B. (1993) Fourier transform analysis of epileptiform discharges recorded from rat neocortical slices in vitro, Proceedings of the Australian Physiological and Pharmacological Society, 24(2): 172P.

Hashemi-Sakhtsari, A., Bouzerdoum, A. and Kerr, D.I.B. (1994) Spectral analysis of discharges with after-activity recorded from rat neocortical slices in vitro, Proceedings of the First World Congress on Computational Medicine, Public Health and Biotechnology, accepted, pending publication.

RECEPTOR MECHANISMS - DEFINITION OF SOME COMMON TERMS

Receptor - A protein molecule which is capable of selectively binding a drug, hormone or neurotransmitter, thereby eliciting a physiological response.

Agonist - A drug, hormone or transmitter substance that elicits a cellular response when it combines with receptors.

Antagonist - A drug that prevents the effect of an agonist.

Competitive antagonists - Act by binding to agonist receptors.

Non-competitive antagonists - Do not bind to the same receptor sites as the agonist, but reduce its effect in some other way.

Ligand - Any substance that binds to a particular type of receptor.

Occupancy - The fraction of the receptors occupied by a ligand.

UNIVERSITY OF ADELAIDE LIBRARY

CHAPTER 1

INTRODUCTION

1.1 GENERAL ANAESTHESIA

1.1.1 Definition of General Anaesthesia

The anaesthetic state is defined in practical, clinical terms as a reversible loss of awareness and memory of external stimuli, especially of painful ones, of sufficient degree to be compatible with surgery. There is, however, difficulty in arriving at a satisfactory definition of general anaesthesia. It is perhaps best considered as a condition induced by pharmacological, or other, means which results in all of the following effects:-

1. Loss of conscious awareness and no recall of events at the conscious level. In terms of the effects of anaesthetics on cognitive function, 3 stages have been suggested: (i) conscious awareness with explicit recall, (ii) conscious awareness without explicit recall, and (iii) subconscious awareness without explicit but with implicit recall.

2. Loss of motor control, changes in cardio-respiratory function and lack of overt muscular response to surgical stimulation. An exception is the respiratory musculature, which usually responds to surgical stimulation by an increase in pulmonary minute volume, even in deep anaesthesia.

3. A state of analgesia with minimal autonomic response to surgical stimulation, although this cannot be totally abolished.

4. In addition there may be some muscular relaxation.

5. The process should be reversible.

The term "increasing depth of anaesthesia" implies the effect of an increasing anaesthetic dose in a progressive impairment of cognitive function. The extremes are commonly described as "light" and "deep" anaesthesia. As a guide to the depth of anaesthesia, the anaesthetist uses clinical signs such as changes in the breathing pattern, blood pressure, heart rate, pupil size and the absence of sweating or lachrymation in response to painful stimuli. Surgical stimulation produces activation in the EEG and may arouse a patient from a deeper to a lighter state of anaesthesia. It may be difficult, particularly in patients with neuromuscular blockade, to identify a change in state which results in conscious awareness. Jessop and Jones (1992) review evidence to suggest that the median EEG frequency, which is 10 Hz in conscious subjects, should be kept below 5 Hz during anaesthesia to ensure that there is no response to verbal command. They also advocate that the auditory evoked potential should be used to measure depth of anaesthesia, but the utility of these methods is by no means established.

1.1.2 A Brief History of Anaesthesia

General anaesthetics are used as an adjunct to surgical procedures in order to render the patient unaware of, and unresponsive to, painful stimulation. They are given systemically, and exert their main effects on the central nervous system (CNS), in contrast to local anaesthetics which work by producing a local block of conduction of sensory impulses from the periphery to the CNS.

The word "anaesthesia" is derived from the Greek meaning insensible or without feeling. This word appears in the Encyclopaedia Brittanica published in Edinburgh in 1771 as signifying "a privation of the senses". Oliver Wendell Holmes, a neurologist, was first to coin the word Anaesthesia in 1847.

The usefulness of nitrous oxide in relieving the pain of surgery was first suggested by Humphrey Davy in 1800. It caused euphoria, analgesia and loss of consciousness. Horace Wells, an American dentist, had a tooth extracted under its influence while he himself squeezed the inhalation bag. Henry Morton, also a dentist and a student at Harvard Medical School, used it to successfully extract a tooth in 1846. Morton then suggested it to Warren, the chief surgeon at Massachusetts General Hospital, and administered nitrous oxide with success for one of Warren's operations. In 1847, James Simpson, professor of obstetrics in Glasgow, used chloroform to relieve the pain of childbirth, bringing on himself fierce denunciation from the clergy. Opposition was effectively

silenced in 1853 when Queen Victoria gave birth to her seventh child under the influence of chloroform.

In early to mid 1900, ether and chloroform were most commonly used anaesthetic agents. It is interesting that Diethyl ether, with spontaneous breathing, dominated the scene in 1946 as it had in 1846.

The introduction of neuromuscular blocking agents after World War II alleviated the need for deep anaesthesia to achieve muscle relaxation, and led directly to the concept of anaesthesia as a triad: an anaesthetic agent for loss of consciousness, an analgesic agent for reflex suppression and insensitivity to pain, and a neuromuscular blocker for marked muscle relaxation. No single drug is known to produce this triad of requirements without causing unpleasant or undesirable side effects. Often rapid unconsciousness is produced by an intravenous induction agent (e.g. thiopentone). One or more inhalation agents (e.g. nitrous oxide) is then used to maintain anaesthesia, and produce some analgesia. As well as a neuromuscular blocking agent, a supplementary intravenous analgesic agent is sometimes administered.

1.1.3 Sites of Action of Anaesthesia

Much effort has gone into identifying a particular brain region on which anaesthetics act. Unconsciousness can be produced by damage to the brainstem reticular formation, the

hypothalamus or the thalamus. Cortical damage produces profound sensory and motor disturbances, but not the actual loss of consciousness. Anaesthetics, even in low concentrations, cause short-term amnesia. It is likely that interference with hippocampal function produces this effect, but as the concentration of anaesthetic is increased, many other functions are affected. However, since the cellular effects produced by anaesthetics can influence the function of the nervous system in many different ways, it is most probably quite unrealistic to seek a critical 'target site' in the brain responsible for all the phenomena of anaesthesia.

At the cellular level, some anaesthetics inhibit the conduction of action potentials, but all inhibit transmission at certain synapses. The effect on axonal conduction requires considerably higher concentrations than the effect on synaptic transmission (Lin et al., 1993b). However, a great body of research *in vivo* stress that much synaptic transmission persists in fully anaesthetised animals. The inhibitory effect on synaptic transmission could be due to reduced transmitter release and reduced post-synaptic sensitivity to the transmitter, but these effects are not universal and caution is required in selecting a particular nerve cell or synapse for study, as anaesthetics actually facilitate transmission at some synapses (Krnjevic, 1992)

1.1.4 Mechanisms of Anaesthesia

The mechanism of general anaesthesia at a molecular level are still far from clear. However, any neurotransmitter receptors involved in producing anaesthesia should be sensitive to all anaesthetic agents (Lin et al., 1993b). A remarkable phenomenon of general anaesthesia is that a common action, reversible loss of consciousness, can be produced by a wide variety of chemical agents, including inert rare gases, hydrocarbons, halocarbons, ethers, ketones, carbamates, barbiturates, amines, arabinosides, and steroids (Miller, 1985).

Earlier observations that the only physicochemical characteristic common to all known general anaesthetics was their liposolubility, led Meyer to propose a lipid theory of anaesthesia in 1937. This was based on earlier work by Overton and Meyer, published during 1899-1901, who showed a close correlation between anaesthetic potency and lipid solubility in a diverse group of simple and unreactive organic compounds, and resulted in the assumption that anaesthetics acted on the hydrophobic parts of membrane lipids. The lipid theory was followed by a number of other theories, whose common characteristic was the non-specificity of the target site of anaesthetics. For example, a critical volume hypothesis, in which anaesthesia occurs when a critical volume fraction of anaesthetic molecules is achieved in the neuronal membrane, or similarly, anaesthetic induced volume expansion of the lipid phase leading to disturbance of function, have been proposed (Smith, 1988).

A further Hydrate theory, proposed independently by Pauling and Miller in 1961, suggest that general anaesthetics cause the ordering of water molecules in their vicinity. This theory was based on the notion that anaesthetics might act by 'freezing' water molecules in the form of an anaesthetic-hydrate complex, close to the surface of the cell membrane, which can disturb the function of membrane protein, and interfere with ionic movements. Other models have suggested that general anaesthetics fluidise the phospholipid moieties of cell membranes, or increase the thickness of lipid bilayers. Yet other theories have proposed that anaesthetic drugs produce conformational changes leading to the loss of function of membrane proteins (Keane and Biziere, 1987).

Amongst all these notions, it is generally agreed that most anaesthetics are hydrophobic, and that lipid solubility of anaesthetics is highly correlated with anaesthetic potencies, but this is a general property of all effective drugs which must penetrate into the brain from the circulation in order to exert their effects (Smith, 1988). The oil-water partition coefficient is thus a standard measure in all such studies, but this does not mean that all drugs act on lipids in the cell membranes; to the contrary, protein receptors or enzymes are most likely almost universally involved in such actions. Moreover, although modified bilayer properties such as volume, order, or fluidity support the lipid hypothesis in a general way, the changes induced in lipid bilayers at clinical doses of anaesthetics are small and seem unlikely to be able to result in physiological effects (Miller, 1985). Thus, it

should be emphasized that although anaesthetics do increase fluidity, nevertheless this effect at clinical concentrations would correspond only to a minute increase in fluidity, such as might occur if the temperature was increased by less than 1 °C (Slater et al., 1993). Most lipid theories of anaesthesia have therefore assumed that some preferential perturbation of boundary lipids surrounding membrane proteins, or lipo-protein, underlies anaesthetic action.

Franks and Lieb (1982) put forward a hypothesis that membrane proteins are themselves the target of anaesthetic actions; more specifically, that the ultimate targets are ion channels in nerve membranes (Franks and Lieb, 1988). In support of this notion, Franks and Lieb (1994) refer to a demonstration where a range of general anaesthetics, at IC_{50} concentrations very close to animal EC_{50} values, inhibit the activity of the soluble lipid-free enzyme, firefly luciferase, providing strong evidence that general anaesthetics bind directly to proteins. However, Franks and Lieb (1994) question that if general anaesthetics act by binding directly to proteins, then, why are some proteins sensitive to anaesthetics and others are not, and what is the nature of the binding sites on sensitive proteins? It is likely that the relevant binding sites are hydrophobic pockets exposed to water rather than interfacial sites exposed to lipid hydrocarbon chains. This is because the former, water-filled pockets might be expected to bind hydrophobic anaesthetics more tightly, avoiding competition from lipid hydrocarbon chains, and can more easily account for the cut-off effect due to increased chain length. However, there is as yet no definitive evidence as to the

exact nature of anaesthetic binding sites on membrane proteins, although increasing evidence implicates receptors for certain neurotransmitters, or their associated channels, as the most likely sites.

Progress on protein-based theories requires, first, a more complete demonstration that a protein site can account both for the diverse chemical structures which induce anaesthesia, and for the reversal of anaesthesia by pressure (Miller, 1985), which has been observed for intravenous agents such as barbiturates, and with local anaesthetics as well as inhalation agents. Perhaps the strongest criticism of a purely lipid theory of anaesthesia comes from the realisation that many anaesthetic agents exhibit chiral specificity of the anaesthetic effects. Prior to 1991 many investigators had failed to find differences in effects between stereoisomers of anaesthetic drugs, or had attempted to link stereospecific effects to lipid perturbation. Franks and Lieb (1991) however demonstrated that the (+)- and (-)-enantiomers of isoflurane have, as expected, identical effects on lipid bilayer properties, but have different effects on specific invertebrate ion channels. This demonstration of chiral selectivity argues strongly against a nonspecific lipid perturbation-mediated effect, and is in favour of a stereospecific interaction with a protein site.

The selectivity and specificity of anaesthetic "side-effects", which are superimposed on the central mechanisms of anaesthesia, may also be explained on a molecular level by the

diversity of protein structures associated with different functions (Miller, 1985; Halsey, 1989).

Since a variety of central neurotransmitter receptors and ion channels have been implicated as possible targets for intravenous general anaesthetics (Hale and Lambert, 1991; Moody et al., 1993), it is conceivable that anaesthetics do not produce their effects by any unitary molecular mechanism of action. Nevertheless a variety of structurally diverse anaesthetics including anaesthetic barbiturates, steroidal anaesthetics, chlormethiazole, propanidid and etomidate do share a common property, namely the ability to enhance the action of GABA on $GABA_A$-receptors at clinically relevant concentrations. Again, the relative selectivity of different anaesthetics at excitatory amino acid receptor-associated ion channels, as well as the potentiation of the GABAergic responses for a number of anaesthetics (barbiturates, steroids or ethanol), implicate both receptor types as being of possible fundamental importance to the overall pharmacological actions of anaesthetic agents (Carla and Moroni, 1992).

In summary, although the molecular mechanisms responsible for the anaesthetic properties remain controversial, nonetheless converging electrophysiological, biochemical, and pharmacological evidence indicates that proteins of neuronal plasma membranes, in particular ion channels and their associated receptors, are possible molecular targets for general anaesthetics.

1.1.5 Stereoselectivity of Anaesthetic Agents

As stated earlier general anaesthetics can be produced by a remarkable variety of chemical agents. Clearly no specific chemical group is required for the activity. But this background of nonspecificity has tended to obscure the fact that most clinically useful agents are more complex compounds; in particular, their structures generally include an asymmetric carbon atom, so that the anaesthetic can exist in two enantiomeric forms (mirror images). Since the only physical difference between these isomers is the ability to rotate plane polarised light, such demonstration of stereoselectivity would strongly support an interaction with protein rather than lipid targets. It is to be noted that whilst the absolute potency differences between isomers are a function of both ligand and receptor structures, it is difficult to assess accurately the extent to which pharmacokinetic factors (rates of metabolism, permeabilities, plasma protein binding, and so on) may influence measured differences in potencies of anaesthetic agents.

In practice, anaesthetic agents are currently, almost invariably, administered as racemic mixtures. However when the potencies of individual optical isomers have been tested on mammals, they are stereoselective, with one isomer being more potent. Stereoselectivity was first observed with the barbiturates. The optical isomers of thiopental and pentobarbital, for example, differ in their potencies in mammals by approximately 2-fold, with the S(-) isomer being in general more potent than the R(+) isomer (Franks and Lieb,

1994). Furthermore the S(+) isomer of ketamine is reported to be 2 to 4 times more potent than the R(-) isomer in both mice and humans, whilst etomidate exerts a potent effect on the GABAergic neuronal systems in the CNS, with the (+)-isomer being much more potent (about 20 times) as an anaesthetic than its (-)-isomer (Keane and Biziere, 1987).

Amongst the volatile anaesthetics, isoflurane, the most commonly used anaesthetic in the United States, shows stereospecificity, where (+)-isoflurane is more potent than the (-)-isomer in enhancing [^{3}H]flunitrazepam binding to benzodiazepine receptors (Moody et al., 1993). Although the absolute potency differences between isomers is approximately 2 fold, these effects are manifested at clinically relevant concentrations of isoflurane and are consistent with the observation of stereospecific differences on K^+ conductances in a mollusc ganglion by Franks and Lieb (1991). Moreover, Jones and Harrison (1993) observed larger increases in the time to half-decay of I_{Cl}, and charge ratio by (+)-isoflurane than by (-)-isoflurane, and propose that it is unlikely these differences are mediated by lipid perturbation, but reflect a structural specificity of interaction between the isoflurane molecule and some regions of the $GABA_A$ receptor-channel protein complex. In keeping with stereoisomerism, the S(+) enantiomer of isoflurane is reported to be about twice as effective as the R(-) isomer in prolonging evoked inhibitory postsynaptic currents mediated by $GABA_A$-receptor channels in cultured rat hippocampal neurones, and about 50% more potent than the R(-) isomer as an anaesthetic in mice. Interestingly, melting curves show that both isomers depress the chain-

melting phase-transition temperature of a pure lipid bilayer (a measure of bilayer disruption) by the same amount (Franks and Lieb, 1994).

There is also evidence that clinically relevant concentrations of volatile anaesthetics increase the binding of a GABA-receptor agonist ([^{3}H]muscimol), and decrease the binding of [^{3}H]SR 95531, a GABA-receptor antagonist (Harris et al., 1994). This bidirectional modulation of radioligand binding to $GABA_A$-receptors is stereoselective, since, as discussed, (+)-isoflurane is more potent than the (-)-enantiomer.

These results are consistent with the hypothesis that volatile anaesthetics produce their pharmacological actions at specific loci on the $GABA_A$-receptor complex, whilst the lack of stereoselectivity in other physical and physiological measures suggest that these are not related to anaesthetic action, and further underscores the potential relevance of $GABA_A$-receptors as targets for inhalation anaesthetics, as reviewed later.

1.2 POTASSIUM CHANNELS

1.2.1 An Introduction to Potassium Channels

There is a substantial interest in specifying the characteristics that define different types of potassium (K^+) currents, particularly since an increase in some K^+ current could mediate anaesthetic depression of neuronal functions

(Krnjevic, 1992). Originally, a K^+ current contributing to the mechanism of action potential in squid giant axons was described by Hodgkin and Huxley (1952). This current is responsible for the repolarisation of the action potential. Since then, K^+ channels have been observed in a greater diversity and prevalence than any other ion channels. In neurones, all K^+ currents can be regarded as basically inhibitory, since they provide the outward currents which the inward Na^+ and Ca^{2+} currents must overcome to produce depolarising signals. As a result, K^+ channels are of paramount importance in regulating membrane potentials, the level of excitability, and the firing properties of neurones (Cook, 1988; Rudy, 1988; Akins and McCleskey, 1993; Zorn et al., 1993). The diversity of K^+ channels may be an evolutionary response to the need for a large variety of discharge patterns required in nervous system function, since they are found to be targets for many ligands such as drugs, hormones, toxins, neurotransmitters and second messengers. K^+ channels thus underlie numerous neuronal firing patterns, and play a an important role in neuronal network information coding and integration.

Although drugs which block Na^+ channels have been used for many years as local anaesthetics, until recently, one factor which has hindered the development of compounds modulating K^+ channels is the multiplicity of these channels, and the lack of specific ligands to activate or block them. However, a number of animal toxins, e.g. apamin, dendrotoxins and charybdotoxin have now been found which potently and rather selectively block certain K^+ channels. Also, application of

whole cell voltage clamp and single channel recording has allowed properties of any single class of K^+ channels to be investigated in the absence of noise from other ion channels (Cook, 1988). This has allowed a more definitive classification of K^+ channel types to be made (Bartschat and Blaustein, 1985a; Bartschat and Blaustein, 1985b; Cook, 1988; Rudy, 1988; Aronson, 1992).

1.2.2 Voltage-Activated K^+ Currents

1.2.2.1 Delayed (outward) rectifier current ($I_{K(V)}$) - This current is activated by depolarisation with some delay, and is the classical Hodgkin-Huxley current. $I_{K(V)}$ acts to repolarise the cell and therefore influences the duration of action potential and possibly the refractory period.

1.2.2.2 Fast transient current ($I_{K(A)}$) - This current activates in response to depolarisation, but much more rapidly than the delayed rectifier (under 20 ms in most species). As this current is inactivated very rapidly during depolarisation, it operates around resting voltages. $I_{K(A)}$ may control the rate of depolarisation, and may be responsible for the transient hyperpolarisation which sometimes occurs after repolarisation.

1.2.2.3 Rapid delayed current ($I_{K(Vr)}$) - This current is activated rapidly (within ms), but takes much longer to inactivate. It delays the onset of action potentials.

1.2.2.4 Slow delayed current ($I_{K(Vs)}$) – This current is activated and inactivated very slowly. The current is increased by cAMP-dependent phosphorylation.

1.2.2.5 Muscarinic-inactivated current ($I_{K(M)}$) – This current was first identified in muscarinic neurones. It is activated slowly, but is not inactivated, and may provide a background of current opposing depolarisation. Cook (1988) refers to this current as a receptor-coupled current, closed by muscarinic agonists acting at M_1-receptors.

1.2.2.6 Inward (anomalous) rectifier current ($I_{K(IR)}$) – This current is activated by hyperpolarisation around resting membrane potential. They may be involved in maintaining the plateau of the action potential and in controlling the duration of hyperpolarisation after repolarisation. There are at least 2 types of inward rectifier currents (Aronson, 1992), one of which is ligand-activated.

1.2.2.7 Calcium-activated K^+ currents – Three types of Ca^{2+}-activated K^+ currents ($I_{K(Ca)}$) have been identified: high-conductance ($I_{BK(Ca)}$), medium-conductance ($I_{IK(Ca)}$) and low-conductance ($I_{SK(Ca)}$) currents, also known as big, intermediate and small, or fast, medium and slow. These currents are responsible for repolarisation, and contribute to the delayed after-hyperpolarisation.

A Ca^{2+}-activated nonspecific cation channel ($I_{K/Na(Ca)}$) is also reported which does not discriminate between Na^+ and K^+.

$[Ca^{2+}]i$ increases its open probability. It is generally voltage-sensitive with a linear current-voltage relationship and long openings (usually 100-1000 ms).

1.2.3 Ligand-Activated K^+ Currents

Ligand-activated K^+ currents are elicited by a variety of neurotransmitter ligands activating associated G-protein coupled receptors. Such ligands include noradrenaline (at α_2 receptors), acetylcholine (at M_2 receptors), dopamine (at D_2 receptors), 5-hydroxytryptamine (at 5-HT 1A receptors), opiates (at μ receptors) and GABA (at $GABA_B$ receptors). These channels are activated by direct interaction of the α- or sometimes ß- or gamma-subunits of G-protein, or else via a second messenger cascade mediated through the receptor-coupled G-proteins. For instance, activation of these channels may be mediated via stimulation of the arachidonic acid cascade by a phospholipase which in turn is activated through a protein kinase, or a G-protein (Aronson, 1992).

1.2.4 Other K^+-Specific Channels

ATP-sensitive channel (K_{ATP}) - The presence of sulphonylurea binding sites in brain suggest these channels exit. They are found in hippocampal (CA_3-region), and in substantia nigra neurones.

5-HT(via cAMP)-inactivated channel (K_{5-HT})

Na^+-activated K^+ channel (K_{Na})

Cell-volume-sensitive K^+ channel (K_{Vol}) -
Opens when cells swell.

Residual leak Currents

1.3 GABA PHARMACOLOGY

In the present context, GABA-receptors are considered prime targets for anaesthetic or analgesic agents. GABA (4-aminobutanoic acid), which is an inhibitory neurotransmitter, can intensely inhibit synaptic activity in the brain.

1.3.1 History of GABA

GABA is present within a large proportion of neurones in the CNS, where it is a major inhibitory transmitter controlling synaptic transmission and neuronal excitability. Evidence for this has steadily accumulated over the 40 years since it was first identified in brain extracts by Awapara et al. (1950) and Tallen et al. (1950). Although GABA was known to exist in the CNS, and much was known of its biochemistry, GABA was not generally accepted as a transmitter until Krnjevic and Schwartz (1967) equated synaptically mediated inhibition with the inhibitory action of GABA on the same cerebral cortex neurones. Perhaps the most crucial evidence was provided by Curtis et al. (1970) who discovered bicuculline as a prototypical competitive GABA antagonist. As

reported by Curtis and Johnston (1974) and Krnjevic (1974), GABA has fulfilled all the criteria for identification as a neurotransmitter. The development of a variety of agonists and antagonists has led to the notion of heterogeneity among GABA receptors. As a result, at least two broad classes of receptors for GABA are recognised, $GABA_A$- and $GABA_B$-receptors. Each of these receptor types has distinctive GABA-binding properties on neuronal membranes, and each mediates characteristically distinct functional responses to GABA, although both are ultimately concerned with inhibition in the CNS.

1.3.1.1 History of $GABA_B$-receptors

Bowery and Hudson (1979) set out to establish a model for terminal depolarisation and receptors mediating presynaptic inhibition in peripheral tissue. They discovered that GABA decreased the stimulated release of ^{3}H-noradrenaline in a dose-dependent manner. However the action was insensitive to bicuculline and other recognised GABA antagonists such as picrotoxin. The known GABA-receptor agonists, such as isoguvacine and THIP, were also inactive. This implicated a GABA-induced inhibition of transmitter release that was not associated with membrane depolarisation, and was not via the then familiar GABA receptor.

Shortly afterwards, Bowery et al. (1981) characterised the pharmacological profile of this novel receptor, and

demonstrated that K^+ evoked release of radiolabled noradrenaline from brain slices could also be inhibited by GABA, and this inhibition was not blocked by bicuculline. Moreover, the GABA analogues that were inactive in the peripheral model were also inactive in brain-slice release experiments, whereas baclofen was an agonist which had no action at bicuculline-sensitive GABA-receptors. Hill and Bowery (1981) ultimately developed a radiolabled receptor-binding assay in brain synaptic membranes, using (^{3}H)-baclofen, that enabled them to distinguish two recognition sites for GABA with entirely separate profiles. At that point, they introduced the terms "$GABA_A$" and "$GABA_B$", as there seemed little doubt that separate receptor types for GABA exist.

1.3.2 An Introduction to GABA-Receptors

Two distinct types of receptors mediate synaptic transmission by the inhibitory amino acid neurotransmitter GABA in the CNS.

1.3.2.1 $GABA_A$-receptors

By definition, $GABA_A$-receptors are linked to chloride channels, and are activated by isoguvacine, modulated by barbiturates and benzodiazepines, and antagonized by bicuculline.

$GABA_A$-receptor complex comprises of an integral chloride ion channel and at least 4 major $GABA_A$-receptor subunits. These are α, ß, gamma and δ. On the receptor, the binding sites identified are (i) the GABA agonist/antagonist site, (ii) the benzodiazepine site, ligands for which can be further subdivided into anxiolytic agonists and anxiogenic inverse agonists, (iii) the barbiturate site, which mediates some of the anaesthetic and anticonvulsant actions of barbiturates, and (iv) the picrotoxin site, where many convulsant agents bind. Each of these sites is thought to be physically distinct, and can be occupied simultaneously to induce their effects.

Activation of $GABA_A$-receptors results in a net influx or efflux of chloride ions, depending on the prevailing concentration gradient. $GABA_A$-receptors are found as postsynaptic (axo-somatic or axo-dendritic), and presynaptic (axo-axonic) receptors, including auto-receptors. The postsynaptic $GABA_A$-receptors regulate the passage of chloride ions, in such a way that receptor activation causes hyperpolarisation of the cell membrane and, thus, decreases sensitivity of the postsynaptic neurone to excitatory inputs (Krogsgaard-Larsen et al., 1988; Kerr and Ong, 1992). Activation of presynaptic $GABA_A$-receptors normally leads to a net efflux of chloride ions causing partial depolarisation (Krogsgaard-Larsen et al., 1988) and modulation of transmitter release from synaptic terminals, whilst autoreceptors inhibit the release of GABA itself (Kerr and Ong, 1992).

1.3.2.2 $GABA_B$-receptors

The bicuculline-insensitive $GABA_B$-receptor is linked to guanosine triphosphate binding proteins (G-proteins), and is activated by GABA and the selective $GABA_B$-receptor agonist (R)-(-)-baclofen. $GABA_B$-receptors are heterogeneous. The receptors are located both pre- and post-synaptically, as well as on glial cells (Bowery, 1993). Pre- and post-synaptic membranes are likely to be different from one another, and might show different sensitivities to the antagonists, particularly since these receptors are linked through different G proteins to pre-synaptic Ca^{2+} and post-synaptic K^+ channels (Kerr and Ong, 1992). Neuronal $GABA_B$-receptors either inhibit Ca^{2+} currents or activate K^+ currents depending on the cellular localisation of the receptor. $GABA_B$-receptors are antagonized by phaclofen and 2-hydroxysaclofen, which were discovered by Kerr and colleagues (see Kerr et al., 1987; Kerr et al., 1990a; Kerr et al., 1990b), whilst newer, more potent antagonists based on phosphonous or phosphinic analogues of GABA have been described (Bowery, 1993).

$GABA_B$-receptor agonists can act through a second messenger system to inhibit basal or forskolin-stimulated cyclic AMP (cAMP) formation, potentiate cAMP formation induced by other neurotransmitters, or modulate histamine and serotonin stimulated inositol phospholipid turnover (Krogsgaard-Larsen et al., 1988; Turgeon and Albin, 1993; Bowery, 1993).

Like $GABA_A$-receptors, $GABA_B$-receptors are found as presynaptic receptors, including autoreceptors, and as postsynaptic

receptors. Amongst these, presynaptic receptors modulate transmitter release from synaptic terminals, whereas autoreceptors inhibit the release of GABA itself, whilst postsynaptic receptors are responsible for inhibiting excitability of the postsynaptic cells (Kerr and Ong, 1992; Bowery, 1993). Thus depending on the brain region examined, $GABA_B$-receptor activation can decrease neurotransmitter release, hyperpolarise postsynaptic neurones, or act presynaptically to inhibit GABA release at inhibitory neurones.

1.3.2.3 GABA-autoreceptors

The role of autoreceptors in regulating endogenous GABA release is well known (Davies et al., 1991; Kerr and Ong, 1992; Bonanno and Raiteri, 1993). There are distinct $GABA_A$- and $GABA_B$-autoreceptors which are activated by GABA and baclofen. Importantly, it is reported that the induction of long-term potentiation is influenced by autoreceptor activation, or its antagonism (Mott and Lewis, 1991).

1.3.3 GABA-Receptor Distribution

Regional distributions of $GABA_A$- and $GABA_B$- receptors in the CNS are different (Krogsgaard-Larsen et al., 1988; Bowery, 1993). In most areas of the CNS, $GABA_A$ binding sites are more

abundant than the $GABA_B$ type, but significant numbers of the latter are found in many brain areas. $GABA_B$-receptors are not confined to neurones but are also present on glial cells. Importantly, high densities of neuronal $GABA_B$-receptors occur in the cerebral cortex and certain thalamic nuclei, particularly the reticular and midline nuclei. Moderate densities of $GABA_B$-receptors are also present throughout the hippocampal formation. The presence of the sites in this brain region may be significant in cognitive functions, since it has been proposed that the induction of long-term potentiation is influenced by $GABA_B$ receptor activation/antagonism (Burgard and Sarvey, 1991; Mott and lewis, 1991).

1.3.4 GABA-Receptors and Excitatory Transmission

There is abundant evidence for $GABA_B$-mediated presynaptic inhibition of excitatory transmitter release in the brain (Bowery, 1993), sensitive to $GABA_B$-receptor antagonists (Krogsgaard-Larsen et al., 1988; Lambert et al., 1989). Evidence derived from lines of research strongly suggests that hyperactivity of the central excitatory neurotransmitter, glutamate, is a major factor in causing certain neurodegenerative disorders, and selective activation of presynaptic $GABA_B$-receptors may represent a flexible way of reducing excessive activation of neurones in the brain by glutamate (Belhage et al., 1993).

1.3.5 $GABA_B$-Receptor Electrophysiology

From electrophysiological studies, $GABA_B$-receptors are indirectly coupled through G-proteins, and possibly second messenger systems, to either Ca^{2+} or K^+ channels, where they mediate a presynaptic reduction in Ca^{2+} influx or a postsynaptic increase in K^+ conductance. GTP-binding proteins (Gi/Go) act as an essential biochemical link in these actions. The late inhibitory postsynaptic potentials (late IPSPs) are responses to activation of $GABA_B$-receptors, and are known to result from activation of inwardly rectifying K^+ channels (Gahwiler and Brown, 1985).

1.3.5.1 $GABA_B$-receptors and Ca^{2+} channels

Amongst Ca^{2+} channels, T- and L-types are present in a wide variety of both excitable and non-excitable cells, whereas N- and P-type channels are found mainly in neurones. Originally, neurochemical evidence suggested that baclofen and GABA can diminish the evoked release of neurotransmitters (Johnston et al., 1981; Hill and Bowery, 1981), whilst a $GABA_B$-receptor mediated depression of the Ca^{2+} component of the action potential in dorsal root ganglion cell was described by Dunlap and Fischbach (1981). A diminution in Ca^{2+} flux would provide an obvious explanation of this effect, but Gahwiler and Brown (1985) found no evidence for involvement of Ca^{2+} in the response to $GABA_B$-receptor activation in hippocampal slices, but instead they attribute any change in

Ca^{2+} conductance to an initial increase in the inward rectifier K^+ conductance. More recently, Ca^{2+} currents in cultured hippocampal neurones have been shown to be modulated by $GABA_B$-receptors which may be responsible for mediating presynaptic inhibition, implicating the N-, T- and possibly L-types Ca^{2+} channels (Scholtz and Miller, 1991). However a direct mechanism involving Ca^{2+} currents in the $GABA_B$-receptor control of transmitter release has yet to be established, although such a mechanism seems most likely at the primary afferent fibres in the spinal cord, where $GABA_B$-receptor activation decreases the evoked release of the putative neurotransmitter peptide, substance-P (Bowery, 1993).

1.3.5.2 $GABA_B$-receptors and K^+ channels

Within higher centres of the mammalian brain an increase in K^+ channel conductance, rather than involvement of Ca^{2+} channels, appears to be the primary neuronal response to postsynaptic $GABA_B$-receptor activation. Nevertheless, the $GABA_B$-receptor agonist baclofen depresses excitatory and inhibitory synaptic transmission, and hyperpolarises neurones in area CA_1 of hippocampus by increasing the K^+ conductance (Lambert et al., 1991); but the precise mechanism of synaptic depression produced by activation of presynaptic $GABA_B$-receptors is not yet established. The postsynaptic K^+ channels, modulated by baclofen in hippocampal neurones, are affected by numerous substances which include internal Cs^+, external Ba^{2+}, the local anaesthetic QX-314 which appears to

have no effect on Cl^- channels associated with $GABA_A$-receptors (Nathan et al., 1990; Andrade, 1991), as well as quisqualic acid and kainic acid (Rovira et al, 1990).

$GABA_B$-receptor induced hyperpolarisation within higher brain centres, which reflects the late IPSP demonstrated after afferent stimulation, is also sensitive to pertussis toxin which ribosylates the Gi/Go α-subunits responsible for activating the K^+ channels. The early fast IPSP, mediated via $GABA_A$-receptors through an increase in Cl^- conductance, is unaffected by pertussis toxin in keeping with the notion that only $GABA_B$- but not $GABA_A$-receptors are linked through G-protein(s) to K^+ channels. Whether the same G-proteins are responsible for coupling K^+ and Ca^{2+} channels is unknown (Bowery, 1993).

1.3.6 Absence Epilepsy

Many drugs for treatment of epilepsy enhance GABA-mediated inhibition or prevent repetitive action potential discharges. Since epileptiform activity is likely to arise from an imbalance of excitatory and inhibitory inputs, the putative role of glutamate receptors and ionic perturbation are, however, likely to play an important role (Aram and Lodge, 1988). However, absence epilepsy appears to be of thalamo-cortical origin, and manifests in humans as an abrupt decrease in motor activity without loss of consciousness, which is a unique syndrome. The role of GABA, gamma-

hydroxybutyric acid (GHB), and $GABA_B$-receptor antagonists in experimental absence seizure models has been investigated. $GABA_B$-receptors are of primary importance in experimental absence epilepsy, and $GABA_B$-receptor antagonists may represent a new class of anti-absence drugs (Soltesz et al. 1988, Bernasconi et al., 1992; Hosford et al., 1992; Marescaux et al., 1992).

Intracellular recordings in slices of guinea pig substantia nigra revealed that, GHB, a metabolite of GABA, lowers the input resistance of pars compacta neurones, hyperpolarises the membrane in a concentration-dependent manner, and facilitates Ca^{2+} conductance (Harris et al., 1989). The effect of GHB is partially reduced in the presence of bicuculline, but neither K^+ nor Cl^- channels seem to be directly implicated in the mechanism of action of GHB. It is possible that GHB functions as an inhibitory neurotransmitter in the CNS, acting on dopaminergic neurones. Once used as an anaesthetic, GHB produces epileptiform activity which, especially at lower concentrations, resembles petit mal epilepsy rather than sleep (Tunnicliff, 1992; Banerjee et al., 1993).

1.4 ANAESTHESIA AND EXCITATORY OR INHIBITORY TRANSMISSIONS

One property of some anaesthetic agents appears to be preferential block of excitatory synaptic transmission at low concentrations, leaving inhibitory transmission, at least unaffected if not enhanced. The result is a shift in balance

between excitatory and inhibitory inputs to a given neurone in favour of inhibition. Depression of postsynaptic responses to excitatory neurotransmitter (glutamate and aspartate) may therefore be important in anaesthesia. Decreased sensitivity to excitatory transmitters occurs at both peripheral and central synapses, whereas the action of inhibitory synapses may be enhanced.

A wide variety of anaesthetics including chloralose, chloral hydrate, diethyl ether, urethane, chloroform, nitrous oxide, propanidid, halothane and magnesium sulphate all markedly enhance presynaptic inhibition. Halothane, urethane, chloralose and chloral hydrate produce the same effect as barbiturates on GABA-mediated postsynaptic inhibition. Chlormethiazole, an anticonvulsant, also potentiates the inhibitory effects of GABA (Keane and Biziere, 1987). Unlike barbiturates, volatile anaesthetics do not consistently potentiate IPSPs, but at low concentrations, can depress evoked IPSPs in cortical slices (Fujiwara et al., 1988). Moreover, inhalation agents prolong the decay of individual spontaneous post-synaptic currents (IPSCs) through $GABA_A$-receptor mediation (Gage and Robertson, 1985; Mody et al., 1991), but the peak IPSC amplitude is decreased at clinically relevant concentrations (Jones and Harrison, 1993). These synaptic currents arise from brief activation of a large number of Cl^- channels, upon the release of GABA from the presynaptic terminals. Furthermore, the prolongation effects may be due to an alteration in the gating kinetics of the $GABA_A$ receptor/channel complex. The prolongation of synaptic inhibition in the CNS is consistent with the physiological

effects that accompany anaesthesia, and may contribute to the mechanism of anaesthetic action. However, surprisingly little unambiguous evidence is available to answer a key question of whether the remarkably consistent potentiation of postsynaptic currents translates into an enhancement of inhibitory synaptic transmission, since some GABAergic synapses appear to be inhibited, perhaps because inhibitory synaptic activity often requires activation of local interneurones by excitatory synapses, which may themselves be depressed by anaesthetics (Franks and Lieb, 1994).

Volatile agents appear to be relatively inactive at all glutamate receptor sub-types (Franks and Lieb, 1994). The antagonism to excitatory amino acids (EAA) responses exerted by some non-volatile general anaesthetics is non-competitive in nature. The variability in interaction between the non-volatile agents and EAA indicates that particular care should be taken when pharmacological agents are tested on glutamate-related mechanisms in anaesthetized animals (Carla and Moroni, 1992). Since some agents like pentobarbital are clearly effective at both inhibitory and excitatory postsynaptic receptors, the balance between the inhibition of excitatory synapses and the potentiation of inhibitory synapses in causing general anaesthesia still needs to be assessed (Mody et al., 1991).

1.5 ANAESTHESIA AND GABA-RECEPTORS

Although general anaesthetics have been used in clinical practice for 150 years, the mechanism responsible for anaesthesia is still not understood. GABA-mediated synaptic transmission has been suggested to be potentiated by general anaesthetics. GABA is the major inhibitory neurotransmitter in the brain and augmentation of GABA-mediated inhibition would induce an overall suppression of neuronal activity in the CNS (Lin et al., 1993b). Although anaesthetic agents could affect presynaptic GABA synthesis or release to enhance synaptic transmission, accumulating evidence indicates that the postsynaptic $GABA_A$-receptor may be the site for anaesthetic augmentation of GABAergic transmission. Evidently several anaesthetics with varied and complex structures, including barbiturates, neurosteroids and propofol, bind to specific sites on the $GABA_A$-receptor complex to allosterically enhance Cl^- channel opening (Jones and Harrison, 1993).

A number of corollaries support the notion that a casual relationship exists between stimulation of GABA-receptor complexes and anaesthesia (Keane and Biziere, 1987). Firstly THIP, a $GABA_A$-receptor agonist, has been shown to produce analgesia and anaesthesia in mice and rats. Secondly the pharmacological effects of drugs which stimulate GABAergic processes is reduced or abolished in anaesthetised animals, which suggests that GABA-receptors are already highly stimulated in anaesthetised animals so that further activation of this neuronal system produces little or no additional effect. Thirdly, while non-specific theories would predict a

generalised reduction in brain metabolic activity under anaesthesia, a specific site of anaesthesia such as the GABA-receptor complex might imply more selective modifications in brain metabolism, as supported by a number of studies using the 2-deoxyglucose technique which have shown very marked regional differences in cerebral metabolism in response to anaesthesia, with the activity of some nuclei even being enhanced.

Amongst the more compelling evidence in support of a GABAergic basis of anaesthesia is the finding that, in oocytes expressing total mRNA, potentiation of GABA-activated Cl^- currents by general anaesthetics is dependent on GABA concentrations, the potentiation being marked with low (5 or 10 μM) levels of GABA, and exponentially decreasing as GABA concentrations increased from 3 to 300 μM (Lin et al., 1993b). As most anaesthetics shift the GABA dose-response curve to lower concentrations, peak Cl^- currents elicited by high levels of GABA are virtually unaffected (Franks and Lieb, 1994).

In order to answer the 'lipid or protein' question for anaesthetics with simple chemical structures, Lin et al. (1993b) attempted to study the role of different $GABA_A$-receptor protein subunits in the modulatory action of anaesthetics, using an expression system that maintained the same lipid matrix for different proteins. They compared the effects of enflurane, a widely used volatile anaesthetic, on GABA-activated Cl^- currents in oocytes injected with mixtures of cRNA encoding α_1, β_1, $gamma_{2S}$, or $gamma_{2L}$ receptor

subunits, and found that potentiation of the GABA-activated Cl^- current by enflurane is influenced by the composition of $GABA_A$-receptor protein subunits, the order of sensitivity to enflurane being $\alpha_1\beta_1 > \alpha_1\beta_1 gamma_{2S} = \alpha_1\beta_1 gamma_{2L} >$ total mRNA. Lin et al. (1993b) observed that benzodiazepine potentiation requires $gamma_2$ subunits, whilst a low dose (20 mM) of ethanol requires $gamma_{2L}$ subunits for potentiation of GABA action. Furthermore, Franks and Lieb (1994) report that 20 µM pentobarbital increased the peak GABA responses by approximately 3 fold in xenopus oocytes expressing whole brain messenger RNA. These results suggest that different $GABA_A$-receptor populations are involved in pharmacological actions of barbiturates, benzodiazepines, ethanol, and general anaesthetics.

The distribution of subunits varies greatly throughout the CNS, and the differences between $GABA_A$-receptor subunits reside mainly in the cytoplasmic loops or the extracellular domains rather than the transmembrane regions. This is important as the transmembrane regions are more likely to be affected by changes in physical properties of the lipid bilayer. These considerations suggest that the structurally simple anaesthetic enflurane acts directly on the $GABA_A$-receptor complex rather than the surrounding lipid membranes to modulate the Cl^- channel opening (Lin et al., 1993b).

Inhalation agents share many properties and exhibit cross-tolerance with non-inhalation agents such as barbiturates, alcohols and benzodiazepines. The ability of barbiturates and benzodiazepines to augment the action of inhalation agents is

routinely exploited in clinical practice to optimize anaesthesia. Also, radioligand binding studies confirm that, like barbiturates, inhalation agents enhance the binding of benzodiazepines in a chloride-dependent fashion, and inhibit the binding of convulsants to the $GABA_A$-receptor complex (Moody et al., 1993). Volatile anaesthetics also increase chloride uptake through GABA-receptor gated chloride channels in synaptoneurosomes (Moody et al., 1988), and potentiate GABA-receptor induced hyperpolarisation in hippocampal cultures (Jones et al., 1992). The latter in vitro actions are shared by other non-volatile anaesthetics, including barbiturates, ethanol, and propofol (Harris et al., 1994).

As with barbiturates and etomidate, inhalation anaesthetics increase the [^{3}H]muscimol binding through a change in the number of binding sites rather than binding affinity (Harris et al., 1994). This effect, which is also reported for alphaxalone (Harrison and Simmonds, 1984), suggests that volatile anaesthetics allosterically modulate GABA-receptors possibly, by recruiting the low affinity sites.

1.5.1 Effect of Anaesthetics on $GABA_A$-Receptor Channel Kinetics

It appears that, in general, volatile agents, barbiturates, propofol and anaesthetic steroids show no change in channel conductance, but the channel open time increases, consistent with the prolongation of postsynaptic currents. For

example, in bovine chromaffin cells, the probability that a channel is in a conducting state is increased by approximately 4-fold by 1.7 μM propofol (Hale and Lambert, 1991).

Despite similarities between barbiturates and benzodiazepines in potentiating the interaction of GABA with its receptors, fluctuation analysis has shown that pentobarbital prolongs Cl^- channel opening, whereas benzodiazepines increases the frequency of channel opening. However, unlike barbiturates, the effects of benzodiazepines on the GABA-receptors do not need the presence of chloride ions (Keane and Biziere, 1987).

1.6 ROLES OF ION CHANNELS, TRANSMITTER RELEASE AND SECOND MESSENGERS IN ANAESTHESIA

A subset of one or more particularly sensitive potassium channel targets may underlie anaesthesia. The intracellular level of Ca^{2+} may or may not influence the anaesthetic response. Also, anaesthetic responses may be modulated by second messenger systems, which can vary from cell to cell. The possible roles played by ion channels, transmitter release and second messenger systems are discussed in the following sub-sections.

1.6.1 Anaesthesia and Na^+ Channels

Studies of population currents recorded from a large number of channels indicate that both volatile anaesthetics

and barbiturates can block Na^+ channels and thus prevent action potential formation (Kendig, 1989). Amongst sub-types of Na^+ channels, the slow-inactivating I_{Na} is probably not very sensitive to volatile anaesthetic agents, and study of the fast I_{Na} in slice preparation has not been plentiful (Krnjevic, 1992).

1.6.2 Anaesthesia and K^+ Channels

Activation of persistent K^+ conductances could result in a generalised decrease in neuronal excitability, at both pre- and post-synaptic levels, leading to a state of general anaesthesia. General anaesthetics are reported to increase the proportion of non-inactivating voltage-dependent K^+ channels in the closed inactive state (Kendig, 1989). Clinically relevant concentrations of halothane has been shown to affect radically different K^+ channel proteins, suggesting that no single, uniquely sensitive, target protein underlies the effects of halothane (Zorn, 1993).

Franks and Lieb (1994), however, suggest that although it is conceivable for small perturbations of voltage-gated Na^+ and K^+ channels to alter patterns of neuronal firing, it is unlikely that these channels play a substantial role in the production of the anaesthetic state.

1.6.2.1 A novel neuronal K^+ current

Franks and Lieb (1988) reported identifying a novel K^+ current, $I_{K(An)}$, reversibly activated by low levels of volatile anaesthetics, in a single cell amongst a group of apparently identical molluscan neurones which show endogenous firing activity. Anaesthetic-induced hyperpolarisation is believed to be responsible for the inhibition of neuronal firing in this sensitive cell. $I_{K(An)}$ is ionic dependent, insensitive to some K^+ and Ca^{2+} channel blockers, only slightly voltage-gated, and shows no inactivation at depolarised potentials. This current resembles a serotonin-sensitive K^+ current, but is insensitive to serotonin, or to an intracellular injection of cAMP. More recently Franks and Lieb (1994) report that $I_{K(An)}$ responds stereoselectively to the optical isomers of isoflurane, but it has to be determined if $I_{K(An)}$ is found in mammalian neurones.

1.6.3 Anaesthesia and Metabotropic Receptors

Studies on general anaesthetics focus mainly on membrane excitability regulated by ionotropic receptors, such as GABA receptor-gated Cl^- channels, and NMDA receptor-gated ion channels, but little attention is paid to neuronal excitability regulated by "metabotropic" receptors, which activate ion channels via second messengers. However, inhalation anaesthetics do modulate metabotropic receptor-mediated second messenger production (Lin et al. 1993a).

1.6.4 Anaesthesia and Ca^{2+} Channels

Three significant processes are believed to be relate to the anaesthetic block of calcium currents: (i) suppression of the low voltage activating (LVA) Ca^{2+}-current, that facilitates burst-type firing, could explain the uncoupling of EPSPs from neuronal firing produced by anaesthetics (Fujiwara et al., 1988), (ii) much evidence show that high voltage activating (HVA) type of Ca^{2+}-currents are involved in neurotransmitter release (Miller, 1987; Lemos and Nowicky, 1989; Suszkiw et al., 1989), and anaesthetic-mediated suppression of HVA-current would account for the depression of transmitter release observed during anaesthesia, and (iii) post-synaptic suppression of voltage-dependent $I_{K(Ca)}$ could be significant, as such currents are involved in long-term changes, and may play a role in processes underlying memory and awareness (Krnjevic, 1992).

Two voltage-clamp studies have demonstrated that halothane is able to prolong the time course of IPSCs in the hippocampal slice (Gage and Robertson, 1985; Mody et al., 1991). The latter propose that elevation of intracellular Ca^{2+} is fundamental to this effect since intracellular administration of the Ca^{2+} chelator BAPTA, or the Ca^{2+} release inhibitor dantrolene blocked the effect of halothane. On the other hand, Jones and Harrison (1993) found that neither Ca^{2+}/EGTA nor BAPTA alone, added to the recording pipette, prevented the prolongation of IPSCs by halothane, suggesting that variations

in $[Ca^{2+}]i$ are not required for the effect of halothane on the time course of IPSC.

Again, Franks and Lieb (1994) argue that although there is a steep dependence of synaptic transmission on Ca^{2+} entry, it seems unlikely that small inhibitions of Ca^{2+} channels, sometimes observed at surgical concentrations of volatile anaesthetics and barbiturates, are sufficient to produce anaesthesia; it is also unlikely that anaesthetics release Ca_{2+} from internal stores, causing an increase in $I_{K(Ca)}$.

1.6.5 Anaesthesia and Transmitter Release

Although in general the evidence linking anaesthesia to transmitter release is weak, there is a stronger supposition that, at excitatory synapses, depression of the postsynaptic response to transmitter might be an important factor in anaesthesia. After release from the presynaptic nerve terminal, neurotransmitters diffuse across the cleft between cells and bind to specific receptors on the postsynaptic membrane. The EAA receptors are linked to normally closed cation-permeable channels. When transmitter binds, the channels open, the membrane of the postsynaptic cell becomes depolarised, and the cell becomes more excited. Whether the fundamental mechanism of anaesthetic action on excitatory ion channels is to modify transmitter-receptor binding, to block the channel, or to favour the transition to a closed channel, there is evidence to support the supposition that anaesthetic

effects on the postsynaptic membrane are important in anaesthesia, as volatile anaesthetics depress excitatory postsynaptic potentials (Krnjevic, 1992).

Once again, Franks and Lieb (1994) suggest that halothane or thiopental are likely to reduce neurotransmitter release at many synapses, but the effects are relatively small.

1.6.6 Anaesthesia and Second Messengers

Second messengers regulate the activity of many enzymes and ion channels, sometimes by direct binding, but more often by phosphorylation, and play a key role in signal transduction.

General anaesthetics may interact with lipid oxygenases to disrupt the eicosanoid second messenger system cascade, and to suppress intracellular and intercellular signalling. P450-mediated metabolism of arachidonic acid, an eicosanoid second messenger which can be derived from inositol phospholipids, is also inhibited by general anaesthetics (Franks and Lieb, 1994). As lipid mediators, the eicosanoids directly modulate a multiplicity of channel species, in particular by activating K^+ channels, and inhibiting Na^+ and Ca^{2+} channels, they can suppress the amplitude and duration of action potentials, and hyperpolarise membranes (Labella and Queen, 1993).

Anaesthetics also inhibit protein kinase C (PKC) which regulates synaptic function by phosphorylation of membrane proteins, including ion channels (Franks and Lieb, 1994). In a lipid-dependent assay, a potential role for lipids modulating anaesthetic effects is implicated, possibly by influencing the conformation of PKC inserted into the lipid bilayer (Slater et al., 1993).

In contrast, Franks and Lieb (1994) argue that there is little hard evidence that second messenger systems are involved in general anaesthesia. Their argument is based on observations that a reduction in cerebellar cGMP with barbiturates occurs at concentrations that do not reduce locomotor activity, suggesting that the effect may be unrelated to anaesthesia, and that most *in vitro* studies on cyclic nucleotides have used high anaesthetic concentrations.

Against this background, the present study has attempted to examine some influences of the possible modes of anaesthetic action, such as increased chloride conductance, increased potassium conductance, and reduced calcium influx, on spontaneous neural discharges in rat neocortical slices maintained in Mg^{2+}-free medium.

CHAPTER 2

SPONTANEOUS EPILEPTIFORM DISCHARGES

Spontaneous epileptiform discharges (SEDs) from neocortical wedges, in the magnesium (Mg^{2+}) free model, are a special case of epileptogenesis. Generally speaking, the cellular basis of epileptogenesis is an increase in membrane excitability in a large population of neurones, or initiation of wide-spread activity from a relatively small groups of pacemaker cells. Since such activity arises from an imbalance of excitatory and inhibitory influences, excitatory glutamate receptors are likely to play an important role in its genesis. Nevertheless, disinhibition can make a significant contribution, as seen from the epileptiform activity generated in neocortical wedges by reducing $GABA_A$-receptor mediated inhibition with bicuculline or picrotoxin (Horne et al., 1986; Traub et al., 1994).

Glutamic acid is the major excitatory neurotransmitter in the brain. Therefore alteration in its function must be responsible for the appearance of SEDs in the cortical wedge, under Mg^{2+} free conditions. Cortical neurones express three major classes of glutamate receptors:

(i) NMDA (N-methyl-D-aspartate) receptors are linked to calcium (Ca^{2+}) channels, modulated by glycine and blocked by Mg^{2+} at resting potentials; the block is relieved by depolarisation.

(ii) AMPA ((RS) 2-amino-3-(3-hydroxy-5-methyl-isoxazol-4-yl)propionate), also known as quisqualate receptors, are divided into ionotropic receptors which are linked to sodium (Na^+) and Ca^{2+} channels, and metabotropic receptors.

(iii) Kainate are fast acting ionotropic receptors and are linked to Na^+ and Ca^{2+} channels.

AMPA and particularly Kainate receptors mediate non-NMDA fast excitatory postsynaptic potentials (EPSPs), whilst NMDA receptors mediate delayed Ca^{2+} and Na^+ entry by initiating action potentials at already depolarised membranes.

In the Mg^{2+}-free model, without external stimulation, the source of excitatory drive comes from NMDA receptors responding to endogenous glutamate, with the Mg^{2+}-dependent channel block at resting potentials removed by the low Mg^{2+} concentration. The resulting discharges show considerable synchrony between different layers of the cortex (Aram and Lodge, 1988), which suggests that whole columns of neurones in the cortex discharge together. Coupling of the neurones generating the bursts uses short latency white matter pathways as well as longer latency polysynaptic pathways in the grey matter. Such SEDs are evidently dependent on the spontaneous release of excitatory amino acids, and the subsequent firing of action potentials in the excited neurones. This closely resembles the behaviour of neurones in the CNS, under excitatory drive, generating a burst of action potentials as seen in figure 2.1.

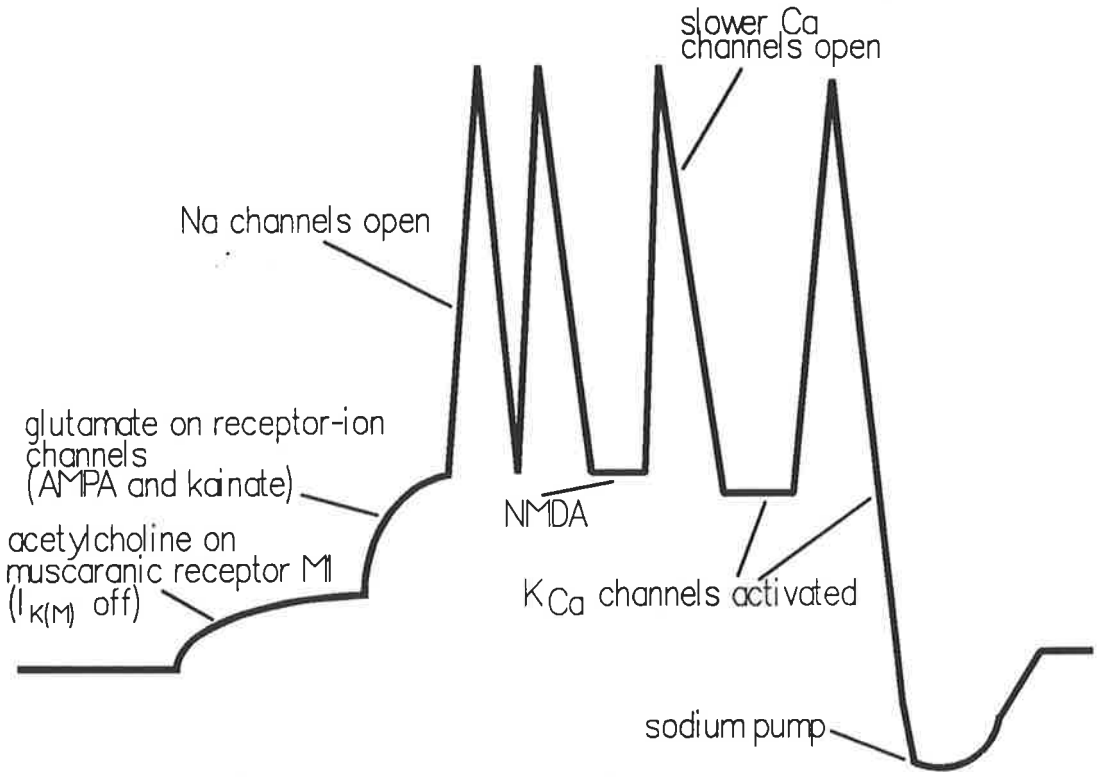

Figure 2.1 Some of currents which govern the behaviour of a central mammalian neuron

Acetylcholine transmitter acting at M1 receptors turns off a persistent potassium current, $I_{K(M)}$, reducing the membrane potential and bringing the cell towards its firing level. Whilst this partially primes the NMDA receptors, the transmitter glutamate also activates non-NMDA receptor-ion channels, further depolarising the membrane and opening Na^+ channels which give rise to fast EPSPs which then trigger action potentials. During depolarisation some Ca^{2+} also enters the cell, particularly when NMDA receptors become activated. As the depolarisation-induced repetitive activity continues, maintained by NMDA receptors, slower voltage-activated Ca^{2+} channels open, prolonging the action potential. The repolarisation of action potentials depends on the activation

of potassium (K^+) conductance as well as on Na^+ inactivation process. The increase in intracellular Ca^{2+} activates calcium-dependent potassium (K_{Ca}) channels which restore the membrane potential and even drive it more negative than the resting level (hyperpolarisation), slowing and finally terminating the burst of activity. Activation of the sodium pump, due to the increase in intracellular Na^+ may also contribute to the restoration of resting potential (Bartschat and Blaustein, 1985b; Kendig, 1989).

In the Mg^{2+}-free model, spontaneous discharges spread throughout the slices. Cells exhibiting spontaneous bursting have been demonstrated in neocortical layers IV/V (Connors, 1984; Armstrong-James et al., 1985). In the neocortical isolated wedge model, the extracellular currents appear first in layers IV/V but are maximal in layer II/III (Aram and Lodge, 1988). Both these layers have a high density of NMDA receptors (Monaghan et al., 1983). Flint and Connors (1993) observed 2 forms of spontaneous rhythmic field potentials in a slice preparation of rat somatosensory cortex. The first, activated by low [Mg^{2+}], has dominant frequencies between 8-12 Hz. The rhythms originate within layer V but not upper layers, and are abolished by NMDA receptor antagonist. The duration of these 'NMDA receptor oscillations' can be potentiated by either blockade of $GABA_A$-receptors with 50 μM bicuculline or activation of metabotropic glutamate receptors. A second form of synchrony, with dominant frequencies between 1-5 Hz, is activated by 10 μM Kainic acid in neurones of layers II/III. Such 'Kainate receptor oscillations' are not affected by $GABA_A$- or NMDA-receptor antagonists or by the activation of

metabotropic glutamate receptors. Nevertheless confirmation that layers II/III are the principal source of the discharges recorded from the wedges in the Mg^{2+}-free model has been provided by Kerr and Pike (1993, unpublished), and examples of such discharges are given in chapters 5, 6,7 and 8.

Horne et al. (1986) showed that one class of excitatory amino acid receptors is activated by NMDA, and it is the response to NMDA that is very sensitive to Mg^{2+}. The antagonism results from a voltage-sensitive block by Mg^{2+} of the channels operated by the NMDA receptor.

It is now widely believed that relief of the voltage-sensitive Mg^{2+} block of the channel associated with the NMDA receptor is the major factor initiating epileptiform bursts in Mg^{2+}-free medium, particularly as NMDA antagonists block the discharges (Aram and Lodge, 1985; Harrison and Simmonds, 1985; Aram and Lodge, 1988; Robichaud et al. 1994). NMDA has been shown to induce burst firing (Flatman et al., 1983; Aram and Lodge, 1988; Aram et al., 1989; Merlin and Wong, 1993; Traub et al., 1994), as has frequently been seen by Ong and Kerr in their laboratories. There is a clear concentration dependency (0-400 μM) of the magnesium block of epileptiform activity in the neocortical slice (Aram et al., 1989), which correlates well with its effect on NMDA channels (Mayer and Westbrook, 1987). However, other actions such as a reduction in surface screening (Hille, 1968) as well as increased transmitter release (Linas and Walton, 1980) are also likely to be important in the Mg^{2+}-free model, since removal of Mg^{2+} ions from the medium superfusing the cortex may result in an

increase in excitability due to a reduction in surface charge screening, which could profoundly influence the effect of drugs upon NMDA receptor mediated activity.

At the resting membrane potential in vitro, and in the presence of 1 mM Mg^{2+}, NMDA receptor-mediated events are markedly suppressed (Aram et al., 1989). Indeed, superfusing the cortical slices with high [Mg^{2+}] and low [Ca^{2+}] produces no epileptiform activity (4 mM Mg^{2+}, 6.5 mM K^{+} and 0.25 mM Ca^{2+}) even after 4 hours (Aram and Lodge, 1988). This is the conventional way to block synaptic transmission, by decreasing the [Ca^{2+}] to 0.2-0.5 mM and increasing [Mg^{2+}] to 6-8 mM, or by adding Co^{2+} or Mn^{2+} (Karnup, 1992), although the latter, particularly Co^{2+}, can block $GABA_A$-receptor activated chloride channels. Apart from which, the raised [Mg^{2+}] would effectively block NMDA receptors in the unstimulated state.

Any depolarisation of the membrane progressively relieves Mg^{2+} block, so that a rapid increase in SED frequency is to be seen when a non-depolarising concentration of NMDA (3 µM) is continuously applied (Robichaud and Boxer, 1993). Conversely, continuous application of a depolarising application of NMDA (10 µM) rapidly blocks SED frequency, whilst serial 10 µM additions of NMDA increased burst rate in a manner qualitatively similar to KCl additions in a cultured fetal murine spinal cord network preparation (Rhoades and Gross, 1994).

NBQX (2,3-dihydroxy-6-nitro-7-sulfamoyl-benzo[F]quinoxaline), a potent and specific non-NMDA glutamate antagonist, has no

effect on low Mg^{2+}-induced SEDs at concentrations that completely block depolarisation to AMPA or kainate in the cortical wedge (Robichaud and Boxer, 1993). This effect suggests that NMDA activation alone is sufficient to produce the synchronous firing needed to produce the discharges, and that measurement of SED frequency is a simple and sensitive measure of endogenous NMDA receptor activation. Nevertheless, the spontaneous discharges require not only the release of glutamate (or other excitatory amino acids) but also the synchronised activation of inhibitory processes, including release of GABA and turning on $I_{K(Ca)}$ to stop the discharges. Thus the SED rate does not depend exclusively on NMDA receptor function.

2.1 ROLE OF NON-NMDA GLUTAMATE RECEPTORS IN EPILEPTOGENESIS

Evidently, in the cortical wedge model, AMPA or kainate subtypes of glutamate receptor do not appear to play an important part in the initiation of epileptogenesis (Aram et al., 1989). However, synaptic mechanisms which are mediated through non-NMDA receptors can be responsible for generating ictal epileptiform activity in juvenile rat hippocampus (Avoli et al., 1993), and the balance between excitation and inhibition in low Mg^{2+}-induced bursts from rat hippocampal slices can be altered by blockade of AMPA receptors (Traub et al., 1994). Moreover, in spinal-cord cultures, glutamate consistently produces desynchronised, irregular, high frequency tonic spiking with no discernible intraburst

quiescent periods (Rhoades and Gross, 1994). It is thus notable that a bath application of kainate or glutamate to a synaptically active network not only depolarises neurones through kainate receptors, but also preempts the effects of endogenously released neurotransmitter at those receptors, since the neurotransmitter both tonically depolarises and synaptically uncouples the network.

2.1.1 Kainic Acid

Kainic acid, which is obtained from seaweed, is about 50 times as potent as glutamate, but also has a delayed toxic effect on neurones whose cell bodies are exposed to it. This toxic effect is known to result from an interaction with the kainate class of glutamate receptors, though the detailed mechanism is not understood. Microinjection of kainic acid into the brain provides a useful way of destroying small groups of nerve cells, for it acts only on cell bodies and not on axons or nerve terminals. It has been suggested that this agent causes an increase in Ca^{2+} permeability, and produces an excessive rise in $[Ca^{2+}]i$, possibly leading to protease activation and cell death (Meldrum and Garthwaite, 1991).

2.2 ROLES OF CALCIUM CHANNELS AND NEUROTRANSMITTER RELEASE IN EPILEPTOGENESIS

It is generally argued that, during neuronal depolarisation, Ca^{2+} enters the terminals through voltage-regulated Ca^{2+} channels and triggers neurotransmitter release. Immediately after this neuronal activity, the Ca^{2+} is rapidly buffered, sequestered and extruded. This Ca^{2+} induced neurotransmitter release is important in epileptiform activity and rhythmic firing generated in vitro. It appears to occur mainly via the P- and N-type Ca^{2+} channels. Antagonists for these Ca^{2+} channels at the presynaptic terminals decrease neurotransmitter release, significantly reducing epileptiform activity (Boulton and O'Shaughnessy, 1991). Furthermore prolongation of Ca^{2+} channel current activation and transmitter release may be due to interaction of a transient N-type current that reveals a more slowly activated L-type current (Formenti and Sansone, 1991). Blockade of N-type Ca^{2+} channels with w-CTX-GVIA minimally inhibits glutamate and GABA release, whereas pretreatment with 200 nM w-Aga-IVA, a P-type channel blocker, reduces K^{+}-induced release of glutamate, aspartate and GABA in rat hippocampal slices (Robichaud et al., 1994). The presynaptic site of action for w-Aga-IVA as a P- channel Ca^{2+} blocker and w-CTX-MVIIC as a blocker of a newly identified Q-type Ca^{2+} channel is supported by the fact that neither of these toxins inhibit direct depolarisations to NMDA in the rat cortical wedge neurones.

In neocortical slices, removal of Ca^{2+} from the superfusing medium leads to a marked reduction in the frequency of

paroxysmal events. This is a result of interfering with initiation of ictaform events. A decrease in the amplitude of events is due to a reduction in the recruitment of neurones. These effects indicate that the neurotransmitter release is essential to the initiation of events, and to the recruitment of neurones to generate the waveform (Horne et al., 1986).

Epileptiform activity in the neocortical slices is most pronounced in terms of amplitude and duration over the lower concentration range of 0.75 to 1 mM Ca^{2+}, although the frequency of spontaneous bursts is reduced (Aram and Lodge, 1988). However, below 0.5 mM Ca^{2+}, the number of afterpotentials is reduced, consistent with the importance of efficient synaptic transmission in recruiting cells to fire in prolonged bursts (Miles et al., 1984) and the presence of regenerative Ca^{2+}-dependent conductances (Dingledine, 1983).

2.3 ROLE OF POTASSIUM CHANNELS IN EPILEPTOGENESIS

Depolarisation of neuronal membranes by K^+ channel blockers unmasks NMDA receptor-mediated excitation, where the different channel blocking agents induce the characteristic patterns of prolonged activity as described in chapter 5. This is in keeping with the proposed role for K^+ channels in terminating the epileptiform bursts (Alger and Nicoll, 1980; Aram and Lodge, 1988). However the failure of applied K^+ to induce afterpotentials may indicate reduced synaptic transmission, due to direct depolarisation of presynaptic

terminals. On the other hand, excitatory amino acids which preferentially depolarise postsynaptic membranes are able to induce bursts with many afterpotentials. It is likely that depolarisation of neurones by high K^+ results in the release of endogenous glutamate and secondary activation of the NMDA receptors, since a depolarising concentration of 20 mM K^+ produces a rise in internal Ca^{2+} concentration of 362 ± 65 nM (Irwin et al., 1992).

2.4 ROLE OF CYCLIC AMP IN EPILEPTOGENESIS

Derivatives of Cyclic AMP (cAMP) block the late after-hyperpolarisation by closing the long lasting K_{Ca} channels. This reduces the frequency of interictal bursts and prevents train adaptation, but does not affect the spike duration (Rudy, 1988; Lewis et al., 1989). Activation of a cAMP-dependent protein kinase enhances the opening frequency and mean open time of non-NMDA type glutamate receptor channels. Cyclic AMP also significantly enhances Ca^{2+} influx resulting in the release of glutamate and aspartate. The potentiated release of excitatory amino acids and increased channel open times may be expected to result in hyperexcitability. Other modulatory effects of cAMP include the mobilisation of intracellular Ca^{2+} and the reduction in $GABA_A$ receptor-mediated Cl^- flux. All these mechanisms may act to increase excitability (Boulton et al., 1993) and regulate burst timing (Rhoades and Gross, 1994).

CHAPTER 3

RECORDING FROM BRAIN SLICES

In this chapter computer based data acquisition and processing is introduced. Merits of recording from brain slices and characteristics of a cortical wedge preparation are reviewed. Details of a grease-gap model used for recording population events from neocortical slices are given. Constituents of a computer-based system developed for acquiring, processing and presenting such neocortical discharges are also discussed.

3.1 COMPUTER-BASED ELECTROPHYSIOLOGICAL DATA ACQUISITION AND ANALYSIS

Personal computers (PCs) are now very common in biological laboratories, and some additional hardware and software make them a complete workstation for data acquisition and analysis as well as other routines such as word processing, spreadsheet and database analyses. One way of setting up such a system is to add an analogue-to-digital (A/D) board, containing an A/D converter, which takes as its input the analogue signal from the physiological preparation via recording electrodes or a transducer and produces digital data which are output to the computer to be read by a software. Analogue signals are conveniently amplified to bring them up to the input range of the A/D converter. An interface circuit is needed for terminating input cables. A ribbon cable connects the interface circuit to the A/D board.

A variety of systems based on a PC have been developed and are reported in the literature:

Ratzlaff and Siegel (1990) present a low-cost DOS-based system for acquiring and storing 1 to 4 channels of interspike interval data. An amplified action potential activates a window discriminator. This generates a digital trigger pulse in order to (i) record the event in a (home-made) event memory circuit, (ii) store the interval period within a commercially produced interval timer interfaced to a 80X86 host processor, and (iii) interrupt the processor to read the event memory. The event memory is reset after being read, the interval period transferred to memory and the host processor resumes its activity. The system was tested for accurate recording and response times for single and multiple channels with and without intensive foreground multitasking. Spike events from the *inferior parietal cortex* of a monkey were demonstrated, while the processor was presenting visual stimuli and monitoring the eye position.

Stromquist et al. (1990) have described a system based on an IBM-PC compatible, a four-channel Burr-Brown A/D converter, a custom built interface module, and custom software written in 'C' language which operates within the Microsoft Windows environment. The software comprises acquire and review modules which allows for averaging, addition and subtraction of various channels and feature extraction of the acquired data on-line. Data can be transferred to Excel for Windows

spreadsheet for further mathematical and statistical analysis, as well as graphical presentation.

Turner and Schlieckert (1990) present a comprehensive large-scale system designed mainly for intracellular patch-clamp studies. A data recording program provides on-line waveform analysis for half-width, rise time and peak value. Off-line analyses include current-voltage relationship, synaptic potential averaging, two-cell interaction and histogram operations. Other attributes reported are definition of a large binary digital database for easy access and a provision for rapid and high-quality output of results. The software, written in FORTRAN and Assembly languages, is tailored for the Data Translation DT2821 series of boards for IBM PC/AT compatibles. Direct Memory Access (DMA) mode of operation for data transfer from A/D to memory is used for faster speed.

Alarcon et al. (1991) have described an Assembler routine for on-line data acquisition and graphical display. User instructions are written in GWBASIC, whilst acquisition and analysis routines are written in Assembly language. The hardware set-up consists of a Microlink data acquisition system connected to an IBM AT through a standard IEEE interface. The user specifies input parameters relating to data collection, for up to 16 input channels. The software allows the computer to behave as a multi-channel digital oscilloscope which has access to large memory data buffer, has disk storage, averaging capabilities and artefact rejection. The authors include the program listing, and acquisition of *somatosensory* evoked responses is provided as a demonstration.

In the present studies, a DASH-16F data acquisition and control interface board, resident in an AT-386 IBM compatible computer, has been used under ASYST data acquisition and analysis software control. ASYST is a high level programming language designed for physiological data collection and processing.

3.2 POPULATION DISCHARGE (EXTRACELLULAR FIELD POTENTIAL) RECORDING

Brain slice preparations permit rather detailed investigations of neurones in a relatively undisturbed, but controlled environment. As awareness and memory are critically modified during anaesthesia, the study of the effects of anaesthetic agents on in vitro preparations of mammalian brain, especially cortex, is justified. The neocortical slice is also a highly useful medium for the investigation of focal and certain generalised seizure types (Connors, 1984), as the spontaneously occurring ictaform activity produced in Mg^{2+}-free medium is sensitive to inhibition by N-Methyl-D-Aspartate (NMDA) antagonists and clinical anticonvulsants.

Additionally, in order to assess the physiological and/or pathological consequences of excitatory amino acid receptor-mediated events, one must be able to obtain accurate and reproducible pharmacological data on a preparation which preserves as much of the tissue structure present in situ as

possible, and which permits quantitative comparison amongst animals subjected to different treatments. Grease-Gap techniques adapted from the cortical wedge preparation demonstrate stable activity for long periods of time (Mody et al., 1987) and allow quantitative pharmacological studies to be performed (Martin et al., 1989). Extracellular recordings using a grease-gap in vitro model suggest the simultaneous discharge of a large population of neurones (Merlin and Wong, 1993). Although spike trains do not provide direct information about cellular ionic mechanisms, they nonetheless reflect the principal traffic in interneuronal network communication (Rhoades and Gross, 1994), and presumably underlie the field potentials recorded in such preparations.

3.3 A GREASE-GAP RECORDING MODEL

Figure 3.1 is a simplified block diagram of the complete grease-gap recording and processing system.

3.3.1 Experimental Procedures

Rats of either sex weighing 230-250 grams were stunned, immediately decapitated, and the brain quickly removed into ice-cold artificial cerebro-spinal fluid (ACSF); composed in mM of, NaCl 118, KCl 2.15, KH_2PO_4 1.175, $NaHCO_3$ 25, D-glucose 11, $CaCl_2,6H_2O$ 2, $MgSO_4,7H_2O$ 2, and equilibrated with 5% CO_2

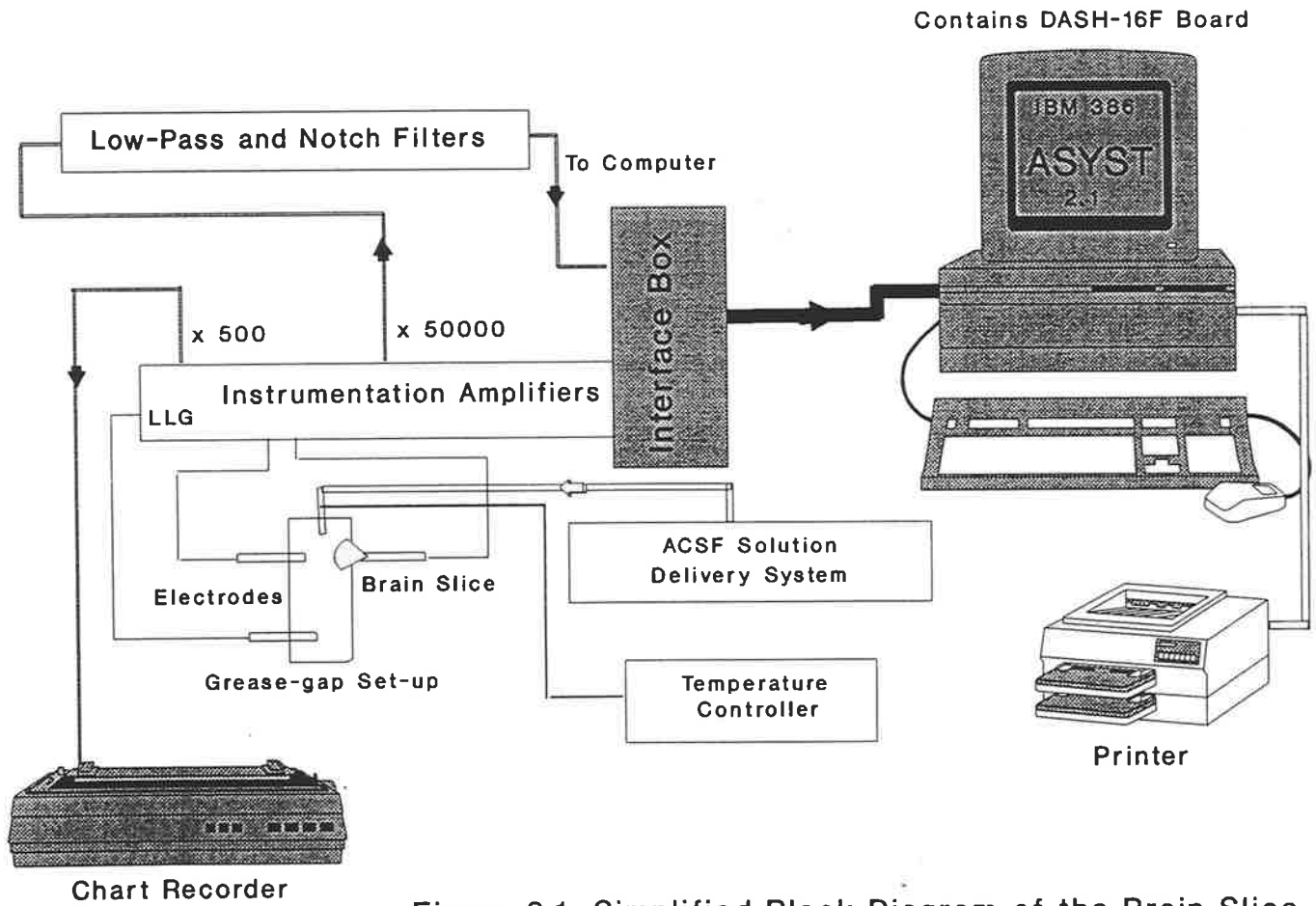

Figure 3.1 Simplified Block Diagram of the Brain Slice Data Acquisition and Processing System

in O_2 to maintain a pH of 7.3. After being allowed to cool in the ACSF for 30 minutes, the brain was placed on a glass surface on ice with the ventral surface uppermost, and two coronal sections were made. The first at a level just behind the optic chiasm, and the second 4-5 mm caudally at approximately the level of the mammilary bodies. The caudal surface of the resulting tissue block was fixed with cyanoacrylate to the prespex carrier block of a vibrating microtome (Lancer, series 1000), and kept in ice cold ACSF. 0.4-0.5 mm slices were then cut and placed in chilled ACSF solution. These slices were bisected at the midline, and further cut to produce wedge-shaped slices of cingulate cortex, or frontal cortex, and corpus callosum (see figure 3.2).

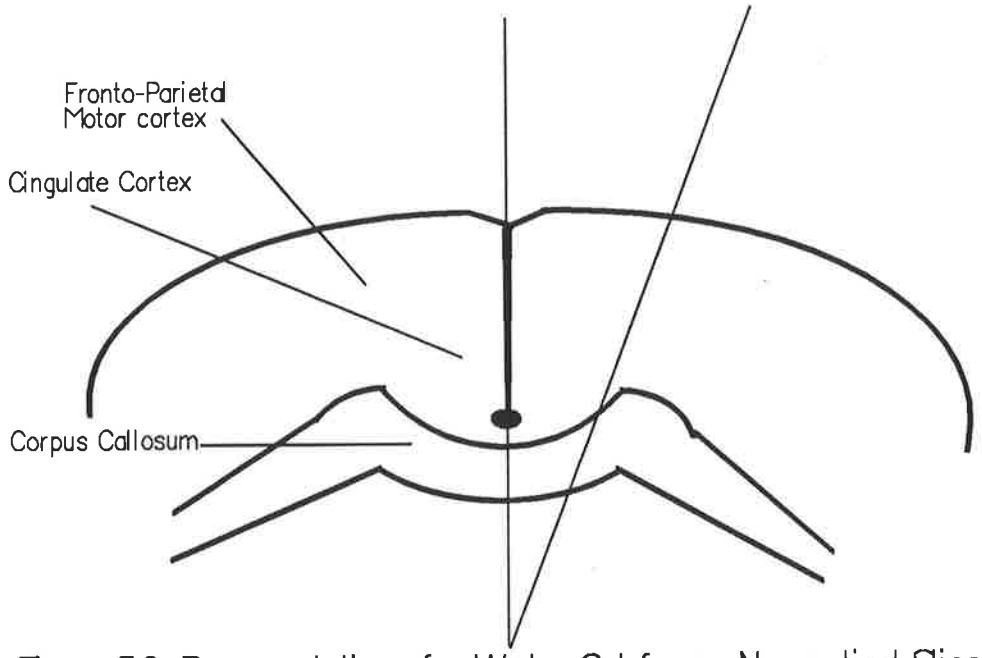

Figure 3.2 Representation of a Wedge Cut from a Neocortical Slice

These wedges were transferred to nylon mesh in a chamber for 1-2 hours of incubation in oxygenated ACSF which was allowed

to reach room temperature. A wedge was then placed on a nappy-liner covered prespex slope of a grease-gap recording system (Wheatley, 1986; Blake et al., 1988), adapted from Harrison and Simmonds (1985) and Horne et al. (1986). Most of the cortical grey matter rested on the nappy-liner of the slope, covered with a thin strip of nappy-liner, and irrigated with ACSF solution in the vicinity of one recording electrode. The ventral margin passed over a small (< 1 mm) grease-gap to the side of the slope so that the corpus callosum (and a small amount of gray matter) lay upon the cloth wick of another pick-up electrode, surrounded by the grease, which was a mixture of equal proportion of Vaseline and Paraffin oil, to provide insulation. Differential potentials between the two electrodes (Williams et al., 1988) were monitored by chlorided silver (99.99% pure) electrodes via a saline bridge, using an instrumentation amplifier, with an earth electrode placed further down the solution soaked, nappy-liner-covered slope.

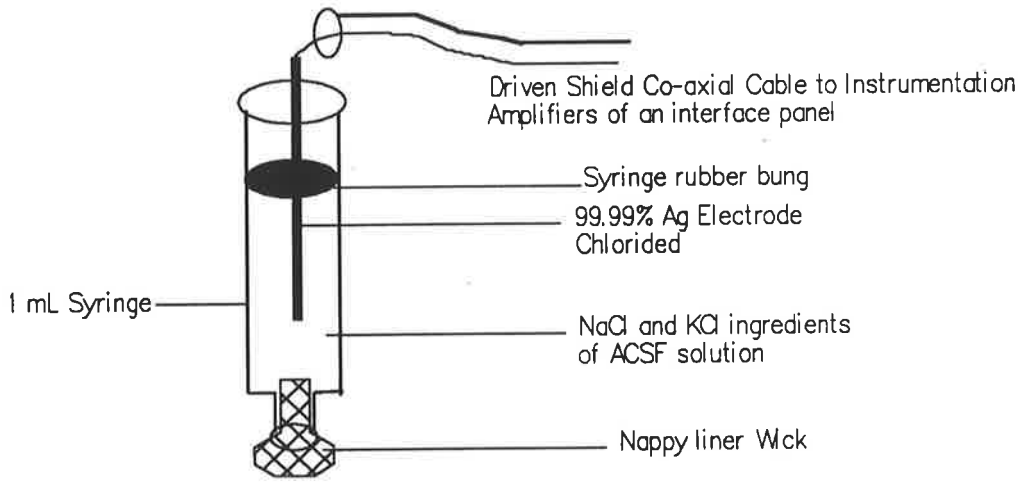

Figure 3.3 Details of a Recording Electrode

Figure 3.3 shows the recording electrode design, assembled in-house, and figure 3.4 shows the grease-gap set-up employed in this research project. The figure in appendix A.3.1 represents a simple electrical circuit for chloriding the silver rods.

Williams et al. (1988) give an equivalent circuit of the neocortical slice preparation, originally described using rat tissue by Harrison and Simmonds (1985) and subsequently for mouse brain by Burton et al. (1988).

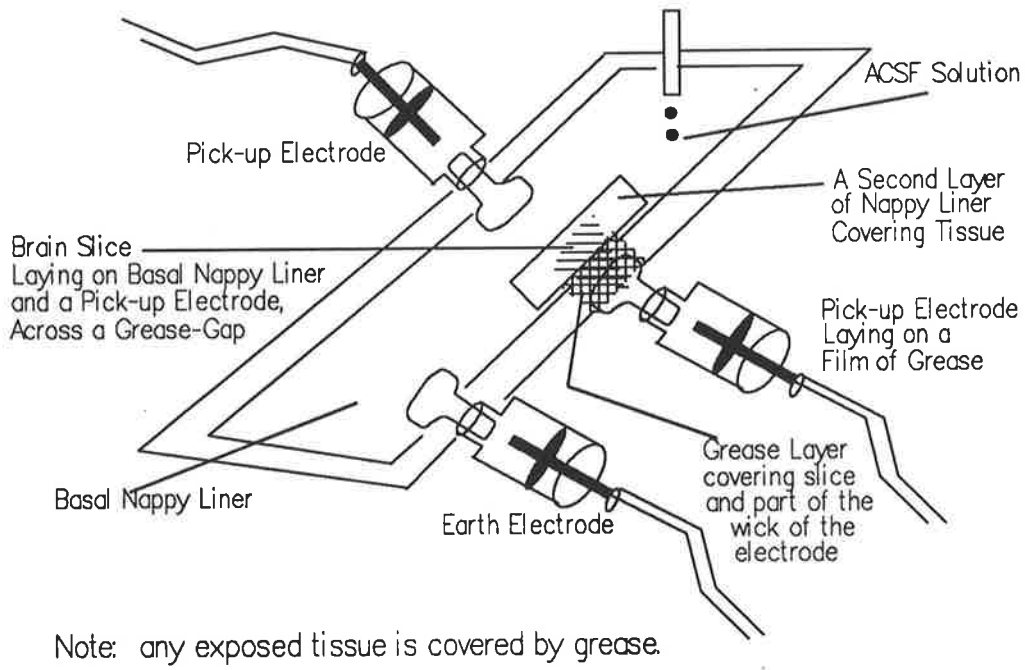

Figure 3.4 Details of the Grease-Gap Set-up Used in Recording Discharges from Neocortical Slices

Figure 3.5 represents the electrical equivalent circuit of a single pyramidal cell, but the same equivalent circuit pertains to many cells with similar properties in parallel. Furthermore, the cable properties of the axons do not affect the form of equations but only the values of the parameters R_i and g_a. There are two current pathways connecting the soma and axon chambers, the first through the axons of the pyramidal

cells which enter the corpus callosum (R_i) and the second an extracellular pathway limited by the grease seal (R_w). All voltage measurements are made in the steady state, so that the membrane capacitance is ignored. The measured D.C. voltage (V) between the two compartments depends upon the efficiency of the seal and upon the conductance of the ionic pathway opened by receptor activation, or on synchronous discharging of the relevant neurones. Subscript r denotes a receptor-activated channel.

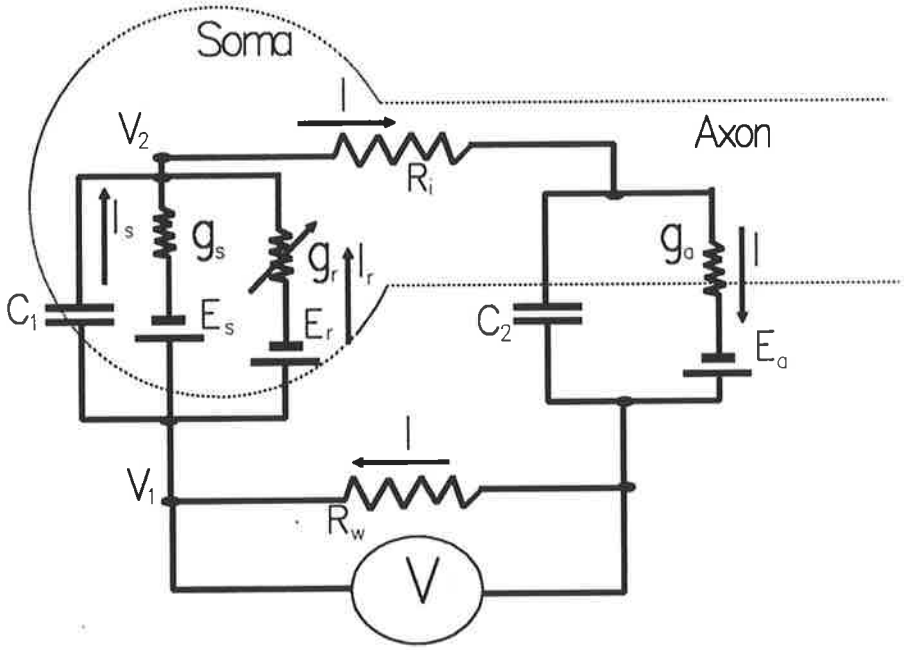

Figure 3.5 Electrical Equivalent Circuit of Cortical Slice Preparation

After placement, the slice was superfused with oxygenated ACSF solution at a rate of 1.2 $mlmin^{-1}$ for 20 minutes during which the temperature was slowly raised from room temperature to 29 °C. This temperature was maintained by a feedback temperature controller, which operates by controlling the current flow through insulated resistance wire wrapped around a stainless steel syringe needle through which the solution drips onto the

nappy-liner-covered slope above the level of the slices. The annotated temperature controller circuit diagram is given in appendix A.3.2. Once stabilised, the solution was changed to Mg^{++} free ACSF to unmask NMDA induced responses, leading to spontaneous discharges (Harrison and Simmonds, 1985; Horne et al., 1986), most often with after-activity on the falling phase.

Discharges were inputted to an instrumentation amplifier through driven-shield cables. Signals were amplified 500 times and fed to a chart recorder, and normally amplified a further 100 times through another instrumentation amplifier and fed into a 12th-order switch-capacitor Butterworth Low-pass filter with the adjustable 3-dB cut-off frequency set to 45 Hz. The low-pass filter was preceded by an active 2nd order analogue low-pass filter, with the 3-dB cut-off frequency of 150 Hz which prevents frequency aliasing, and followed by a passive low-pass filter with the 3-dB cut-off frequency of 500 Hz to remove the digitising effect on the filtered output waveform. Note that the cut-off frequencies of the associated analogue filters need to be correspondingly modified if the cut-off frequency of the main 12th order low-pass filter is drastically changed. Although a 4th-order Elliptic switch-capacitor 50 Hz Notch filter, with the associated anti-digitising filter, was initially incorporated, it was never found necessary. Details of the filter circuits, which were designed and developed for this project, as well as an explanatory block diagram are attached in appendix A.3.3.

The filtered signal passed through an interface box to be digitised using a DASH-16F data acquisition and control interface board, resident in an AT-386 IBM compatible computer, under ASYST data acquisition and analysis software control.

The temperature controller and filters share a specifically designed and developed regulated power supply.

3.3.2 An Introduction to ASYST Version 2.1

ASYST (amongst a family of packages ASYST, ASYSTANT + and ASYSTANT GPIB) produced by Macmillan Software Company is a high level language used in data acquisition, data analysis, data presentation and data storage. Functions such as storage and retrieval of files, data plotting, complex numerical analysis and other useful features are applied through the use of a command Language. Data can be acquired from a variety of A/D boards, from RS-232 serial communications port and from boards which can handle digital data in IEEE-488 format (also known as GP-IB or HP-IB after Hewlett-Packard interpretation of the IEEE-488). Such a form of communication allows data transfer rates of over 400 Kbits per second. Simultaneous data acquisition and control functions can be made through a combination of RS-232, A/D, Digital Input/Output (DIO) and GP-IB boards. Additionally, data can be imported or exported to a variety of popular packages such as DBASE and LOTUS-123.

An ASYST programmer uses ASYST words to build other words, and these new words (c.f. procedures or functions in other languages) can be linked into a final programme. Each word can be debugged and tested. ASYST has an Interactive mode of operation for immediate execution of short words and word clusters. A Compiled programme converts such words into a more efficient form of execution.

ASYST is divided into four modules. The base system module provides graphics capabilities, statistics, and a system for programming. The analysis module includes regression, curve fitting, spectral analysis and fast Fourier transform (FFT). The data acquisition module has facilities for A/D sampling, digital-to-analogue (D/A) output, DIO and simple timing of external events. The GPIB/IEEE-488 interface module interfaces ASYST to over 10000 GPIB-compatible instruments.

The system allows the environment to be customised for particular applications by the use of overlays that perform specific functions to save valuable memory. ASYST version 2.1 is configured through a series of screens to set up the overlay structure, graphics system, hardware configurations and acquisition details.

Barton (1991) classifies ASYST amongst many A/D data acquisition software packages as Difficult, but Flexible and Fast.

3.3.3 Metrabyte DASH-16F Board

This is an Analogue/Digital Input/Output board, produced by MetraByte Corporation, which is installed internally in an expansion slot of an IBM PC/AT (or a bus compatible) computer. The conversion time for the A/D converter is 8 µs which allows a throughput rate of 100 KHz to be achieved in DMA mode of operation. Some features of the DASH-16F board are listed below (see the DASH-16F manual for additional features):

* Higher cost, higher speed
* 16 single-ended or 8 differential input channels
* Gain is hardware selectable
* 8 digital input/output lines
* 2 analogue output (12 bit D/A converter)
* 2 counter/timers
* A pacer clock

In order to use the DASH-16F board with ASYST, the following parameters were selected by setting the appropriate switches on the board:

Number of channels:	16
Base address:	300 Hex
Polarity:	bipolar
Input voltage range (gain):	±10 V
DMA setting:	on 1 not 3 (only if DMA is used)

3.3.4 Interface Circuit Box

The interface circuit, which was designed and built for this project, interfaces the DASH-16F board with the outside world. It is connected to the 37 pin male "D" input/output connector of the DASH-16F board via a ribbon cable. As well as straight through BNC connectors for multiple input-channel communication, the interface box has 3 instrumentation amplifiers which can be used to directly interface to the recording electrodes via special driven-shielded cables in differential mode of operation. The interface box allows communication through 16 single-ended or 8 differential input channels. The schematic drawing in appendix A.3.4 shows how 3 instrumentation amplifiers and other direct channels are connected to the DASH-16F board.

Additionally, the interface box provides an analogue stimulator output signal and contains a circuit which enables the A/D converter to be triggered externally. These latter components were used in whole-animal experimentation, described in the next chapter.

As channels 0 to 2 are allocated as inputs to the instrumentation amplifiers, channel 3 was normally used for single-channel data acquisition i.e. the filtered signal was fed to pin 34 (CH3 HI IN) of the DASH-16F input/output connector through the interface box.

It should be noted well that, in order to run ASYST,

pins 24 (IP2 / CTR0 GATE) and 25 (IP0 / TRIG0) of the DASH-16F interface connector need to be connected together. In order to use D/A outputs, pins 8 (VREF -5 V) and 10 (D/A 0 REF IN) need to be connected together.

3.3.4.1 Instrumentation amplifiers

The interface box contains 3 identical instrumentation amplifiers (Analog Devices AD625) constituting Channel 0 (CH0), CH1 and CH2. An instrumentation amplifier provides:

* High input impedance (input impedance of AD625 exceeds 1 GΩ)

* High Common Mode Rejection Ratio (CMRR)

$$CMRR = 20\log_{10}\left(\frac{\text{Differential gain}}{\text{Common Mode gain}}\right)$$

Common mode signal is not amplified by the gain stage. High CMRR rejects 50 Hz as a common mode signal.

* High gain

Each amplifier has 2 BNC differential input Sockets shown as I/P+ and I/P-, the outer shields of which are driven by a 741 unity gain buffer. The driven-shield arrangement is recommended for reduction of transmission line capacitive effects over long cable distances. A gain switch provides

amplification in the range of 2 to 2000. Two banana sockets permit external monitoring of the output of each instrumentation amplifier, allow for amplifier cascading and access to LLG which is the DASH-16F board LLG. A D.C. offset adjustment facility for each amplifier, a necessary feature in grease-gap recording, is provided by a TL084 (1/4) operational amplifier. When not in use, the instrumentation amplifier inputs and the offset amplifier inputs are set to LLG. Circuit diagram of one of the instrumentation amplifiers (channel 0) is shown in appendix A.3.5.

3.3.4.2 Earthing and power supply arrangements for the interface box

(i) Chassis Ground: This is connected to Mains earth. As shown in appendix A.3.5, the guard drive is connected to the body of the set/use switch which is isolated from chassis. The guard drive voltage is one diode voltage drop above the actual common mode voltage.

(ii) Power (Digital) Ground: This is taken from the 0 V rail of the DASH-16F board 5 V supply through pin 7 of the 37 way connector.

(iii) Low Level Ground: The 0 V rail of an external ±15 V power supply is common with the 0 V of a ±7.5 V regulated power supply internal to the interface box. The 0 V is taken to low level ground (LLG). The ±7.5 V

supplies power to the instrumentation amplifiers and associated operational amplifiers. LLG carries signal currents (a few mA) and is the ground reference for all analogue inputs and A/D channels. The instrumentation amplifiers outputs are with respect to the LLG. The shields of all straight through inputs are also connected to the LLG. A circuit diagram showing the LLG rail is attached in appendix A.3.6.

Acquiring discharges in this neocortical wedge model presented a number of problems; spontaneous cortical discharges occur at random, usually ranging from 1 every few minutes to 1 every 20 seconds, and the baseline shows drift. Additionally, agents such as some K^+ channel blockers, and GABA agonists, cause a large depolarization, on top of which such discharges are superimposed.

ASYST software was developed by the author to acquire data at a variable sampling rate frame-by-frame and perform a series of data analysis functions, such as on-line low-pass filtering, off-line FFT and phase-plane plotting. The programme for the acquisition and processing of discharges with after-activity from neocortical slices is listed in appendix A.3.7. Many examples of the acquired and analysed discharges will be presented in chapters 5, 6 and 7. The software is produced in modules and is menu-driven through the use of function keys. Any combination or permutation of various functions is possible by rearranging the modules. For example, relevant sections of the programme can easily be rearranged to perform off-line filtering or on-line FFT, or to

perform an on-line sequence for the phase-plane plot of a low-pass filtered signal.

CHAPTER 4

EVOKED POTENTIAL RECORDING FROM RABBIT BRAIN

The aim of this part of research has been to investigate the modification of evoked potentials recorded from brain structures in rabbits under general anaesthetic. In this chapter, a computer based data acquisition and processing system for recording evoked potentials from rabbit brain is introduced. The procedure used for rabbit anaesthesia is discussed and examples of recorded potentials are presented. Unlike discharges from cortical slices, these responses were averaged to improve their signal-to-noise (S/N) ratio.

4.1 AN INTRODUCTION TO WHOLE-ANIMAL DATA ACQUISITION AND PROCESSING SYSTEM

Means by which an experimenter can acquire, display and process electrical activities in the nervous system are integral parts of an electrophysiological set-up. Permanent and cheap storage of results which are easily accessible is also desirable. Originally, a camera was used to photograph waveforms displayed on an oscilloscope. This arrangement produced a one-off trace and did not allow for on-line manipulation or post-processing of the original data. It was also unsuitable for signals with poor S/N ratio which required averaging. Cost of film purchase and processing was also a consideration. The computer of average transients which allowed averaging, and addition or subtraction of responses became available in 1968, providing a range of processing

routines. The next stage was the appearance of expensive and dedicated microcomputers during the 1970s.

Limited resolution of analogue FM tape recording, as well as problems mentioned above, makes the FM recording technique unsuitable for recording smaller signals from some regions of brain with good S/N. Digital recording technique using pulse code modulation (PCM) provides S/N ratio of 80 dB or more compared to 50 dB achieved with the analogue method. PCM digital recording may be the most suitable technique for continuous electrophysiological data recording.

Stand-alone oscilloscopes (increasingly digital) have become available that are capable of storing, printing and performing some limited on-line signal processing, such as signal averaging. However their storage capacity is likely to be limited and non-permanent, their signal analysis capability is limited and they are often quite expensive.

As in chapter 3 where the method for recording responses from neocortical slices is discussed, a PC based system for acquiring and processing evoked potentials from rabbit brain was developed using the available commercial devices, and adding the required components as necessary. The block diagram of the system is shown in figure 4.1.

The relevant DASH-16F board, and ASYST data acquisition and analysis software, have been introduced in chapter 3. Details of the interface box, including the instrumentation amplifiers was also discussed in the previous chapter. However, the

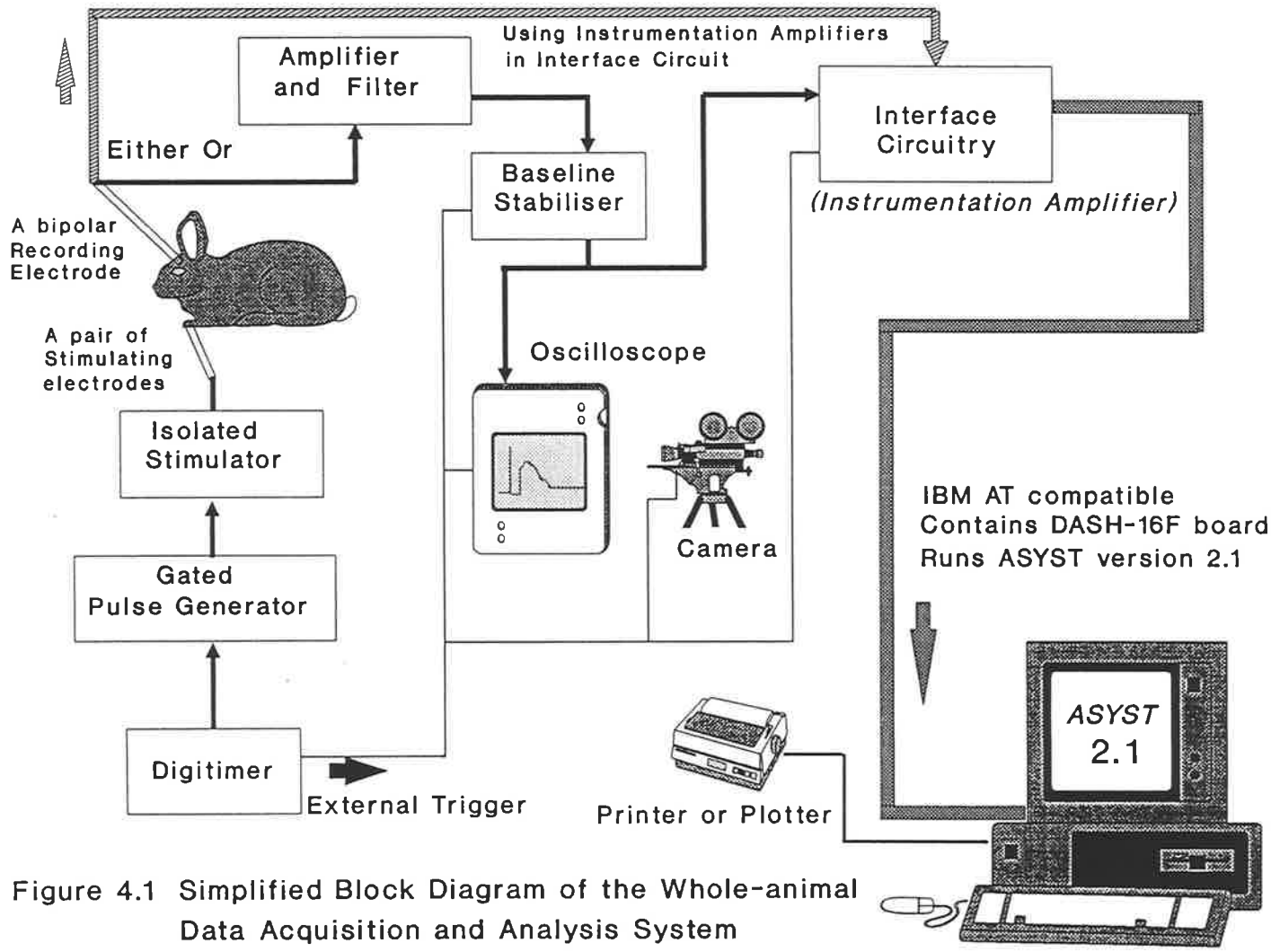

Figure 4.1 Simplified Block Diagram of the Whole-animal Data Acquisition and Analysis System

interface box contains circuits for analogue stimulator output and A/D external trigger input, with the latter being used in this section of the project.

4.1.1 Analogue Stimulator Output

As shown in appendix A.4.1, the analogue stimulus trigger output provides an external stimulus with respect to the LLG. The non-inverting input of the operational amplifier is connected to pin 9 of the DASH-16F board which is the D/A converter channel 0 output. The gain of the amplifier is set to unity and offset adjustment is provided through the inverting input. The output voltage of stimulator is 6.87 V with respect to the LLG.

4.1.2 Analogue-to-Digital External Trigger Input

The input for triggering the A/D on the interface box is arranged with respect to power ground. Power (digital) ground is the noisy ground carrying all digital signals and power supply currents. The circuit diagram of the A/D trigger circuit is shown in appendix A.4.2. Trigger pulse amplitude 5 to 40 V of either polarity (minimum pulse width of approximately 100 *ns*) can be applied to the input, which is connected to pin 25 (IP0 / TRIG0) of the DASH-16F board.

Automatic resetting after approximately 1 or 10 seconds, as well as manual resetting, is provided.

The +5 V supply voltage for the D-type flip-flop (see appendix A.4.2) is taken from the DASH-16F board and is with respect to the power ground. The outer shell of the A/D trigger BNC socket, pin 7 of the flip-flop, and the reset switch earth are also at the power ground level. The 5 V buffered pulse output is with respect to the LLG. The power ground and the LLG are connected together inside the DASH-16F board.

4.1.3 Digitimer

This instrument, which is produced by Devices (a U.K. manufacturer), through a crystal clock provides:

(i) An external trigger pulse at a fixed time interval in order to synchronise the operation of other components in the system, as shown in figure 4.1,

(ii) A single stimulus pulse of defined duration as the input to the gated pulse generator; or, originate 2 consecutive stimulus pulses of defined durations with a certain time interval between them to act as a combined input to the gated pulse generator.

The pulses are negative with approximately -12 V amplitude.

4.1.4 Gated Pulse Generator

This instrument, which is also produced by Devices, generates a single pulse or a train (burst) of pulses which are sent to the Isolated Stimulator as shown in figure 4.1. The instrument generates a −12 V, 0.1 ms pulse when set to Single trigger mode. This pulse is coincidental with the negative going leading edge of the input pulse i.e. the A or B outputs of the Digitimer. Output C results in generation of 2 pulses separated in time as dictated by the values of the Digitimer counters. In Gated mode of operation, for a set gating input pulse duration, a variable number of pulses in a fixed duration train are obtained by the counter settings. The duration of a pulse train is equal to the gating pulse duration from A or B, as determined by Digitimer counters. In the case of a combined C output, 2 pulse trains equal in duration to the 2 Digitimer counter settings are obtained.

For the *in vivo* study reported here, beside using pulse outputs (isolated or combined as necessary), trains containing 5 or 6 pulses with the approximate burst duration of 20 ms, and inter-burst duration of 40 ms were also obtained.

4.1.5 Isolated Stimulator

This instrument is also manufactured by Devices. It is battery operated and generates one or more stimulus pulses. The pulse amplitude varies between 0 and 90 V and its duration

is also controllable. The device is usually triggered externally by the gated pulse generator. Facilities for single shot and stimulus pulse polarity reversal also exist. With a gated setting, the number of pulses in a stimulator output train depends upon the isolated stimulator frequency and the duration of the train as set by the output of the gated pulse generator.

In the course of experiments reported in this chapter, stimuli were a single 0.1 ms pulse or paired pulses of the same duration at intervals set by the Digitimer. Amplitude of the pulses usually ranged between 20 and 90 V according to the region being stimulated, depth of anaesthesia, type of stimulating and recording electrodes in use, and other experimental variables.

4.1.6 Stimulating Electrodes

A pair of hollow stainless steel electrodes fashioned from hypodermic needles (2.5 cm in length and 0.0725 cm in diameter), with the shank covered in epoxy resin but tips exposed for about 1 mm, mounted on a piece of perspex were inserted through the skin to stimulate nerves transcutaneously in a rabbit shaven forelimb. Distance between the 2 electrodes was set to about 0.5 cm.

Ochs and Booker (1961), Akaishi et al. (1988), Legoratti-Sanchez (1989), Amri et al. (1990), Hamba et al. (1990), West

and Michael (1990), have each described their methods of constructing stimulating electrodes for electrophysiological research.

4.1.7 Recording Electrodes

The evoked potentials from the rabbit brain were picked up by a bipolar recording electrode. This was constructed from an approximate length of 10 cm hollow stainless steel tubing, 0.0725 cm or 0.04 cm in diameter. The tip was etched in a diluted HCl solution for a few minutes by passing current between the electrode tip and a carbon rod to remove any jagged metal (a few drops of paraffin floating on the surface of the acid solution prevented acid from splashing up). The tip was degreased with xylol after etching. Enamelled Teleconstan wire (34 swg) or enamelled Constantan wire (36 swg) was passed through the steel tubes, extending beyond the tip. The assembled electrode was held by a stereotaxic electrode holder, dipped into epoxy resin for insulation and slowly withdrawn to ensure an even coat. The coated electrode was baked to cure in an oven for ½ hour at 100 °C. It was baked for a further ½ hour at 170 °C after again being dipped in epoxy resin solution. At one end, excess inner wire was cut and tip and shank were bared of insulation under a microscope by a sharp blade to leave a tip-shank separation of 1 mm.

The inner cores of a pair of coaxial cables were soldered to the bipolar electrode at one end and attached to 3 mm banana

plugs at the other end (the sockets on an interconnection board accepted the 3 mm plugs). The outer shields of the cables were joined together and soldered to an earth pin. The electrical continuity of the assembled electrode was checked. The electrode was placed in a stereotaxic electrode carrier. It was inserted in rabbit brain to access structures according to stereotaxic coordinates calculated with reference to an atlas. Figure 4.2 shows the electrode configuration.

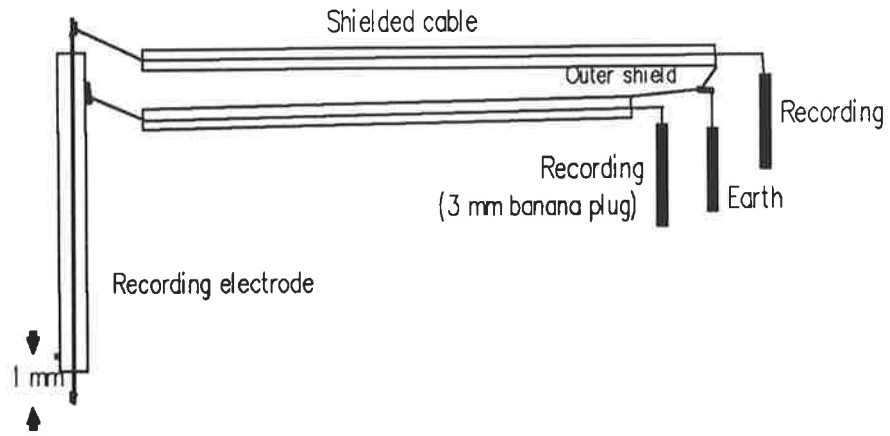

Figure 4.2 A Bipolar Electrode for Recording Evoked Potentials from Rabbit Brain

A variety of electrodes have been described for electrophysiological signal recording. Ochs and Booker (1961), Sander et al. (1986), Amri et al. (1990), Tsuruoka et al. (1990) used insulated steel wire, platinum glass-coated or tungsten microelectrodes in their applications.

Liebeskind and Mayer (1971) have described recording electrodes fashioned from teflon coated stainless steel wire for acute and chronic experiments, and also processes in making stimulating electrodes.

4.1.8 Amplifier and Filter

As shown in figure 4.1, differential signal from the recording electrode was fed to a Grass P511 AC preamplifier for filtering and amplification. Alternatively the signal could have been digitally filtered, using the ASYST software development system, and taken directly to one of the instrumentation amplifiers in the interface box through a pair of driven-shielded cables.

The Grass preamplifier accepts direct differential inputs from the recording electrode and performs 2 tasks. It band-pass filters the input signal prior to amplification. The grass P511 is an AC differential amplifier and should therefore reject any DC component in the physiological signal.

In recording evoked afferent responses from rabbit brain, a gain setting in the range of 2000 to 20000 was required to bring the signal level to Volts before digitisation. Lower and upper half-amplitude cut-off frequencies of 0.15 Hz and 10 KHz were usually selected for the band-pass filter.

4.1.9 Baseline Stabiliser

Low frequency DC voltage fluctuations can be removed by high-pass filtering. Analogue filtering however introduces time-delay errors and phase distortion. Digital filtering, on the other hand, is time consuming and introduces variable phase shifts which makes it inadequate for fast on-line processing.

Marion-Poll and Tobin (1991) describe the implementation of low-pass filtering and differentiation into a single linear stage referred to as a low-Pass filtered derivative, which is reported to be efficient and fast. Action potentials are detected by comparing the low-pass filtered first derivative of the signal with a preset threshold constant.

Stabilising the baseline following the AC preamplification stage, especially when recording smaller signals, was regarded as desirable. All stages in the preamplifier circuit except the final stage are AC coupled. The preceding band-pass filter with the lower cut-off frequency of 0.15 Hz (or higher) should have filtered any DC component prior to amplification.

Although the AD625 instrumentation amplifier inherently accommodates a degree of DC offset through a negative feedback control mechanism, a baseline stabilizer was designed and developed to remove any baseline DC offset at the beginning of each data acquisition frame. The circuit diagram of the baseline stabiliser is included in appendix A.4.3. The original design, published by Weinberg et al. (1985), was

modified so that the -12 V pulse from the Digitimer triggers the circuit in line with other elements in the data acquisition and analysis system.

Basically, each time sample and difference amplifier is triggered through a 555 timer, the voltage across the hold capacitor, V_{CH}, which is the DC offset voltage, is subtracted from the input voltage i.e. the baseline is reset to zero.

4.1.10 Data Acquisition and Analysis Software

As shown in figure 4.1. output signal from the baseline stabiliser is fed to the interface box. Channel 3 was used for single-channel data acquisition. The software was developed using ASYST version 2.1, and is enclosed in appendix A.4.4. The A/D is externally triggered by a pulse originating from the Digitimer, and the A/D board is initialised on entry to the acquisition routine. The programme acquires data frames with each external trigger and performs analysis functions such as averaging, and interacting between conditioning and test responses. The programme is menu-driven, and has been made into turnkey application for general users.

Action potential frequency content ranges from 10 Hz to 10 KHz. On the basis of Nyquist sampling theorem, in order to avoid aliasing, it is necessary to sample at least at twice the highest frequency component to reconstitute an original analogue signal from the sampled data. This could be

accomplished as the combination of DASH-16F hardware board and ASYST software allowed sampling at rates approaching 100 KHz, without the need to resort to the DMA mode of operation.

4.2. EVOKED POTENTIAL RECORDING FROM STRUCTURES IN RABBIT BRAIN

Our interest in neural mechanisms of anaesthesia encompasses analgesia. The mechanism for pain perception and modulation may occur in part through action on *raphe nuclei* and the associated *periaqueductual gray* (PAG), particularly in generating an aversive responses to noxious stimulation and in modulating the input interpreted as a painful experience. This proposed role in antinociception and analgesia has been investigated by Meller and Dennis (1986, 1990a, 1990b, 1991).

It is still unknown what aspect of brain function is involved in nociception or its modification by analgesic or anaesthetic agents. Evoked potential recording was undertaken with the aim of investigating the modification of potentials from brain structures by various anaesthetic and analgesic agents. In particular the form and extent of neural interactions between particular brain regions, and how the proposed neural circuits respond to various anaesthetic agents. It was deemed appropriate to investigate the electrical properties of the somaesthetic system, and record changes in electrical activity of the PAG as a result of stimulating those structures which send afferent projections to it. In this connection targeting

some midline *thalamic*, *hypothalamic* and *amygdaloid nuclei* as part of the *limbic* system was also considered.

However this aspect of the work was not pursued since baseline conditions proved impossible to assess and maintain or replicate between animals. Indeed such an in-depth investigation of the neural interactions between different brain regions in a given anaesthetised animals was impossible. It was most difficult to establish, amongst other factors, the depth of anaesthesia to make inferences as to how a given anaesthetic agent, or conversely electrical stimulation, might be affecting a particular region in the brain. Neither was it possible to know to what extent a particular region was under influence from many other brain regions in the *in vivo* preparations. Hence a switch was made to investigate the responsiveness of neocortical brain slices to neuroactive agents in a more controlled environment, which will be discussed in detail later. Meanwhile, experimental findings from whole animal experiments are reported. Some examples of evoked responses recorded from different afferent pathways are given, by way of illustration, but it is emphasised that this aspect was not pursued in depth.

4.2.1 General Anaesthesia

A number of different anaesthetic agents were tested in order to establish those suitable for work in the rabbit. The use of paralysing agents, such as D-tubocurarine or Flaxedil

as used by Ochs and Booker (1961) and Gallamine Triethiodide as used by Guilbaud (1981), was avoided for ethical reasons as such agents do not have analgesic effect, i.e. the animal feels the noxious stimuli, but is unable to protest. Indeed, the University of Adelaide Ethics Committee now prohibits such experiments under paralysing agents. Nembutal, Urethane, Dial, as well as mixtures of Dial plus Urethane, and α-Chloralose plus Urethane were tested as intravenous anaesthetic agents. Halothane was used as an inhalation anaesthetic in the course of this study.

* **Nembutal – Ceva (pentobarbitone sodium)** – 60 mg/ml saline. The recommended dose according to Barne and Eltherington (1966) is 30 mg/Kg intravenously.

Like thiopentone, barbitone and pentobarbitone are members of the barbiturate group of central nervous system depressants which have been in use since 1935 or earlier. Intravenous injection of pentobarbitone, which differs from thiopentone only in possessing an oxygen atom instead of sulphur attached to the ring and is less lipid-soluble, produces unconsciousness after 1-2 minutes delay. It does not cross the blood-brain barrier as efficiently as thiopentone which is more lipid soluble. Very little of these agents is metabolized in the first 10 minutes after injection. The long after-effect, associated with a slowly-declining plasma concentration, means that drowsiness and some degree of respiratory depression persist for about 2 hours. These agents are commonly used for induction but not maintenance of surgical anaesthesia. Ochs and Clark (1967), Besson et al.

(1971), Liebeskind and Mayer (1971), Sander et al. (1986) and Sanchez et al. (1988) report using this agent, mainly for anaesthesia in the rat.

At the neural level, barbiturates potentiate inhibition due to increased affinity of GABA and other ligands at the $GABA_A$-receptor complex (Franks and Lieb, 1994). Potentiation of GABA-induced responses is related to a prolongation of chloride channel open time (Keane and Biziere, 1987; Kerr and Ong, 1987). Pentobarbital prolongs the decay time constant of $GABA_A$-mediated spontaneous inhibitory postsynaptic currents (sIPSCs), and this effect is reportedly not blocked by intracellular administration of the Ca^{2+} chelator BAPTA or the Ca^{2+} release inhibitor dantrolene (Mody et al., 1991).

Barbiturates produce their main effect on GABA-mediated postsynaptic inhibition (Keane and Biziere, 1987). However they are well known to potentiate presynaptic inhibition due to GABA and, more importantly, some barbiturates at higher concentrations directly activate $GABA_A$-receptors, resulting in GABA-mimetic responses (Kerr and Ong, 1992).

The actions of barbiturates are in fact complex. For instance pentobarbitone blocks the open quisqualate/kainate receptor channel (Miljkovic and MacDonald, 1986). Indeed, barbiturates potentiate GABA-mediated inhibition, antagonise the quisqualate sub-type of glutamate receptors (Simmonds and Horne, 1987), and are likely to depress excitatory amino acid release (Kerr and Ong, 1992). Moreover, Carla and Moroni (1992) report that thiopentone antagonises both AMPA and NMDA

responses, whereas Franks and Lieb (1994) argue that conflicting evidence exists for barbiturate inhibition of sub-types of glutamate receptors, with NMDA currents being very insensitive to pentobarbital. Certainly barbiturates also reverse GABA antagonism at the picrotoxin site. The potentiation of GABA by barbiturates has a different structure-action profile from that found in the picrotoxin reversal property, and the two effects are probably independent (Kerr and Ong, 1992).

Despite similarities between barbiturates and benzodiazepines in potentiating the interaction of GABA with the $GABA_A$-receptor, their molecular mechanisms differ. Benzodiazepines increase the frequency of Cl^- channel opening, and unlike barbiturates, the effects of benzodiazepines on the GABA receptor does not require the presence of chloride ions. Subanaesthetic concentrations of pentobarbitone stimulate GABA-enhanced benzodiazepine binding, whereas anaesthetic concentrations enhance benzodiazepine binding in the absence of added GABA, an effect attributed to the GABA-mimetic actions of barbiturates in opening the cholride channel of the $GABA_A$-receptor complex (Keane and Biziere, 1987; Kerr and Ong, 1992).

* **Urethane (ethyl carbamate)** - 25% (25 g/100 ml saline). The anaesthetic dose is 1000 mg/Kg, usually injected intravenously in a divided dose.

Akaishi et al. (1988) report using urethane in the rat. It enhances presynaptic inhibition as well as producing the same

effect as barbiturates on GABA-mediated postsynaptic inhibition (Keane and Biziere, 1987).

* **Dial (diallyl barbituric acid)** - 0.25 g/5 ml saline. The recommended dose is 50 mg/Kg by intravenous injection.

Dial is a hypnotic and a sedative agent. Being a barbiturate derivative, similar neural mechanisms of action are presumably attributable to Dial.

* A mixture of **(a) Dial** (0.25 g/5 ml saline intravenously), and **(b) Urethane** (1.5 g/7.5 ml saline intraperitoneally). This is an effective experimental anaesthetic combination.

* A mixture of **(a) α-Chloralose** (2.5%) and **(b) Urethane** (25%):

(a) α-chloralose - 0.5 g in 20 ml water (0.025 g / ml dose), with the solution heated to 65 °C and a few drops of propylene glycol (propane-1, 2-diol) added to dissolve it, and
(b) urethane - 6.25 g in 25 ml saline. The final recommended dose for this mixture was 40 mg/Kg α-chloralose and 750 mg/Kg for urethane.

Sanders et al. (1980) used chloralose to anaesthetise rats and Hamba et al. (1990) used intraperitoneal injection of urethane (0.7 g/Kg) plus α-chloralose (65 mg/Kg) for rat.

Chloralose, like urethane, enhances presynaptic inhibition as well as producing the same effect as barbiturates on $GABA_A$-mediated postsynaptic inhibition, the effect of α-chloralose

being dependent on $GABA_A$-receptors. Overall, it markedly enhances GABAergic transmission and potentiates the synaptic effects of GABA at these receptors (Keane and Biziere, 1987; Kerr and Ong, 1992).

* A Mixture of 2% **Halothane** and Oxygen as an Inhalation Anaesthetic.

Halothane was introduced in 1957 as a halogenated, inhalational anaesthetics. Capable of rapidly attaining different levels of anaesthesia, being both non-irritant and pleasant to inhale, being non-explosive and easy to administer with a calibrated vaporiser, and having minimal side effects (Nunn et al., 1989), halothane was at one time the most widely used inhalation anaesthetic. It is non-explosive. Induction and recovery from it are faster than with ether, because of its relatively low solubility in blood. It is more potent than ether (minimum alveolar concentration of 0.8% compared with 1.9% for ether), but can easily produce respiratory and cardiovascular failure. Halothane also causes a fall in blood pressure. The main disadvantage of halothane is liver damage. About 25% of the absorbed dose of halothane undergoes metabolism.

Guilbaud et al. (1981) used a gaseous mixture of halothane, 0.5% in nitrous oxide (2/3) and oxygen (1/3) for a stable depth of anaesthesia in rat. Amri et al. (1990) used sodium thiopentane (25 mg/Kg) as a short-lasting anaesthetic agent followed by a mixture of air and 2% halothane to sustain anaesthesia.

At the cellular level, a major action of halothane is to enhance $GABA_A$ receptor-mediated inhibition leading to depressed neuronal excitability. In an earlier voltage clamp study, Gage and Robertson (1985) found that halothane prolonged the decay time constant of $GABA_A$-mediated sIPSCs. This effect is also seen by Mody et al. (1991) who propose that enhancement of $GABA_A$-mediated inhibition through release of intraneuronally stored Ca^{2+} is a fundamental action of halothane leading to CNS depression. Jones and Harrison (1993) however found that neither Ca^{2+}/EGTA nor BAPTA alone added to the postsynaptic recording pipette prevented the prolongation of IPSCs by halothane, suggesting that variations in intracellular calcium, $[Ca^{2+}]i$, are not required for the effect of halothane on the time course of IPSC. Also, it has been reported that halothane preferentially antagonises AMPA responses (Carla and Moroni, 1992).

4.3 EXPERIMENTAL PROCEDURE

Young male Rabbits were weighed to assess the required anaesthetic dose. The anaesthetic was injected slowly through the marginal ear vein by an intravenous catheter over a long time (½ hour or more). Supplementary doses of most anaesthetics were sometimes given intraperitoneally as required.

Originally, a series of experiments were carried out under urethane anaesthesia. It appeared that urethane markedly suppressed the activities of deeper structures in brain, making recording of evoked responses difficult. A mixture of α-chloralose and urethane, as described above, was then used with better success. Also a gaseous mixture of 2% halothane (fluothane, by ICI Australia) and oxygen was often given, for maintaining anaesthesia.

The head of the anaesthetised rabbit was supported by a clamping device which holds the head stable by counter pressure between the upper molars and orbital bones. The clamping device was attached to a stereotaxic frame. Some Xylocaine, a local anaesthetic, was injected to the pressure points of the facial area to relieve discomfort from the clamping device. Before surgery the depth of anaesthesia was checked by corneal reflex and flexor withdrawal response to noxious stimuli, such as pinching a forelimb.

After removing hair from the scalp, the skin was incised, and craniotomy was performed to expose the brain, by drilling through the skull between *bregma* (ß) and *lamda* (*l*). Bone from both sides of the midline (mainly opposite side to the limb being stimulated) was removed. Extra bone was removed with a pair of Ronguer bone clippers. Care was taken in removing *periostium* and *dura matter* not to rupture the central sinus. Gelfoam was sometimes applied to promote blood clotting. The brain was kept moist with application of paraffin oil over its surface. Bone wax was also used to stop any bleeding from bones. A tracheal cannula was placed to ensure free air flow,

and connected to a ventilator, in case breathing problems developed. After placing the tracheal cannula, a narrow cannula was inserted in the jugular vein so that anaesthetic agents could be administered.

The central sinus was used as the midline in a 3-dimensional stereotaxic coordinate measurement. Coordinates for ß and *l* (or any other marker) were registered as references, prior to electrode penetration. Anterior/posterior with reference to ß, lateral to left/right of the midline, and depth reading on and below the brain surface provided the 3 coordinate measurements registered during each experiment. 'P' represents posterior with reference to ß, 'L' represents lateral to the midline and 'H' represents the distance below the brain surface. Two different stereotaxic atlases for rabbit brain were used. Firstly, Meller's atlas (1987) for which the rabbit head was slightly tilted, with ß 7 mm above *l*, and the ß to *l* distance being 18 mm. In Meller's atlas, a vertical electrode penetrates plane to the aqueduct as it descends through the brain. Secondly, Girgis and Shih-Chang's atlas (1981) for which the longitudinal axis of the brain was assumed to be plane to a true coronal section of the forebrain. In lowering the recording electrode through the brain, care was taken not to rupture the central sinus vein.

The rabbit body temperature (37 °C) was maintained by a feedback temperature-controlled blanket. These experiments were performed in a partially shielded Faraday cage.

4.3.1 Perfusion and Sectioning

In order to verify the position of recording electrode in the brain, and confirm the origin of responses from particular brain nuclei, the brain was perfused at the end of each experiment, after giving the animal a lethal dose of an intravenous anaesthetic.

The chest was opened in midline through the abdomen. The ribs were cut away, half-way through the rib cage, in order to obtain a window for access to the heart. The descending aorta was clamped with a pair of artery forceps to limit the amount of body tissue perfused. The *pericardium* was removed. The left ventricle *myocardium* was stabbed with a pair of fine scissors to admit a cannula filled with physiological saline (154 mM), and the right atrium was opened to release any excess fluid.

Transcardiac perfusion was performed with a prefixation rinse of about 500 ml 0.9% saline solution, or a 0.067 M phosphate buffer solution with pH 7.4, until the outcoming fluid was fairly clear. This was followed by perfusing 1 l solution of 10% phosphate-buffered formalin at room temperature and sometimes was continued by 500 ml 10% sucrose in phosphate buffer solution.

The brain including part of the upper spinal cord was removed and stored in 30% sucrose in phosphate buffer so that ice crystals would not damage the tissue during sectioning by a freezing microtome, using 'dry-ice' (solid CO_2) and 70%

alcohol which formed a euthetic mixture. 50 μm frozen sections were collected in a 0.1 M phosphate buffer solution.

Sections were mounted on gelatine-subbed slides, air dried, and stained with a Nissl cytoplasmic stain, in order to visualize the nerve cells in various regions. After staining, sections were dehydrated in graded alcohol solutions (70%, 95% and 100%) and then cleared with xylene before being coverslipped using Fluoromount (Gurr).

The sugar solution was not required for perfusion and storage if paraffin sections were to be obtained using a microtome. In this case slides were coated with egg albumin instead of gelatine solution. Alternatively, for some fluorescent substances used in tracing experiments, an air-dried slide was coated with 10% glycerine, coverslipped and sealed round the edges with nail polish.

4.4 RESULTS AND DISCUSSION

In the experiments described below, rabbits were induced with a mixture of urethane and α-chloralose and maintained by halothane using a vaporiser, in accordance with the dosages of anaesthetic agents quoted earlier. In considering the following results it should be noted that, unless otherwise stated,

(a) the lower cut-off frequency for the band-pass filter

associated with the preamplifier was set to 0.15 Hz and the upper cut-off frequency was set to 10 KHz for all records presented,

(b) the preamplified amplitude of a signal is obtainable by dividing the displayed voltage by the amplifier gain,

(c) a single stimulus pulse at 40 ms intervals is applied through the gated pulse generator to a forelimb,

(d) where presented, the stereotaxic coordinates are based on the atlas by Girgis and Shin-Chang (1981).

Figures 4.3 and 4.4. show interaction between responses to paired stimuli to the same site (a forelimb), recorded from the rabbit cortex (recording positive up). Figure 4.3 shows cortical potentials generated from the contra-lateral forelimb somatosensory area of the cortex, approximately 1 mm below the brain surface. stimuli 25 V, 0.1 ms were applied. The onset delay for the first stimulus, referred to as the conditioner, was 20 ms. In figure 4.4 responses recorded from the somatosensory cortex, approximately 3 mm below the brain surface, again in response to contra-lateral forelimb stimulation. The stimulus artifacts are clearly seen with these responses. The bottom trace in both figures show a superimposition of conditioner-test complex, test response, and the difference waveforms.

Response interactions are frequently performed to confirm the polysynaptic nature of pathways and establish their branching and interconnections, as was well demonstrated by Ochs and Booker (1961) and Ochs and Clark (1967). Such interaction studies, sometimes referred to as collision tests, are used to

confirm axonal divergence, or the convergence of neuronal projections onto a particular site or pathway. More commonly, the tests are used to identify whether a response is antidromic, where antidromic and orthodromic impulses are made to collide. Antidromic signals are generally recognised as those having a constant latency and are capable of following a high frequency stimulation.

It can also clearly be seen from the figures 4.3 and 4.4 that a conditioning response, preceding the test response by 40 ms has resulted in 80% diminution of the latter, indicating an inhibitory interaction. When such paired pulses are applied to the peripheral stimulating sites, the amplitude of the cortical potential evoked by the test stimulus is depressed over a range of stimulus intervals, the depression being largely due to presynaptic inhibition generated by the conditioning response. Synaptic transmission can thus be blocked by stimuli delivered in quick succession. The degree of blocking induced by repetitive stimulation seems to be directly related to the number of synapses involved i.e. more blocking reflects a polysynaptic pathway, presumably because inhibitory interactions can occur at each synaptic relay.

High cortical signal to noise discrimination of cortical responses can be achieved with a moderate number of averaging (20 to 50). Under the experimental conditions, the cortical potentials had a latency of 10–15 ms, and a duration of 30–40 ms, whilst the peak amplitude of such signals ranged from 75 μV to 250 μV. A high S/N ratio indicates that cortical neurones are well synchronised, and the pathways very

responsive to external stimulation, probably reflecting transmission in the dorsal column, medial lemniscus and ventral posterior thalamus, projecting to the cortex.

Polysynaptic afferent pathways appeared not only more easily depressed by paired pulse stimulation, but also more sensitive to anaesthetic agents. One approach that could be used in such studies would be to examine the stimulus response properties of these potentials over a range of inter-stimulus intervals, in the presence of increasing concentrations of an anaesthetic agent. However, the problem of shift in response baseline over the periods of averaging, due to the pharmacokinetics of anaesthetic agents *in vivo*, renders interpretation of such studies very difficult, and it was considered unproductive to pursue this problem further. For this reason no detailed studies of interactions were made, since the isolated cortex was clearly a more productive and manageable preparation.

One afferent pathway that is clearly polysynaptic is located in the periaqueductual gray region, an area surrounding the *aqueduct of the midbrain*. The PAG is implicated in a number of roles associated somaesthesia, including analgesia, of particular interest in this project. Figure 4.5 shows a small, noisy signal of 10 µV peak amplitude, 15 ms latency and 40 ms duration, recorded from PAG in response to contra-lateral forelimb stimulation. By comparison with figure 4.6, taken from the medial lemniscus with only one relay, the PAG response has a markedly delayed onset, a slower risetime and a longer duration. The delayed onset could arise from the accumulated synaptic delays of a series of synapses along the

ascending pathway, which would also contribute to the prolonged risetime and duration of the response. However the smaller diameter of the fibres reaching PAG would also contribute to these characteristics of the response.

In figure 4.6, the upper trace shows a response recorded from the rabbit medial lemniscus (ML) at the level of superior colleculus. The medial lemniscus is a band of white fibres, which originates from the *dorsal column nuclei* of the spinal cord, and contains axons that convey impulses for fine touch, proprioception and vibration, running through the *medulla*, *pons* and *midbrain* to reach the ventral posterior thalamus. In general, signals from the ML were found to be relatively noisy, requiring a higher number of averaging to achieve a good S/N ratio. They had peak amplitude in the range of 30 to 120 μV, a mean latency period of 5 ms, and their duration varied between 8 and 20 ms.

The lower trace in figure 4.6 shows how interacting two identical responses resulted in approximately 33% diminution of the second signal. The responses show the characteristic short latency (5 ms), abrupt rising phase, and a period of secondary discharge on the falling phase of the response. The latter was, to some extent, obscured by the use of averaging, since the discharge was asynchronous. The short latency is due to a single relay and the large fibre size of the peripheral and central components of the pathway.

Figure 4.7 again shows the effect of interacting conditioner and test signals from the ML at 40 ms interval. As seen, the

UNIVERSITY OF ADELAIDE LIBRARY

conditioning signal has only partially suppressed the test signal, again by approximately 33%. Yet at the same inter-stimulus interval the test cortical response (figure 4.3) is substantially more depressed (80%). Clearly, the thalamic and intracortical relays contribute to the inhibition of the second response in this pathway.

Figure 4.8 represents a waveform originating from both the ML and *lateral spinothalamic pathway* admixed at the midbrain level, with a delayed component due to the latter pathway. The lateral spinothalamic pathway is a sensory pathway for pain and temperature. This pathway relays in the spinal cord, crosses and ascends in the lateral spinothalamic tract of the spinal cord, medulla and midbrain on its way to *nucleus ventralis postero lateralis* of thalamus, where it synapses on neurones running to the somaesthetic area of cortex.

This fortuitous simultaneous recording from the ML and spinothalamic tract (STT) nicely illustrates the different properties of these two pathways, in response to repetitive stimulation (2 pulses, 24 ms apart). As can be seen the later spinothalamic component is more sensitive to a conditioning response than is the ML component, to the extent that the spinothalamic component is virtually abolished. This is a characteristic of the pathway, most probably due to presynaptic inhibitory interaction between the conditioner and test responses at the level of the relay in the spinal cord.

Finally, the upper trace in figure 4.9 shows a different response originating from the ML, but again with a component

from the lateral spinothalamic pathway. It is a noisy, prolonged response. The bottom trace clearly shows that supplementary intravenous injection of 1 ml (25 mg) α-chloralose resulted in a marked reduction in discharge duration, eliminating much of the later STT component of the response, but leaving the ML component intact. This is a clear example of the way in which an anaesthetic can specifically influence conduction in a sensory pathway, an observation that was the original basis which prompted this aspect of the study.

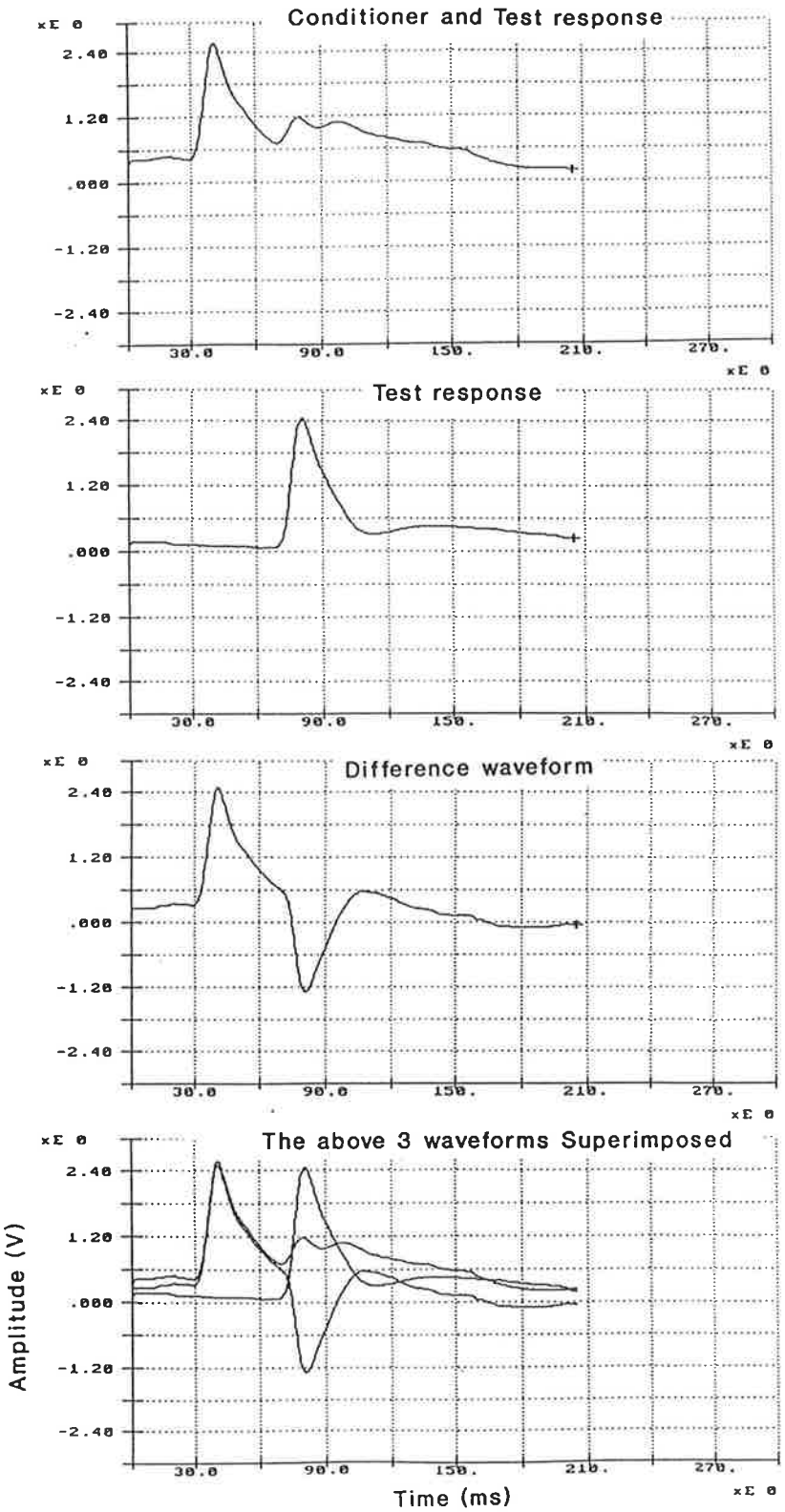

Figure 4.3 Evoked potentials recorded from the rabbit cortex (approximately 1 mm below the brain surface). The effect of interacting conditioning and test responses is illustrated.

In descending order: Conditioner & test, test, difference and all 3 superimposed.

Stimulus pulse: 25 V, 0.1 ms Stimulus interval: 40 ms

Response latency: 10 ms Number of averages: 50

Amplifier gain: 10000

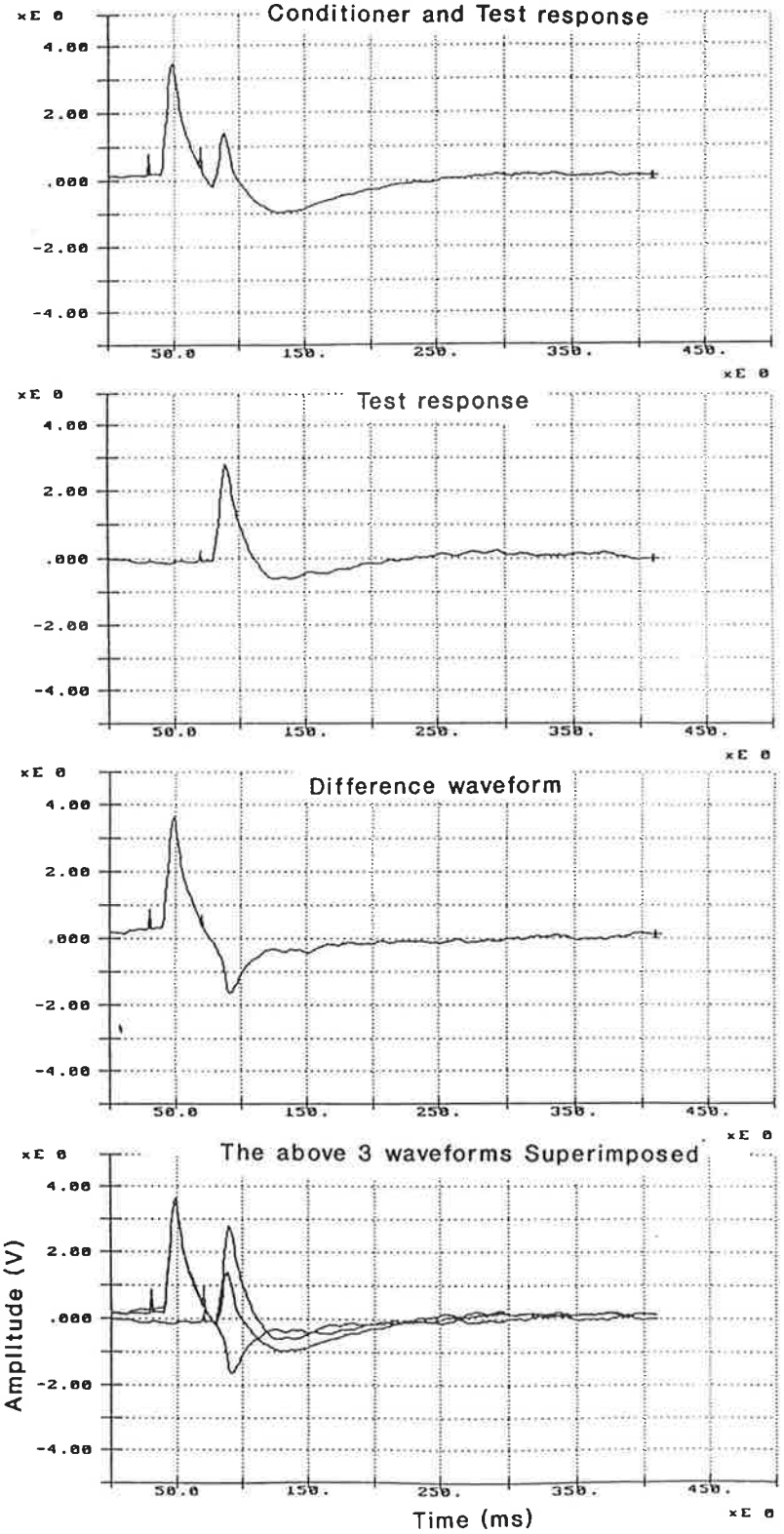

Figure 4.4 Evoked potentials recorded from the rabbit cortex (approximately 3 mm below the brain surface). The effect of interacting conditioning and test responses is illustrated.

In descending order: Conditioner & test, test, difference and all 3 superimposed.

Stimulus interval: 40 ms Number of averages: 25

Amplifier gain: 20000

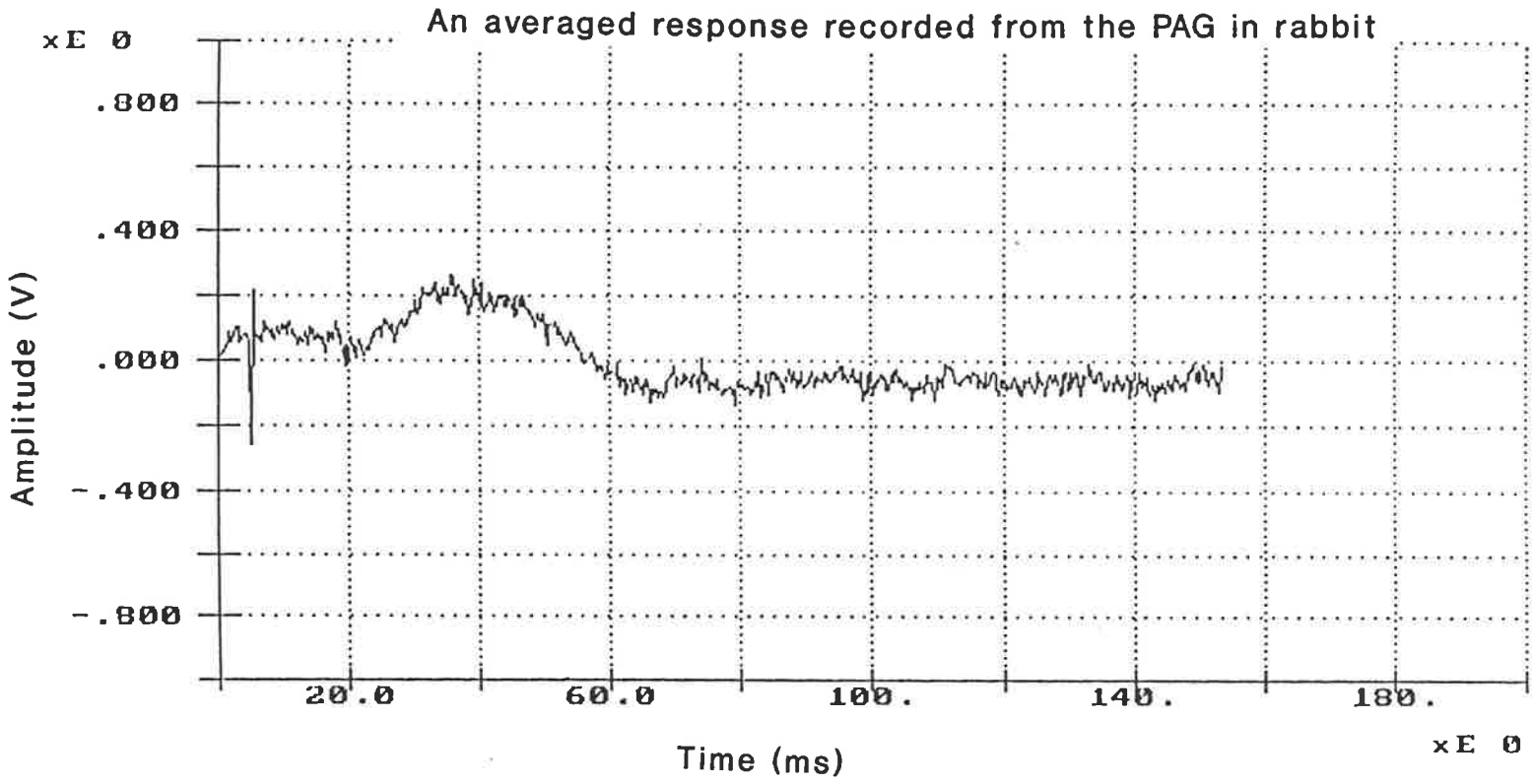

Figure 4.5 A relatively small, noisy signal recorded from the periaquaductual gray in rabbit brain.
Number of averages: 30
Amplifier gain: 20000

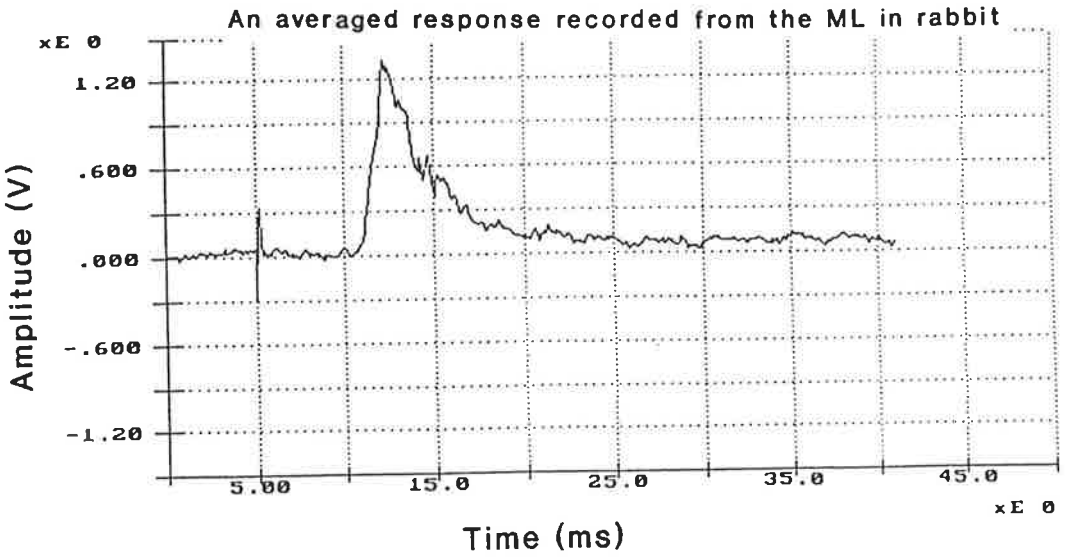

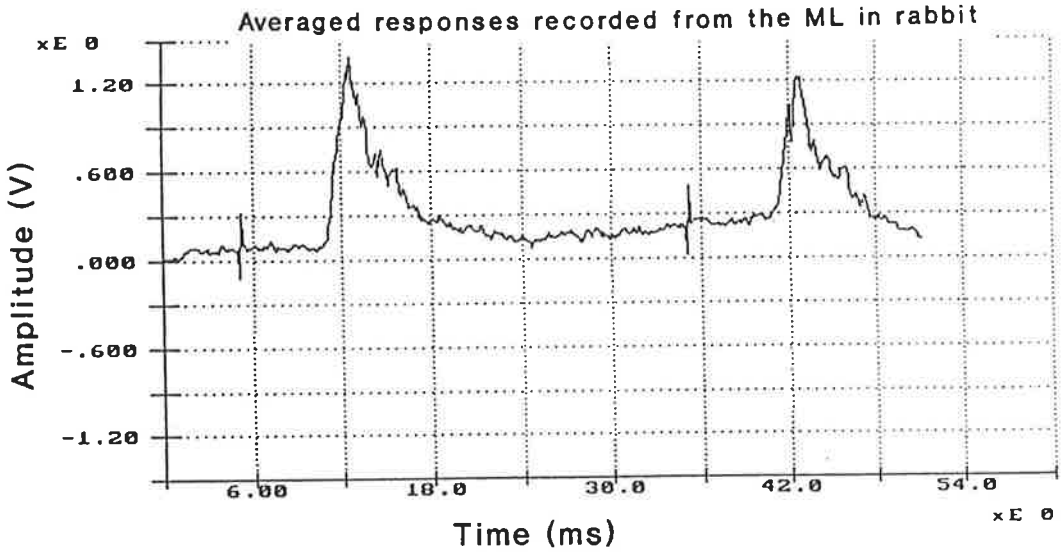

Figure 4.6 Evoked potentials recorded from the medial lemniscus in rabbit brain. Upper trace shows an uninteracted response. Lower trace shows the effect of interacting with a second response at a delay of 30 ms. Seterotaxic coordinates for recording both responses were: P = 10, L = 2, and H = -12 Number of averages: 50 Amplifier gain: 20000

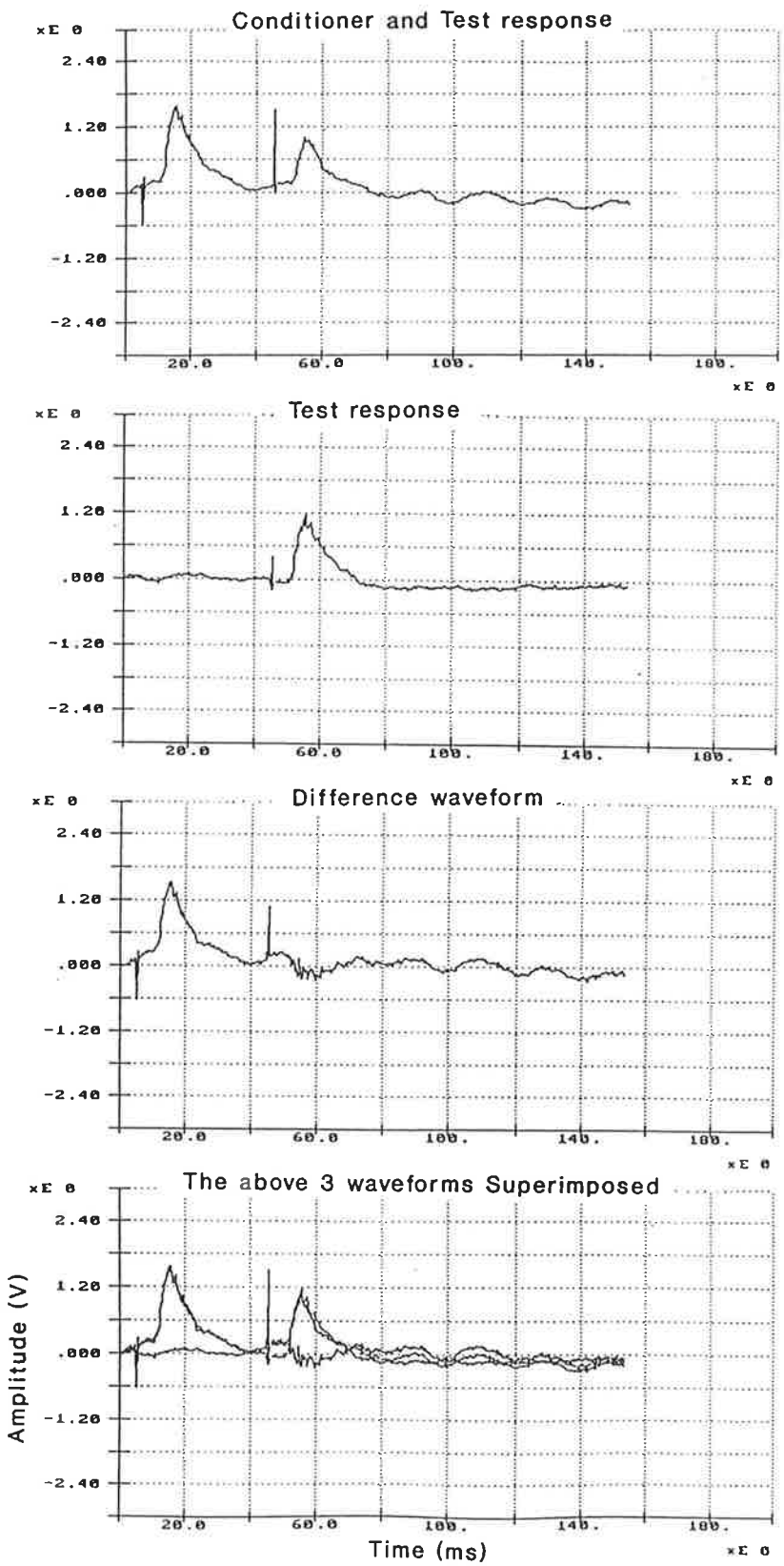

Figure 4.7 Evoked potentials recorded from the medial lemniscus in rabbit brain, showing some interaction between conditioner and test responses. In descending order: Conditioner & test, test, difference, and all 3 superimposed.

Number of averages: 50 Amplifier gain: 20000

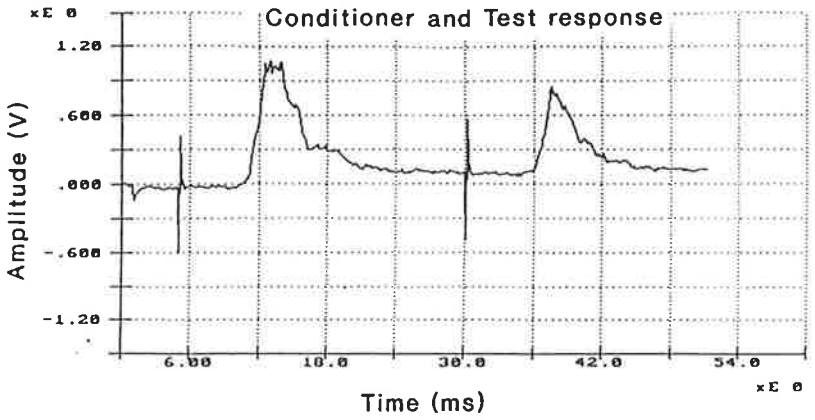

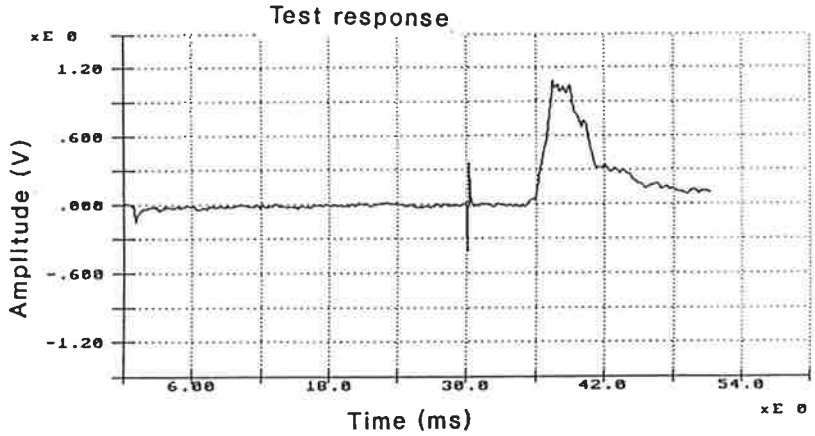

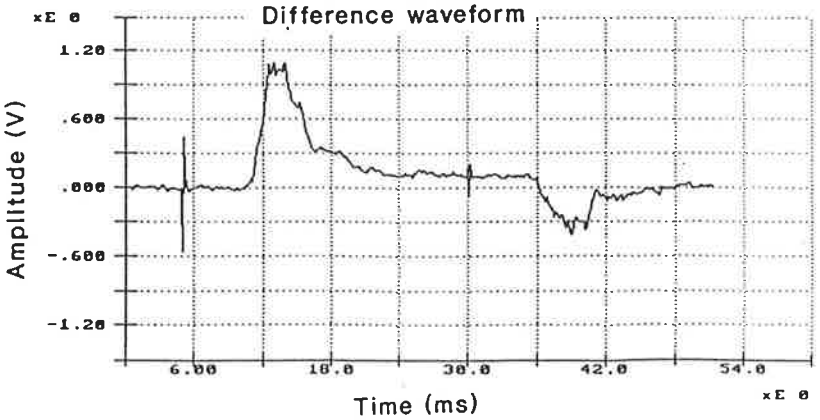

Figure 4.8 Combined evoked potentials recorded from the medial lemniscus and the lateral spinothalamic pathway.

In descending order: Conditioner & test, test and difference waveforms.

Stereotaxic coordinates for recording both responses were:

P = 9, L = 3, and H = -15

Number of averages: 50 Amplifier gain: 20000

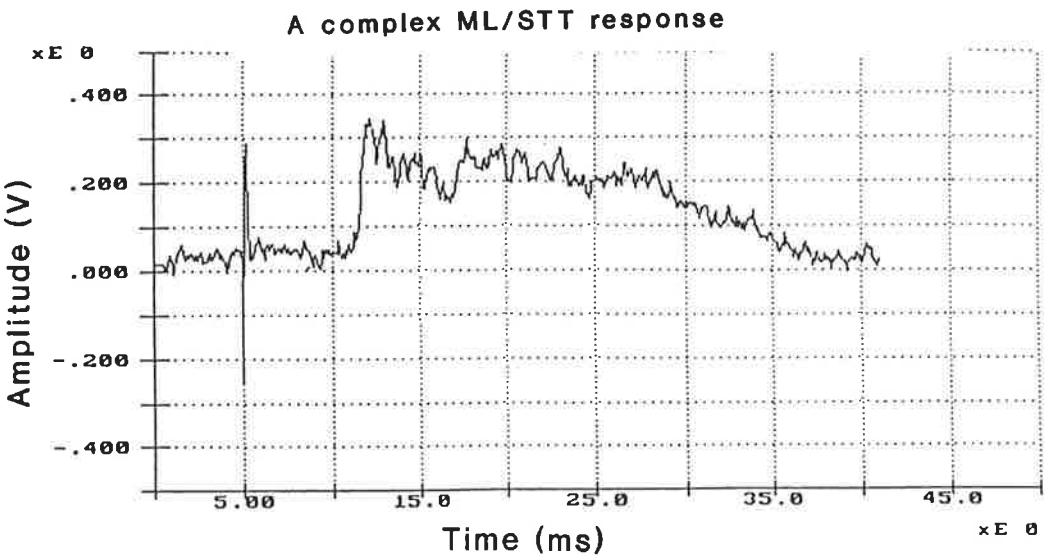

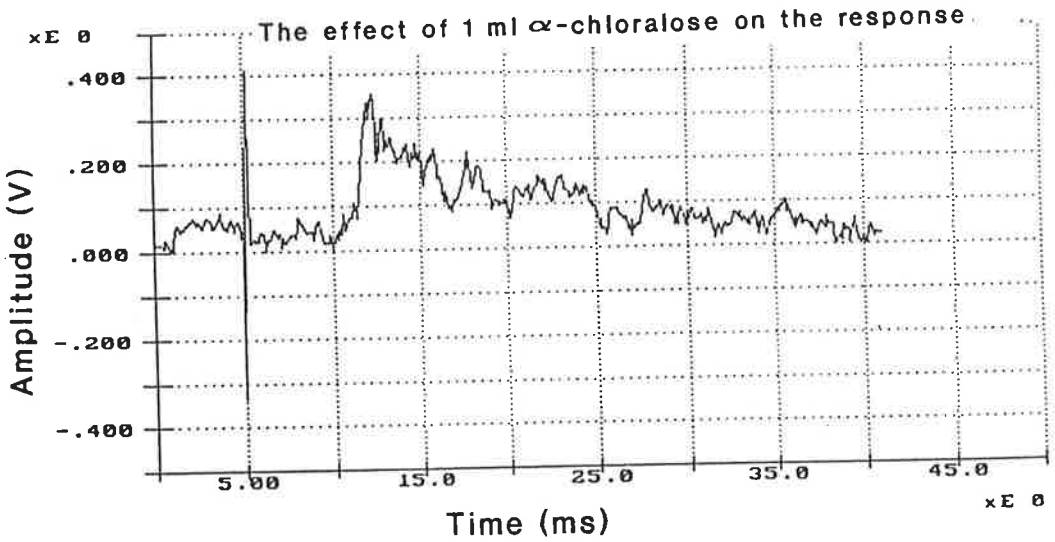

Figure 4.9 A Combined evoked potential recorded from the medial lemniscus and the lateral spinothalamic pathway.

Upper trace shows a small, noisy response. Lower trace shows the effect of a supplementary intravenous injection of 1 ml (25 mg) α-chloralose on the waveform.

Number of averages: 30 Amplifier gain: 20000

CHAPTER 5

EFFECTS OF POTASSIUM CHANNEL BLOCKERS ON EPILEPTIFORM DISCHARGES RECORDED FROM RAT NEOCORTICAL SLICES IN VITRO

The role of potassium (K^+) channels in controlling the membrane potential which influences excitability and discharging characteristics of neurones is well known (Alger and Nicoll, 1980; Aram and Lodge, 1988; Chamrlin and Dingledine, 1988; Akins and McCleskey, 1993; Zorn et al., 1993). K^+ channel blockers have been shown to readily induce epileptiform activity in the grease-gap recording model (Aram and Lodge, 1988). As depression in neuronal excitability is believed to be a plausible mechanism leading to the state of anaesthesia, investigating the biophysical and pharmacological properties of K^+ channels formed an important part of this research project since these, or Cl^- channels, are likely to be involved.

Table 6.1 is reviewed in Hille (1992). It lists some potassium channels, and a selection of blocking agents for each channel.

Studies of interactions between neurotransmitters and K^+ channels can help to identify the underlying mechanisms of the functional role of various neurotransmitters.A list of receptors which are coupled to K^+ channels through G-proteins or second messengers system to act as channel openers would include baclofen $GABA_B$, acetylcholine M_2, adrenergic (NE) α_2, dopamine D_2, 5-hydroxytryptamine 1A and adenosine A_1.

Potassium channel	Acting from outside	Acting from inside
Delayed Rectifier	TEA, Cs^+, Ba^{2+}, 4-AP, Capsaicin, Dendrotoxins, Noxiustoxin	TEA, Cs^+, Na^+, Li^+, Ba^{2+}
A-Channel	TEA, 4-AP, Dendrotoxins	TEA
Ca^{2+}-Activated	TEA (BK), Cs^+, Apamin (SK), Charybdotoxin (BK)	TEA, Na^+, Ba^{2+}
Inward Rectifier	TEA, Cs^+, Rb^+, Na^+, Ba^{2+}, Sr^{2+}	Mg^{2+}
ATP-Sensitive	TEA, Cs^+, Ba^{2+}	TEA, Na^+, Mg^{2+}

Table 5.1 Blocking Agents for Potassium Channels

Conversely, K^+ channel blocking actions of acetylcholine M_1, adenosine A_2, dopamine D_1, adrenergic β_1, and 5-hydroxytryptamine 2 receptors may induce tissue hyper-excitability.

Different means of modulating K^+ channel opening seems to encompass most of the known intracellular second messengers, namely Ca^{2+}, cAMP, cGMP, GTP-binding proteins (α, and a combination of β and gamma), protein kinase C, and ATP. A rise in cAMP leads to channel closure in the case of K_{5-HT}, whereas in most other cases (delayed rectifier, inward rectifier, transient outward current and certain Ca^{2+}-activated K^+

channels), cAMP facilitates channel opening (Cook, 1988). However, high levels of cyclic AMP in hippocampal neurones block the long lasting calcium-dependent potassium channels, K_{Ca}, (Lewis et al., 1989), whilst membrane-permeant analogues of cAMP cause a small reduction in voltage-dependent outward currents, and decrease the $I_{K(Ca)}$ which leads to late after-hyperpolarisations (Akins and McCleskey, 1993). Indeed in general, raised cAMP has wide-ranging intracellular effects, such as inhibiting K^+ currents and facilitating excitatory neurotransmitter release, leading to an increase in cell excitability (Boulton et al., 1993).

As a preliminary investigation, in order to become familiar with the grease-gap recording model, and to ascertain the viability of neocortical slices, a series of experiments were carried out where applying 1 to 10 mM KCl in Mg^{2+}-free ACSF for approximately 4 minutes caused a dose-dependent tissue depolarisation. In these preparatory experiments, the viability of neocortical slices was sometimes ascertained by applying low concentrations of NMDA to the unmasked NMDA receptors, inducing tissue hyperexcitability. The role of NMDA in epileptogenesis is discussed in detail in chapter 2. Aram and Lodge (1988) report that in Mg^{2+}-free ACSF, increasing the K^+ level from its normal value of 4.5 mM to 9 mM leads to a concentration-dependent increase in the frequency and the amplitude of spontaneous epileptiform events. Whilst Irwin et al. (1992) found that a depolarising concentration of K^+ (20 mM) results in an average rise in internal Ca^{2+} concentration of 362 ± 65 *n*M. Most likely, depolarisation of hippocampal neurones by high K^+ results in the release of endogenous

glutamate, with secondary activation of the NMDA receptors. Indeed Rhoades and Gross (1994) report that serial additions of 10 μM NMDA increased the discharge burst rate, in a manner qualitatively similar to the effect of KCl additions, in cultured fetal murine spinal cord networks.

Initially in this chapter the effect of NMDA on spontaneously discharging neocortical slices is presented. The focus of the chapter, however, is on how each of a number of classical K^+ channel blockers, namely tetraethylammonium, carbamyl-choline, ceasium chloride, 4-aminopyridine and barium chloride modify the spontaneous epileptiform activity induced in a Mg^{2+} free medium. Although studies on neocortical discharge patterns do not provide direct information about cellular ionic mechanisms, they nonetheless reflect the principal traffic in interneuronal network communication (Rhoades and Gross, 1994).

5.1 SPONTANEOUS DISCHARGES WITH AFTER-ACTIVITY

As discussed earlier in chapter 2, NMDA receptors are normally closed by Mg^{2+} at resting membrane potential, and depolarisation is produced by glutamate acting on non-NMDA receptors (Kainate and AMPA). In Mg^{2+} containing ACSF, blocking K^+ channels results in depolarisation which assists the NMDA-induced opening of its channels, by displacing Mg^{2+}. This mechanism, which is voltage-dependent, requires the presence of the amino acid glycine. Removal of Mg^{2+} from the ACSF superfusing the neocortical slices releases this Mg^{2+}-

dependent block, and leads to spontaneous discharges due to endogenous glutamate, often with after-activity on the falling phase of discharges. Figure 5.1 illustrates such spontaneous discharges recorded from brain slices in different rats. The shape and size of the after-activity associated with discharges can vary between preparations, and within each preparation. In experiments reported in this chapter, spontaneous discharge rate ranged from 1 every few minutes to 1 every 20 s. The relative discharge amplitude ranged from 30 to 330 μV, although this depends on the efficacy of the insulation across the grease-gap, whilst the discharge duration, as measured from computer records of individual discharges, ranged from 4 to 48 s. In some experiments, where slices were taken from a tissue block further away from the *optic chiasma* towards the *mammilary bodies* (see chapter 3), simpler discharges with no or limited after-activity were recorded. Such simpler discharges naturally had a shorter duration (1 to 3 s), smaller amplitudes, and faster discharge rate. It was also noted that prolonged bursts tended to occur after long periods of quiescence, reminiscent of a Markov process, suggesting that such intervals are important in recruiting neurones to produce synchronous burst discharges (Miles et al., 1984 and Aram and Lodge, 1988). In addition, the longer the period between 2 consecutive discharges, the higher the number of after-potentials associated with the second discharge, as was noted by Miles et al. (1984) and Aram and Lodge (1988). This may reflect a response to a period of quiescence during which neurotransmitter stores are replenished (O'Shaughnessy et al., 1988).

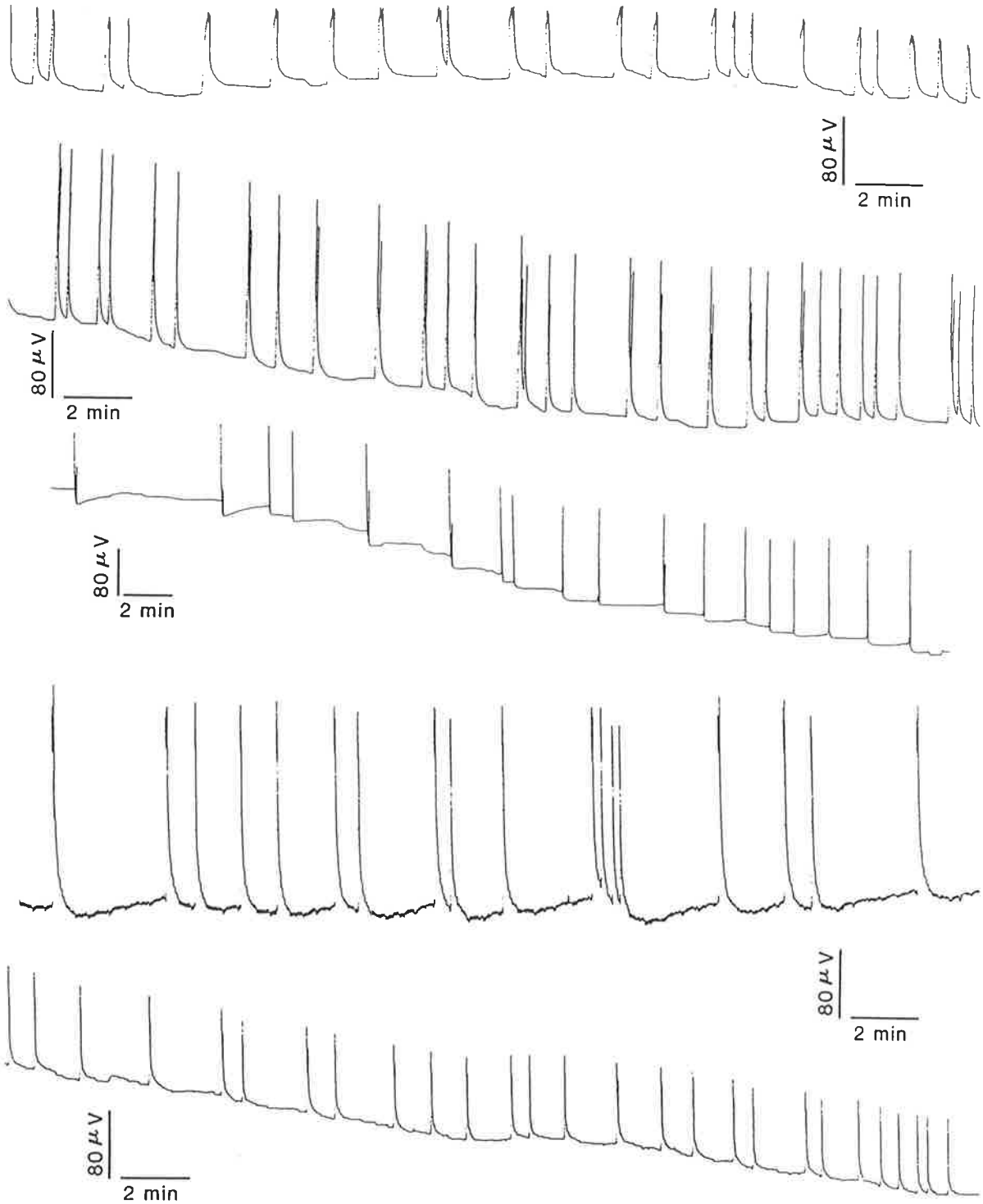

Figure 5.1 Spontaneous epileptiform discharges recorded from neocortical slices, showing how the discharge rate, and the position of after-potentials vary between different slices.

The potentials recorded from slices by O'Shaughnessy et al. (1988) had 5 to 15 after-potentials superimposed on the decay phase, similar to the discharges frequently seen in this project.

The synchrony between events in different layers of the cortex suggests that whole columns of neurones discharge together and spontaneous epileptiform discharges spread throughout the cortical slices (Aram and Lodge, 1988). Earlier Intracellular studies in the cortex (Connors and Gutnick, 1984) and hippocampus (Miles et al., 1984) suggested that after-potentials may represent the recruitment of neurones to fire in bursts via reverberating excitatory synaptic activity.

Endogenous activation of the NMDA receptor is important in the initiation of the paroxysmal events but little involved in the subsequent recruitment of neurones. The amplitude of discharges is related to number of neurones recruited whereas the frequency is related to the initiation of events. Neurotransmitter release may be essential both in the recruitment of neurones and in the initiation of events (Horne et al., 1986).

5.2 EFFECTS OF NMDA ON SPONTANEOUS DISCHARGES

To assess the physiological and/or pathological consequences of excitatory amino acid receptor-mediated events, it is necessary to obtain accurate and reproducible

pharmacological data on a preparation which preserves as much of the tissue structure present in situ as possible, and which permits quantitative comparison among animals subjected to different treatments. The present grease-gap technique, adapted for cortical wedge preparations, allows such quantitative pharmacological studies to be performed (Martin et al., 1989), although not all responses can readily be quantified. Here, NMDA was used to assess the viability of slices, particularly those with only a very slow discharge frequency.

Relief of the voltage-dependent Mg^{2+} block of the channel associated with the NMDA receptor is the major factor initiating epileptiform bursts in Mg^{2+}-free medium. Figure 5.2 is a chart recorder trace showing the effect of applying 30 µM NMDA to a spontaneously active neocortical slice. Although NMDA was normally effective almost immediately after reaching the tissue, there was a delay of nearly 2 minute before the hyperexcitability was induced in this experiment. The NMDA solution was diluted from a 10 mM stock which additionally contained the total ACSF equivalent amounts of NaCl and KCl. NMDA resulted in a dose-dependent tissue depolarisation, and a marked increase in the discharge rate. In general, slices recovered from a four minute application of non-toxic concentrations of NMDA (1 to 10 µM) within 5 to 6 minutes after the application had stopped. However, on several occasions 30 µM NMDA, or higher, concentrations caused neurotoxicity in the slices which consequently failed to recover.

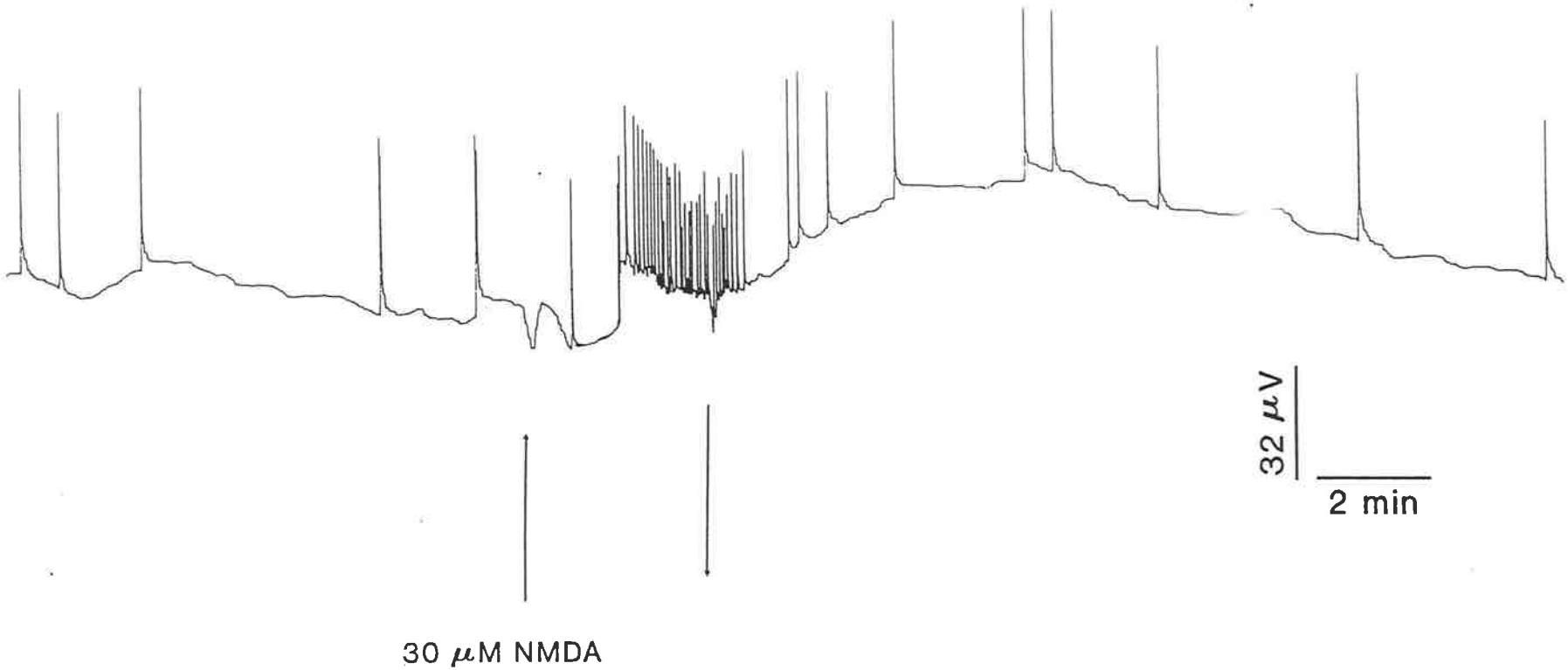

Figure 5.2 The effect of 30 μM NMDA on spontaneous discharges recorded from a rat neocortical slice. There was a delay before NMDA induced hyperexcitability in this slice.

Robichaud and Boxer (1993) also noted a rapid NMDA-induced increase in the spontaneous epileptiform discharge (SED) frequency (approximately 300% of control). However, in their experiment, 3 μM NMDA was applied continuously which led to the increase in frequency being sustained for 2 hours.

Although washout of NMDA reversed its effects on discharge frequency, such slices which showed only slow firing in response to NMDA were not used in the study of the effects of K^+ channel blockers.

5.3 EFFECTS OF TEA ON SPONTANEOUS DISCHARGES

Computerised data acquisition reveals a "microscopic" picture of each neocortical discharges, and permits subsequent digital signal processing. Generally, there has been a tendency to run chart recorders at faster speeds to acquire a detailed trace of individual discharges in the neocortical wedge model (Horne et al., 1986; Aram and Lodge, 1988; O'Shaughnessy et al., 1988; Aram et al., 1989; Martin et al., 1989; Boulton and O'Shaughnessy, 1991; Boulton et al., 1993;). The present results suggest that chart recorders may be best suited to obtain a "macroscopic" picture of the slice activity over a period of time, whilst simultaneous individual frames are required to study detailed responses.

Figure 5.3 represents sample chart recorder data of the effects of 1 and 5 mM TEA, applied for approximately 4

minutes, on spontaneous discharges. In slices from 8 different rats (n=8) used for TEA experiments, the initial rate of spontaneous discharges over at least a period of 1 hour ranged from 1 every 200 s to 1 every 17 s, and the mean duration of spontaneous discharges was 4 s. The increase in discharge rate with 5 mM TEA (n=8) was not statistically significant (t test, 2 tailed at P=0.05) due to development of after-activity on the discharges, whereas in some preparations, 1 mM TEA significantly increased the discharge rate (1-tail test, P=0.1). However, 5 mM TEA generally increased the relative amplitude of discharges by an average of 34%, which was significant (1-tail test, P=0.1), and increased the discharge duration by an average of 31% which was also significant (1-tail test, P=0.1). A dose-dependent baseline potential shift was noted with TEA, presumably by blocking a resting I_K. The depolarisation started within 30 s of TEA reaching the slice. For 5 mM TEA, the duration of the baseline potential shifts were approximately twice the duration of the TEA application, and the amplitude of the shifts were approximately twice the amplitude of pre-treated discharges. 5 mM TEA took approximately 90 s to take effect, and it often took 1½ to 6½ minutes for the discharge amplitude to return to control after the TEA application was completed; but, in some slices, it took as long as 22 minutes for total recovery from the increased discharge rate.

Figures 5.4.a and 5.4.b represent two independent sets of computer acquired responses, showing control, a discharge in the presence of 5 mM TEA, and recovery. As can be seen, the most characteristic feature of the response to 5 mM TEA was an

overshoot of the rising phase, relative to control, as well as an extension of the after-activity. This overshoot in the rising phase was noted consistently in all experiments with TEA over the 0.5 to 10 mM range, whereas the extension in after-activity was most striking with higher TEA concentrations (5 to 10 mM). The bottom trace in both sets of records represents discharges on partial recovery, some residual effect on the initial spike still being evident.

The consistent overshoot of the rising phase of discharges with TEA is most likely due to a block of the classical voltage-dependent Hodgkin-Huxley delayed (outward) rectifier K^+ current, $I_{K(V)}$, by the agent; this current is involved in repolarisation and bursting behaviour of neurones (Aronson, 1992). In marked contrast to the present findings in neocortex, Rhoades and Gross (1994) report that TEA reduced the integrated burst amplitude at 5-10 µM and only marginally increased burst rate at higher concentrations in the cultured fetal murine spinal cord networks.

In these experiments, TEA always caused a dose-dependent baseline shift, on which such discharges were superimposed. In general, such baseline shifts are referred to as depolarisation (or hyperpolarisation), when applying various agents to neocortical slice preparations (Horne et al., 1986; Aram and Lodge, 1988; Aram et al. 1989, Ong et al., 1990). Here, in the extensive study of various potassium channel blockers, the baseline potential shifts appeared inconsistent, and not necessarily concentration-dependent. As will be discussed later in this chapter, the baseline shift may not

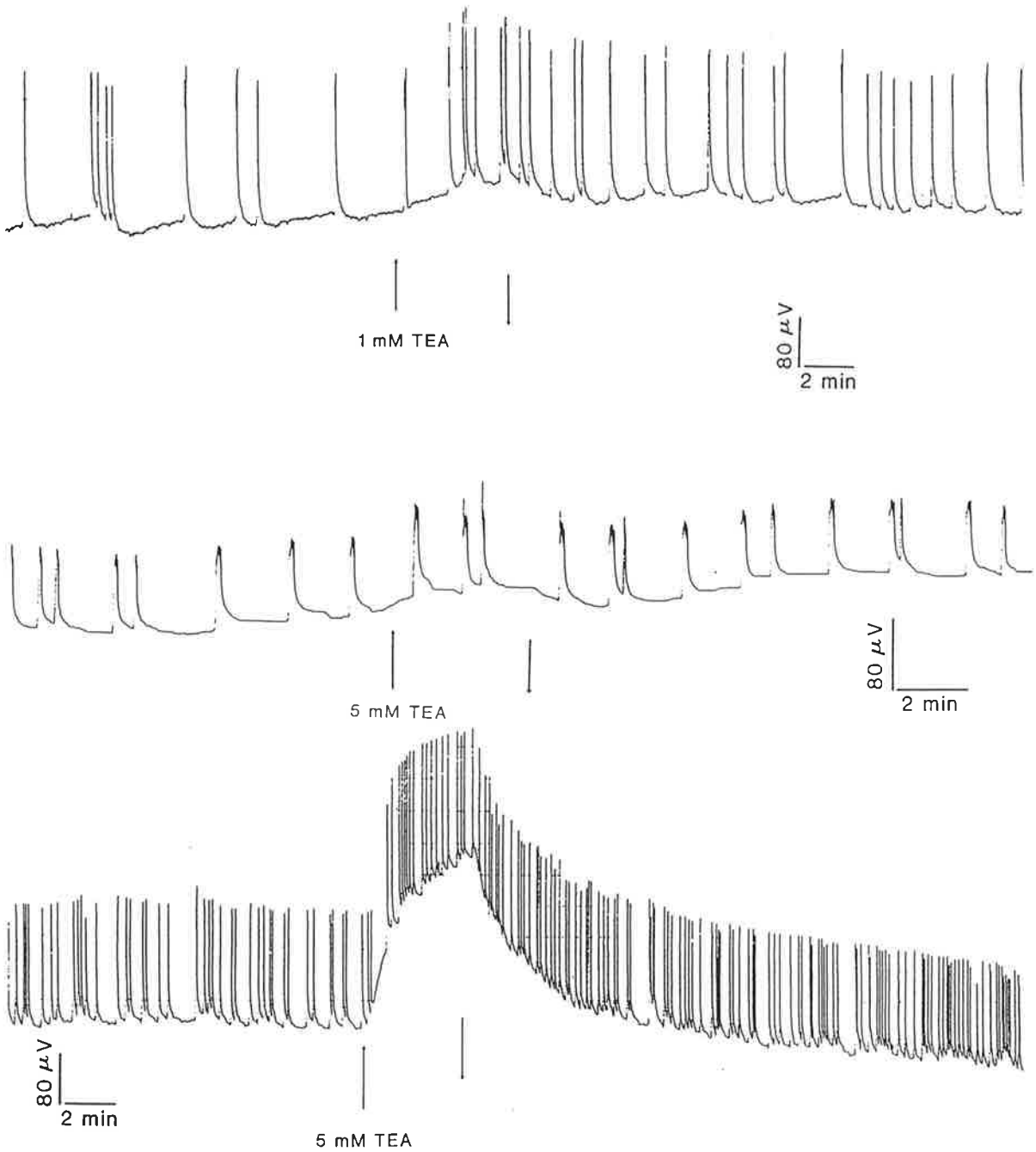

Figure 5.3 Chart recorder traces, from independent experiments, showing the effects of 1 and 5 mM TEA on neocortical discharges.

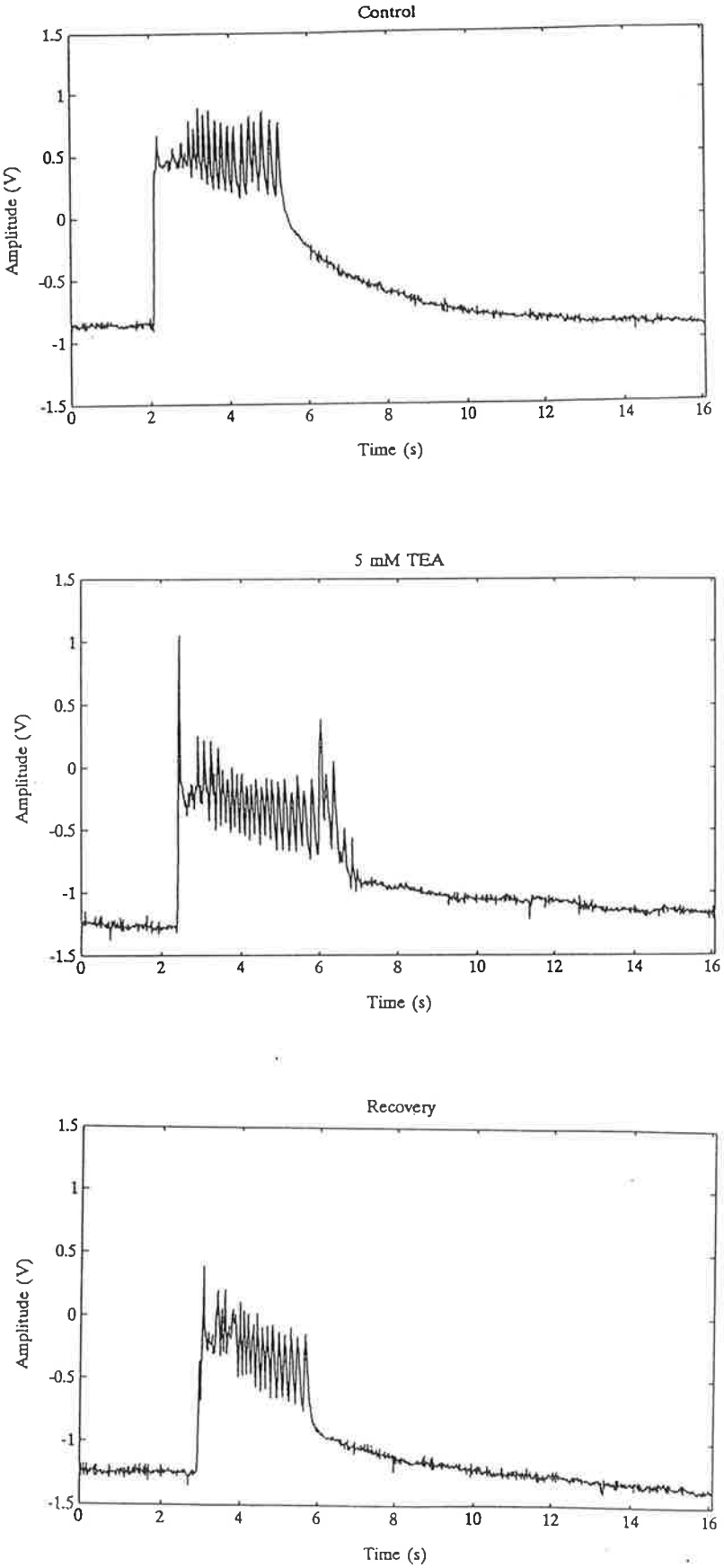

Figure 5.4.a A set of computer recorded responses showing control, a discharge in the presence of 5 mM TEA, and recovery. The effects of TEA are seen in detail.

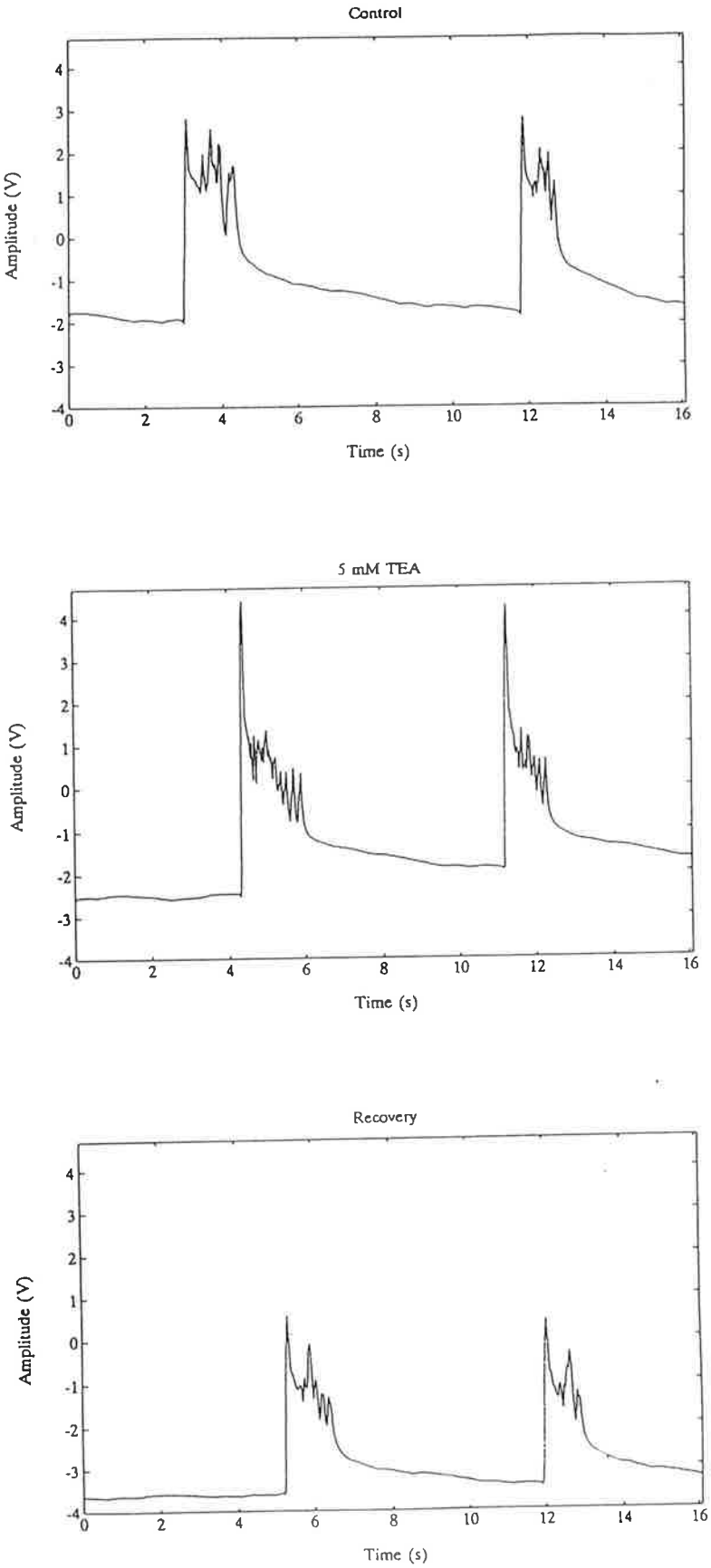

Figure 5.4.b A set of computer recorded responses showing control, discharges in the presence of 5 mM TEA, and recovery. The overshoot of the rising phase of discharges, induced by TEA, is clearly seen.

entirely represent a depolarisation of neurones, but also a physico-chemical ionic effect (a concentration effect) across the grease-gap barrier. TEA was either diluted in ACSF solution (up to and including the 5 mM solution) prior to superfusion, or applied as a stock solution (10 mM) containing the total ACSF equivalent concentrations of NaCl and KCl in an attempt to preserve the molarity of the superfusing medium.

A delayed rectifier K^+ current with shallow voltage-dependent inactivation is known to be TEA sensitive (Cook, 1988; Franks and Lieb, 1988; Rudy, 1988; Oyama et al., 1991; Akins and McClesky, 1993). Although the TEA sensitive K^+ currents are either slowly or very slowly inactivating (Foehring and Surmeier, 1993), inactivation is not a strong measure in K^+ channel classification (Rudy, 1988).

In general, TEA blocks several K^+ currents (Latorre, 1993). These include the delayed rectifier, the muscarinic M, and the inward rectifier currents (Aronson, 1992). However according to Bartschat and Blaustein (1985b), TEA blocks the non-inactivating (or slowly inactivating) voltage-regulated, the inactivating voltage-regulated and the calcium-activated potassium channels in significantly lower concentrations than it blocks the resting K^+ permeability in isolated pre-synaptic nerve terminals from rat brain.

Internal and external cell binding sites for the quantitative effect of TEA should be distinguished (Bartschat and Blaustein, 1985a; Rudy, 1988; Newland et al., 1992), as externally applied TEA blocks some K^+ currents, whereas

internally applied TEA is less specific and usually less potent (Rudy, 1988).

Although as high as 50 mM TEA is reported to have been externally applied to neurones (Franks and Lieb, 1988; Sihra et al. 1993), in these experiments TEA concentrations greater that 5 mM prolonged the after-activity of discharges. It is most likely that the extension of after-activity by TEA is due to its blocking a voltage-dependent high conductance sub-type of K_{Ca} channels, known as BK_{Ca}. The BK_{Ca} is widely reported to be blocked by TEA (Cook, 1988; Rudy, 1988; Yoshida et al., 1991; Aronson, 1992; McLarnon and Sawyer, 1993; Rhoades and Gross, 1994). However in contrast to these results Rudy, McLarnon and Sawyer, and Rhoades and Gross found that a low TEA concentration (0.5-1 mM) was sufficient for the block.

Additionally, K_{Ca} channels are also implicated in regulating the frequency of burst firing (Akins and McCleskey, 1993), regulation of Ca^{2+} entry and burst shortening or termination (Traub and Wong, 1983), and may also contribute to repolarisation and hyperpolarisation which follows the repolarisation (Aronson, 1992). In contrast, Rhoades and Gross (1994) believe that K_{Ca} are not responsible for regulating spontaneous bursting in cultured spinal cord neurones, partly because they found minimal increases in discharge rate only at higher TEA concentrations, and deduced that voltage-gated K^+ conductances and not K_{Ca} conductances must have been blocked. Such conclusions could, of course, be tested by the use of specific blockers for K_{Ca} channels, but time did not permit this aspect to be pursued.

5.3.1 Phase-Plane Plot Study

A capability to produce phase-plane plots was implemented in software, as part of the data processing, so that amplitude, duration and the rate of rise and fall of control and discharges modified by various agents could be closely compared. Figure 5.5 represents steps taken to produce a phase-plane plot for a simple discharge. For this, the discharge is low-pass filtered at 50 Hz by the ASYST software, removing any higher frequency noise. The filtered waveform is then differentiated, and a phase-plane plot is produced by plotting the differentiated signal amplitude versus the original signal amplitude. The signal amplitude (the x-axis) is normalised so that phase-plane plots can be compared. Figure 5.6 represents 3 sets of phase-plane plots comparing a control with two discharges modified by TEA. The first set (a) shows how a simple neocortical discharge is low-pass filtered, the filtered signal differentiated, and a phase-plane plot is produced. The second set (b) follows the same procedure to produce a phase-plane plot for a discharge in the presence of 1 mM TEA, which clearly differs from control. The phase-plane emphasizes the fast descending limb of the overshoot that is produced by TEA. Section (c) represents steps taken to produce a phase-plane plot for a discharge in the presence of 5 mM TEA, with the after-activity clearly highlighted in the phase-plane plot. The software listing in appendix A.3.7 details the procedure to implement phase-plane plotting in ASYST).

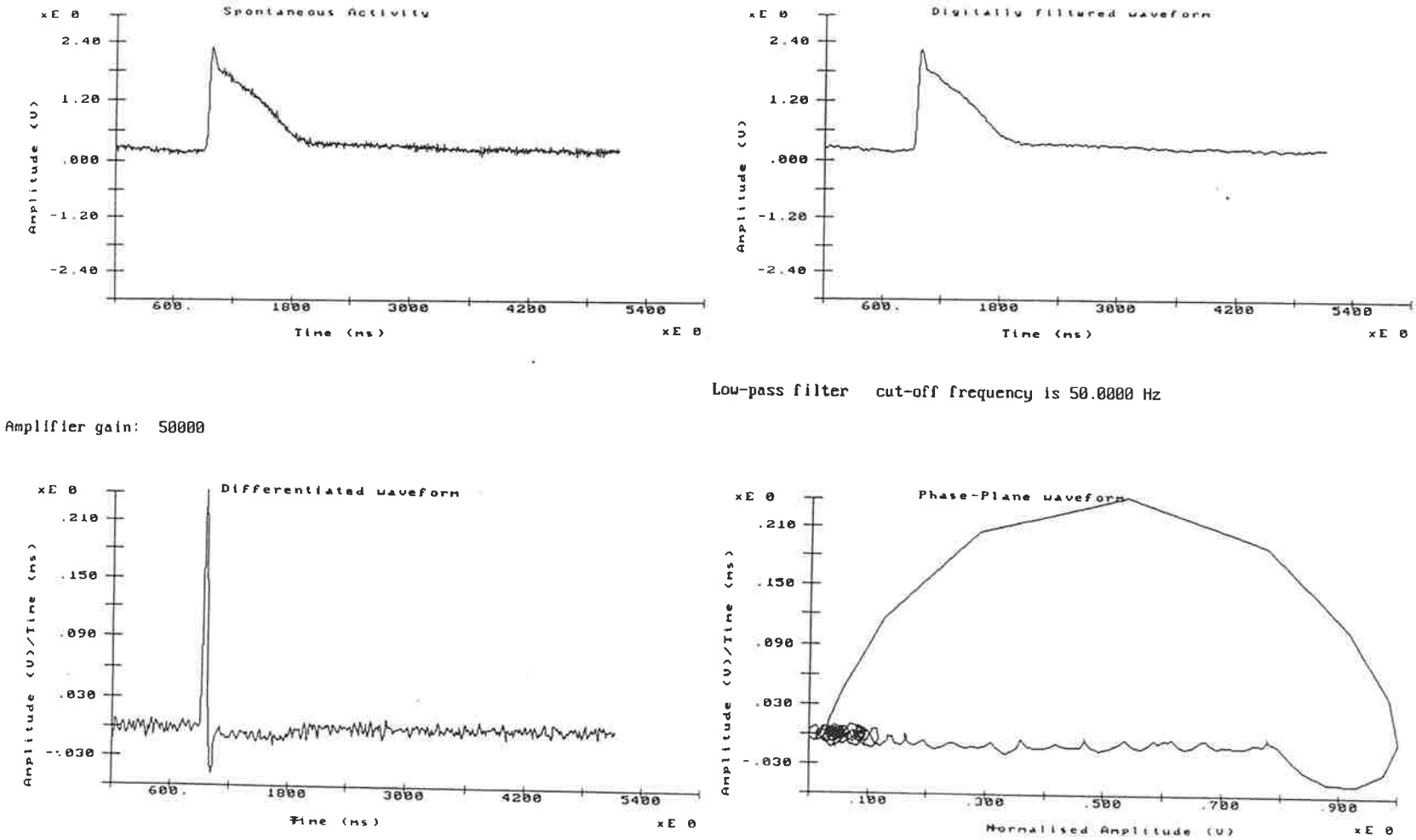

Low-pass filter cut-off frequency is 50.0000 Hz

Amplifier gain: 50000

Figure 5.5 Steps taken to produce a phase-plane plot for a spontaneous discharge. A simple discharge is digitally low-pass filtered at 50 Hz. The filtered signal is differentiated and a phase-plane plot is produced by plotting the differentiated signal amplitude versus the original signal amplitude. Note that the amplitude axis is normalised so that phase-plane plots can be compared.

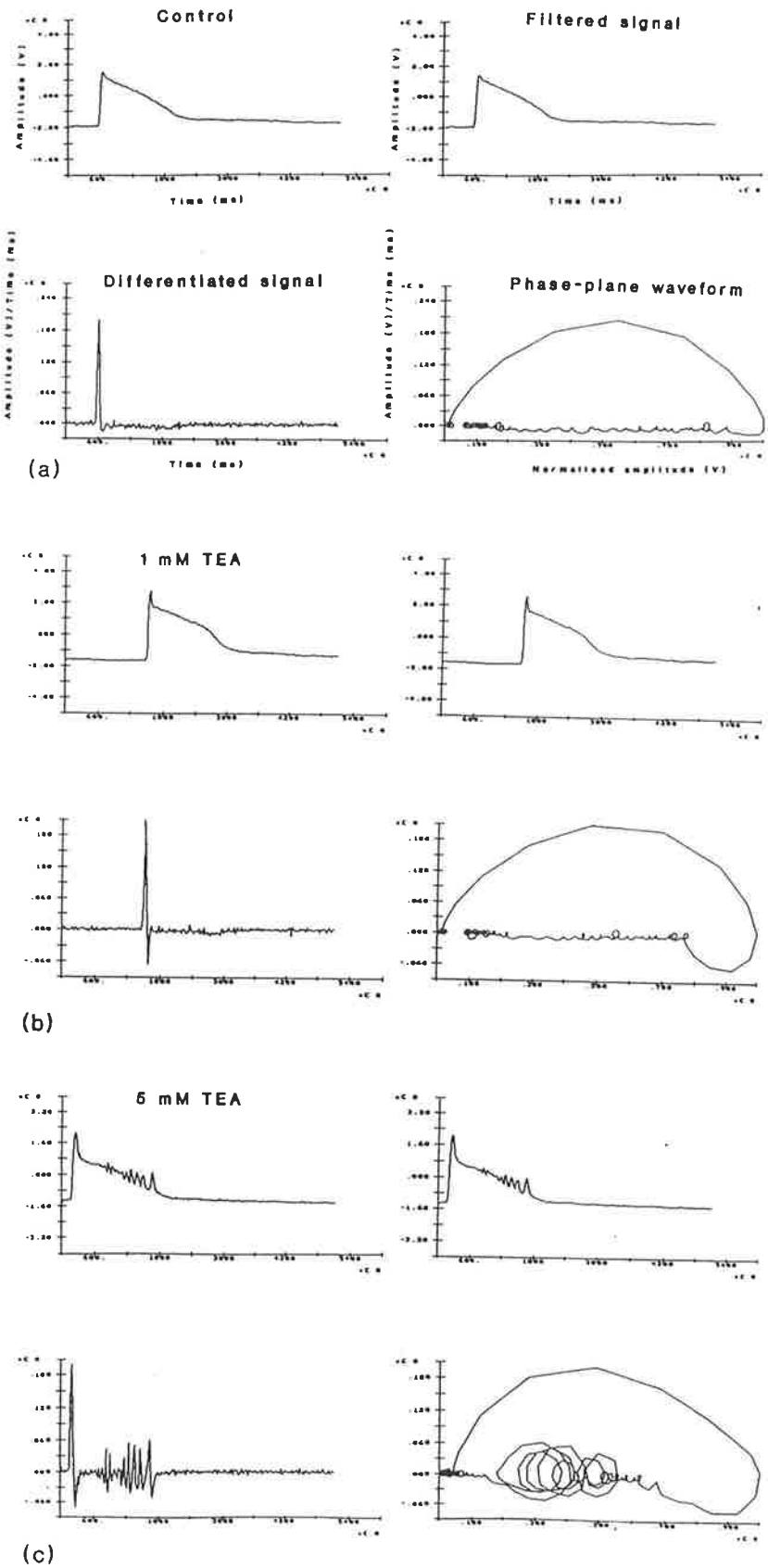

Figure 5.6 Phase-plane plots for control, and discharges in the presence of 1 and 5 mM TEA. (a) A simple discharge is low-pass filtered at 50 Hz. The filtered signal is differentiated, and a phase-plane plot is produced by plotting the differentiated signal amplitude versus the original signal amplitude. The amplitude axis is normalised so that different phase-plane plots can be compared. (b) represents steps taken to produce a phase-plane plot for a discharge modified by 1 mM TEA. (c) Represents the same steps for a discharge modified by 5 mM TEA.

As illustrated here, phase-plane plots accentuate the variations in the rate of rise and fall of discharge components, which is useful in the study of the modification of discharges by channel blockers. However, it appears that phase-plane plots are best suited for highlighting the characteristics of simpler discharges. A discharge with large after-potentials produces a complex phase-plane plot, which would be difficult to interpret.

5.4 EFFECTS OF CCh ON SPONTANEOUS DISCHARGES

Chart recorder traces in figure 5.7 show the effects of 500 µM carbamyl-choline (CCh), applied for approximately 4 minutes, on spontaneous activity from brain slices. For the CCh experiments, the rate of occurrence of spontaneous discharge ranged from 1 every 138 s to 1 every 11 s. Depending on the inherent excitability of slices, 500 µM CCh increased the frequency of discharges in some slices, but decreased it in others. Rhoades and Gross (1994) found that Muscarine and acetylcholine were ineffective in increasing the burst rate in their spinal cord cultured networks.

CCh usually increased the amplitude of discharges. However, in some experiments, the modified discharges were initially larger than control, but their amplitude then fell exponentially in time. On average, 500 µM CCh increased the discharge amplitude by 49% which was significant (1-tail test, P=0.1), and increased the duration of discharges by 179% which

was very significant (1-tail test, P=0.1). A small baseline depolarisation was noted with 500 µM CCh, which started approximately 15 s after CCh reached the tissue. CCh was diluted from a 10 mM stock solution containing ACSF equivalent amounts of NaCl and KCl. In all experiments tissue recovery from CCh was quicker than recovery from TEA. It took between 4 to 8 minutes for CCh to wash off.

Two independent computer recorded responses in figures 5.8.a and 5.8.b show, in detail, how the application of 500 µM CCh resulted in skewing of the rising phase of discharges, an effect quite opposite to that seen with TEA. CCh also prolonged discharges and markedly increased the number of after-potentials. CCh induced discharges are reported to be smaller in amplitude that control (Aram et al., 1988; Vidal and Changeux, 1993). The curving of the rising phase of discharges by CCh could explain how they appear smaller on a chart recorder trace. CCh suppresses the resting K^+ channel, known as the K_M channel (Constanti et al. 1981; Yamaguchi and Ohmori, 1993). The resting $I_{K(M)}$ current is turned off by acetylcholine, to give cell depolarisation (Kendig, 1989). The $I_{K(M)}$ may play a role in regulating repetitive firing (Rudy, 1988), and is not inactivated (Aronson, 1992).

There is disagreement which sub-type of muscarinic receptor is affected by the action of CCh. Yamaguchi and Ohmori (1993) believe that CCh is likely to act on M_1 receptors, whereas Courtney and Nicholls (1992) advocate that it acts on M_3 receptors. Fatatis et al. (1992) report that both M_1 and M_3 receptors subtypes are affected by CCh, and Das et al. (1992)

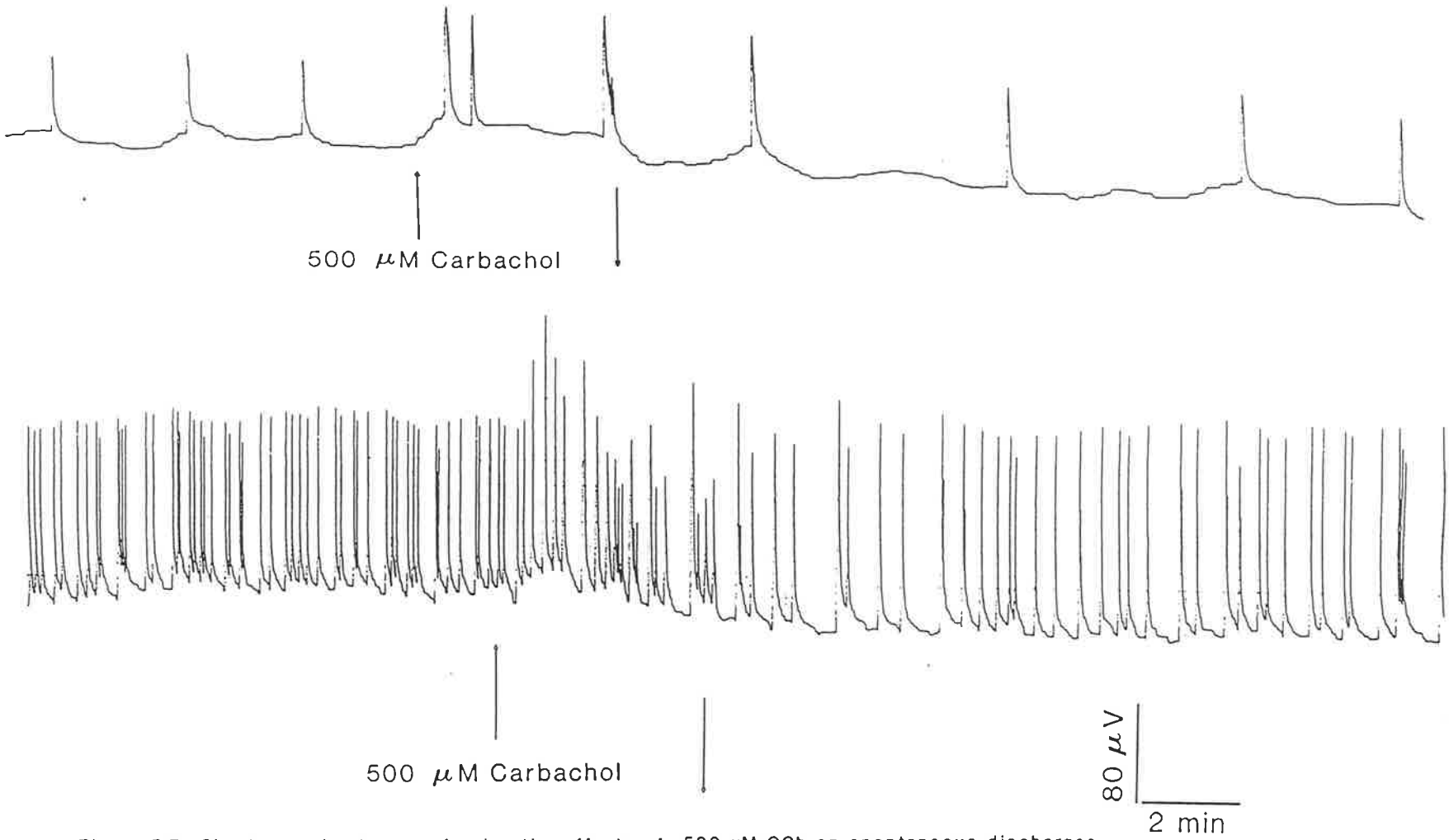

Figure 5.7 Chart recorder traces showing the effects of 500 μM CCh on spontaneous discharges recorded from neocortical slices. CCh had a variable effect on the rate of occurrence of discharges, and its effect on extending the discharge duration is clearly seen in the upper trace.

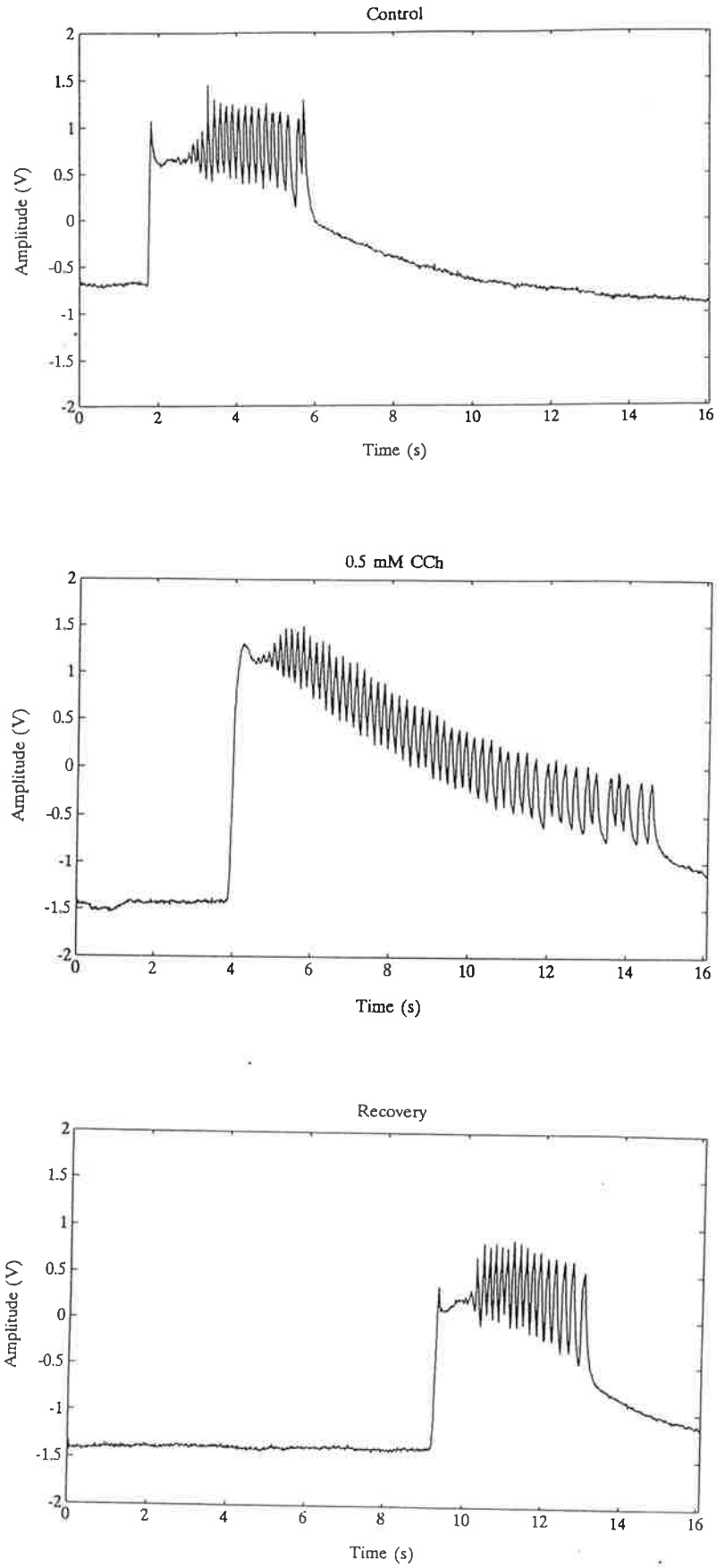

Figure 5.8.a Computer recorded responses showing control, a discharge in the presence of 0.5 mM CCh, and recovery. The effects of CCh are seen in detail.

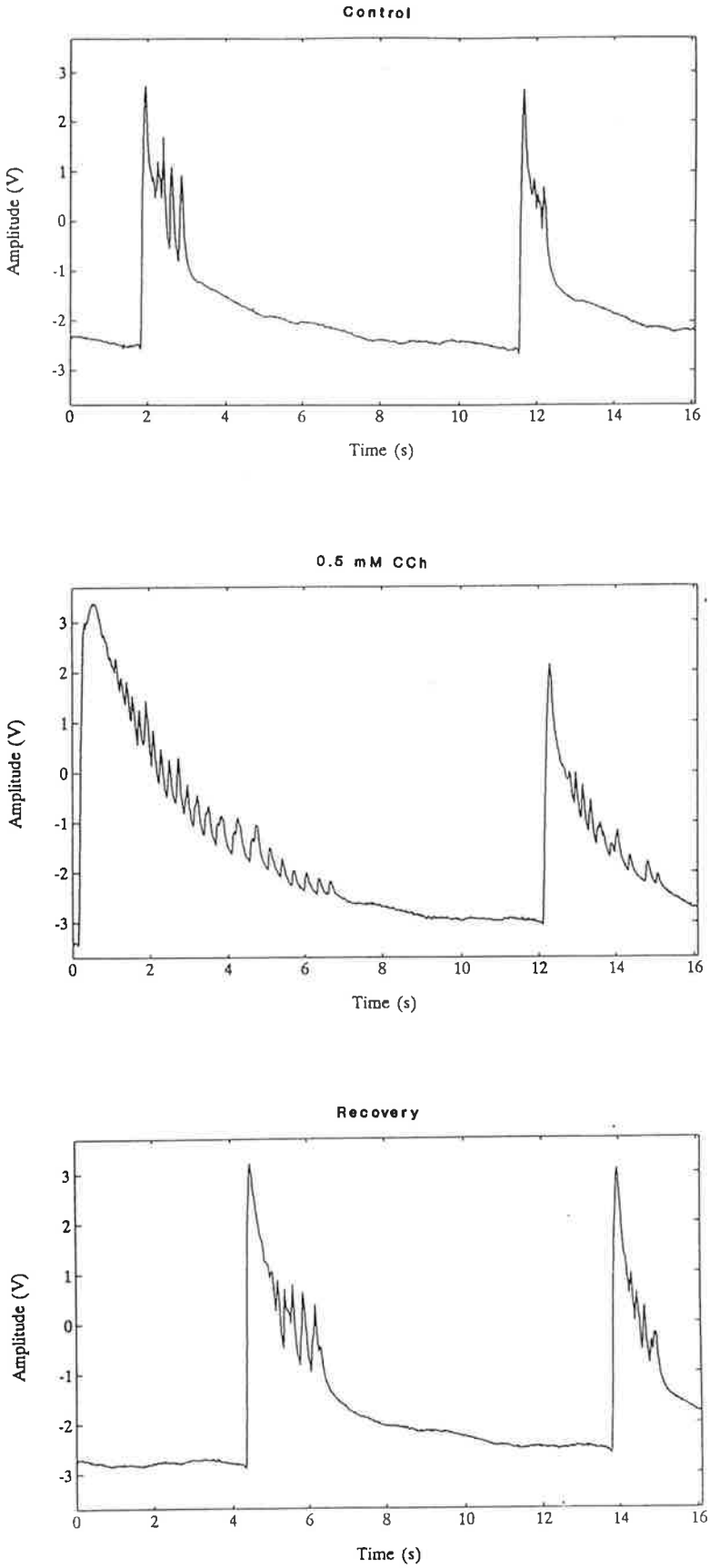

Figure 5.8.b Computer recorded responses showing control, discharges in the presence of 0.5 mM CCh, and recovery. The bottom frame shows discharges on partial recovery.

favour M_1, rather than M_4 receptors mediating the CCh response. It is also widely advocated that CCh induces an increase in intracellular free Ca^{2+} (Huleux et al., 1991; Fatattis et al., 1992; Glaum and Miller, 1992; Lambert et al., 1992).

In addition to its effect on resting K^+ conductances, the present results support that CCh blocks a K_{Ca} channel (Vidal and Changeux, 1993), markedly prolonging the after-activity of discharges (Aram et al., 1988). Additionally, it is reported that CCh, by blocking the K_{Ca} channel, eliminates a long-lasting after-hyperpolarisation which influences the interspike interval during repetitive firing, and produces spike frequency adaptation and habituation.

5.5 EFFECTS OF CsCl ON SPONTANEOUS DISCHARGES

CsCl is known to be a general K^+ channel blocker. In these experiments CsCl in the 0.5-10 mM concentration range were made from a 10 mM stock solution containing the total ACSF equivalent concentrations of NaCl and KCl, but taking into account the contribution of Cs^+ ions. CsCl was normally applied for a 4 minute duration.

As seen clearly from the chart recorder data in figure 5.9 and computer acquired data in figures 5.10.a and 5.10.b, 5 mM CsCl application consistently increased the rate of occurrence of discharges, which on average, was by 160% to 1 discharge every

73 s. 5 mM CsCl also increased the number of after-potentials in each discharge up to 100%. Rhoades and Gross (1994) report that 2-4 mM Cs^+ extended the extracellularly recorded action potential profiles in the cultured fetal murine spinal cord networks.

A fast rate of discharging at 1 every 12 s was induced by 10 mM CsCl, but with this concentration of CsCl, discharges often had few after-potentials. As traces in figure 5.9 show, a large shift in baseline potential was seen within 60 s of 5 mM CsCl reaching the tissue, which lasted up to twice the duration of the CsCl application.

Although frequently applied intracellularly as a 'non-specific' K^+ channel blocker, Cs^+ is also effective upon extracellular administration. Cs^+ is a non-specific blocker of most K^+ channels (Thomson and West, 1990; Rhoades and Gross, 1994) which includes the transient outward, the delayed (outward) rectifier, the intermediate conductance Ca^{2+}-activated, and the 5-HT(via cAMP)-inactivated (K_{5-HT}) channels, but it has a particularly potent blocking effect on the inward (anomalous) rectifier channel (Cook, 1988; Rudy, 1988, Birch et al. 1991).

In rat neocortical neurones, Cs^+ blocks an anomalous rectifier current, $I_{K(IR)}$, with slow kinetics (Sutor and Hablitz, 1993), which is reported to be only partially blocked by Ba^{2+} (Birch et al., 1991).

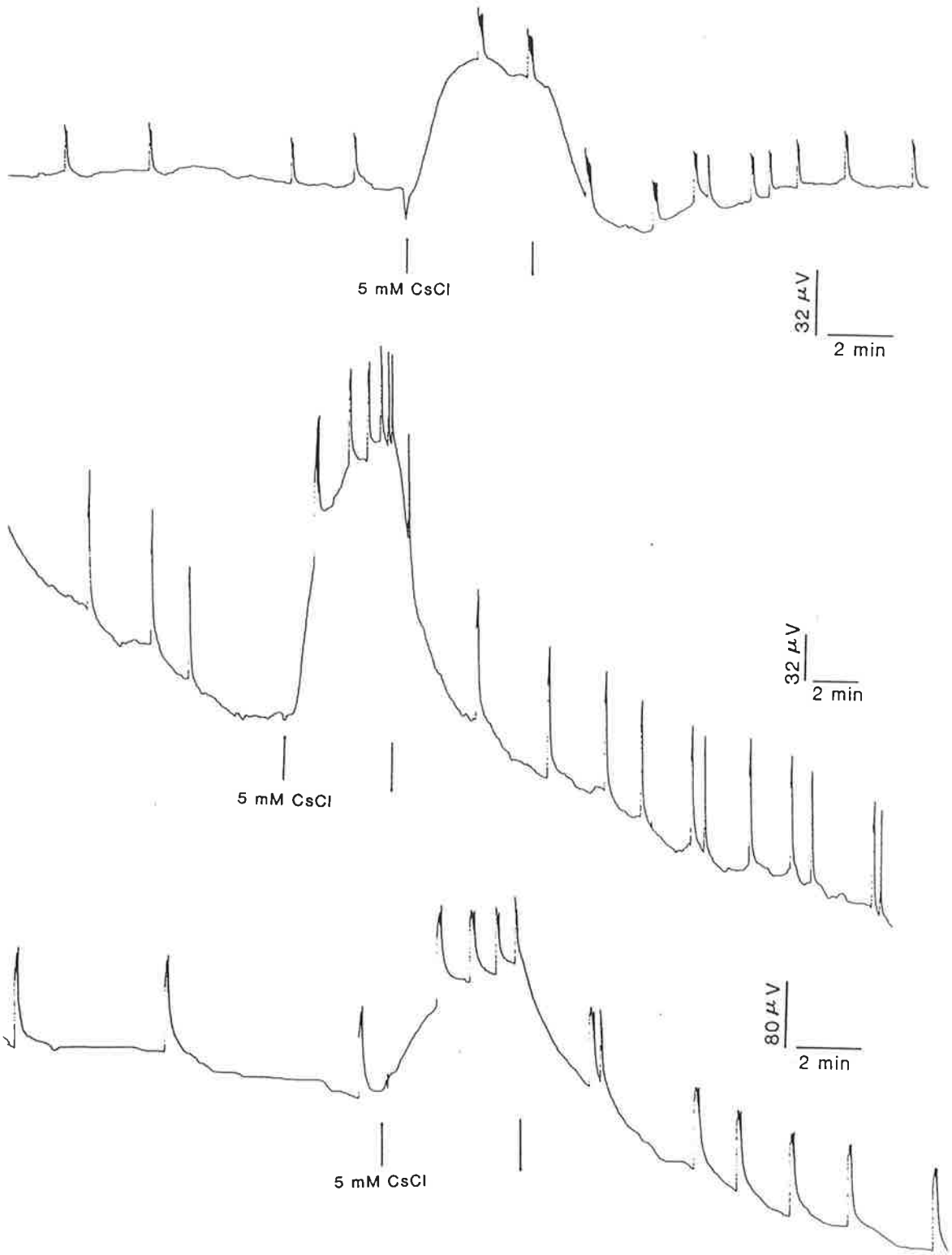

Figure 5.9 Chart recorder traces showing the effect of 5 mM CsCl on spontaneous discharges recorded from neocortical slices. CsCl has extended the after-activity of discharges which are superimposed on a baseline potential.

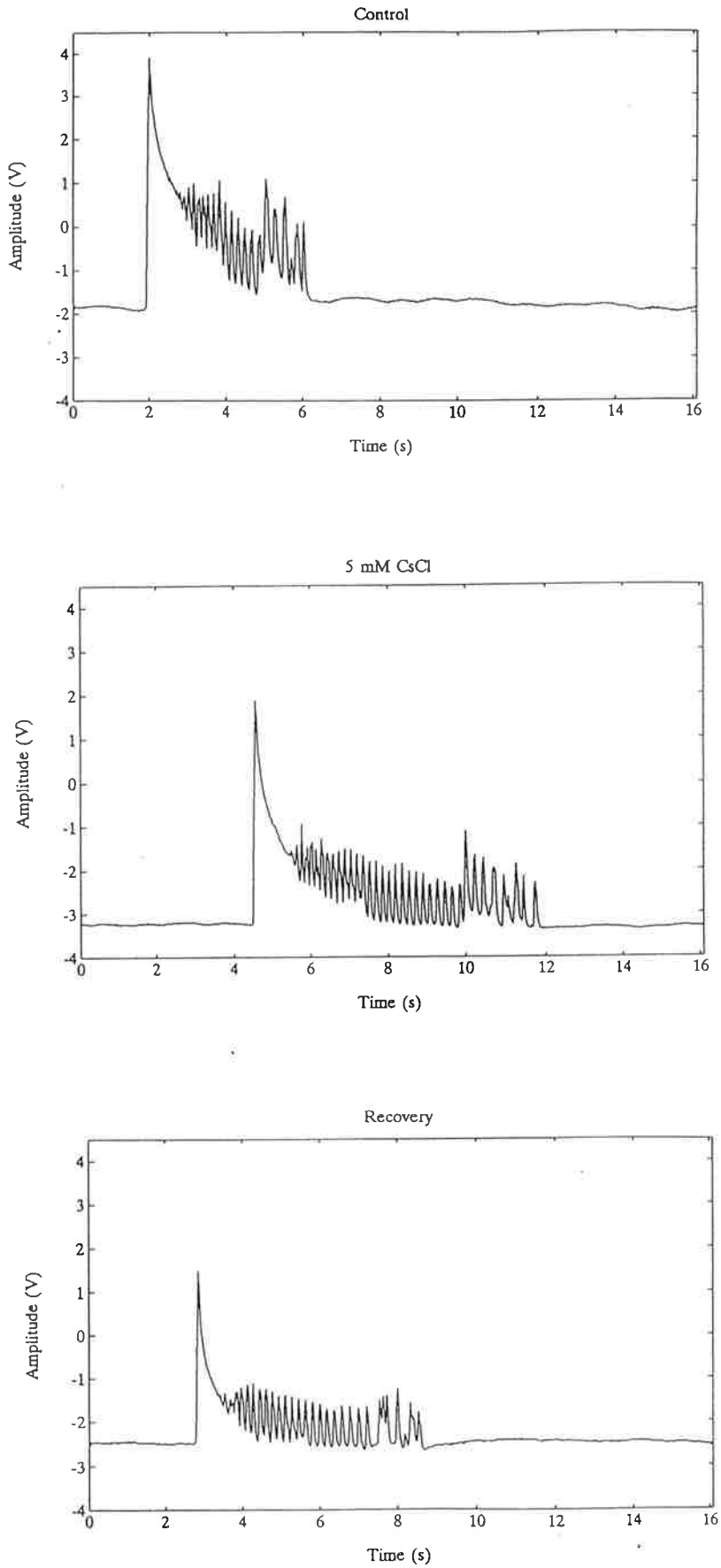

Figure 5.10.a Computer recorded responses showing control, a discharge in the presence of 5 mM CsCl, and recovery. The effect of CsCl in increasing the number of after-potentials is seen in detail. The after-potentials appear low on the falling phase of discharges in this set.

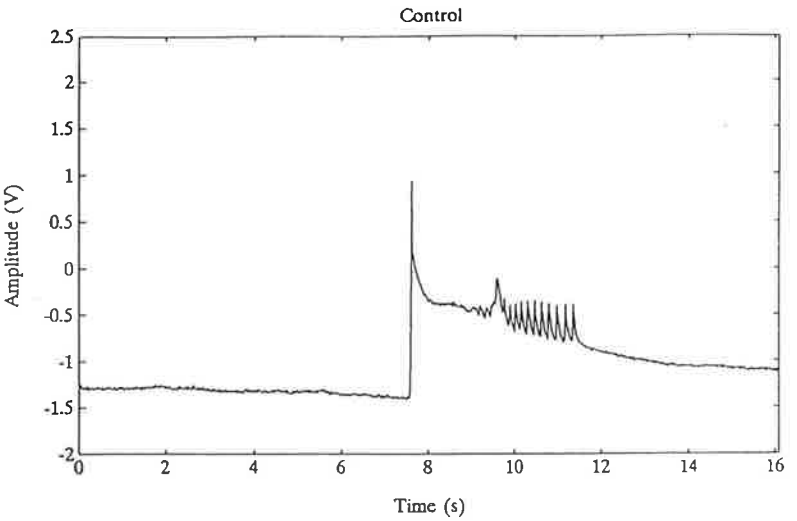

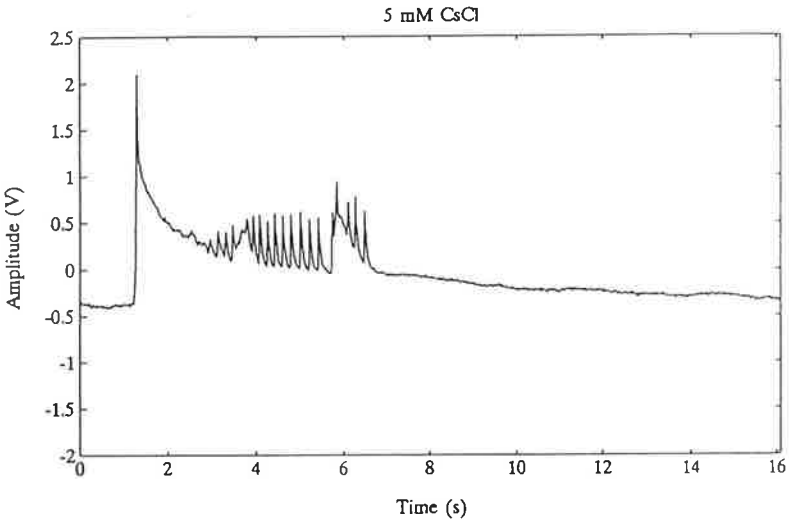

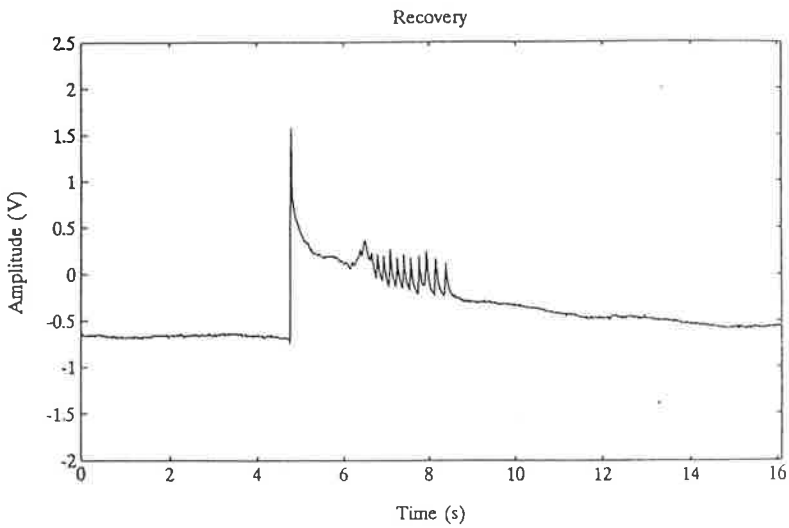

Figure 5.10.b Computer recorded responses showing control, a discharge in the presence of 5 mM CsCl, and recovery. The effect of CsCl in increasing the number of after-potentials is seen in detail.

In experiments reported here, tissue recovery from Cs^+ was similar in time course to recovery from TEA.

5.6 EFFECTS OF 4-AP ON SPONTANEOUS DISCHARGES

Chart recorder traces in Figure 5.11.a show the effect of 10, 20 and 30 μM 4-AP on the activity of a neocortical slice. 4-AP concentrations were made from a 10 mM stock solution containing the total equivalent concentrations of NaCl and KCl, and these were normally applied for a 4 minute duration. As tissue recovery with 4-AP took considerably longer than with CCh or TEA, a period of no less than 30 minutes was allowed between successive applications. Chart recorder data in figure 5.11.b show the effects of 10 and 50 μM 4-AP on discharges recorded from 3 independent slices. An increase in the discharge rate is seen with 4-AP in the 10 to 50 μM concentration range. In one experiment, 10 μM 4-AP increased the discharge rate by 120%, and increased the discharge amplitude by 37.5%. No marked depolarisation was noted with 4-AP applications.

Computer recorded frames in figure 5.12 show that 4-AP not only increased the number of after-potentials, but also caused a 'sharpening' of individual spikes, which suggests multiple-firing.

A fast component of the voltage-regulated K^+ currents, i.e. the transient outward, $I_{K(A)}$, as termed by Connor and Stevens

(1971), is sensitive to 4-AP (Cook, 1988; Rhoades and Gross, 1994). 4-AP also induces neurotransmitter release (Ong et al., 1990, Sihra et al., 1993). The sensitivity of the $I_{K(A)}$ to 4-AP, however, varies between different neuronal cells, in some requiring as much as 1-3 mM 4-AP for inhibition (Franks and Lieb, 1988; Rudy, 1988). The $I_{K(A)}$ current, which activates and inactivates quickly, is distinctive from and clearly separable form the slowly and very slowly inactivating K^+ currents. Overall, the slow components of the voltage-regulated K^+ currents are sensitive to 4-AP (Aronson, 1992; Rhoades and Gross, 1994), but perhaps to a lesser extent than $I_{K(A)}$. This is because these slow components may contain a 'resting' K^+ permeability (Bartschat and Blaustein, 1985a) as well as very sensitive non-inactivating (or moderately sensitive slowly inactivating) voltage regulated K^+ permeabilities (Foehring and Surmeier, 1993).

It is suggested that 4-AP is membrane permeable, and it blocks equally well applied from the inside or outside of a cell, although its blocking site is probably internal (Rudy, 1988).

The repetitive depolarisation induced by 4-AP activates both voltage-sensitive Na^+ channels, which are blocked by TTX, and voltage-sensitive Ca^{2+} channels, which consequently elicits neurotransmitter release (Tibbs et al., 1989; Heemskerk et al., 1991). According to Bartschat and Blaustein (1985b), 4-AP has little effect on K_{Ca} channels in synaptosomes, but stimulates the K_{Ca} channels at higher concentrations by an unknown mechanism.

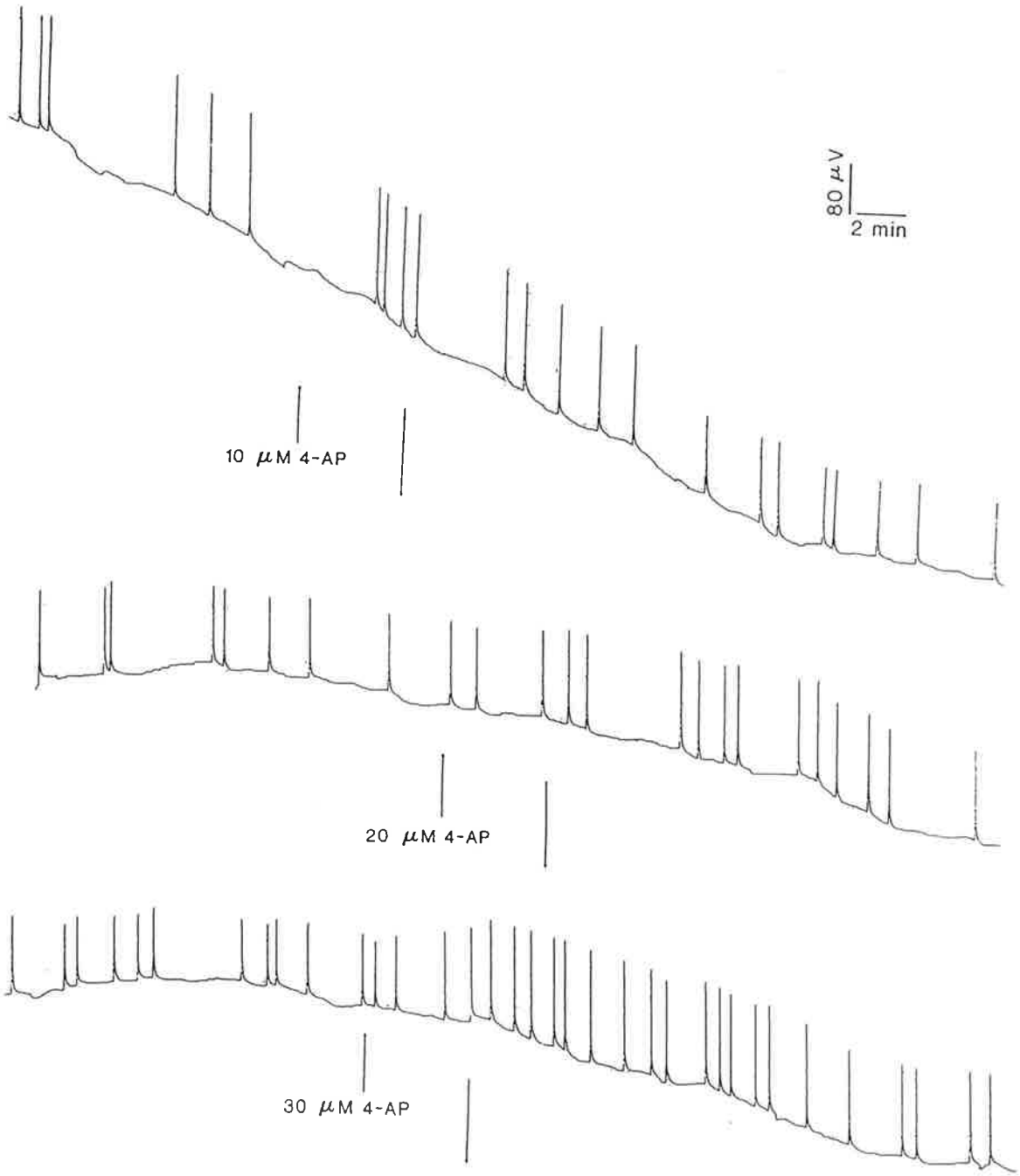

Figure 5.11.a Chart recorder traces showing the effects of 10, 20 and 30 μM 4-AP on spontaneous discharges recorded from the same slice. In excess of half an hour was allowed between applications for tissue recovery.

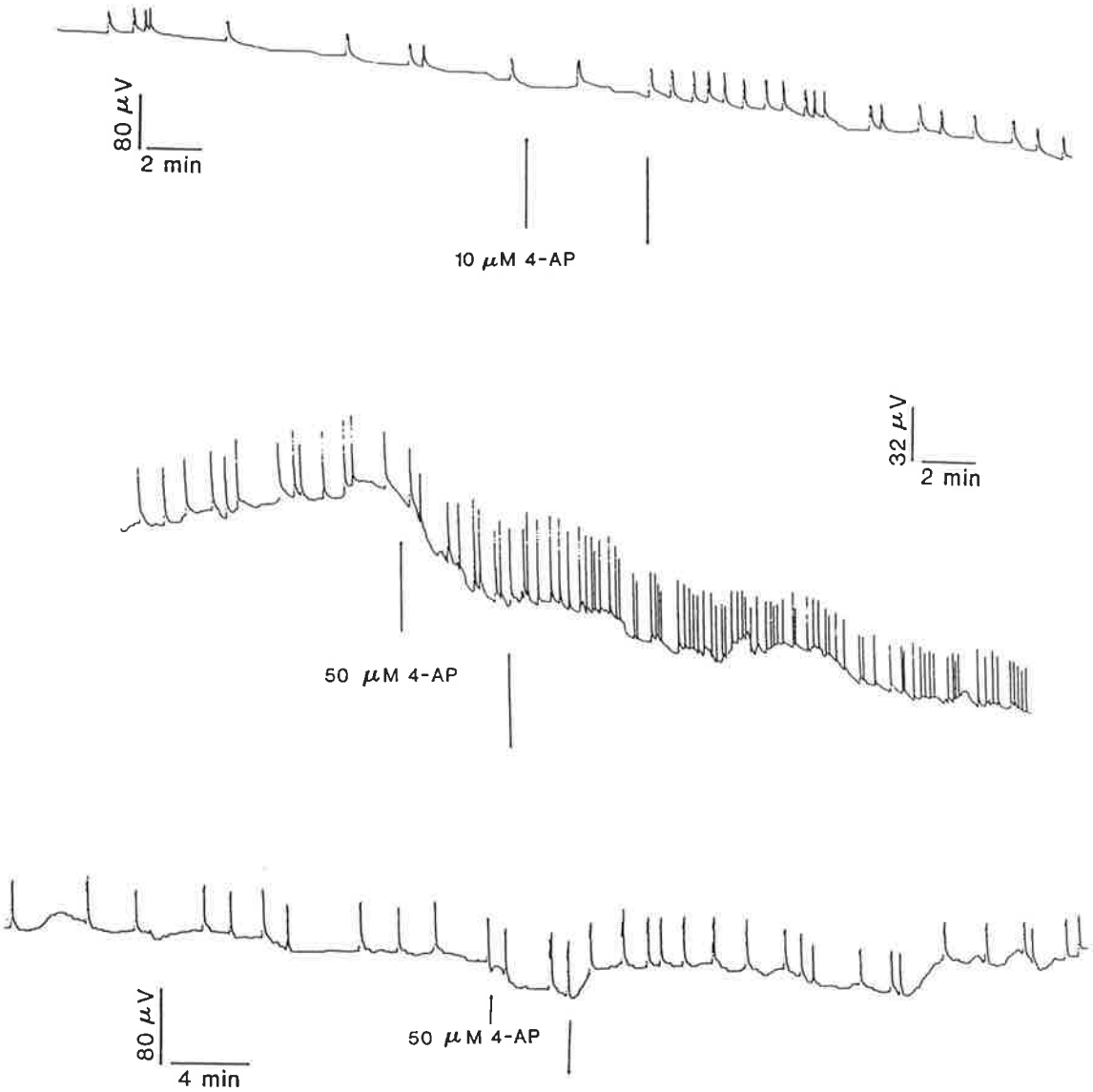

Figure 5.11.b Chart recorder traces showing the effects of 10 and 50 μM 4-AP on spontaneous discharges recorded from slices in 3 experiments.

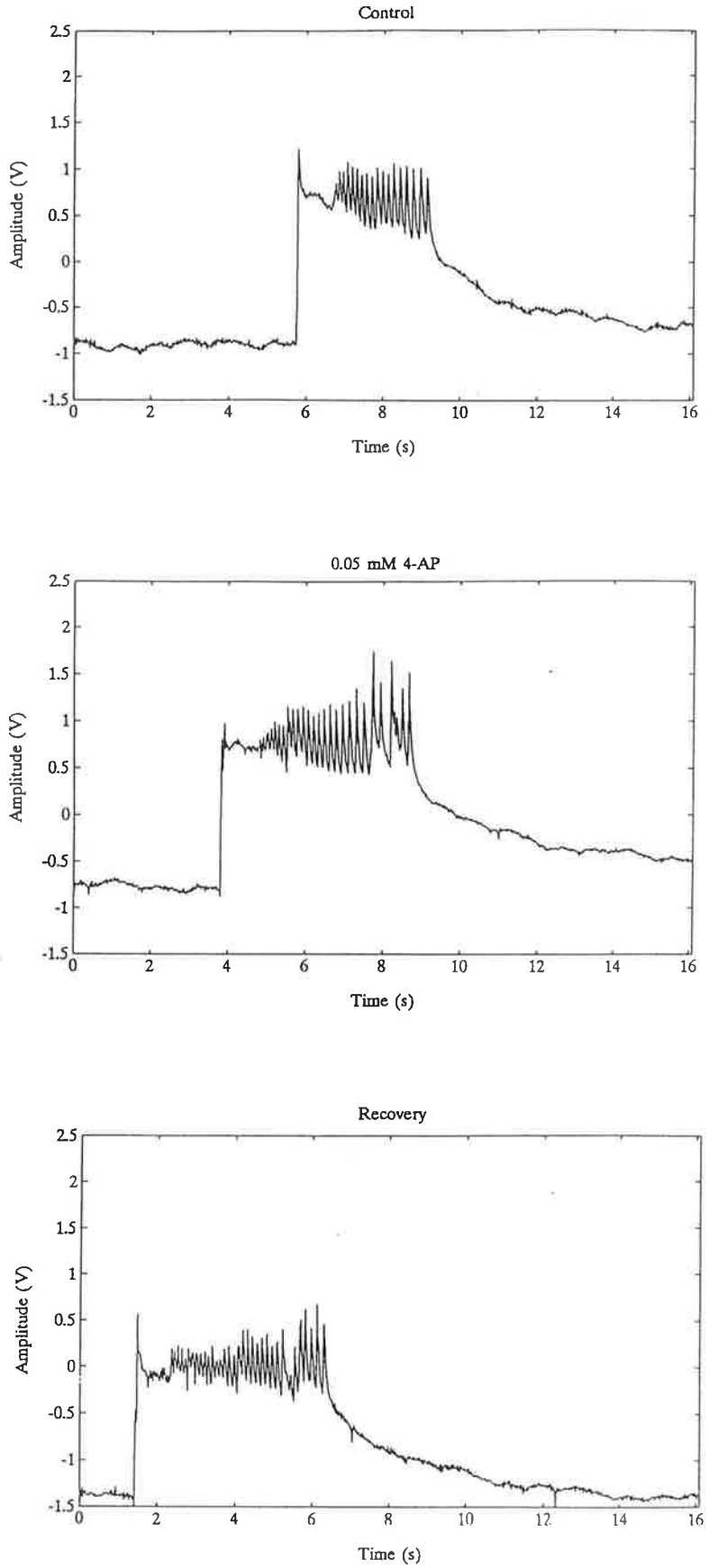

Figure 5.12 Computer recorded responses showing control, a discharge in the presence of 50 μM 4-AP, and recovery. The effect of 4-AP in "sharpening" the after-potential spikes is clearly seen. The bottom frame shows a discharge on partial recovery.

The $I_{K(A)}$ current activates and inactivates quickly, and regulates the frequency of repetitive firing in neurones (Rudy, 1988, Akins and McCleskey, 1993). This current is thought to control the rate of depolarisation, and may be responsible for repolarisation of the pre-synaptic terminal, and for the transient hyperpolarisation which sometimes occurs after repolarisation (Aronson, 1992).

The inward rectifier K^+ channel, K_{IR}, is reported to be insensitive to 4-AP (Cook, 1988; Rudy, 1988). The delayed rectifier K^+ channel is sensitive to 4-AP, albeit at high (mM) concentrations of it (Cook, 1988; Sihra et al., 1993) which implies that TEA and 4-AP have overlapping properties (Cook, 1988), and sometimes difficult to distinguish (Rudy, 1988). This emphasises that 4-AP is not $I_{K(A)}$ specific.

A role for K^+ channels in terminating the epileptiform bursts (Alger and Nicoll, 1980) is supported by Aram and Lodge (1988) who found 10-50 µM 4-AP enhanced the frequency and the number of after-potentials per burst in neocortical slice preparations in Mg^{2+}-free medium, and induced long-lasting paroxysmal activity in the normal medium. Similarly, 100 µM 4-AP is reported to increase the frequency of paroxysmal discharges in neocortical slices (Ong et al., 1990). Furthermore, 4-AP induced both ictal and interictal discharges in juvenile rat hippocampal slices (Avoli et al., 1993). It extended the extracellularly recorded action potential profiles in the cultured spinal cord neurones (Rhoades and Gross, 1994), which increases the strength of excitatory synaptic interactions mediating the increase in discharge

rate. An increase in discharge frequency and the number of after-potentials is also reported in this thesis. However here, an excessive increase in the discharge rate was often associated with a reduction in the number of after-potentials of individual discharges, as prolonged activity could not be sustained during fast discharging.

The 4-AP induced 'sharpening' of after-potentials seen here is not explicitly reported elsewhere. This phenomenon possibly represents renewed firing of the initiating events rather than true after-potentials as seen with CCh. In fact, Rhoades and Gross (1994) report that 4-AP reduced the burst amplitude with successive 20 µM incremental additions, in cultured spinal cord neurones.

5.7 EFFECTS OF $BaCl_2$ ON SPONTANEOUS DISCHARGES

Application of $BaCl_2$ to neocortical wedges, in the present study, extended the discharges and induced a slow, exponentially decaying phase of discharge after-activity. Ba^{2+} concentrations in the range of 100 to 1000 µM were made by diluting a 10 mM stock solution containing the total ACSF equivalent amounts of NaCl and KCl compounds and were normally applied to brain slices for 4 minutes. 500 µM $BaCl_2$ was the standard concentration used, and its effect was ascertained in 8 experiments on different brain slices. This concentration of Ba^{2+} always produced a pronounced shift in baseline within 60 s of reaching the tissue, and induced a massive increase in

the rate of occurrence of discharges, which were superimposed upon such shifts. Ba^{2+}-induced baseline potential changes were dose-dependent, and sometimes attained 100 µV in amplitude of 10 minute duration. Ba^{2+} often increased the amplitude of discharges, especially around the peak of the depolarisation. Tissue recovery with Ba^{2+} was slower than with other K^+ channel blockers described earlier. As supported by Rhoades and Gross (1994), postwash restoration of the initial activity pattern following Ba^{2+} application took 30 minutes or more.

Chart recorder traces in figure 5.13.a show the effects of 50, 100 and 500 µM $BaCl_2$ on the same neocortical slice. Over ½ hour was allowed for tissue recovery between applications, while tissue remained in the optimal condition for the initial 2 to 3 hours of recording. As little as 50 µM $BaCl_2$ increased the discharge rate, on average, by 140%. Figure 5.13.b shows the effect of 1 mM $Bacl_2$, which has not only markedly induced tissue hyperexcitability, but also altered the after-activity of discharges. The mean increase in discharge rate with 500 µM $Bacl_2$ was 275%, and with 1 mM $Bacl_2$ was 360%. The discharge after-potentials sometimes disappeared when the Ba^{2+}-induced firing rate exceeded 5 per second, and these after-potentials reappeared later on partial recovery.

Figure 5.14 shows a set of computer recorded discharges, which illustrate how 500 µM $BaCl_2$ typically shifted the after-potentials down the falling phase, and slowed their frequency.

$BaCl_2$ blocks the anomalous (inward) rectifier current, $I_{K(IR)}$. This is verified by Sutor and Hablitz (1993) who demonstrated

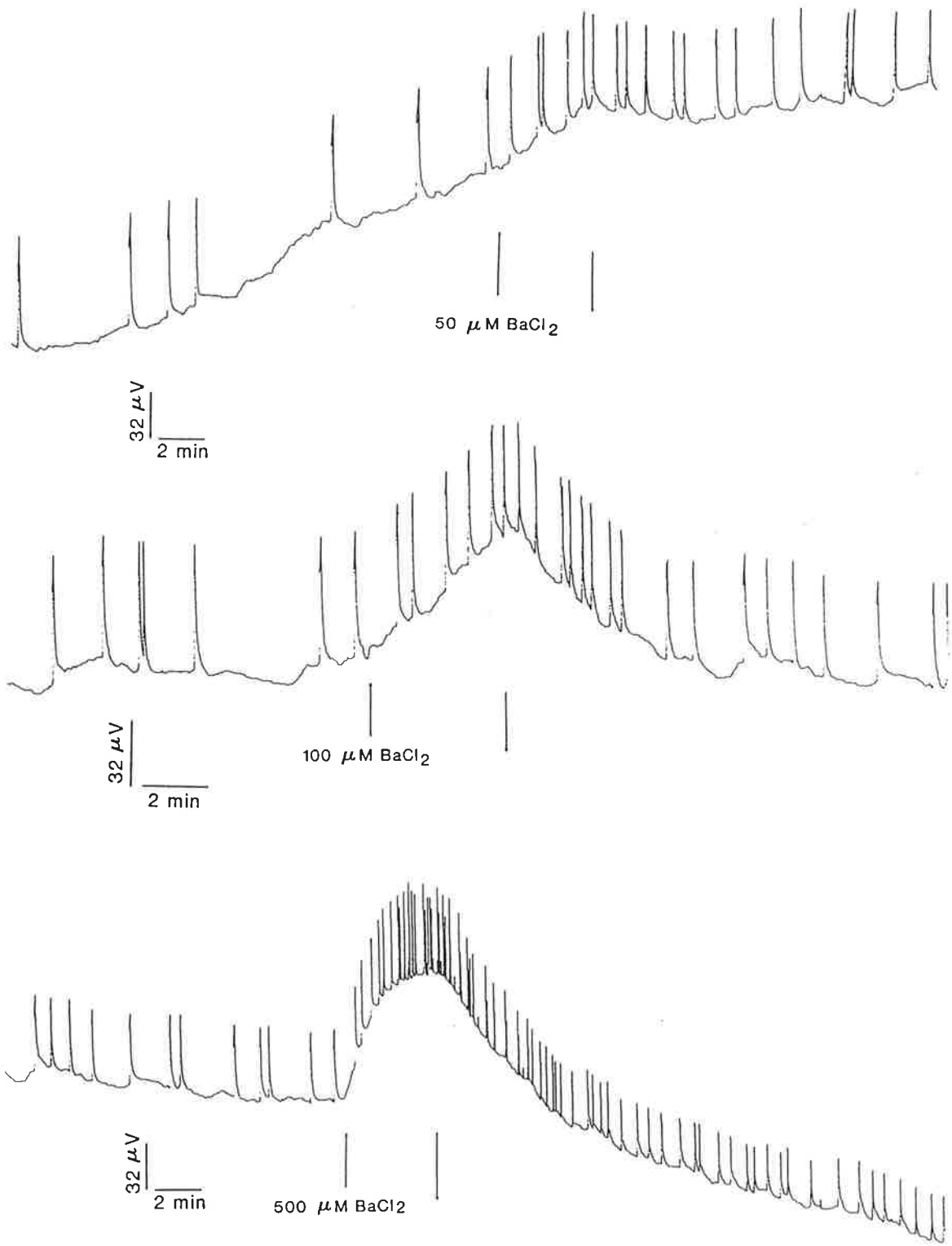

Figure 5.13.a Chart recorder traces showing the effects of 50, 100 and 500 μM $BaCl_2$ on spontaneous discharges recorded from a neocortical slice. As tissue recovery was very slow with $BaCl_2$, up to an hour was allowed between successive 4 minute applications.

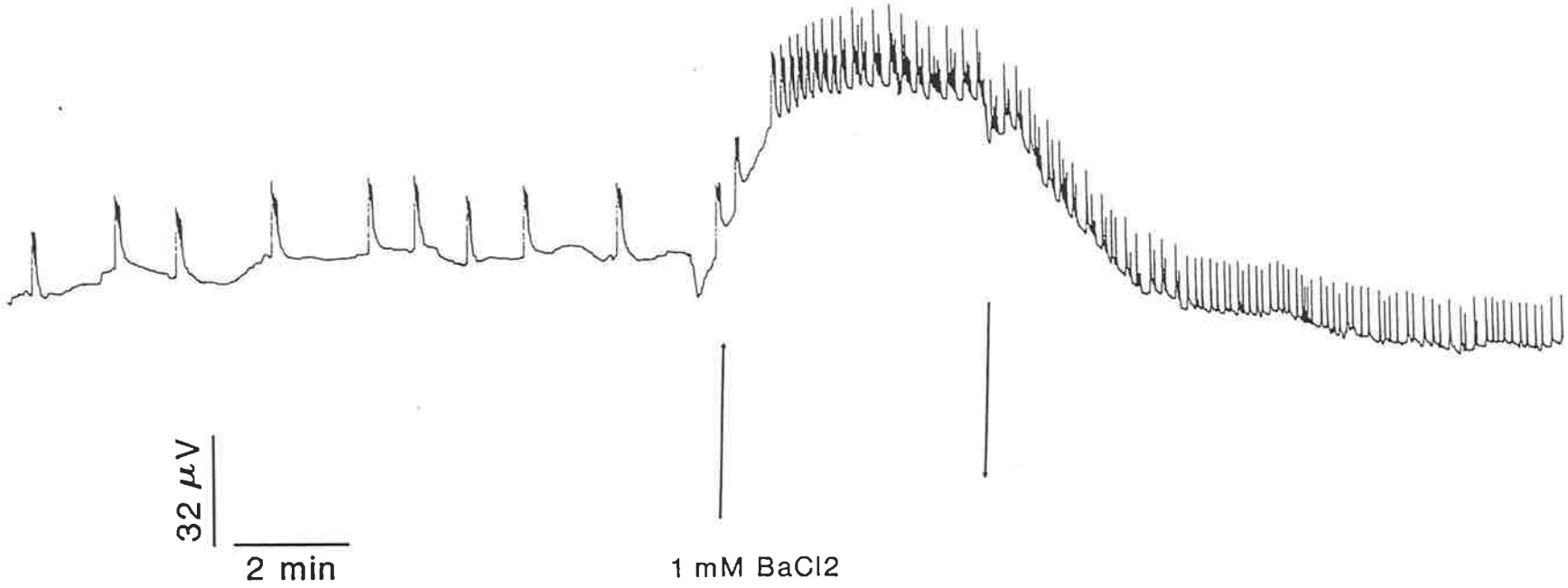

Figure 5.13.b The effects of 1 mM $BaCl_2$ on spontaneous discharges recorded from a neocortical slice. 1 mM $BaCl_2$ induced tissue hyperexcitability and moved the after-activity of discharges down the falling phase.

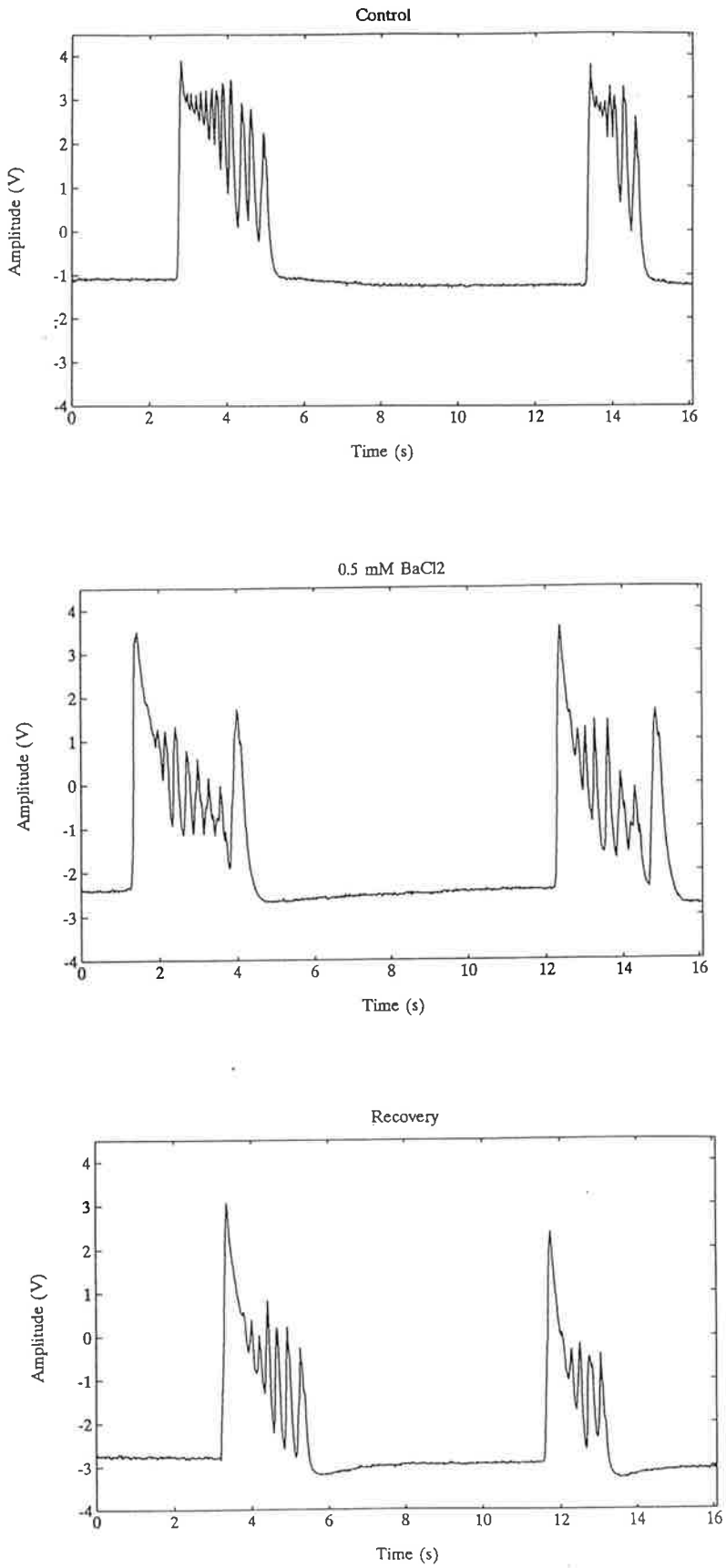

Figure 5.14 Computer recorded responses showing control, discharges in the presence of 500 μM $BaCl_2$, and recovery. The effects of $BaCl_2$ in lowering the after-potentials on the falling phase of discharges, and reducing the frequency of the after-potentials are clearly seen. The bottom frame shows discharges on partial recovery.

that Ba^{2+}, at concentrations of 10-100 µM, blocks an inwardly rectifying potassium conductance, active at rest in layer II-III of rat neocortical neurones. The inward rectifier currents are voltage-activated by hyperpolarisation around the resting potential, and may be involved in maintaining the plateau of action potentials, as well as controlling the duration of after-hyperpolarisation (Aronson, 1992). Ba^{2+} also induces neurotransmitter release (Ong et al., 1990).

Ba^{2+} blocks the inward rectifier channel (K_{IR}), which is G-protein coupled to a range of receptors including $GABA_B$. It is also reported to block voltage-sensitive delayed (outward) rectifier, high conductance Ca^{2+}-activated, and receptor-coupled K_M and K_{5-HT} channels (Cook, 1988; Rudy, 1988). These indicate that, like Cs^+, Ba^{2+} is a broad spectrum K^+ channel blocker. The interaction of Ba^{2+} with the delayed K^+ channel of the mammalian brain neurone is, however, much slower than TEA (Oyama et al., 1991).

Ba^{2+} depolarises the nerve terminal, through blocking the K^+ channels, which activates TTX-sensitive Na^+ channels, causing further depolarisation. It can enter the terminal through the voltage-regulated Ca^{2+} channels during depolarisation. Ba^{2+} is equipermeant with calcium through the T-type Ca^{2+} channels, but is more permeant through the L- and N-type Ca^{2+} channels. Ba^{2+} is unlikely to cause a significant increase in the inward current if only the T channels are active. Following entry, Ba^{2+} accumulates in the nerve terminal to a greater extent than Ca^{2+} because it is not sequestered by the intraterminal buffering systems as effectively as Ca^{2+}. Thus, even if Ba^{2+}

entry under non-depolarising conditions were low, Ba^{2+} would amass in the nerve terminal. It acts on the neurotransmitter release mechanism, either directly or through envoking the release of intracellular Ca^{2+} (Ong et al., 1990; Sihra et al., 1993). In contrast, immediately after neuronal activity, the Ca^{2+} is rapidly buffered, sequestered and extruded. Residual Ca^{2+} may remain in the cytoplasm following a period of activity, and may add to the Ca^{2+} that enters during subsequent neuronal activity to enhance the transmitter release directly (Bartschat and Blaustein, 1985b).

There is conflicting evidence on the effect of internal Ba^{2+} on the K_{Ca} channels. Yoshida et al. (1991) report that an increase in the internal concentration of Ca^{2+}, Sr^{2+}, or Ba^{2+}, increases the open probability of the K_{Ca} channel, whereas McLarnon and Sawyer (1993) observed that Ba^{2+} inhibits K_{Ca} channels when added internally to a high (0.2 mM) or a low (5 μM) concentration of Ca^{2+}.

Overall, the convulsant actions of 4-AP and Ba^{2+} on neocortical slices are therefore likely to involve an increase in neurotransmitter release, by enhancing presynaptic inward calcium current, where both inhibitory and excitatory synaptic transmission may be affected (Aram et al., 1989). Sihra et al. (1993) found that Ba^{2+} (1 mM), and 4-AP (3 mM) plus Ca^{2+} (1.1 mM) are qualitatively similar in evoking both membrane depolarisation and transmitter release, and in inducing responses in the presence of 1 μM TTX. These results indicate that Ba^{2+} and 4-AP act by a similar sequence of events, which includes activation of Na^{+} channels. In experiments reported

here, Ba^{2+} in the 50-1000 μM range was found to be more potent that 4-AP in the 10-50 μM range in both initiating and maintaining neuronal firing.

Many calcium channel studies use Ba^{2+} or Sr^{2+} as the charge carriers for recording voltage dependent currents (Bean, 1989; Huston et al., 1990; Formenti and Sansone, 1991; Pennington et al., 1991; Yoshida et al., 1991; Mulle et al., 1992; McLarnon and Sawyer, 1993; Sutor and Hablitz, 1993). Reportedly, these cations have a higher permeability than Ca^{2+} through the channels, thereby producing larger currents, and they do not inactivate the channels to the same extent, thereby giving more sustained currents (Jones et al., 1992). Although Ba^{2+} and Sr^{2+} readily pass through voltage-gated calcium channels (Hagiwara and Ohmori, 1982), these divalent cations do not mimic the actions of Ca^{2+} on K_{Ca} currents (Gorman and Hermann, 1979), or calcium-dependent metabolic processes (Chad and Eckert, 1986). Therefore it is not unreasonable to suggest that Ba^{2+} and Sr^{2+} currents do not behave identically to Ca^{2+} with respect to the inhibition by neurotransmitters (Jones et al., 1992). Indeed, Ba^{2+} carries through Ca^{2+} channels, but interferes with many Ca^{2+}-dependent intracellular processes (Rhoades and gross, 1994). Network bursting is dependent on Ca^{2+} entry and intracellular Ca^{2+} levels. Blocking the Ca^{2+} entry eliminates bursting and most spike activity, which could partly be due to blockage of the synaptic interactions by reducing transmitter release.

5.8 EFFECTS OF $SrCl_2$ ON SPONTANEOUS DISCHARGES

In a comparative study on the effect of Sr^{2+} and Ba^{2+}, neocortical slices showed much more sensitivity to Ba^{2+} than to Sr^{2+}. Ba^{2+} was found to be 25 to 50 times more potent in increasing the discharge rate than Sr^{2+}. In fact, no significant effect on discharge rate was seen with 1 mM $SrCl_2$, whereas 5 mM $SrCl_2$ did increase the discharge rate although, on average, by only 56%. Occasionally Ba^{2+} was used to initiate neuronal discharging in unresponsive slices, i.e. to test for tissue viability.

Figure 5.15 shows chart recorder data comparing the effects of CsCl, $BaCl_2$ and $SrCl_2$. Section (a) compares the effects of 5 mM CsCl and 1 mM $BaCl_2$ on the firing rate of a neocortical slice. Similarly, section (b) compares the effects of 500 µM $BaCl_2$ and 5 mM CsCl on the activity of a different slice. Both sections (a) and (b) clearly show that Ba^{2+} induced a much higher discharge rate than Cs^+ in this neocortical wedge model. Section (c) shows the effect of 5 mM $SrCl_2$ on epileptiform discharges recorded from a neocortical slice. Clearly, Sr^{2+} is not as potent as Ba^{2+} in modifying the discharge rate. In fact, it behaves more similar to Cs^+ in inducing tissue hyperexcitability. This is confirmed by traces in section (d) showing that 5 and 10 mM $SrCl_2$ failed to initiate neuronal firing in an unresponsive slice, whereas 500 µM $BaCl_2$ initiated intense discharging in the same slice.

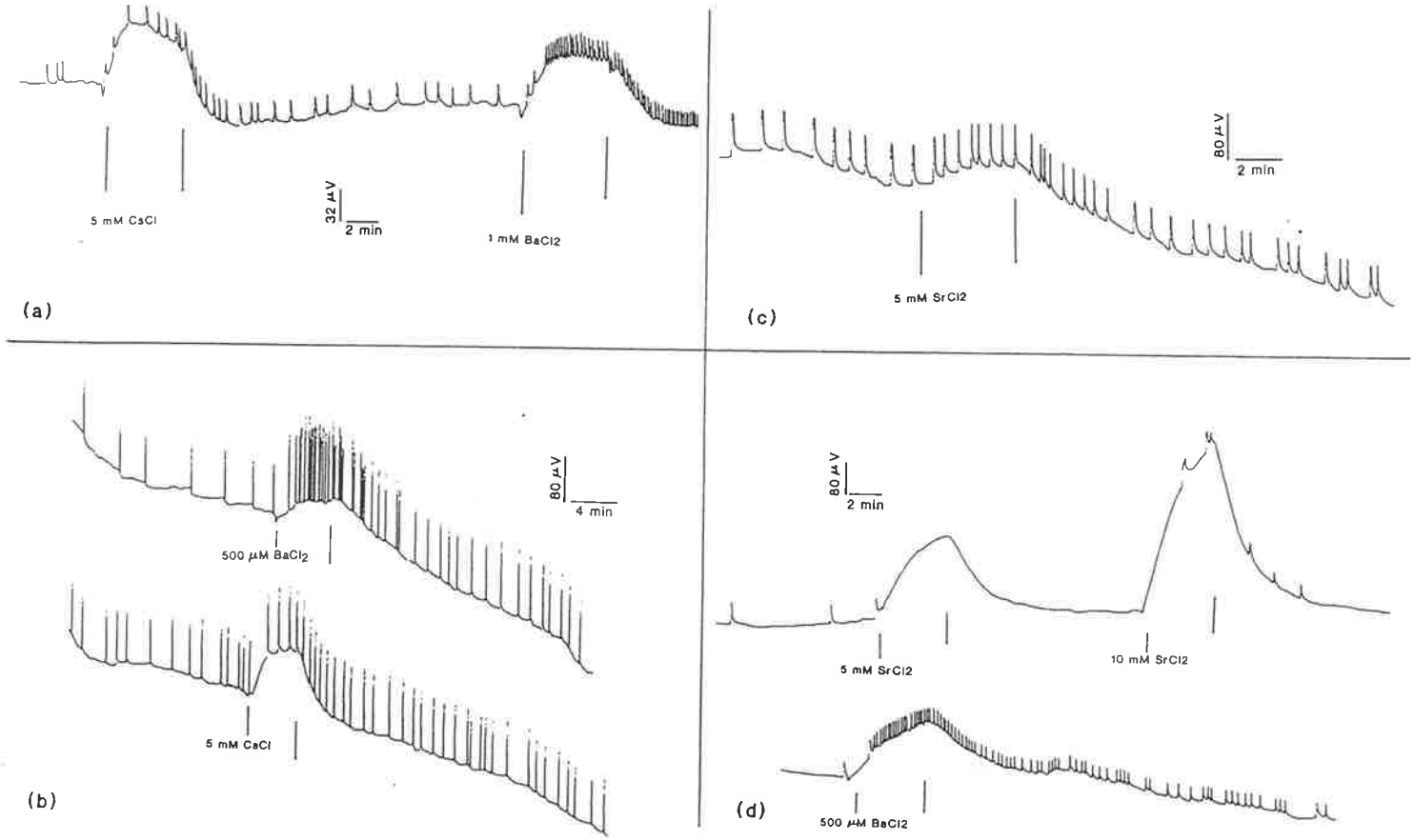

Figure 5.15 Chart recorder data comparing the effects of CsCl, $BaCl_2$ and $SrCl_2$ on epileptiform discharges recorded from neocortical slices. Section (a) shows the effects of 5 mM CsCl and 1 mM $BaCl_2$ on the same slice. Similarly, section (b) compares the effects of 500 µM $BaCl_2$ and 5 mM CsCl on a neocortical slice in another experiment. Section (c) shows only the effect of 5 mM SrCl2 on a slice. Finally, section (d) compares the effects of 5 and 10 mM $SrCl_2$ on a weakly responsive tissue, and shows that 500 µM Ba^{2+} induced tissue hyperexcitability in the tissue. Overall, figure 5.15 suggests that the effect of Sr^{2+} in modifying tissue hyperexcitability resembles Cs^{+} much more than Ba^{2+}.

5.9 EFFECTS OF $CoCl_2$ ON SPONTANEOUS DISCHARGES

The effect of 500 µM $CoCl_2$ on spontaneous activity of neocortical slices was briefly investigated. Co^{2+} is reported to block the K_{Ca} conductance (Franks and Lieb, 1988), as well as the N- and L-type Ca^{2+} conductances (Boulton and O'Shaughnessy, 1991).

Figure 5.16 is a chart recorder trace showing that $BaCl_2$ induced discharges in a neocortical slice, and $CoCl_2$ modified the discharge rate. The upper trace shows that 5 mM CsCl had little effect on an inactive slice, whereas 500 µM $BaCl_2$ initiated paroxysmal firing. The middle trace shows the effects of a repeated application of 500 µM $BaCl_2$, followed by 500 µM $CoCl_2$ on the same slice. The bottom trace shows the effect of a mixture of 500 µM $BaCl_2$ plus 500 µM $CoCl_2$ on the firing rate of the slice. As the same slice was used, over ½ hour was allowed between applications for tissue to stabilise. As noted, Co^{2+} significantly reduced the Ba^{2+}-induced increase in discharge rate, presumably by blocking the Ca^{2+} or K_{Ca} conductances, which are responsible for generating or maintaining the repetitive firing, or by blocking synaptic transmission (Karnup, 1992). Although Rhoades and Gross (1994) report that in cultured fetal murine spinal cord networks bursting was slowed and reduced in amplitude by a 1.8 mM addition of $CoCl_2$, and was generally eliminated by 10 mM, no significant change in amplitude of discharges was noted here. Additionally, Ba^{2+}-evoked release of glutamate is blocked by 10 µM $CdCl_2$ or 10 µM $CoCl_2$ (Sihra et al., 1993). As NMDA receptors are coupled to Ca^{2+} channels, a role for Co^{2+}

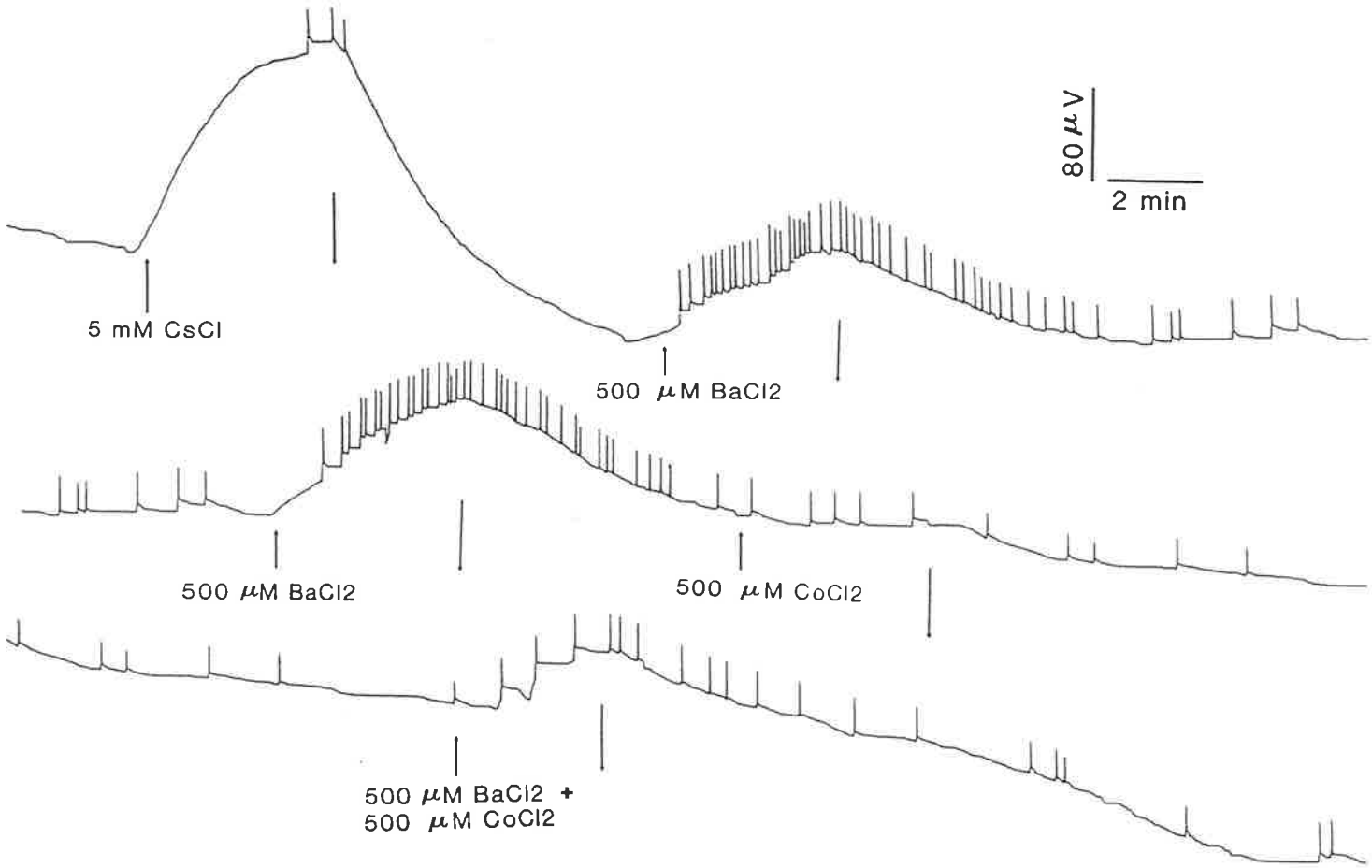

Figure 5.16 The effect of $CoCl_2$ on the activity of a neocortical slice. The upper trace shows how 500 μM $BaCl_2$ initiated regular firing in a slice which showed no significant response to 5 mM CsCl. The middle trace shows how application of 500 μM $CoCl_2$, following 500 $BaCl_2$, reduced the discharge rate. The bottom trace shows the effect of applying a mixture of 500 μM $BaCl_2$ plus 500 μM $CoCl_2$. Tissue was allowed to stabilise between applications.

blocking the NMDA ion channels, which mediate epileptogenesis, may also exist.

5.10 EFFECTS OF REDUCING EXTERNAL Ca^{2+} ON SPONTANEOUS DISCHARGES

Ca^{2+} channels are generally classified into L-, N- and T-types. The most ubiquitous Ca^{2+} channels are the L-type (long-lasting) channels, which are characterised by a high threshold for voltage activation (HVA), slow inactivation kinetics and sensitivity to dihydropyridines. Nifedipine and verapamil are L-channel antagonists. The N-type (neuronal type), which are also HVA (Formenti and Sansone, 1991), are involved in transmitter release. The T-type Ca^{2+} channels are low voltage activating, and exhibit fast inactivation kinetics.

Ca^{2+} influx underlying epileptiform activity in the rat neocortex may occur partially via the activation of the N-type Ca^{2+} channel. L- and N-types channels are blocked by w-conotoxin, Co^{2+} and Cd^{2+}, significantly reducing the epileptiform activity (Boulton and O'Shaughnessy, 1991), although the prolongation of Ca^{2+} channel current activation may be due to a block of the N-type current that reveals a more slowly activated L-type current (Formenti and Sansone, 1991). The peptide w-CTX-GVIA (300 *n*M) is ineffective in altering the rate of spontaneous discharges, and Ni^{2+}, which antagonises the T-type current, shows a variable effect on the epileptiform activity (Robichaud et al., 1994).

Additionally, P- and Q-channels form two further sub-types of Ca^{2+} channels. It is reported that blocking the P-type channel by 300 *n*M w-Aga-IVA reduced the frequency of spontaneous epileptiform discharges in rat cortical wedge by 63%, while 300 *n*M w-CTX-MVIIC peptide blocked the new Q-type channel, which is resistant to dihydropyridines, w-CTX-GVIA and w-Aga-IVA, reducing the frequency by 35% (Robichaud et al., 1994).

Figure 5.17 comprises 4 chart recorder traces. The first 2 traces, (a) and (b), show the effects of 500 µM $BaCl_2$ on the activity of a neocortical slice. A time period exceeding ½ an hour was allowed for tissue recovery after each application. The slice was then superfused by the ACSF containing only 0.5 mM Ca^{2+} for 20 minutes. Section (c) shows that lowering the Ca^{2+} level from 2 to 0.5 mM did not markedly modify the rate of occurrence of discharges, or their amplitude, but 500 µM $Bacl_2$ induced a higher rate of discharging. At the next stage, shown by the chart recorder trace (d), the Ca^{2+} level was further lowered to 0.1 mM. Following superfusion with this low calcium ACSF for 20 minutes, the activity of the slice severely declined, producing much smaller and infrequent discharges. Interestingly, 500 µM Ba^{2+} could not substitute for the low Ca^{2+} level in restoring normal activity. The required $BaCl_2$ concentration for each application was made up by diluting a 10 mM stock in the corresponding Ca^{2+} containing ACSF.

Removal of Ca^{2+} from the medium leads to a marked reduction in the frequency and amplitude of paroxysmal events, suggesting

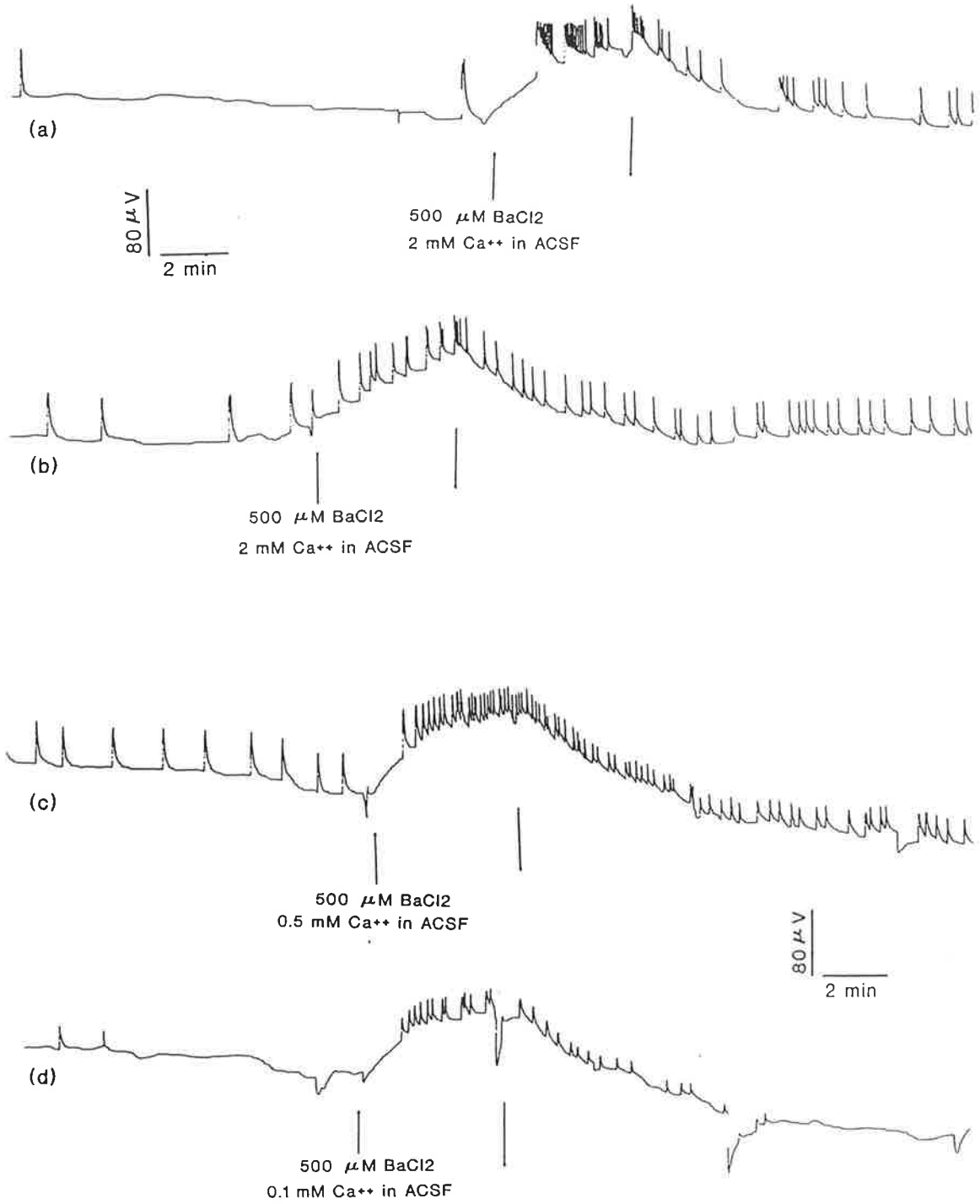

Figure 5.17 The effect of decreasing Ca^{2+} concentration in the superfusing medium on spontaneous discharges recorded from a neocortical slice. Chart recorder traces (a) and (b) show the effect of 0.5 mM $BaCl_2$ on the firing pattern of a neocortical slice. (c) and (d) show the effects of 500 μM $BaCl_2$ on the activity, having first superfused the tissue with the ACSF solutions containing 0.5 or 0.1 mM Ca^{2+}, each for 20 minutes. In excess of half an hour was allowed for tissue recovery after each $BaCl_2$ application.

that neurotransmitter release is essential to the initiation of events and the subsequent recruitment of neurones to generate the waveform (Horne et al., 1986). Aram and Lodge (1988) found that at 1.0 to 0.75 mM calcium, epileptiform activity in the neocortical slices was most pronounced in terms of amplitude and duration, but the frequency of spontaneous bursts was reduced, whereas below 0.5 mM calcium, the number of after-potentials was also reduced. These findings confirm a role for Ca^{2+} in maintaining regenerative conductances. Indeed, in hippocampal neurones neither Mg^{2+} nor Sr^{2+} (0.2 mM) added internally were effective in the activation of K_{Ca} when internal Ca^{2+} was very low (0.1 μM), but both could potentiate Ca^{2+}-induced activation of K_{Ca} in the presence of a slightly higher (5 μM) Ca^{2+} concentration (McLarnon and Sawyer, 1993). This confirms the earlier findings that Ca^{2+} is needed for neuronal activity, and the other divalent ions can not completely substitute for it.

5.11 EFFECTS OF CAFFEINE ON SPONTANEOUS DISCHARGES

There was interest in this project to find means of increasing the number of after-potentials of individual discharges so that modification of their after-potentials by various K^+ channel blockers could be compared by means of spectral analysis, which would provide further indirect information on cellular ionic mechanisms (see chapter 6).

50 to 100 μM Caffeine was applied on one occasion in an attempt to increase the number of after-potentials. Caffeine increased the discharge rate, but had no significant effect on the number of after-potentials. It was later established that CCh was the most suitable agent in extending the activity of individual discharges.

Although it may seem inappropriate to include caffeine in a chapter on K^+ channel pharmacology, nevertheless figure 5.18 is inserted to demonstrate the effects of 50 and 100 μM caffeine on spontaneous discharges recorded from a neocortical slice.

The effect of purines on the CNS neurones is predominantly inhibitory. A pre-synaptic inhibitory effect occurs at many central and peripheral synapses. It is mediated by P_1 receptors, which are more sensitive to adenosine than to ATP, and which are blocked by methylxanthines. Both inhibitory and excitatory post-synaptic effects have been described. The mechanism of action of the methylxanthines e.g. caffeine and theophylline is interesting in relation to the hypothesis of purinergic transmission. These drugs have a stimulant effect on the central nervous system, and are known to be antagonists at the P_1 receptor. However they also inhibit the enzyme phosphodiesterase which destroys cAMP, and it is not clear which (if either) of these biochemical effects underlies their action on the CNS. Caffeine is reported to elevate the internal Ca^{2+} level (Jones and Harrison, 1993).

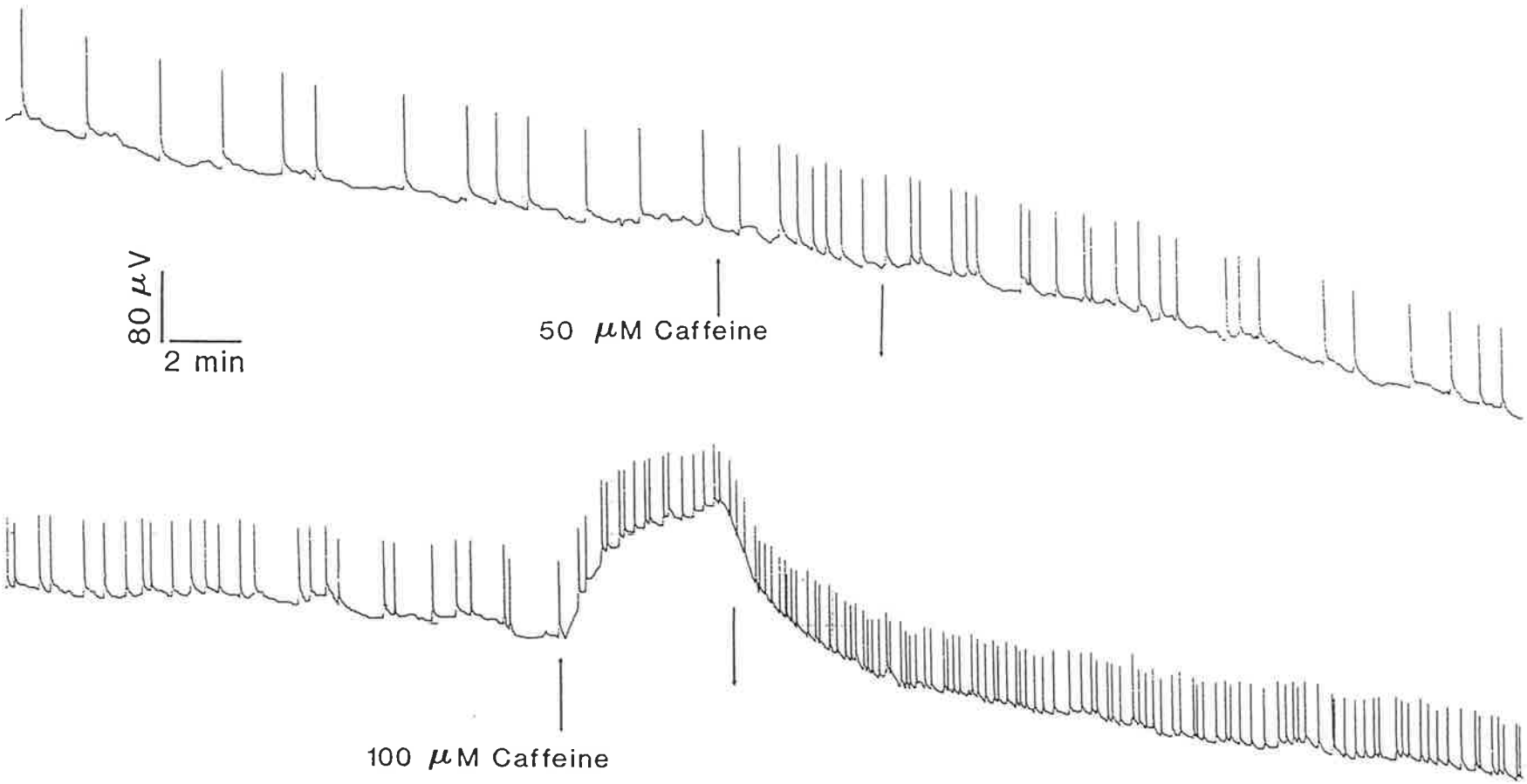

Figure 5.18 The effects of 50 and 100 μM Caffeine on spontaneous discharges recorded from a neocortical slice. A four-minute application of 100 μM Caffeine has markedly increased the discharge rate. No marked change in the duration of discharges is seen with the applications.

5.12 BASELINE POTENTIAL SHIFT

As mentioned earlier, baseline potential shifts were seen with applications of TEA, CsCl and $BaCl_2$. A series of experiments were conducted to establish the nature of these baseline potentials. Commonly used concentrations of CsCl (5 and 10 mM) and $BaCl_2$ (0.5 and 1 mM) were applied to spontaneously active slices. The tissue was then killed by applying a 0.1 M HCl solution to it for a few seconds, or raising the temperature of the superfusing ACSF solution to over 50 °C for a few minutes, and the tests were repeated. In some experiments control responses were recorded, the tissue was then removed and kept in the fridge overnight, and placed back next morning to compare the responses to Cs^+ and Ba^{2+}. Surprisingly, baseline shifts were seen when Cs^+ or Ba^{2+} was applied to the dead tissue, despite the fact that Cs^+ or Ba^{2+} stock solutions contained the total ACSF equivalent concentrations of NaCl and KCl, and the required concentrations were diluted in the ACSF. It was however difficult to ascertain the relative contributions of tissue depolarisation and the ionic concentration effect across the grease-gap to the overall potential, as these potentials were inconsistent. The potential varied with applications to the same slice, as well as between slices. Direct comparisons were made difficult since a long time had to be allowed for recovery between successive applications of Cs^+ or Ba^{2+} during which tissue viability and responsiveness always deteriorated. It appears that the answer may have been found through investigating the baseline potentials on tissues which alternated between being dead and alive, which is of course

inconceivable. Robichaud and Boxer (1993) also remark on non-specificity of the baseline shift in response to application of polyamines in a grease-gap recording model.

5.13 EFFECTS OF TEMPERATURE ON NEOCORTICAL SLICE ACTIVITY

In slices where the effects of temperature were under study, raising it from 23 °C to 29 °C led to an increase in the rate of occurrence, amplitude and particularly duration of spontaneous discharges. Additionally, the number of discharge after-potentials often increased. Above 30 °C, although the rate and amplitude remained high, the number of after-potentials per discharge started to decrease. By 37 °C, the amplitude also decreased, and although tissues discharged well, most discharges had few after-potentials. All these effects of temperature appeared to be fully reversible. In all experiments reported in this thesis, the temperature was reliably maintained at 29 °C, which appeared to be the optimum recording temperature. Synaptic activity in slice preparations has been reported to be optimal between 20 and 30 °C, due to reduced neurotransmitter uptake (Algar and Nicoll, 1982) and/or increased probability of neurotransmitter release (Hubbard et al., 1971). At 29 °C the long-term viability of slices presumably improved, since satisfactory recording could be obtained for up to 10 hours, although, in general, the amplitude and number of after-potentials of discharges always deteriorated after the initial 2-3 hours, irrespective of recording conditions. Aram and Lodge (1988) report

satisfactory recording for up to 24 hours from neocortical wedges.

It may be appropriate to mention here that the temperature controller design presented in appendix A.3.2 performed satisfactorily in this project. However it is proposed that, in order to improve the stability (control of temperature overshoot), the sensed voltage, which is a function of the temperature, should be added to its differentiated signal. The combined signal should then be inverted, and compared to a set point. Additionally, modifying the pulse width modulator, by using a triangular wave generator with the comparator, may provide a better heat switching control.

CHAPTER 6

POWER SPECTRUM ANALYSIS OF DISCHARGES WITH AFTER-ACTIVITY RECORDED FROM RAT NEOCORTICAL SLICES IN VITRO

6.1 INTRODUCTION

As discussed in earlier chapters, rat neocortical slices maintained in Mg^{2+}-free artificial cerebro-spinal fluid (ACSF) exhibit spontaneous "epileptiform" discharges with after-activity (Horne et al., 1986, O'Shaughnessy et al., 1988, and Aram et al., 1989; Ong et al., 1990). Such spontaneous activity can be altered by agents that open or shut neuronal potassium (K^+) channels controlling their overall excitability (Rudy, 1988; Zorn et al., 1993). Anaesthetic and analgesic agents generally inhibit such discharges (Krnjevic, 1992).

In order to study biophysical and pharmacological properties of isolated neocortical tissue showing prolonged discharging, effective quantification of the spontaneous discharge complex and its modification by various neuroactive agents is necessary. This can be achieved by sampling each discharge to obtain a detailed picture which includes the after-activity.

Aram and Lodge (1988) assigned a repetition rate of approximately 5 Hz to afterpotentials during each burst of extracellularly recorded discharges from layer II/III of neocortex. Their "coastline" analysis may however not be much superior to using a higher order "Simpson's rule" to integrate the waveform.

Traditionally periodogram and correlogram methods have been used in biomedical signal processing. Karnup (1992) applied autocorrelation to derive power spectra revealing predominant frequencies of regular action potentials in spike trains recorded extracellulary from guinea-pig neocortex in vitro. Flint and Connors (1993) report that two distinct forms of synchronous rhythmic field potentials were recorded from separate population of neurons in rat somatosensory cortical slices, with dominant frequencies of 8 to 12 Hz and 1 to 5 Hz. It is, however, unclear how these frequencies were derived and whether they represent the rate of occurrence of discharges, or the frequency of after-potentials.

Here, in order to improve resolution for analysing short data segments, a number of modern techniques, namely Welch as a non-parametric method, and Yule-Walker and Unconstrained Least Squares as parametric methods have been investigated. These methods are compared to the classical Fourier transform technique. Grant (1993) and Grant and McDonnell (1993) give an introduction to the discrete Fourier transform and spectral analysis techniques.

As discussed in chapter 5, each K^+ channel blocker has a distinctive effect on the spontaneous epileptiform discharges. Spectral analyses of spontaneous discharges and those modified by each of the K^+ channel blockers are presented in this chapter. These provide numerical values for frequency and power density, supplementing the time domain observations.

6.2 FOURIER TRANSFORM AS A CLASSICAL SPECTRAL ANALYSIS METHOD

As seen in figure 6.1, performing fast Fourier transform (FFT) on a complete spontaneous discharge produces a frequency spectrum with a very large initial component near D.C., due to baseline and discharge offset potentials that swamp the after-activity frequencies of interest. This makes spectral interpretation of the raw data in the discharges very difficult.

In order to remove the dominating initial component in the FFT pattern, any offset had to be eliminated so that the underlying frequencies could be detected (figures 6.2 and 6.3). A signal processing software was developed using the MATLAB package (by MathWorks Inc.) where the following steps were implemented:-

(a) The acquired data frame was converted from Binary to ASCII within the ASYST environment,

(b) The data frame was imported into MATLAB and a suitable segment of the signal containing the after-activity was selected,

(c) If necessary an exponential was fitted to data so that the falling exponential component of the after-activity could be removed,

(d) The mean value of the signal was removed,

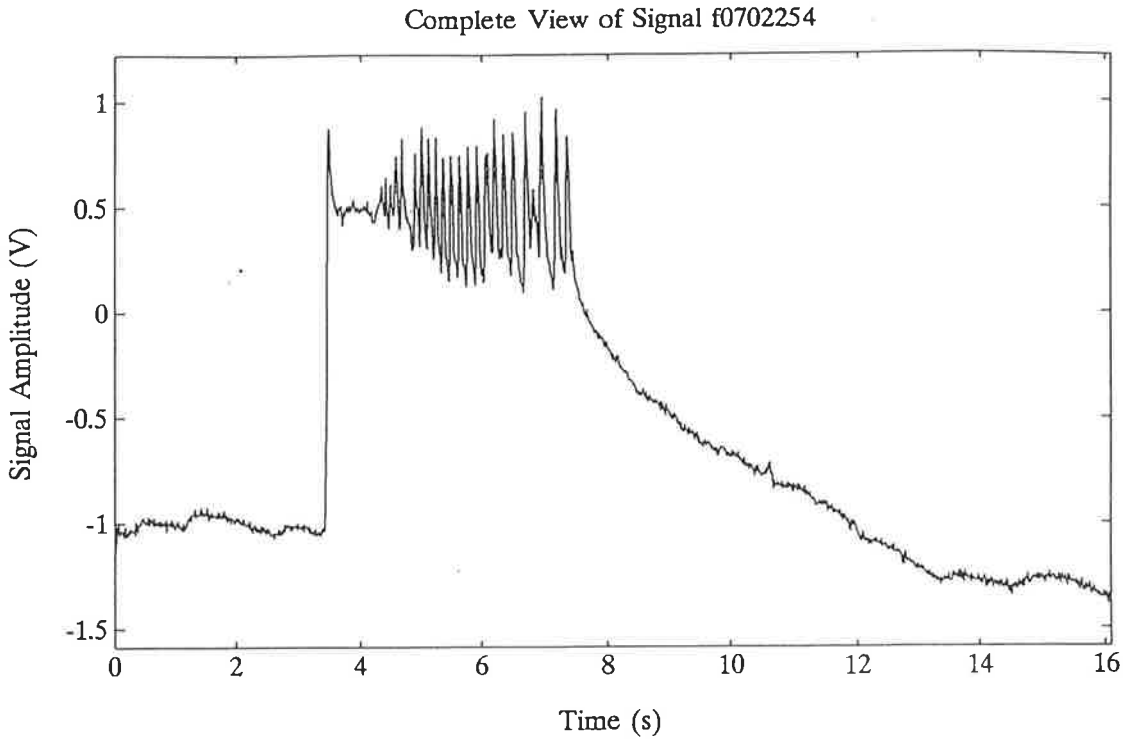

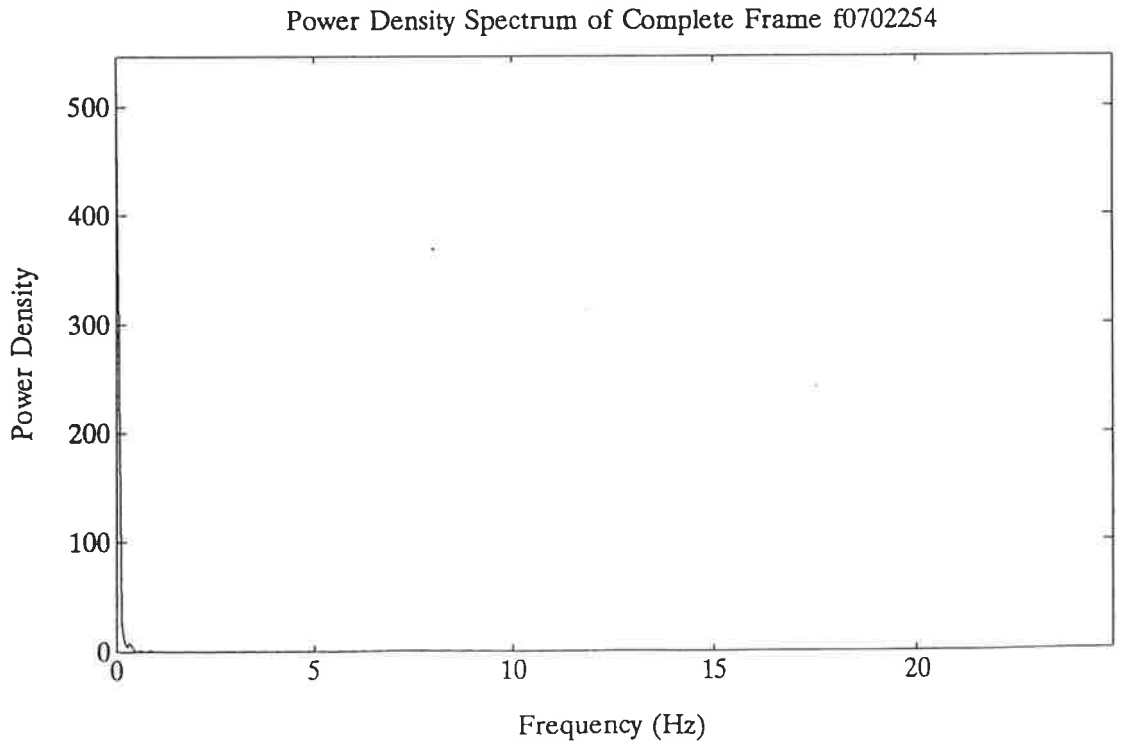

Figure 6.1 Fourier transform based power density spectrum of a complete spontaneous discharge recorded from a neocortical slice.

(e) The signal was then multiplied by a window, usually a Hamming window, to isolate the relevant data.

(f) The windowed signal was then Fourier transformed, and the power spectrum density was also produced.

Figures 6.2 and 6.3 demonstrates the above steps (a) to (f) taken to produce power density spectra of the spontaneous discharge shown in figure 6.1, with and without an exponential fitting.

6.3 MODERN SPECTRAL ANALYSIS TECHNIQUES

At the inception of this work, the *periodogram calculation* method based on FFT was used for power estimation of the after-activity of discharges, but this requires long data sequences for good spectral resolution since the method assumes a stationary time series. It also suffers from spectral leakage (side-lobes appearance) and does not provide a consistent estimate of the true power density. Different window functions are used to reduce the spectral leakage, but windowing makes an unrealistic assumption that the data sequence is zero outside the windowed region. Windowing also reduces the frequency resolution, requiring a compromise between good frequency resolution and minimal leakage to be made (see Proakis and Manolakis, 1992).

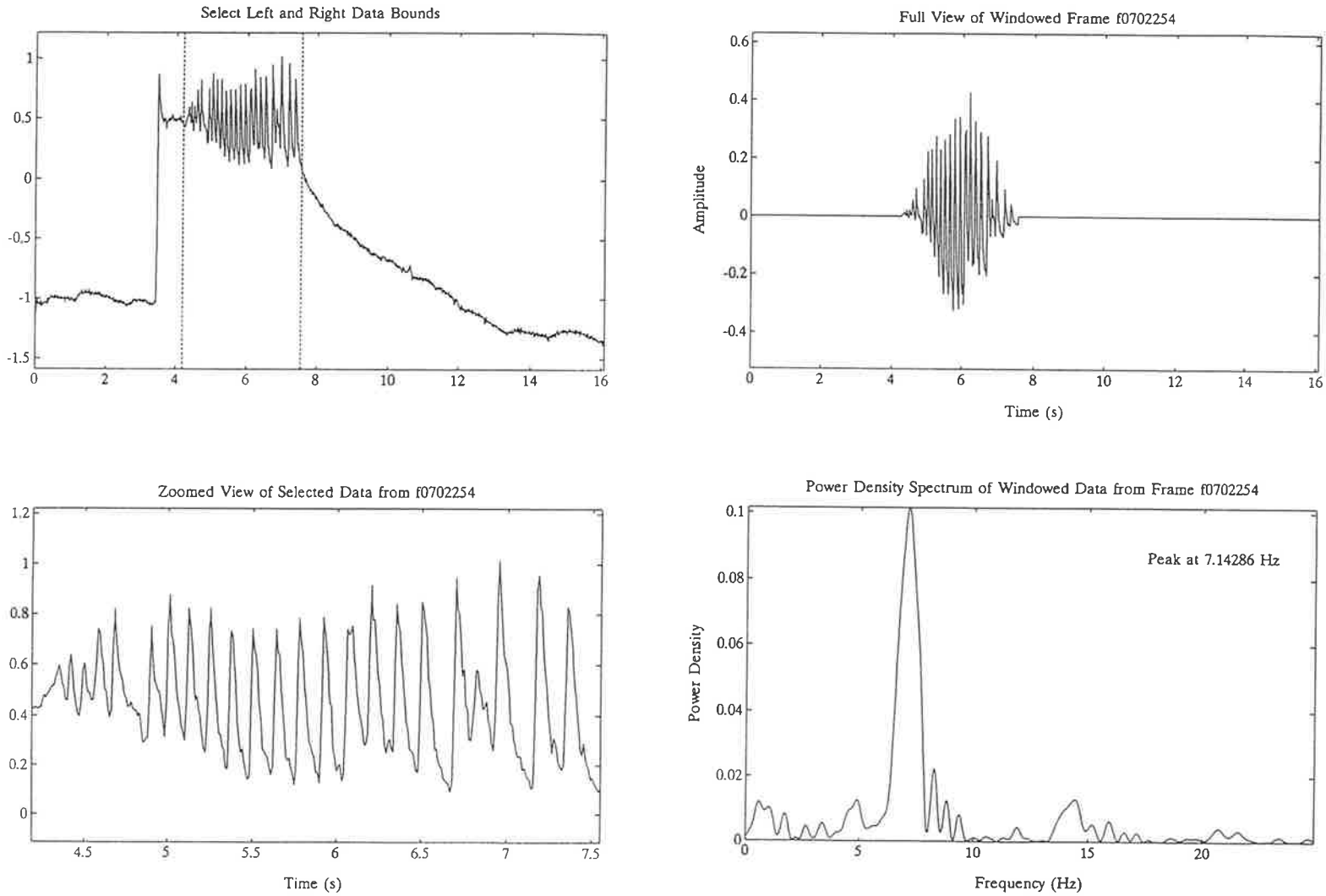

Figure 6.2 Steps taken to produce a power density spectrum of the discharge after-activity. The segment containing after-potentials is selected. The mean is removed. The signal is multiplied by a Hamming window. Fourier transform based power density spectrum of the windowed signal is obtained.

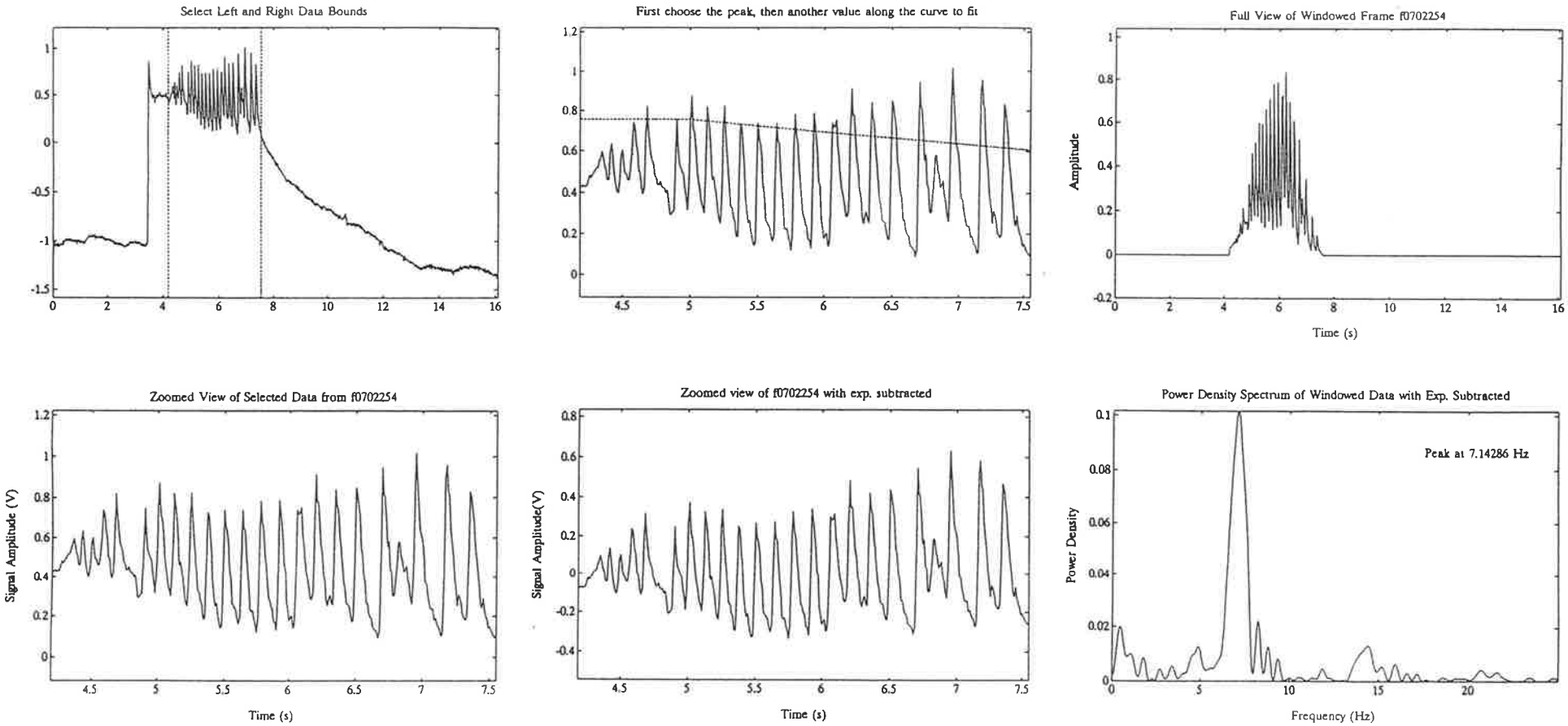

Figure 6.3 Steps taken to produce a power density spectrum of the discharge after-activity. The segment containing after-potentials is selected. An exponential is fitted to the data. The mean value is removed. The signal is multiplied by a Hamming window. Fourier transform based power density spectrum of the windowed signal is obtained.

6.3.1 Non-Parametric Methods

Non-parametric methods try to improve the periodogram calculation method, using division and windowing techniques to obtain a consistent estimate. The *Welch non-parametric* method, for example, decreases the variance of the periodogram calculation method at the expense of frequency resolution. A no-overlap Welch method, however, provides a better resolution. Increasing the degree of overlap decreases the variance in the Welch periodogram. A signal consisting of 2 sinusoids of 10 and 17 Hz frequencies distorted by a zero mean noise sequence, with the amplitude of sinusoids 10 times larger than the noise amplitude, was used to test the periodogram calculation and Welch methods. The periodogram calculation method resolved the 2 sinusoids, but was biased. For shorter data lengths, the Welch method was, however, clearly inferior to the periodogram calculation method. The no-overlap method resolved the two sinusoids but was more biased than the periodogram calculation method.

6.3.2 Parametric Methods

A parametric method is based on modelling the data observed, x(n), as the output of a linear system model, expressed by a rational system function of the form:

$$H(z) = \frac{B(z)}{A(z)}$$

$$= \frac{\sum_{k=0}^{q} b_k z^{-k}}{1 + \sum_{k=1}^{p} a_k z^{-k}}$$

The random process x(n) generated by the model is called the autoregressive moving average (ARMA) model process. If the input and output of the system are assumed to be stationary random processes, then

Power Density Spectrum $\Gamma_{xx}(f) = |H(f)|^2 \Gamma_{ww}(f)$

$\Gamma_{ww}(f)$ = pds of input sequence
$H(f)$ = frequency response of the model

if we also assume that the input was a zero mean white noise sequence with autocorrelation

$$\gamma_{ww}(m) = \sigma_w^2 \delta(m)$$

$$\therefore \quad \Gamma_{ww}(f) = \sigma_w^2$$

where $\sigma_w^2 = E[|W(n)|^2]$

then, Power Density Spectrum

$$\Gamma_{xx}(f) = \sigma_w^2 |H(f)|^2$$

$$= \sigma_w^2 \frac{|B(f)|^2}{|A(f)|^2}$$

Therefore the power density spectrum can be estimated if the model parameters are obtained.

Two other models can be derived from this model. The first model is obtained by setting q = 0. This produces a system model with a system function H(z) = 1/A(z), the output of which is called the autoregressive (AR) process of order p. The second model is obtained by setting p = 0. This produces a system function of H(z) = B(z). Its output is called the moving-average (MA) process of order q. Thus an AR model of

possibly infinite order can be used to represent the two other models (see Proakis and Manolakis, 1992).

Yule-Walker and *Unconstrained Least Squares* methods use the AR model. The AR model is suitable for representing spectra with narrow peaks. The parametric methods do not suffer from spectral leakage, do not make unrealistic assumption that the data was zero outside the selected regions and possess better resolution capabilities. The simple linear equations for the AR parameters were easily solved in MATLAB, allowing for implementation of both methods. The Yule-Walker method is briefly described below.

6.3.2.1 Yule-Walker method

The Yule-Walker method assumes the observed signal, x(n), is the output of an autoregressive system, H(z) = 1 / A(z), driven by a white noise process w(n).

Thus the power density spectrum $\Gamma_{xx}(f)$ of the signal x(n) is given by

$$\Gamma_{xx}(f) = \left| H(f) \right|^2 \sigma_w^2$$

where σ_w^2 is the variance of the white noise process w(n).

When the power density spectrum of a stationary random process is a rational function, a relationship between the autocorrelation and the model parameters exists, resulting in a matrix:

$$\begin{vmatrix} \gamma_{xx}(0) & \gamma_{xx}(-1) & \cdots & \gamma_{xx}(-p+1) \\ \gamma_{xx}(1) & \gamma_{xx}(0) & \cdots & \gamma_{xx}(-p+2) \\ \vdots & \vdots & \vdots & \vdots \\ \gamma_{xx}(p-1) & \gamma_{xx}(p-2) & \cdots & \gamma_{xx}(0) \end{vmatrix} \begin{vmatrix} a_1 \\ a_2 \\ \vdots \\ a_p \end{vmatrix} = \begin{vmatrix} \gamma_{xx}(1) \\ \gamma_{xx}(2) \\ \vdots \\ \gamma_{xx}(p) \end{vmatrix}$$

$$\sigma_w^2 = \gamma_{xx}(0) + \sum_{k=1}^{p} a_k \gamma_{xx}(-k)$$

The Yule-Walker method solves for the model parameters $\{a_k\}$ using the relationship above. It then calculates the power density using the equation:

$$P_{xx}^{yw}(f) = \frac{\sigma_w^2}{\left| 1 + \sum_{k=1}^{p} \hat{a}_p(k)\, e^{-j2\pi fk} \right|^2}$$

Figure 6.4 compares the power density spectrum obtained by Fourier transform to the spectra produced by Welch, Yule-Walker and Unconstrained Least Squares methods. Although the after-activity of the selected discharge does not show a significant exponential decay, nevertheless for all methods an exponential was fitted to the selected data to remove it. The selected data was multiplied by a Hamming window prior to Fourier transformation, whereas no windowing was required for the other methods.

N.B. Applying any of the modern techniques to the complete discharge produced a power density spectrum very similar to that shown in figure 6.1

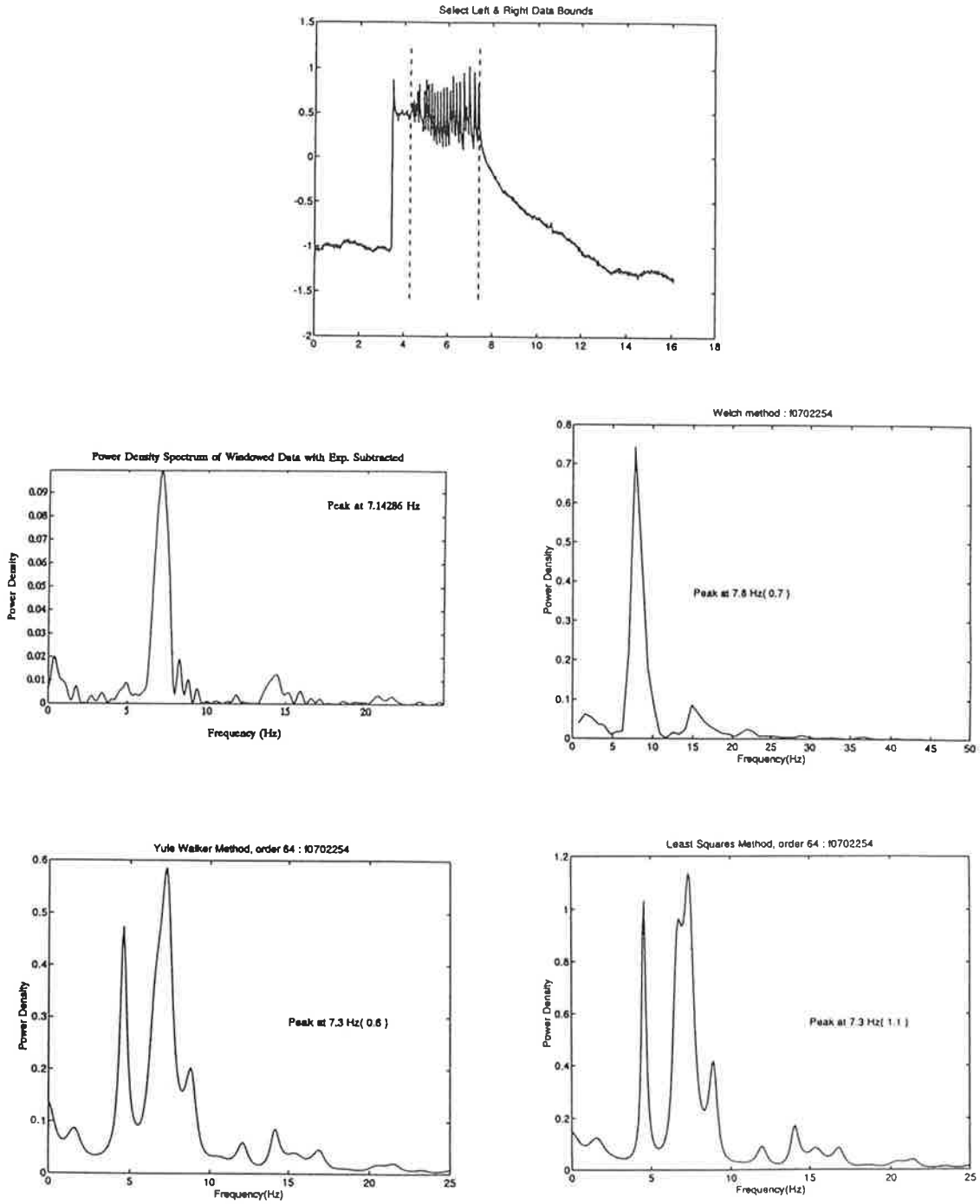

Figure 6.4 Power density spectra obtained by the FFT based method versus modern non-parametric and parametric methods. Welch, Yule-Walker and Least Squares methods are presented. The least squares method provides better resolution, but at the expense of a much longer computation time.

As shown in figure 6.4, for a given order which is related to the number of model parameters used, and which is limited to half the data points available, the Unconstrained Least Squares method resolved the signal peaks better than the Yule-Walker, but it requires a much longer computation time and attenuates signal harmonics.

The Yule-Walker method of a higher order (P = 32 or 64) was selected for power density analysis of neocortical discharges in this project.

6.4 RESULTS AND DISCUSSION

All discharges recorded exhibit non-stationary behaviour i.e. show a shift in frequency from a higher to a lower value across the after-activity. Each period of after-activity was therefore arbitrary broken into 8 segments. The Yule-Walker method for power spectrum estimation was then applied to each short segment, to resolve the peak frequencies and produce moving power density spectra.

The effects of various K^+ channel blockers on spontaneous discharges recorded from neocortical slices in time domain are discussed in detail in chapter 5. In this chapter spectral analysis of two sets of discharges will be described: control, TEA-modified discharge, with recovery; and control, CCh-modified discharge, with recovery. The results of spectral

analysis applied to the remaining K^+ channel blockers, namely CsCl, 4-AP and $BaCl_2$ will be also presented. However the effects of the latter K^+ channel blockers are not discussed in detail, as they can be interpreted in a similar manner to the first two blockers.

The upper frames (a_1, b_1 and c_1) in figure 6.5 represent sample control, 5 mM TEA modified discharge and recovery. As discussed in chapter 5, 5 mM TEA causes an overshoot of the rising phase of the control discharge as well as extending the after-activity. The a_3 plot represents a discharge on partial recovery.

In the same way, the upper frames (a_1, b_1 and c_1) in figure 6.6 represent control, 500 µM CCh modified discharge and recovery. 500 µM CCh causes a marked skewing of the rising phase of discharges (in marked contrast to TEA) and also extends the after-activity enormously (up to 3 times). Partial recovery to baseline is seen in the c_1 plot. Such effects were not so marked over the lower range of 1 to 100 µM CCh.

Sections a_2, b_2, c_2 in both figures 6.5 and 6.6 represent the moving power density spectra for each of the 8 segments across the discharge after-activity in descending order. The Yule-Walker method was applied to each short segment to resolve the peak frequencies, and produce the spectra. Sections a_3, b_3, c_3 in both figures 6.5 and 6.6 are image plots of the same signal segments versus frequency. The darker the segments in the images, the higher the power density at those frequencies. These images also convey information on the sharpness of

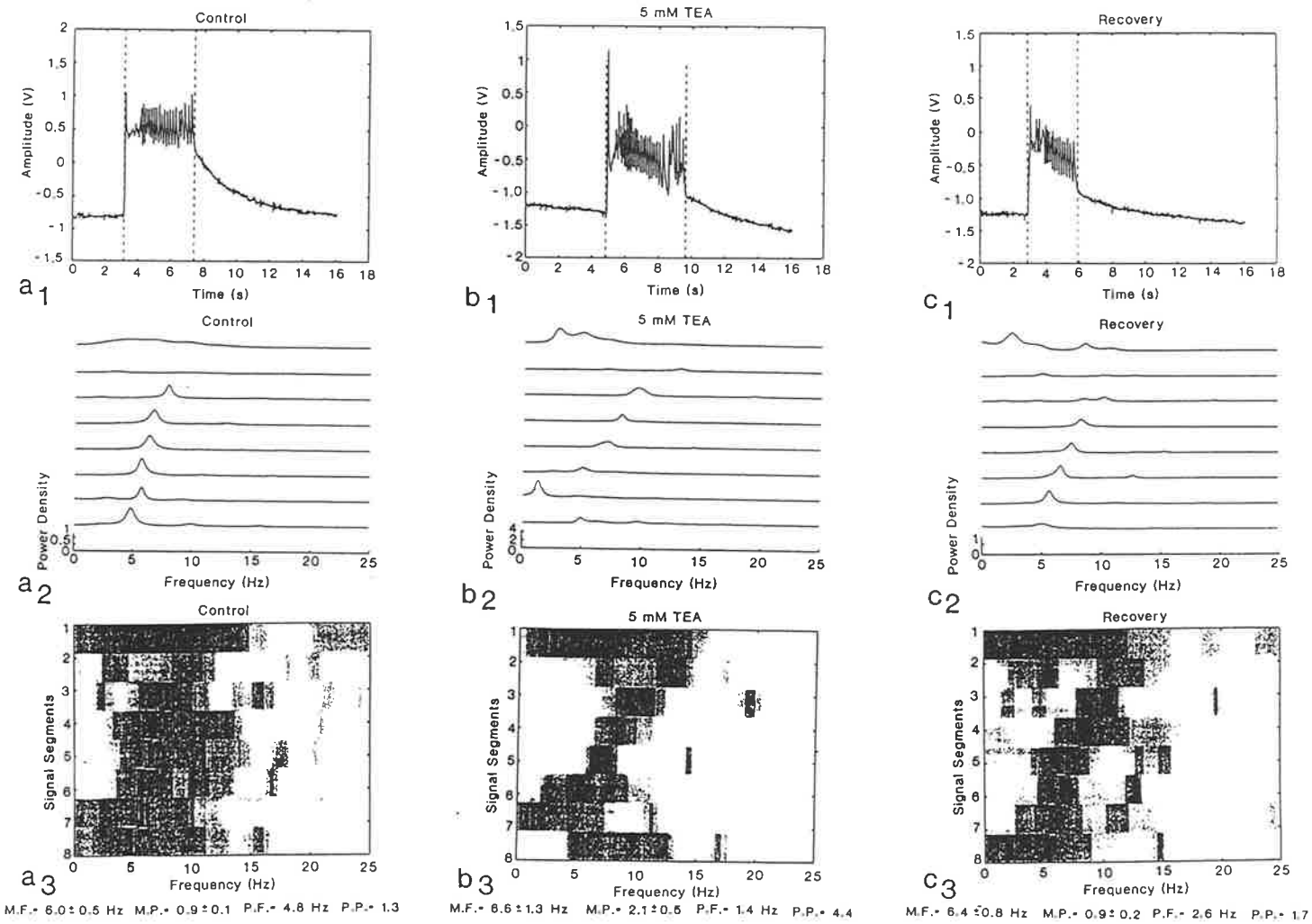

Figure 6.5 Computer collected responses showing control, a discharge in the presence of 5 mM TEA, and recovery (a_1, b_1, c_1). The moving power density spectra (a_2, b_2, c_2) were computed using the Yule-Walker method with model order $p = 32$. The image plots (a_3, b_3, c_3) show the frequency distribution of signal components.

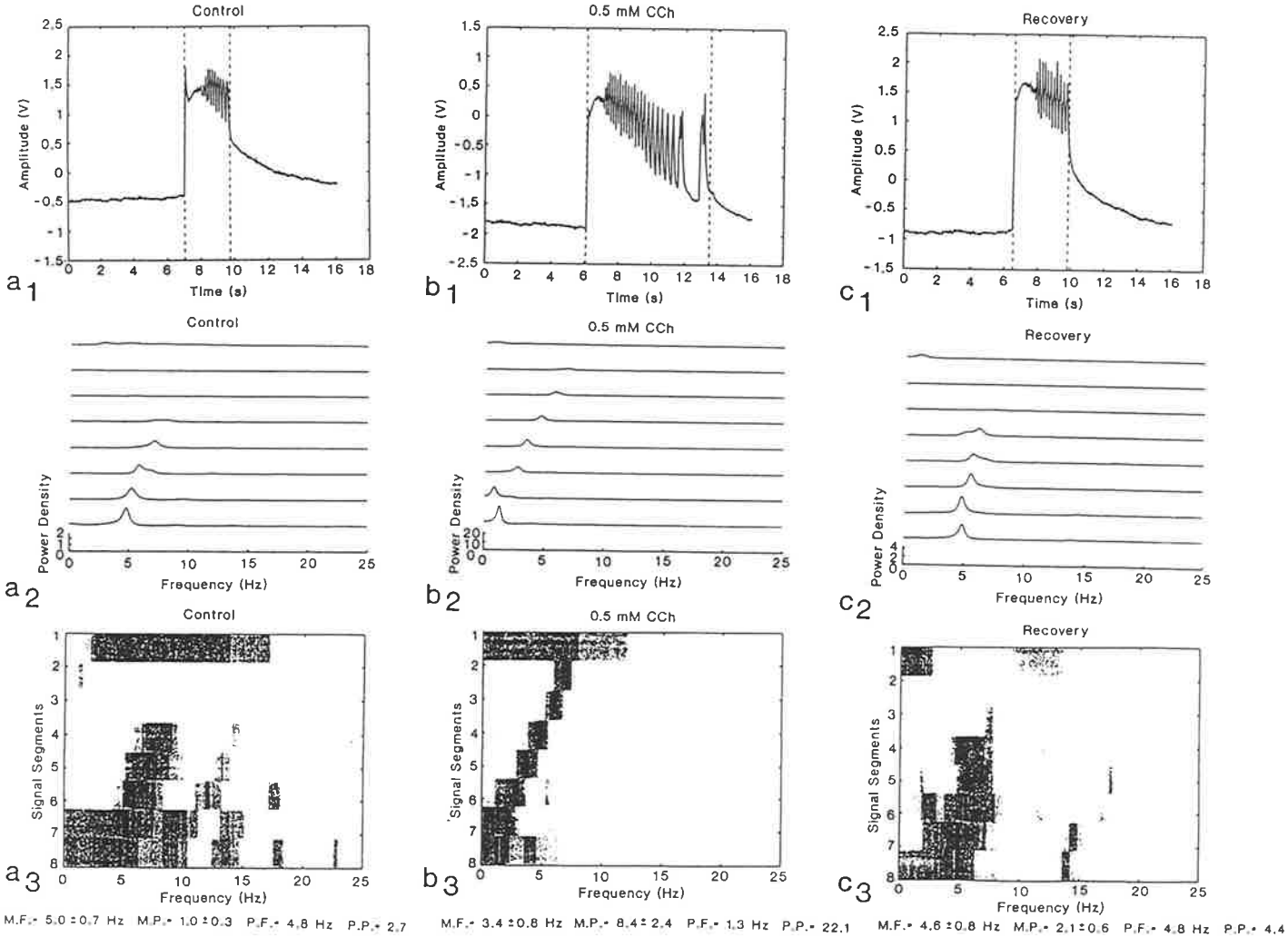

Figure 6.6 Computer collected responses showing control, a discharge in the presence of 0.5 mM CCh, and recovery (a_1, b_1, c_1). The moving power density spectra (a_2, b_2, c_2) were computed using the Yule-Walker method with model order $p = 32$. The image plots (a_3, b_3, c_3) show the frequency distribution of signal components.

frequency peaks and the distribution of signal harmonics. It can be clearly seen that both TEA and CCh increased the power density of control signals and lowered the frequency corresponding to the maximum power density (shifts to left). The values printed under the image plots represent the mean of 8 peak frequencies ± standard error of mean (M.F. ± s.e.), the mean of 8 corresponding peak power densities ± standard error of mean (M.P. ± s.e.), the frequency at which the power density was maximum (P.F.) and the maximum power density (P.P.). In figure 6.5, comparing control to TEA, M.F. has slightly increased and M.P. has approximately doubled, whereas in figure 6.6, comparing control to CCh, M.F. has decreased, but M.P. has greatly increased. As mentioned above P.F. has decreased and P.P. has increased with both drugs. The increase in power density induced by CCh is, however, most striking.

Table 6.1 lists the mean values of M.F., M.P., P.F. and P.P. as explained above for control, drug-modified discharges and recovery sets of TEA and CCh. The number of individual discharges in each category is given by n, and the sets are from 2 different experiments. Mean values show that in the TEA case, M.F. is not largely affected, whereas M.P. has increased, P.F. has decreased and P.P. has increased. In the CCh case, M.F. has decreased, M.P. has increased, P.F. has decreased and P.P. has increased.

Sections marked as (a) and (b) in figure 6.7 are a collection of 8 sample mean plots representing mean values of peak frequencies and the corresponding peak power densities versus signal blocks (segments) for control and drug-modified

	Control (TEA) n=6	Control (CCh) n=7
Mean Frequency (M.F.)	5.9917 ± 0.2167	5.1571 ± 0.2706
Mean Power Density (M.P.)	0.8456 ± 0.0655	1.7285 ± 0.1886
Peak Frequency (P.F.)	4.9500 ± 0.7402	4.8571 ± 0.1131
Peak Power Density (P.P.)	1.3833 ± 0.1376	3.8143 ± 0.5147
	5 mM TEA n=4	0.5 mM CCh n=6
Mean Frequency (M.F.)	5.7656 ± 0.5273	3.7896 ± 0.2860
Mean Power Density (M.P.)	1.4179 ± 0.1965	4.1023 ± 0.5491
Peak Frequency (P.F.)	1.6500 ± 0.2901	2.4333 ± 0.8082
Peak Power Density (P.P.)	3.6000 ± 0.3742	8.8833 ± 2.8865
	Recovery (TEA) n=5	Recovery (CCh) n=4
Mean Frequency (M.F.)	6.0075 ± 0.3588	5.0750 ± 0.3399
Mean Power Density (M.P.)	0.8632 ± 0.0755	2.4488 ± 0.3260
Peak Frequency (P.F.)	5.1600 ± 0.7004	4.7750 ± 0.6537
Peak Power Density (P.P.)	1.4400 ± 0.2482	5.0500 ± 0.4992

Table 6.1 Mean ± s.e. values for frequency and power density calculated for n discharges from 2 independent sets. Statistical data for control, discharges modified by TEA, and those on partial recovery are tabulated.

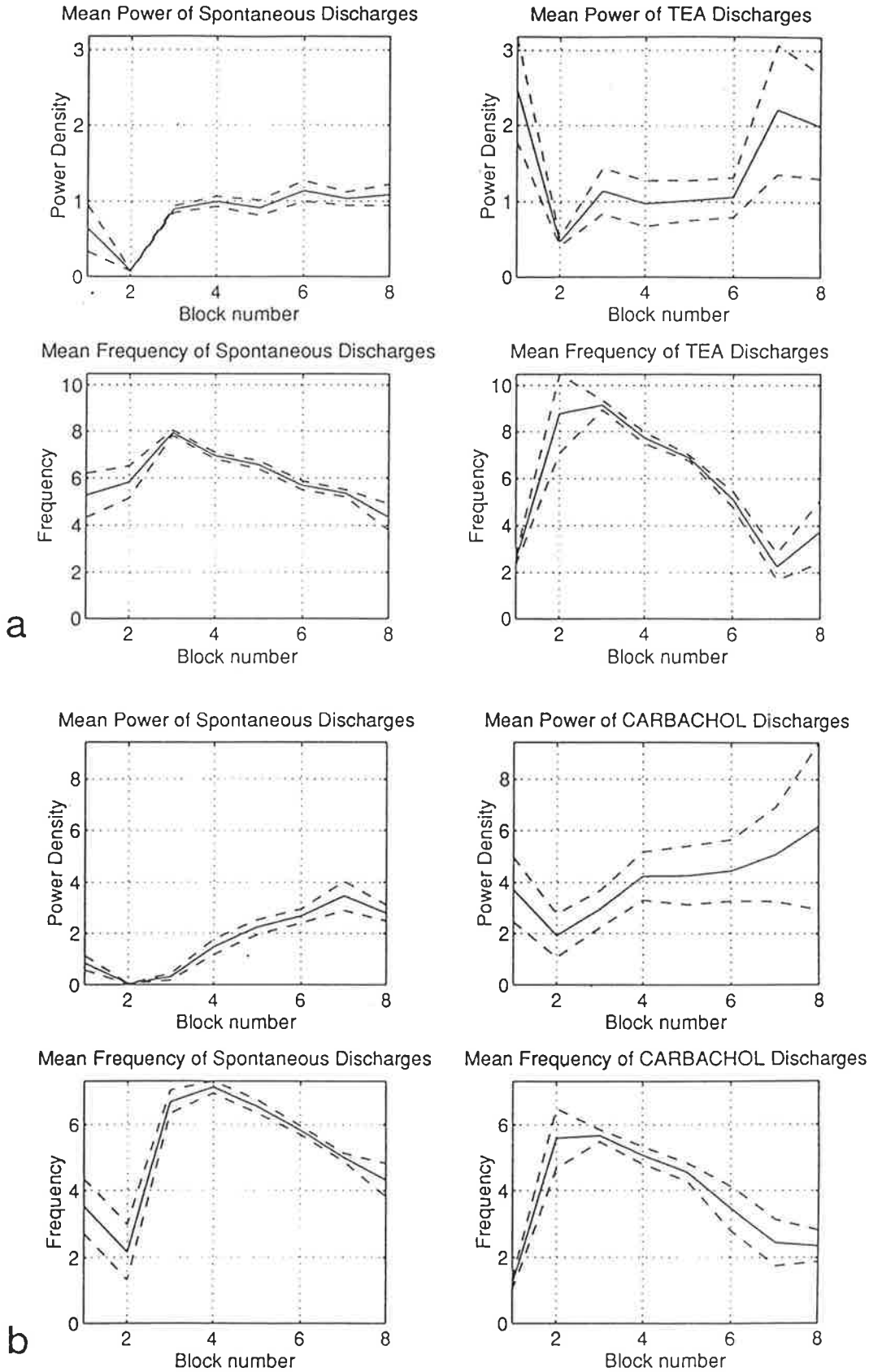

Figure 6.7 Graphs plotted from points representing the mean values of peak power density and peak frequency, for each signal segment, from (a) control and TEA-modified, and (b) control and CCh-modified discharges. The graphs show the variations in frequency and power density patterns. The dashed lines represent standard errors of the means. Discharges for (a) and (b) are from 2 independent slices, and the number of discharges for each plot is given by n in table 6.1.

discharges. However here each of the 8 discrete values in each plot represents the mean for that segment from all the n discharges in a group, with n as in table 6.1. The graphs aim to show the variations in frequency and power density between independent sets of control discharges, as well as comparing the control with the drug-modified discharges. Expectedly, the mean power and the mean frequency patterns for the two independent sets of control discharges are similar, but not identical. The mean frequency of the third segment from control discharges, as shown in figure 6.7 section (a), is approximately 8 Hz and the mean frequency of the fourth segment from control discharges, as shown in figure 6.7 section (b), is approximately 7 Hz. The shift in these peak frequencies to the left and the increase in peak power density are clearly seen in response to both TEA and CCh.

Overall, the plots in figure 6.7 show the after-activity pattern of discharges from neocortical slices (Spontaneous or drug-modified) peaks early to a high frequency and slows down in time along the after-activity. As the after-activity slows, the power density increases. Thus lower frequency discharges contain more power.

Figure 6.8 is an enlarged reproduction of the control discharge in figure 6.5 showing the discharge (a_1), its power density spectrum (b_1), and its image plot (c_1). Details in the image plot are clearer in this larger diagram.

Frequency spectral data showing the effect of 5 mM CsCl on a discharge are illustrated in figure 6.9. Once again the

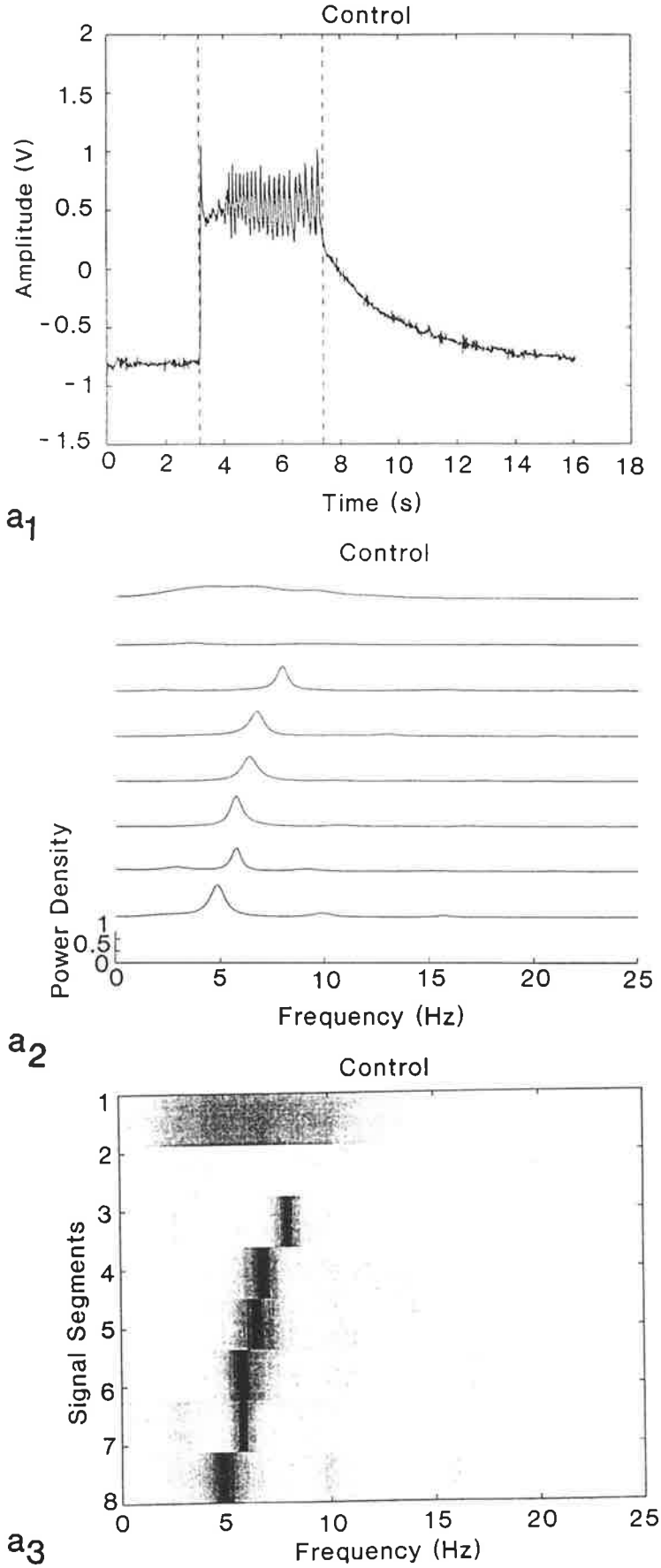

Figure 6.8 This figure represents the control discharge (a_1), and its power density spectrum (a_2) and image plot (a_3) as shown in figure 6.5. Details in the image plot are clearer in this larger diagram.

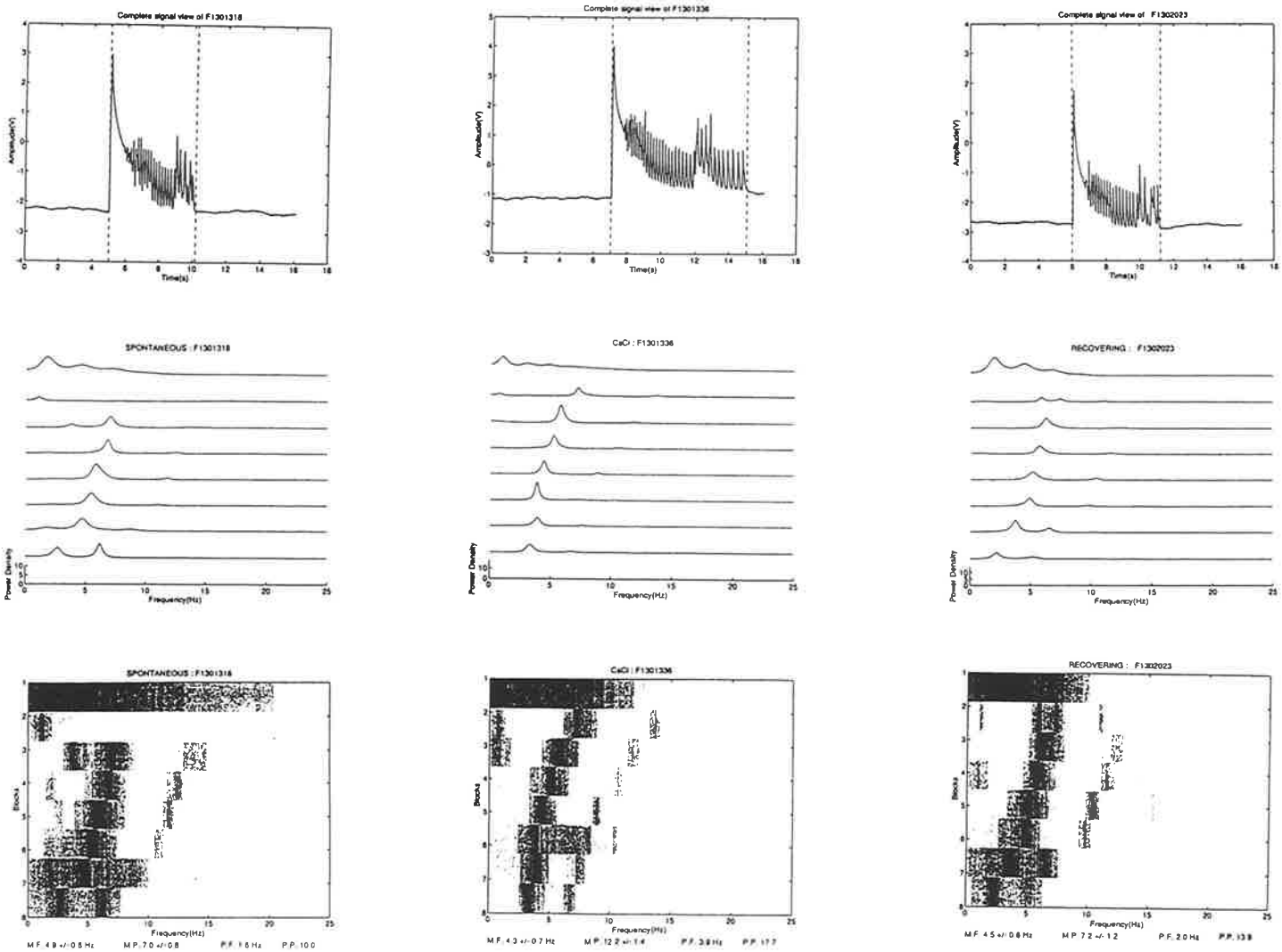

Figure 6.9 From left to right: Computer collected responses showing control, a discharge in the presence 5 mM CsCl, and recovery. Power density spectra and image plots for the responses are also presented.

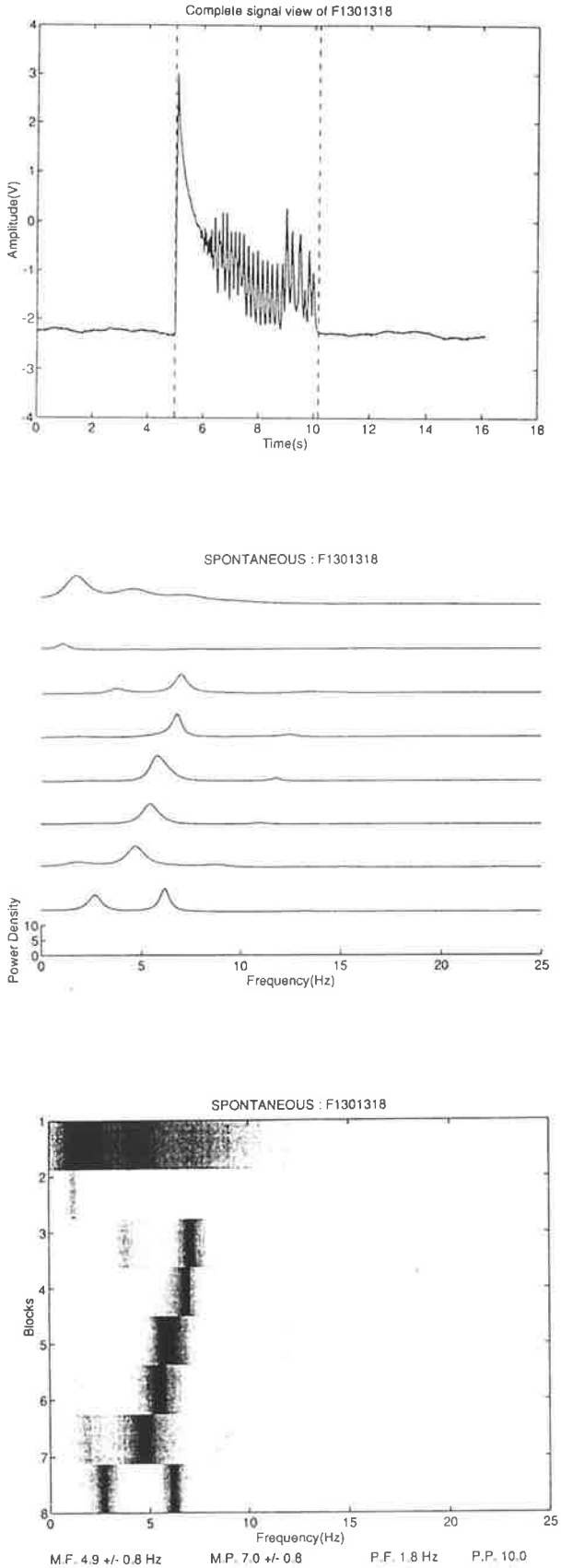

Figure 6.10 This figure represents the control discharge, its moving power density spectrum and image plot as shown in figure 6.9. Details in the image plot are clearer in this larger diagram.

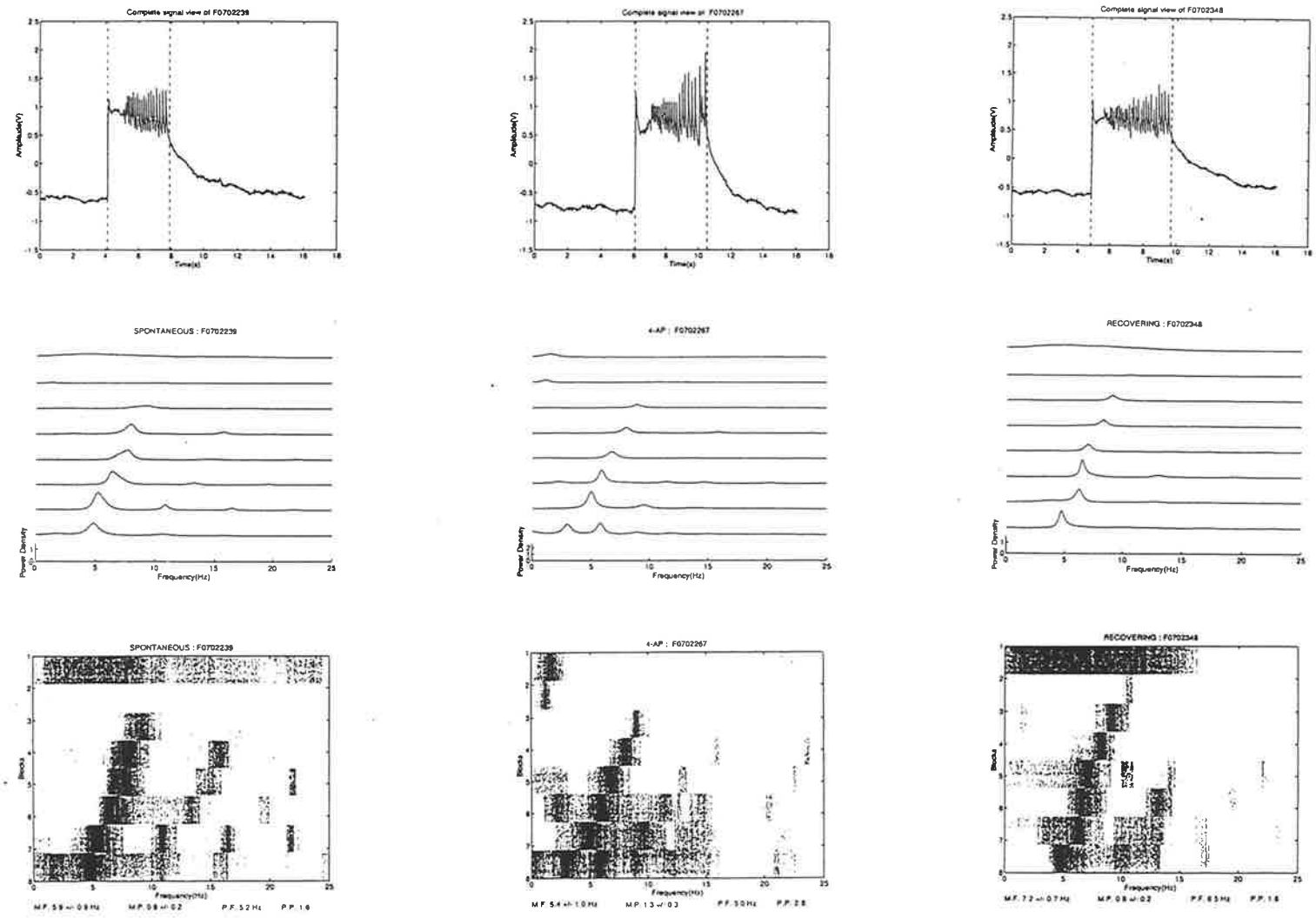

Figure 6.11 From left to right: Computer collected response showing control, a discharge in the presence 50 μM 4-AP, and recovery. Power density spectra and Imag plots for the responses are also presented.

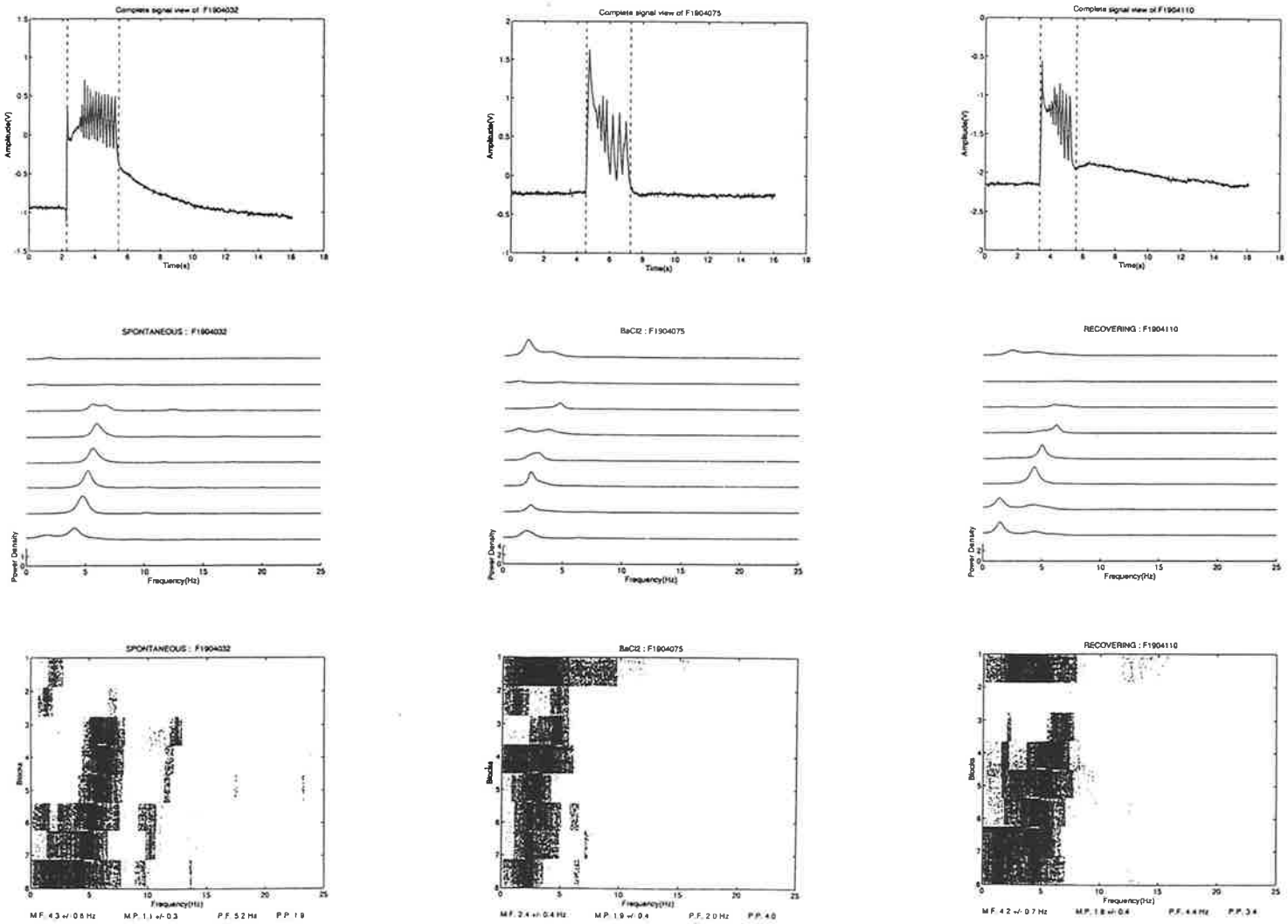

Figure 6.12 From left to right: Computer collected respons showing control, a discharge in the presence 0.5 mM $BaCl_2$, and recovery. Power density spectra and image plots for the responses are also presented.

control discharge from figure 6.9, together with its moving power density spectrum and image plot, are shown in figure 6.10. A larger image plot has provided a better visualisation of spectral details. Similarly, spectral analyses which show the effects of 50 μM 4-AP and 0.5 mM $BaCl_2$ are presented in figures 6.11 and 6.12 respectively.

Table 6.2 lists the mean values of M.F., M.P., P.F. and P.P. for 2 sets of CsCl related responses, each comprising control, discharges in the presence 5 mM CsCl and recovery. The number of individual discharges in each category is given by n. The sets are from 2 different experiments.

Sample mean plots in sections (a) and (b) of figure 6.13 represent mean values of the peak frequencies and the corresponding peak power densities versus signal blocks (segments) for the 2 sets of control and discharges modified in the presence of CsCl. The number of discharges for each graph is given by the n value in table 6.2. The dashed lines represent the standard errors of the means.

Table 6.3 lists the mean values of M.F., M.P., P.F. and P.P. for a set of responses comprising control, discharges in the presence of 50 μM 4-AP, and recovery. The number of individual discharges in each category is given by n.

Sample mean plots in figure 6.14 represent mean values of peak frequencies and corresponding peak power densities versus signal blocks (segments) for the set of control and discharges modified in the presence of 4-AP. The number of discharges for

each graph is given by the n value in table 6.3. The dashed lines form a band which represents the standard errors of the means.

Finally, table 6.4 lists mean values of M.F., M.P., P.F. and P.P. for 2 sets of $BaCl_2$ related responses comprising control, discharges in the presence of 0.5 mM $BaCl_2$, and recovery. Again, the number of individual discharges in each category is given by n, and the sets are from 2 different experiments.

Sections (a) and (b) in figure 6.15 represent sample mean plots representing mean values of the peak frequencies and the corresponding peak power densities versus signal blocks (segments) for the 2 sets of control and $BaCl_2$-modified discharges. The number of discharges for each graph is given by the n value in table 6.4. The dashed bands represent the standard errors of the means.

As well as demonstrating the effects of K^+ channel blockers on spontaneous discharges recorded from neocortical slices in time domain, Spectral analysis has enabled us to perform detailed quantitative analysis of frequency and power density characteristics of individual discharges and how such characteristics are modified by the blockers.

	Control (CsCl) n=3 First Set	Control (CsCl) n=4 Second Set
Mean Frequency (M.F.)	4.4167 ± 0.4590	4.9781 ± 0.7099
Mean Power Density (M.P.)	8.5176 ± 1.2818	0.3199 ± 0.0750
Peak Frequency (P.F.)	2.4667 ± 0.8743	1.9500 ± 0.2630
Peak Power Density (P.P.)	19.2333 ± 7.3698	1.2250 ± 0.2839
	5 mM CsCl n=5	5 mM CsCl n=9
Mean Frequency (M.F.)	4.1525 ± 0.3176	3.8000 ± 0.2850
Mean Power Density (M.P.)	10.0706 ± 0.6697	0.5521 ± 0.0621
Peak Frequency (P.F.)	1.8600 ± 0.5492	2.8778 ± 0.7168
Peak Power Density (P.P.)	17.3800 ± 1.4005	1.3333 ± 0.3456
	Recovery (CsCl) n=9	Recovery (CsCl) n=1
Mean Frequency (M.F.)	4.5139 ± 0.2358	3.5875 ± 0.8262
Mean Power Density (M.P.)	6.7228 ± 0.4216	0.4526 ± 0.1775
Peak Frequency (P.F.)	1.3222 ± 0.1152	1.3000 ± 0.0
Peak Power Density (P.P.)	14.0222 ± 1.2683	1.6000 ± 0.0

Table 6.2 Mean ± s.e. values for frequency and power density calculated for n discharges from 2 independent sets. Statistical data for control, discharges modified by CsCl, and those on partial recovery are tabulated.

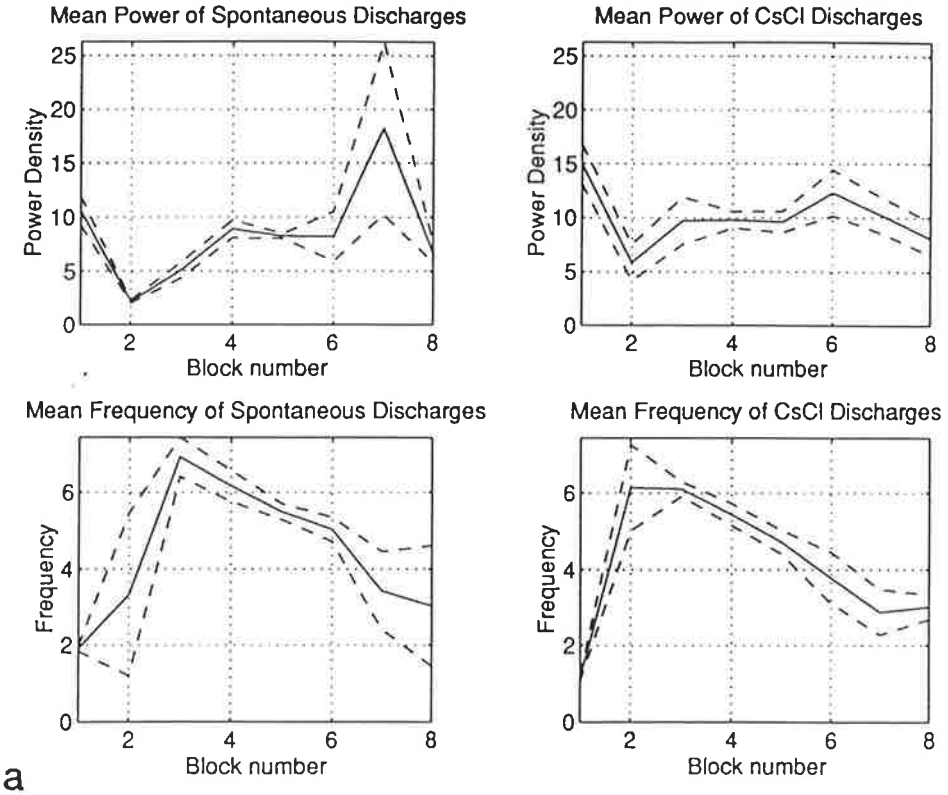

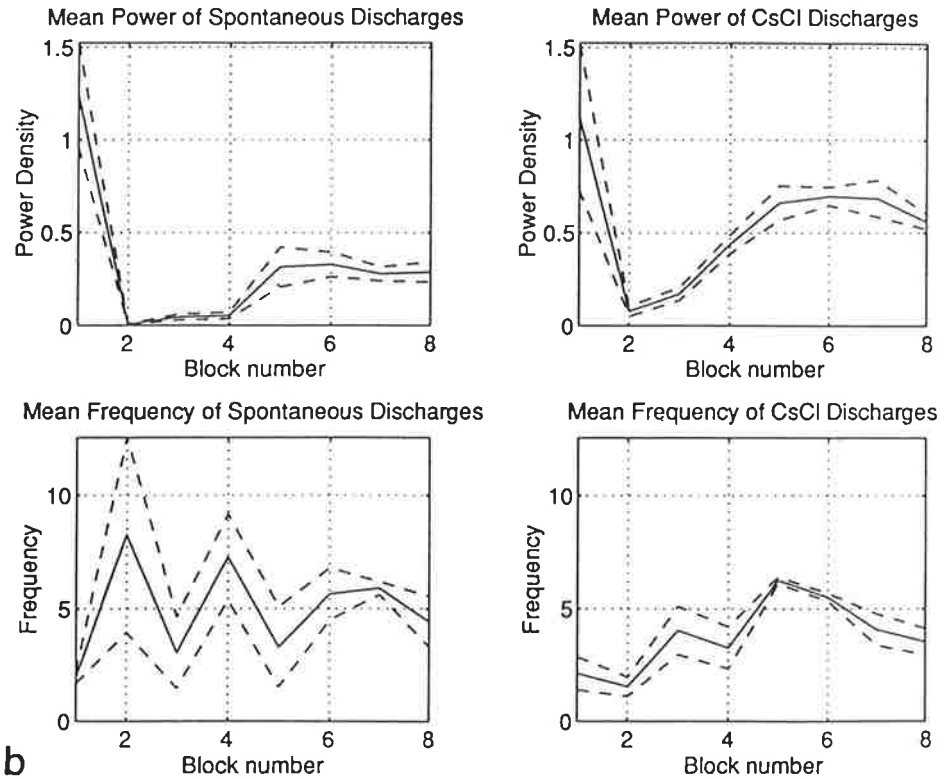

Figure 6.13 Two sets of graphs (a and b) plotted from points representing the mean values of peak power density and peak frequency, for each signal segment, from control and discharges in the presence of CsCl. The graphs show the variations in frequency and power density patterns. The dashed lines represent standard errors of the means. Discharges for (a) and (b) are from 2 independent slices, and the number of discharges for each plot is given by n in table 6.2.

	Control (4-AP) n=7
Mean Frequency (M.F.)	5.6821 ± 0.3504
Mean Power Density (M.P.)	0.8783 ± 0.0831
Peak Frequency (P.F.)	6.2000 ± 0.2469
Peak Power Density (P.P.)	1.7571 ± 0.2256
	50 μM 4-AP n=5
Mean Frequency (M.F.)	5.5050 ± 0.4317
Mean Power Density (M.P.)	1.1779 ± 0.1689
Peak Frequency (P.F.)	4.4200 ± 0.8610
Peak Power Density (P.P.)	2.8200 ± 0.6168
	Recovery (4-AP) n=2
Mean Frequency (M.F.)	6.5437 ± 0.7068
Mean Power Density (M.P.)	0.7671 ± 0.1212
Peak Frequency (P.F.)	7.0500 ± 0.5500
Peak Power Density (P.P.)	1.4500 ± 0.1500

Table 6.3 Mean ± s.e. values for frequency and power density calculated for n discharges from a 4-AP set. Statistical data for control, discharges modified by 4-AP, and those on partial recovery are tabulated.

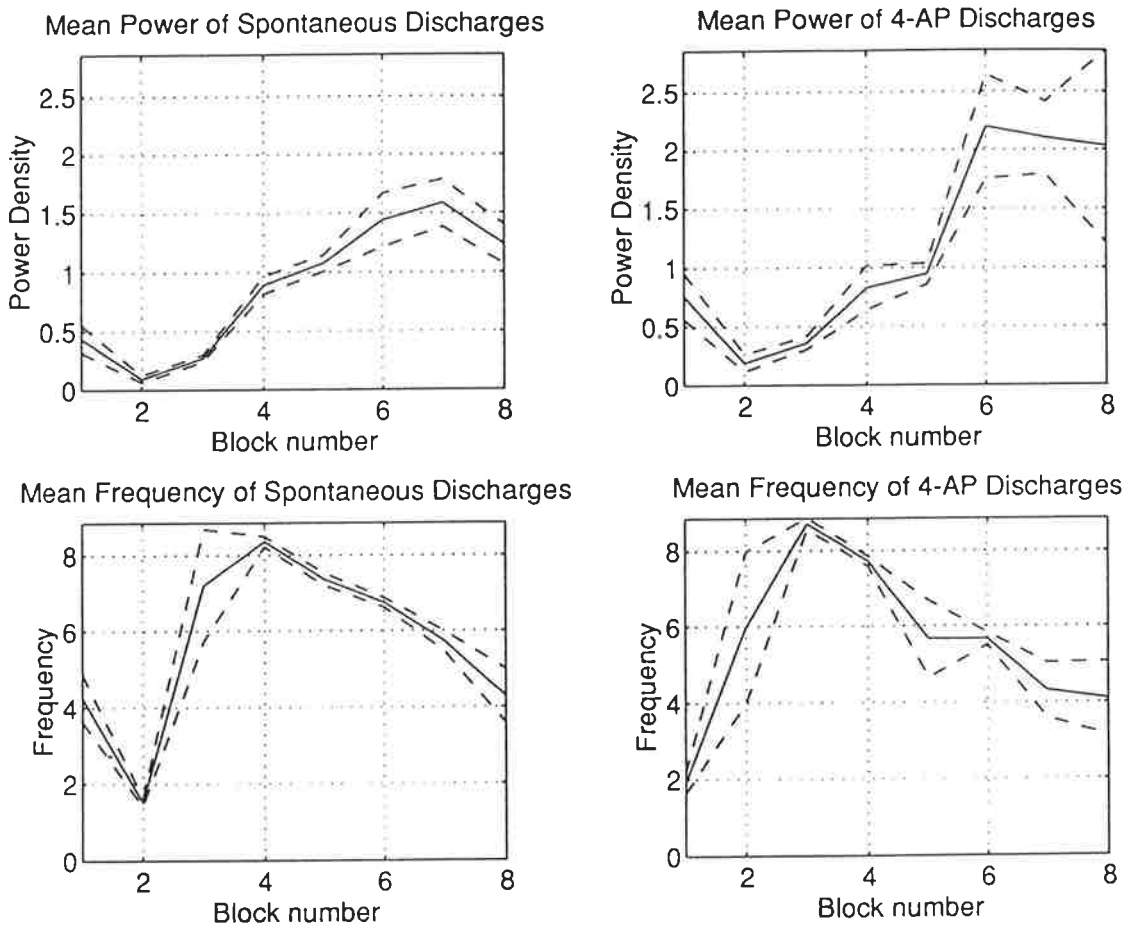

Figure 6.14 Graphs plotted from points representing the mean values of peak power density and peak frequency, for each signal segment, from control and discharges in the presence of 4-AP. The graphs show the variations in frequency and power density patterns. The dashed lines represent standard errors of the means. The number of discharges for each plot is given by n in table 6.3.

	Control ($BaCl_2$) n=3 First Set	Control ($BaCl_2$) n=4 Second Set
Mean Frequency (M.F.)	4.4333 ± 0.3469	4.5625 ± 0.4191
Mean Power Density (M.P.)	1.1344 ± 0.1560	16.9087 ± 3.4067
Peak Frequency (P.F.)	4.8667 ± 0.1764	2.0500 ± 0.7182
Peak Power Density (P.P.)	2.0667 ± 0.2186	49.8250 ± 17.1371
	0.5 mM $BaCl_2$ n=4	0.5 mM $BaCl_2$ n=5
Mean Frequency (M.F.)	2.8906 ± 0.2438	3.1025 ± 0.1954
Mean Power Density (M.P.)	2.2366 ± 0.2405	22.1432 ± 2.5156
Peak Frequency (P.F.)	2.2000 ± 0.2345	1.8200 ± 0.0735
Peak Power Density (P.P.)	4.7750 ± 0.4289	52.7400 ± 8.1602
	Recovery ($BaCl_2$) n=2	Recovery ($BaCl_2$) n=3
Mean Frequency (M.F.)	4.0063 ± 0.5259	3.8667 ± 0.4588
Mean Power Density (M.P.)	1.4665 ± 0.2754	22.2104 ± 4.6688
Peak Frequency (P.F.)	4.3500 ± 0.0500	1.9000 ± 0.6000
Peak Power Density (P.P.)	3.2500 ± 0.1500	59.4667 ± 7.2577

Table 6.4 Mean ± s.e. values for frequency and power density calculated for n discharges from 2 independent sets. Statistical data for control, discharges modified by $BaCl_2$, and those on partial recovery are tabulated.

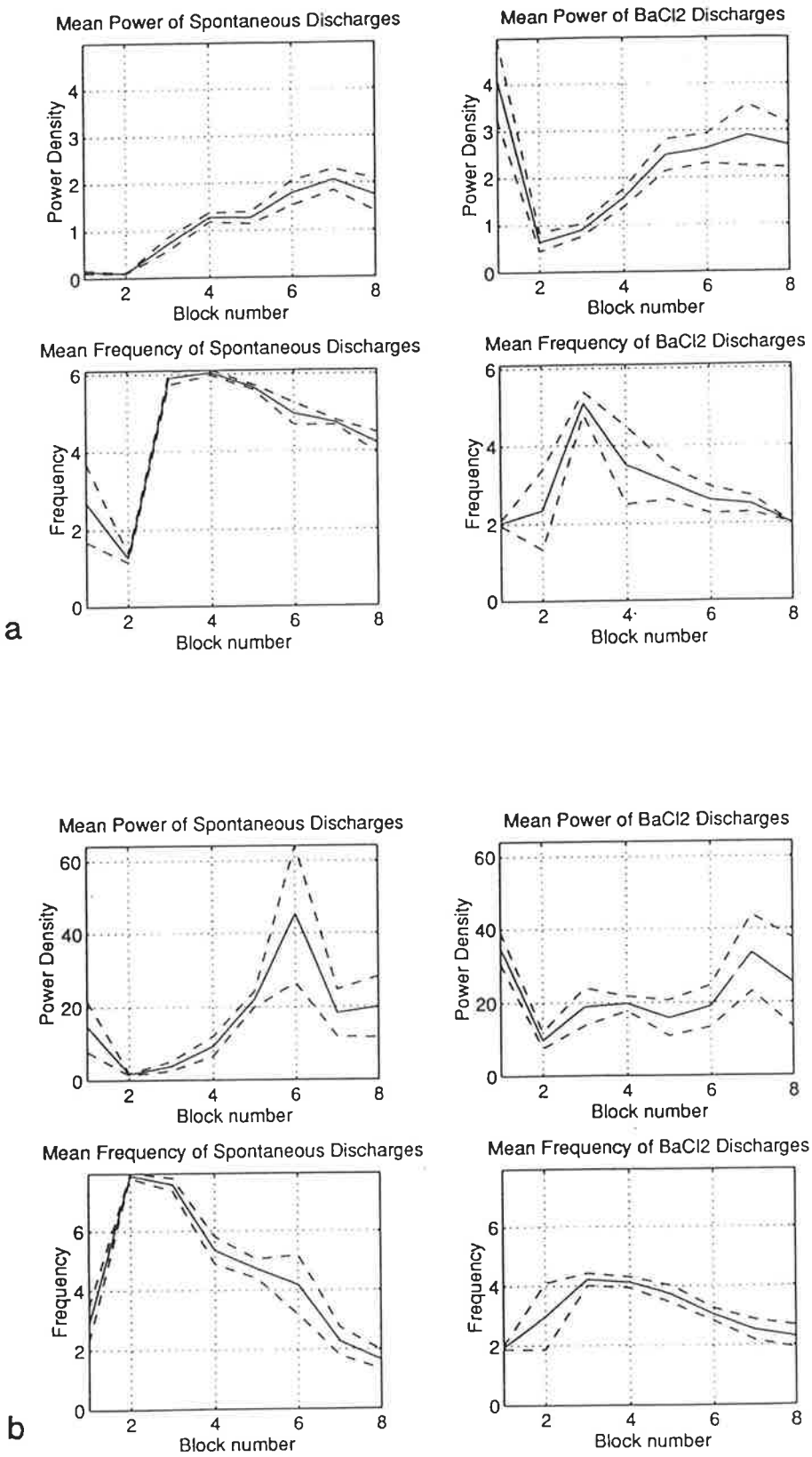

Figure 6.15 Two sets of graphs (a and b) plotted from points representing the mean values of peak power density and peak frequency, for each signal segment, from control and discharges in the presence of $BaCl_2$. The graphs show the variations in frequency and power density patterns. The dashed lines represent standard errors of the means. Discharges for (a) and (b) are from 2 independent slices, and the number of discharges for each plot is given by n in table 6.4.

6.5 CONCLUSIONS

In this chapter, the Yule-Walker parametric technique was applied to the after-potentials of discharges so that their frequency and power density could be unequivocally quantified. Here, the application of spectral analysis to discharge from neocortical wedges has been valuable in revealing that the mean frequency of the after-activity segments of spontaneous discharges normally ranges between 4.5 to 6 Hz, and that the frequency of after-potentials on the falling phase of any discharge peaks early and decreases in time as the event continues. Furthermore, the analysis revealed that K^+ channel blockers clearly modify discharges in frequency as well as time domains. Both TEA and CCh, for example, significantly increased the peak value of the power density and decreased the frequency at which the power was maximum.

The spectral analysis in this chapter has provided graphical display and accurate numerical values for the frequency and power of signals under study. It is undoubtedly a useful tool for characterising changes induced in a single discharge by a neuroactive agent, and aids the unravelling of cellular mechanisms underlying neurophysiological states, such as anaesthesia. The challenge remains to relate these changes to effects of the K^+ channel blockers on various channel types.

CHAPTER 7

EFFECTS OF $GABA_A$- AND $GABA_B$-RECEPTOR AGONISTS AND ANTAGONISTS ON SPONTANEOUS EPILEPTIFORM DISCHARGES RECORDED FROM RAT NEOCORTICAL SLICES IN VITRO

4-aminobutanoic acid (GABA), as the major inhibitory amino acid neurotransmitter in the central nervous system (CNS), was introduced in chapter 1. Two distinct types of receptors mediate synaptic transmission by GABA, these are the $GABA_A$- and $GABA_B$-receptors.

$GABA_A$-receptors are comprised of a hetero-pentameric complex with at least 4 types of binding sites, together with an integral enclosed chloride ion channel. $GABA_A$-receptors are activated by isoguvacine, modulated by barbiturates, benzodiazepines and steroids, and antagonized by bicuculline. On the other hand, $GBAB_B$-receptors are linked to calcium channels pre-synaptically or potassium channels post-synaptically through second messenger systems, are activated by (-)-baclofen, and antagonized by phaclofen and 2-hydroxysaclofen, but are insensitive to bicuculline. Both $GABA_A$- and $GABA_B$-receptors are found as presynaptic receptors including autoreceptors, as well as postsynaptic receptors. Presynaptic receptors modulate transmitter release from synaptic terminals. Autoreceptors act as regulators, inhibiting the release of GABA itself. Postsynaptic receptors are responsible for inhibiting excitability of the postsynaptic cells.

In this chapter the effects of some $GABA_A$- and $GABA_B$-receptor agonists and antagonists on spontaneous discharges recorded from neocortical slices will be presented and discussed. The following conditions apply to all sub-sections and should be borne in mind:

(i) Agents were made up as stock solutions containing the total ACSF equivalent amounts of NaCl and KCl. Particular concentrations were obtained by diluting the stock solution in ACSF, and then by successive dilution.

(ii) Agents were normally applied for a four-minute duration. Where one or more agents were applied in succession to the same slice, at least ½ an hour was allowed for tissue recovery between applications, to ensure that control was re-established as far as possible.

(iii) In studies where mixtures were applied to slices, equivalent volumes of each agent were added together.

7.1 EFFECTS OF GABA AND 3-AMINOPROPYLSULPHONIC ACID ON SPONTANEOUS NEOCORTICAL DISCHARGES

Replacement of the carboxyl group that still provides $GABA_A$-receptor activity are found in the sulfonic and sulfinic analogs of GABA, whereas the phosphonic and phosphinic acids are selective ligands for $GABA_B$-receptors, and are inactive at $GABA_A$-receptors (Kerr and Ong, 1992). Amongst these, 3-

aminopropylsulphonic acid (3-APS) is known to be a potent $GABA_A$-receptor agonist, and also has $GABA_B$ antagonist properties on peripheral $GABA_B$-receptors, but does not interact selectively with $GABA_B$-receptors (Krogsgaard-Larsen et al., 1988) as it is a $GABA_A$-receptor agonist. 3-APS exhibits weak $GABA_B$-receptor antagonism (Bowery, 1993), especially at higher concentrations.

Figure 7.1.a. shows chart recorder traces (a and c) of the effects of 100 and 500 µM GABA on spontaneous activity of a neocortical slice in Mg^{2+}-free ACSF. GABA is active at both $GABA_A$- and $GABA_B$-receptors. It is noted that 100 µM GABA (trace a) did not have a significant effect on the amplitude or frequency of discharges, whereas 500 µM GABA (trace c) clearly abolished or diminished tissue activity for the period of its application. Trace (b) shows the effects of 1 µM 3-APS which resembles those of GABA at the higher concentration, confirming that 3-APS is a potent agent (Krogsgaard-Larsen et al., 1988; Bowery, 1993). Trace (d) is recorded from a separate slice showing how 10 µM 3-APS eliminated discharges for a period almost twice as long as the duration of its application. 3-APS is reported to be at least as active as GABA at $GABA_A$ sites (Bowery, 1993). However, as was noted by Kerr and Ong (1992) and is shown by these experiments, partly due to lack of uptake, 3-APS is more potent than GABA. At the concentrations used here, 3-APS has only minimal antagonist actions on $GABA_B$-receptors, since doses greater than 50 µM is required for the antagonist effects.

Applications of 500 μM or 1 mM GABA caused baseline hyperpolarisation in the present model (trace c). It is reported that in normal conditions GABA-mediated inhibition in the neocortex leads to hyperpolarisation and a reduction of membrane excitability by shunting of epsps (Aram et al., 1989). In agreement with the present finding, Horne et al. (1989) report that superfusion of 1 mM GABA for 2 minutes significantly reduced the frequency of paroxysmal events during the first 5 minutes. However, Horne and colleagues observed the effect of GABA was associated with a reduction in amplitude of the paroxysmal events only when it produced a depolarisation.

Computer-recorded data in figure 7.1.b show the effects of (a) 50 μM GABA and (b) 100 μM GABA on 2 independent slices. It appears that, in the absence of a GABA uptake blocker, such relatively low concentrations of GABA only marginally modify the amplitude or the number of after-potentials of discharges compared to control. However, figure 7.1.c shows a discharge modified by a higher concentration of 1 mM GABA, which is clearly smaller than control.

Two sets of computer collected responses in figure 7.1.d show how discharges were modified by two successive applications of 1 μM 3-APS. Sufficient time, exceeding 30 minutes, was allowed between applications for tissue recovery. The computer records show that 1 μM 3-APS slightly reduced the discharge amplitude compared to control. As mentioned earlier, 10 μM 3-APS eliminated discharges. The middle computer data frame in figure 7.1.e shows the first discharge on return from a period

when discharges were eliminated. This discharge which exhibits extended after-activity can also be picked from the chart recorder trace (d) in figure 7.1.a. As explained in introductory chapters, initial discharges on resumption of activity after a period of suppression are often prolonged, possibly as neurotransmitter stores are replenished during the quiescent period.

It can be concluded that due to uptake, the effect of GABA in modifying spontaneous neocortical discharges is only significant with 0.5 or 1 mM concentrations, but this requires experiments with and without GABA uptake blockers to confirm its validity, as discussed later in sub-section 7.5.1. The results here also confirm that 3-APS is a potent $GABA_A$-receptor agonist.

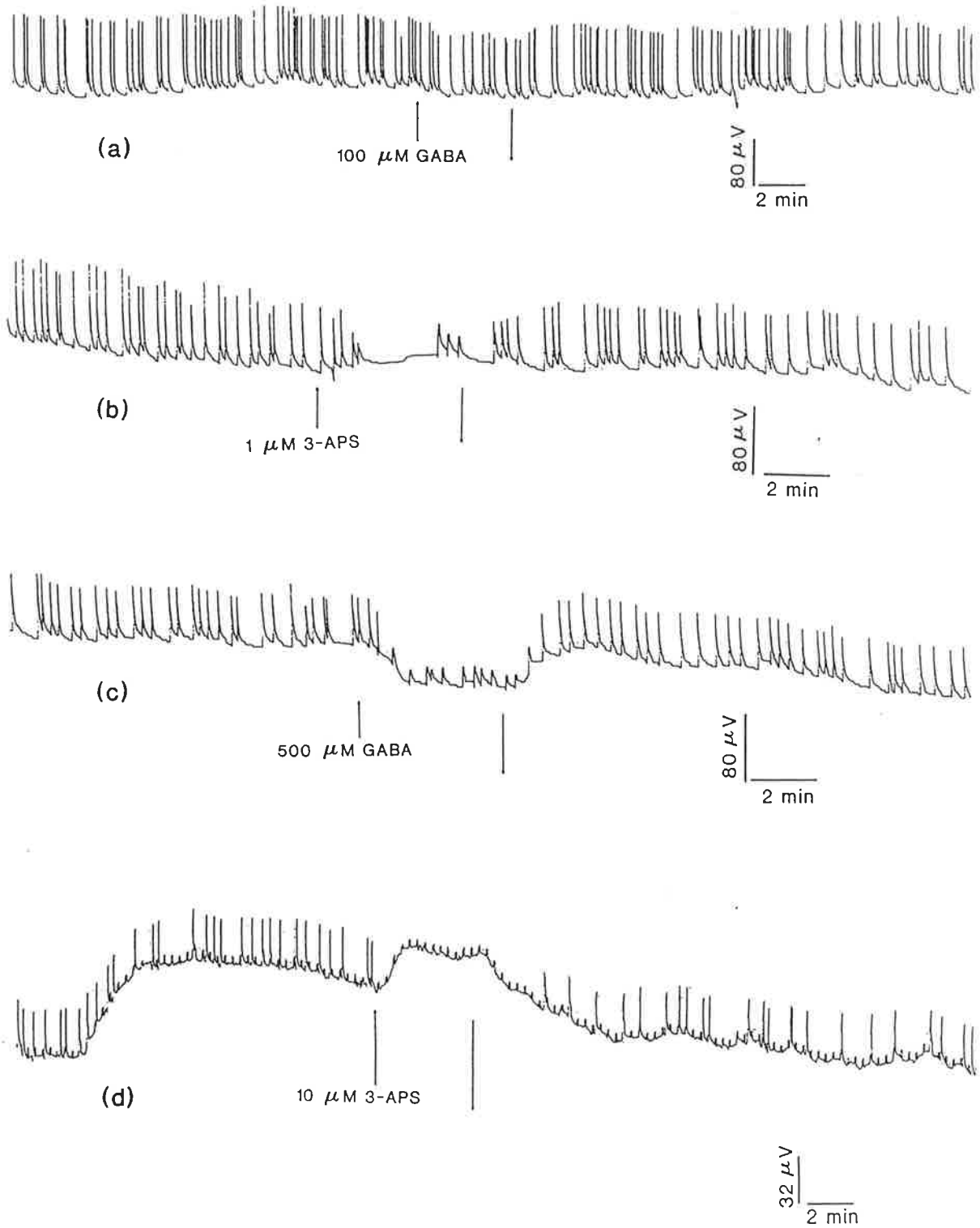

Figure 7.1.a Chart recorder traces showing the effects of 100 and 500 μM GABA, as well as 1 and 10 μM 3-APS on spontaneous activity recorded from neocortical slices in Mg^{2+}-free ACSF. Traces (a), (b) and (c) are from the same slice. Trace (d) is from a different slice showing how 10 μM 3-APS produced a period of complete inactivity, and a slower discharge frequency after its application.

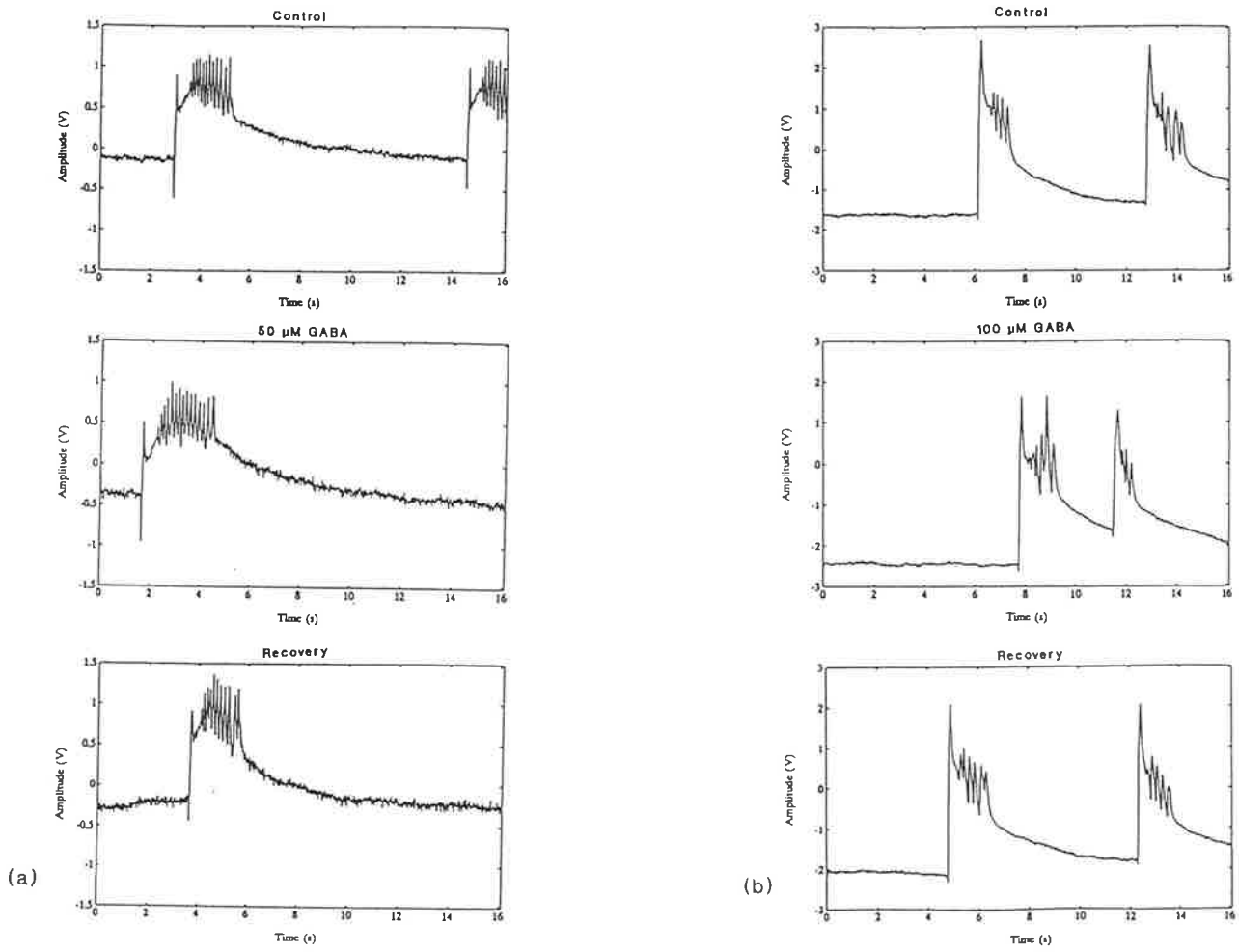

Figure 7.1.b Two independent sets of computer recorded responses showing the effects of (a) 50 µM GABA and (b) 100 µM GABA on discharges. Although no marked effects are noted, most likely due to GABA being taken up, 50 µM GABA seems to have somewhat reduced the amplitude and increased the number of after-potentials of the discharge compared to control.

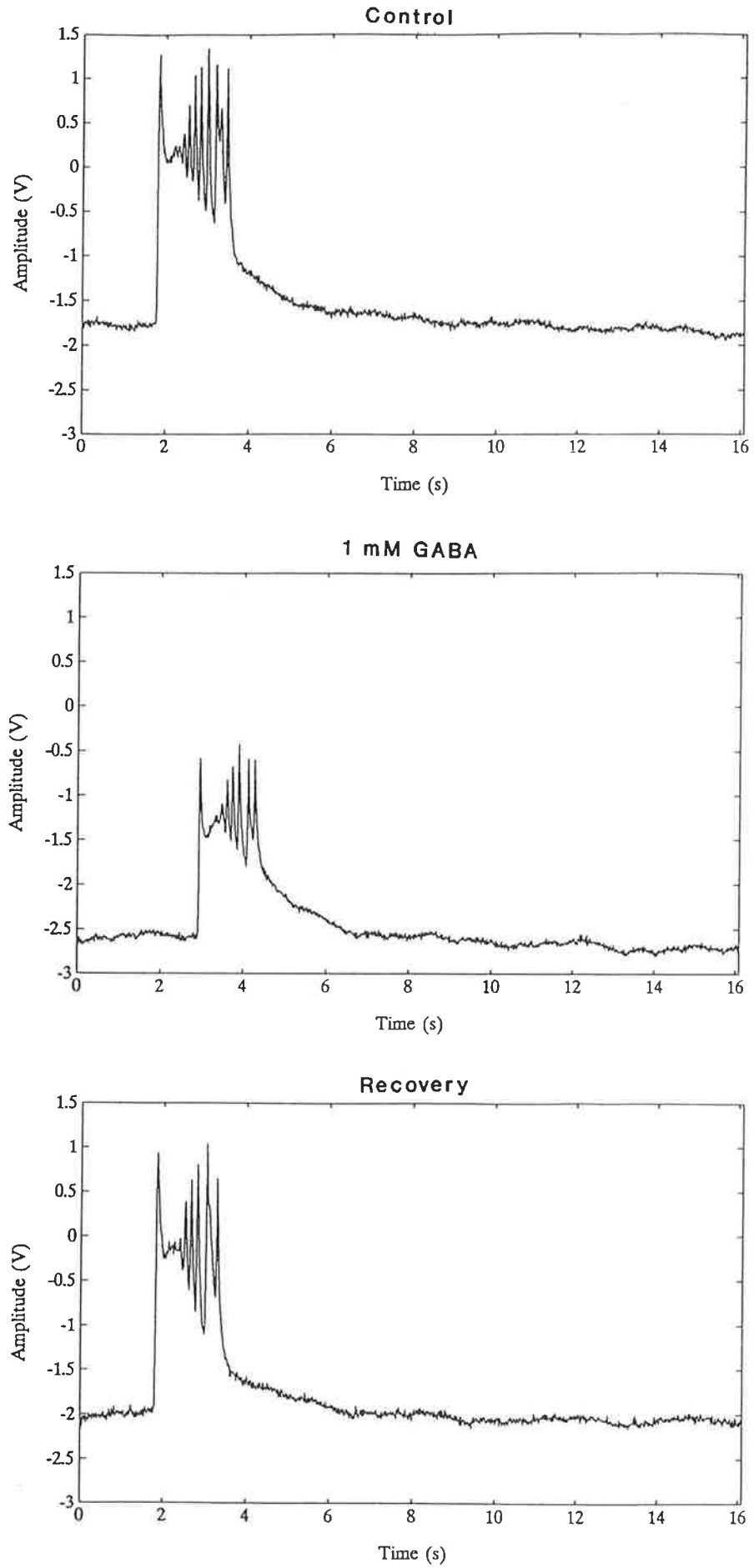

Figure 7.1.c Computer recorded responses showing control, a discharge in the presence of 1 mM GABA, and recovery. Miniaturisation of the discharge by 1 mM GABA is illustrated.

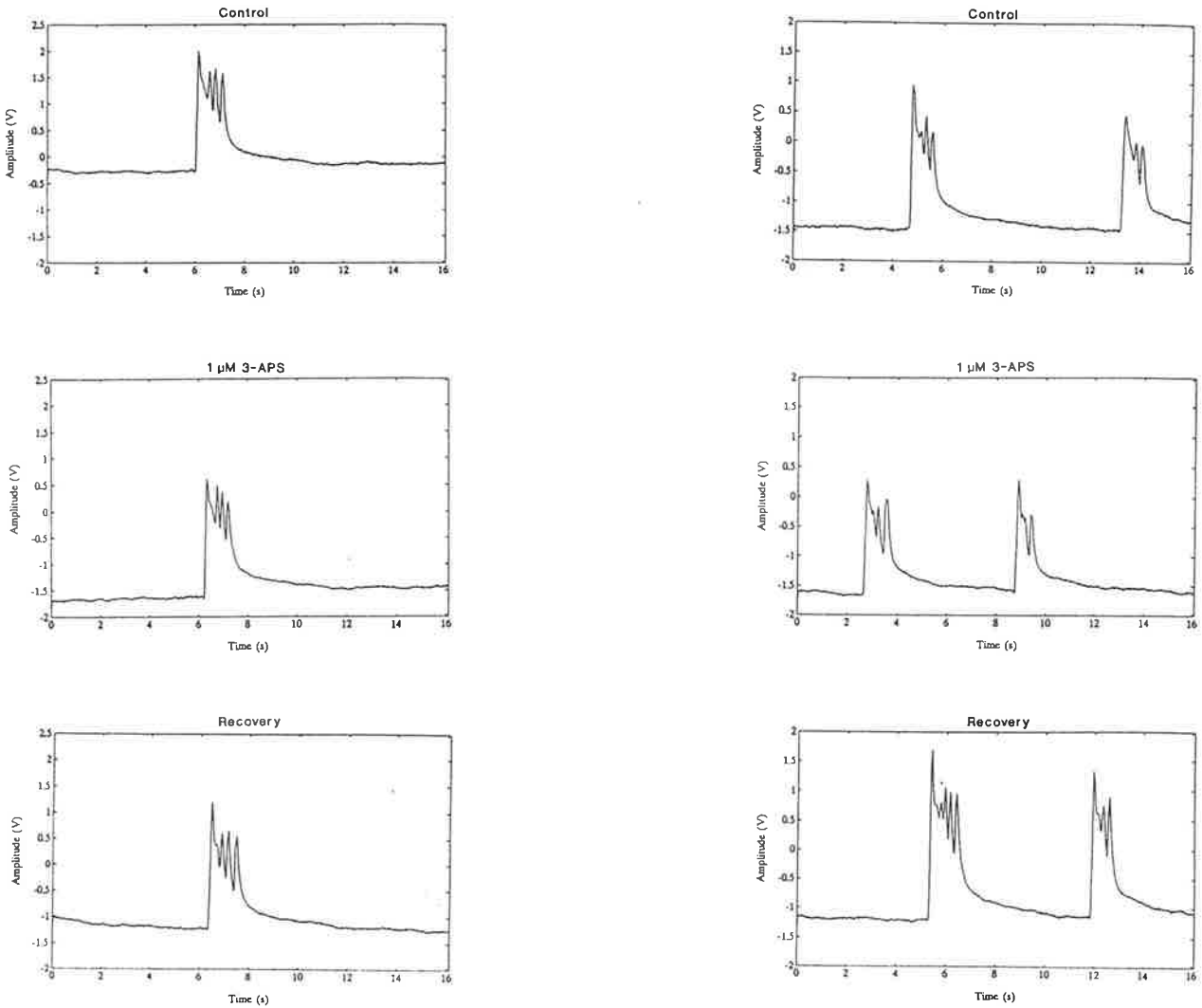

Figure 7.1.d Two sets of computer recorded responses showing the effects of 1 μM 3-APS on discharges recorded from the same slice. Discharges in the presence of 1 μM 3-APS appear slightly smaller than control.

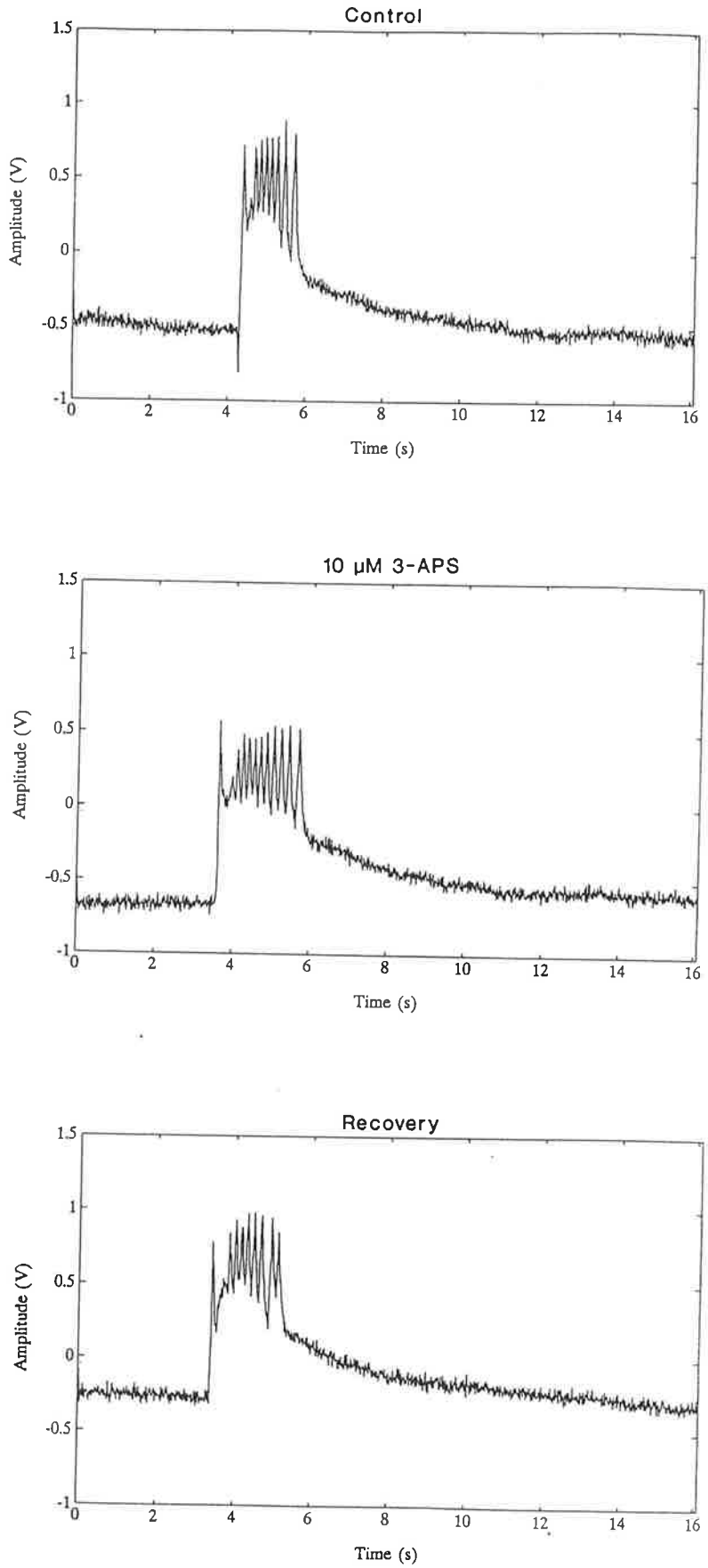

Figure 7.1.e Computer recorded responses showing control, a discharge in the presence of 10 µM 3-APS, and recovery. The middle response shows the first discharge on resumption of activity, after a period of suppression (c.f. figure 7.1.a, trace d).

7.1.1 Muscimol, THIP, and Propofol as Notable $GABA_A$-Receptor Agonists

A great advance in structure-action studies at $GABA_A$-receptors has been provided by the discovery that the naturally occurring isoxazolol muscimol (MUSC) is a potent agonist at $GABA_A$-receptors, with a strong structural resemblance to GABA. Incorporating the basic function of muscimol into a ring structure gives THIP, (4,5,6,7-tetrahydroisoxazolo[5,4-c]pyridine-3-ol), which is a moderately potent $GABA_A$-receptor agonist. Unlike Muscimol which is toxic and is rapidly metabolised, THIP has undergone clinical trial. It does not cause respiratory depression, but shows sedative effect. THIP perhaps represents the true muscimol conformation for activating low-affinity $GABA_A$-receptors (Kerr and Ong, 1992), although an earlier study by Hill et al. (1981) indicated direct involvement of the classical bicuculline-sensitive GABA-receptor was unlikely. Amino acids are likely to cross the brain-blood barrier (BBB) in the unionized form. GABA and isoguvacine do not permeate the BBB, whereas THIP and muscimol enter the brain easily after peripheral administration in animals. Dihydromuscimol (DHM) in the forms of (S)-DHM, (S)-4,5-DHM, are reported to be the most powerful agonist at $GABA_A$-receptors (Krogsgaard-Larsen et al., 1988).

It is worth noting that currently one of the more interesting short acting general anaesthetics in clinical use is Propofol (2,6-diisopropylphenol). It is a short acting anaesthetic, well suited to day-surgery. Propofol is chemically unrelated

to other general anaesthetics, or to any previously found agents acting at $GABA_A$-receptors (Kerr and Ong, 1992). It enhances $GABA_A$-receptor-induced responses in neurones (Hale and Lambert, 1991) which may be the basis of its anaesthetic and sedative actions. It has been observed that Propofol inhibits spontaneous activity in neocortical slices in Mg^{2+}-free ACSF.

7.2 EFFECTS OF BICUCULLINE METHIODIDE ON SPONTANEOUS NEOCORTICAL DISCHARGES

Picrotoxin was, at first, the only $GABA_A$-receptor antagonist available. It has a poor aqueous solubility and no charge on the molecule. Picrotoxin is a non-competitive $GABA_A$-receptor antagonist. Specific picrotoxin sites are likely found on all subunits of the $GABA_A$-receptor complex, certainly on the α and ß subunits where they are closely associated with the GABA-receptor region. The barbiturate and picrotoxin sites, even if different, are closely coupled since ligands for each mutually prevent the actions of one another (Kerr and Ong, 1992).

Bicuculline, a phthalide isoquinoline alkaloid, was the first competitive $GABA_A$-receptor antagonist shown to be specific against GABA (Curtis et al., 1970). It was the introduction of this antagonist that eventually led to general acceptance of the notion that GABA is an inhibitory transmitter in the mammalian CNS. Bicuculline is now used routinely to define

$GABA_A$-receptor-mediated processes, where the receptors are coupled to chloride conductance mechanisms in neuronal membranes. All the effects of GABA and GABA-related analogues on these receptors can be prevented by this antagonist (Bowery, 1993). Antagonism with bicuculline is stereospecific. The more stable and soluble quaternary derivatives of (+)-bicuculline are bicuculline methochloride (BMC) and bicuculline methiodide (BMI). However, bicuculline and its quaternary derivatives do show some effects that suggest mode(s) of action unrelated to its $GABA_A$-receptor antagonist or anticholinesterase properties (Kerr and Ong, 1992).

BMC and picrotoxin have different sites of action at the postsynaptic GABA-receptor complex (Krogsgaard et al., 1988). Bicuculline behaves as a true competitive antagonist, competing for the GABA binding site and directly interacting with the $GABA_A$-receptor. Bicuculline does not behave as a chloride channel blocker, nor does it alter the kinetics of the channel. In contrast, all non-competitive antagonists, such as picrotoxin, are ion channel modifiers (Kerr and Ong, 1992).

It is a characteristic feature of bicuculline interaction with $GABA_A$-receptors that this antagonist preferentially combines with low-affinity sites (Krogsgaard et al., 1988) and that chaotropic agents enhance the ability of bicuculline to displace [^{3}H]-GABA from its low-affinity binding sites (Kerr and Ong, 1992).

Chart recorder traces in figure 7.2.a show the effects of 25 and 50 μM BMI on spontaneous activity from the same neocortical slice. These concentrations of BMI did not appear to have a pronounced effect on the amplitude of discharges. A reduction in discharge frequency as well as an increase in the number of after-potentials of individual discharges were however noted, where BMI had some effects. Secondary discharging was particularly notable with 50 μM BMI application. These extended discharges are faintly detectable in the lower chart recorder trace in figure 7.2.a. Computer collected responses in figure 7.2.b and 7.2.c show detail of the effects of 25 and 50 μM BMI in modifying discharges.

In line with these observations, Traub et al. (1994) found that $GABA_A$-receptors blockade was important in determining the number of secondary bursts in discharges from hippocampal slices, and Merlin and Wong (1993) observed the addition of picrotoxin or bicuculline elicited burst discharges in individual cells which consisted of a primary burst followed by a series of secondary bursts. Other studies of the effects of $GABA_A$-receptor antagonists on neocortical slices report mixed findings. Gutnic et al. (1982) found that penicillin and bicuculline, induced neither spontaneous membrane potential depolarising shifts nor convulsive discharges, whereas Robichaud and Boxer (1993) found that, in the spontaneous epileptiform discharge model, the $GABA_A$-receptor antagonists picrotoxin and (-)-bicuculline at relatively high concentrations (50 μM) had little (picrotoxin) or no (bicuculline) effect on amplitude or frequency of spontaneous epileptiform discharges. Karnup (1992) observed that 100 μM

picrotoxin induced no change in spike trains during background firing in guinea-pig neocortex in vitro.

The effects of BMI on spinal cord cultures may be different, as Rhoades and Gross (1994) found that treatment with 60 µM BMI reliably increased the burst amplitude and the regularity of both burst amplitude and burst frequency, inducing a stable, synchronised, quasi-periodic network bursting mode.

BMI suppresses $GABA_A$-receptor mediated inhibition presynaptically, eliciting discharges of a more complex nature.

Since BMI and picrotoxin are effective $GABA_A$-receptor antagonists, more obvious responses to their application in the present slice model are immediately expected. The fact that such responses are not seen raises some interesting points; notably that $GABA_A$-receptor antagonism disinhibits the $GABA_B$-receptors, resulting in the release of $GABA_B$-receptor-mediated inhibition, which depresses the slice activity.

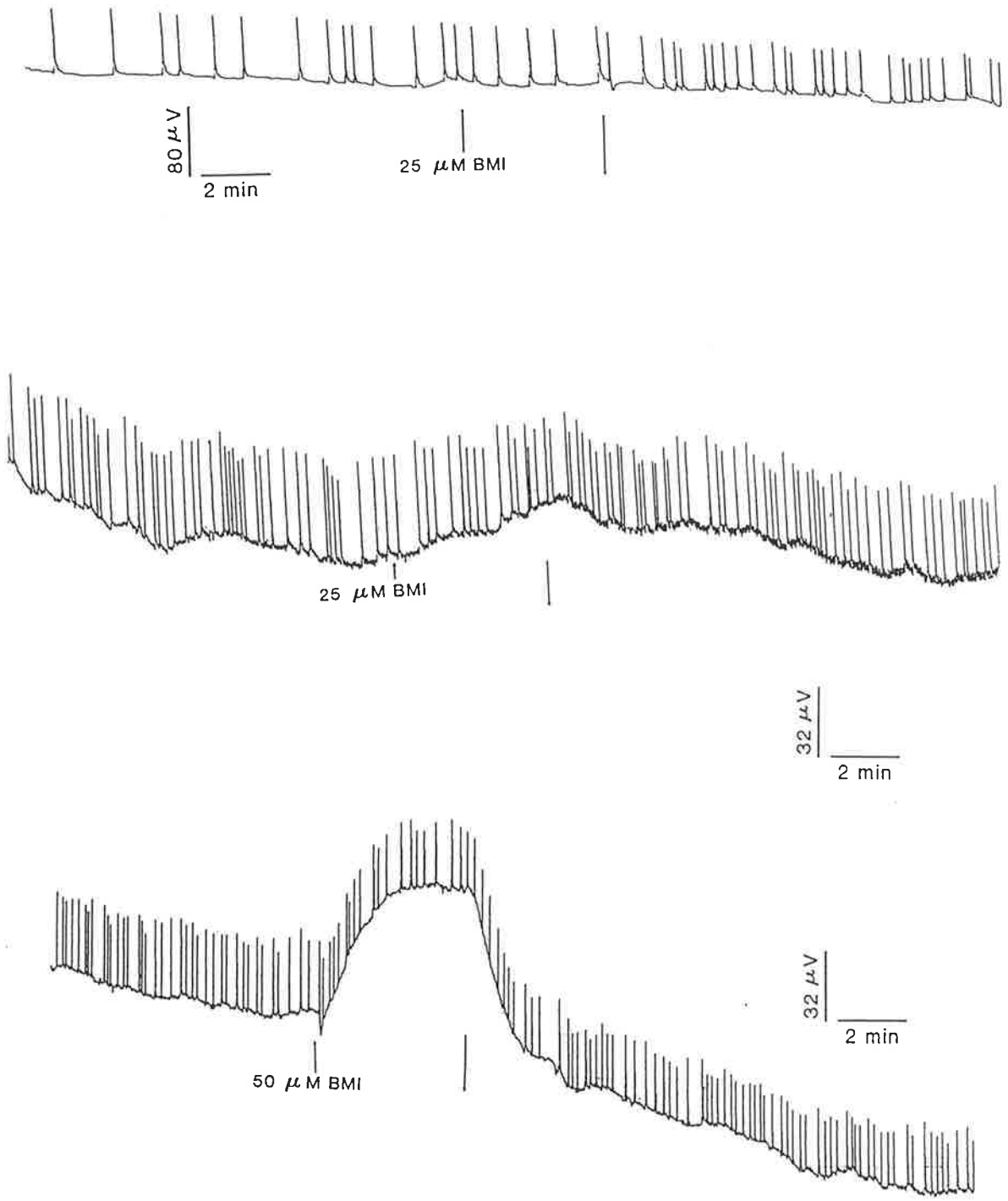

Figure 7.2.a Chart recorder traces showing the effects of 25 and 50 μM BMI on spontaneous discharges from a neocortical slice. The chart recorder sensitivity is set lower for the upper trace. A pronounced baseline potential is seen with 50 μM BMI.

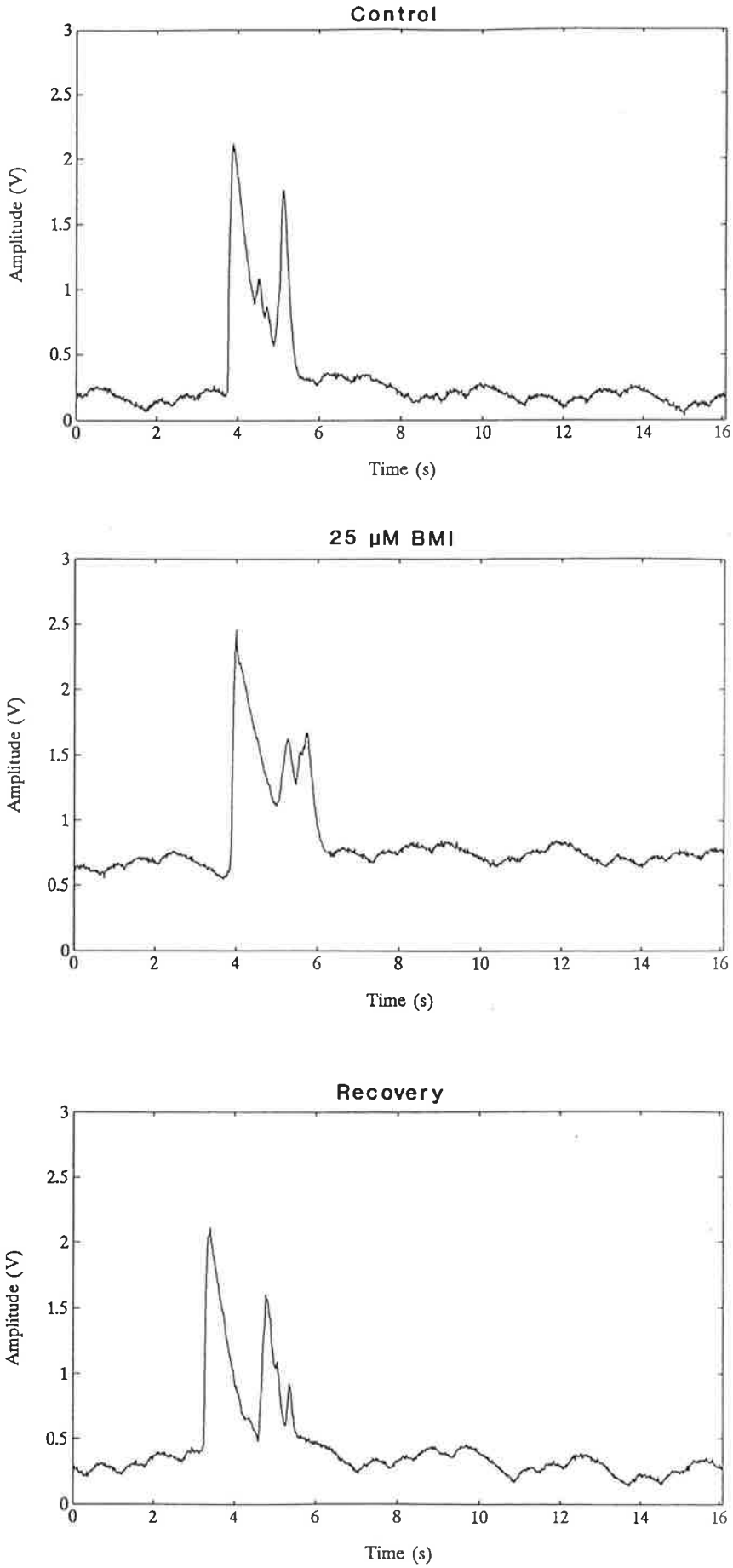

Figure 7.2.b A set of computer recorded responses showing that 25 µM BMI slightly extended a discharge, compared to control. The bottom trace shows a discharge on partial recovery.

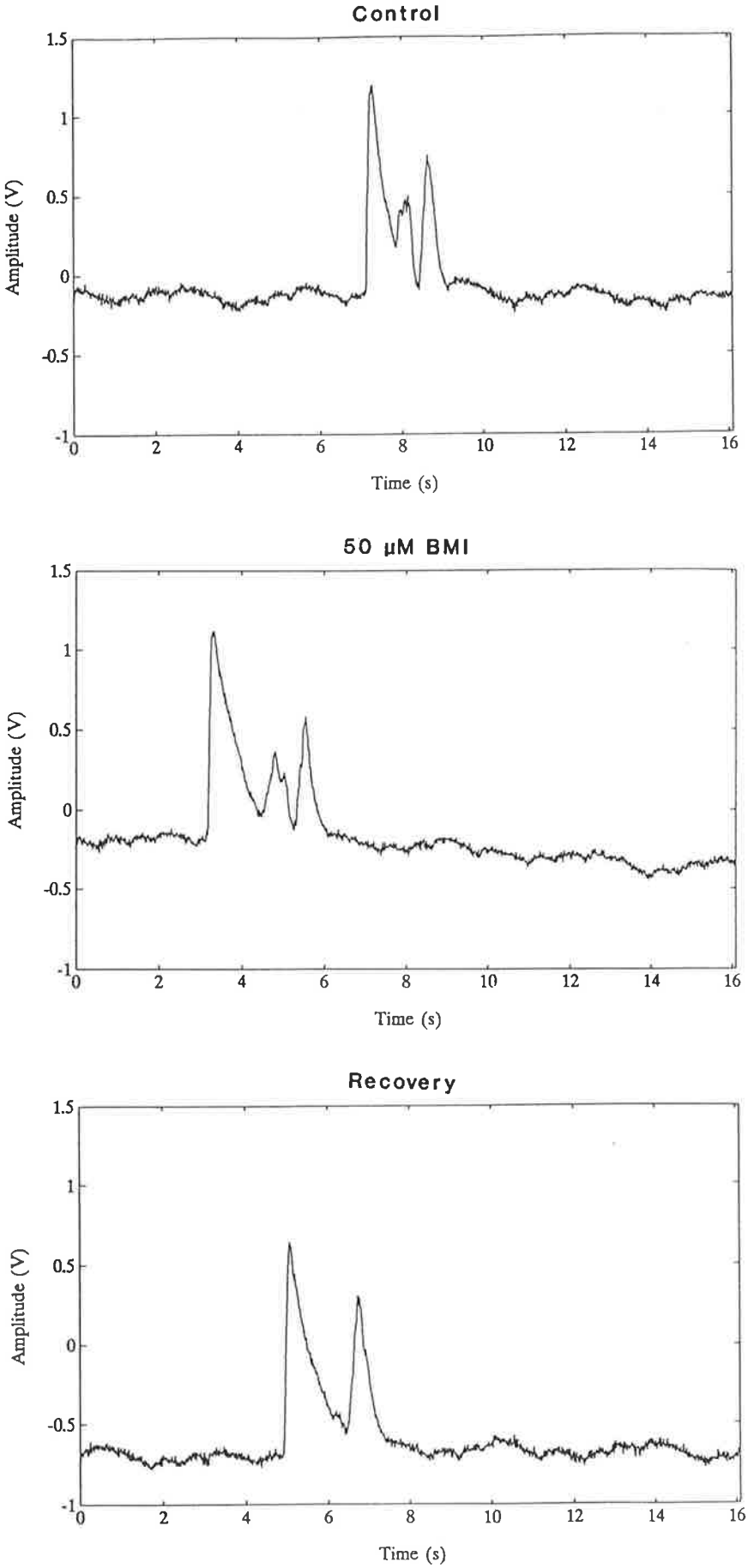

Figure 7.2.c Computer acquired responses showing control, a discharge in the presence of 50 µM BMI, and recovery. 50 µM BMI normally prolonged discharges.

7.3 EFFECTS OF BACLOFEN AS A $GABA_B$-RECEPTOR AGONIST ON SPONTANEOUS NEOCORTICAL DISCHARGES

$GABA_B$-receptors can also be subdivided into presynaptic receptors, including autoreceptors, and postsynaptic receptors. A modulatory role of $GABA_B$-receptors in signal transduction mechanisms, through intracellular messenger systems is suggested. $GABA_B$-receptors are heterogeneous (Bowery, 1993). Pre- and postsynaptic receptors are likely different from one another (Asprodini et al., 1992) and are indirectly coupled through G proteins and second messenger systems to either Ca^{++} or K^+ channels, where they mediate a presynaptic reduction in Ca^{++} influx, or a postsynaptic increase in K^+ conductance (Krogsgaard-Larsen et al., 1988; Kerr and Ong, 1992). $GABA_B$-receptor-mediated inhibition of neurotransmitter release is manifest in a variety of systems (Bowery, 1993).

Baclofen, ß-p-chlorophenyl-GABA, is an analogue of GABA, with a lipophilic substituent on the GABA backbone. Baclofen is virtually inactive at $GABA_A$ sites but is stereospecifically active at $GABA_B$ sites, with R(-)-baclofen being the active form. Baclofen penetrates the brain and acts on $GABA_B$-receptors. Baclofen is in general use as a muscle relaxant and an antispastic agent (Kerr and Ong, 1992). It not only reduces skeletal muscle tone and inhibits spinal monosynaptic and polysynaptic reflex activity, but also depresses activity in higher brain centres. There are no other strict baclofen analogs of note as $GABA_B$-receptor agonists, since the sulphonic and phosphonic analogs are antagonists. However,

some phosphinic analogs of GABA, 3-aminopropylphosphinic acid and its methyl analogue, are highly effective in $GABA_B$ binding and act as agonists in functional tests (Kerr and Ong, 1992; Bowery, 1993).

Figure 7.3.a shows the effects of baclofen in 0.05 to 5 µM range on spontaneous discharges recorded from a neocortical slice. Note that baclofen concentrations below 0.5 µM did not markedly change the discharge frequency. The period of quiescence observed on or following a four-minute application of baclofen was directly proportional to its concentration in the 0.5 to 10 µM range tested i.e. the higher the baclofen concentration, the longer the period during which discharges became irregular or were eliminated.

Figure 7.3.b shows chart recorder traces obtained from another slice confirming that 0.1 and 0.2 µM baclofen did not significantly affect the amplitude or rate of occurrence of spontaneous discharges. A small baseline hyperpolarisation was noted with baclofen concentrations above 0.5 µM.

It is weakly detectable from the chart recorder traces in figure 7.3.a that, on resumption of activity, the first discharge is prolonged with each of the 1, 2 or 5 µM baclofen applications.

As shown by computer records in figure 7.3.c, 0.1 µM baclofen reduced the number of after-potentials, without affecting the amplitude of discharges in two independent experiments. Note how the first discharge on resumption of regular firing is

somewhat prolonged. Figure 7.3.d shows how a discharge modified by 0.2 μM baclofen has smaller after-potentials, but its amplitude is not significantly affected. Computer data in figure 7.3.e show the effects of 1 μM baclofen on neocortical discharges. Discharges occurring during application of 1 μM baclofen were normally reduced both in amplitude and duration. In some experiments, as exemplified in set (b) of figure 7.3.e, 1 μM baclofen lowered the position of after-potentials on the falling phase of discharges as well as increasing the number of after-potentials. This effect suggests that higher and lower concentrations of baclofen may produce different effects. It has been suggested that the presynaptic and postsynaptic actions of baclofen contribute almost equally to suppression of the transmission at 1 μM, whereas the presynaptic action predominates at 5 μM (Hirata et al., 1992).

Lewis et al. (1989) studied the effects of baclofen on epileptiform discharges recorded from hippocampal slices and, contrary to the present results, found that although the discharge frequency increased when baclofen concentration was reduced in steps from 5 to 2 to 0.5 μM, there was no consistent change in the duration of individual discharges, and at a very low concentration of baclofen (0.1 μM), discharges became quite brief and unstable.

Any discharges seen while 10 μM baclofen was effective were always smaller than control. Figure 7.3.f represents a set of computer collected data from a slice showing how a discharge modified by 10 μM baclofen was smaller than control. It is noted how discharges on recovery contain more after-

potentials. "Miniaturisation" of discharges with higher baclofen concentrations were consistently seen in these experiments. In partial agreement, Horne et al. (1986) found that, in Mg^{2+}- free ACSF, superfusion of 10 µM baclofen for 2 minutes significantly reduced the frequency of paroxysmal events for the first 10 minutes, but did affect the amplitude of these events.

These observations that baclofen at higher concentrations produces, if any, smaller discharges during its application, and extends the discharges which re-appear after the period of quiescence, suggest that baclofen and GABA can diminish the evoked release of neurotransmitters. Although diminution in Ca^{2+} flux would provide an obvious explanation, Gahwiler and Brown (1985) found no evidence for Ca^{2+} involvement in the response to $GABA_B$-receptor activation in hippocampal slices, and deduce that any change in Ca^{2+} conductance results from an initial increase in K^+ conductance. In contrast, Scholtz and Miller (1991) indicate that the Ca^{2+} current responsible for mediating presynaptic inhibition in cultured hippocampal neurones is modulated by $GABA_B$-receptors. 10 µM baclofen is known to inhibit Ca^{2+} channel currents in adult rat sensory neurones (Formenti and Sansone, 1991), and in embryonic neurones (Dunlap, 1981). Baclofen suppression is shown to be more potent on the early Ca^{2+} current than the later, thus slowing the rate of Ca^{2+} current activation (Tatebayashi and Ogata, 1992), with some inactivation of the suppressive effect (Dunlap and Fischback, 1981). It may be that in the spinal cord, involvement of Ca^{2+} is most likely at primary afferent fibres, where $GABA_B$-receptor activation decreases the evoked

release of putative neurotransmitter peptides, such as substance-P (Bowery, 1993).

Within higher centres of the mammalian brain an increase in K^+ channel conductance appears to be the primary neuronal response to $GABA_B$-receptor activation and produces membrane hyperpolarisation (Bowery, 1993). Baclofen induced a small hyperpolarisation in rat neocortical slices in experiments reported in this section. In hippocampal neurones, baclofen is reported to depresses excitatory and inhibitory synaptic transmission, and hyperpolarises the neurones by increasing the K^+ conductance (Horne, 1986). Baclofen is also reported to depress excitatory postsynaptic potentials (epsps) and hyperpolarise the basolateral amygdala neurones with an EC_{50} of 1 μM (Asprodini et al., 1992). It is however uncertain whether baclofen exert its action directly through the G-protein or by activation of a second messenger system (Formenti and Sansone, 1991).

In summary, activation of post-synaptic $GABA_B$-receptors hyperpolarises neurones by increasing K^+ conductance, but the mechanism of synaptic depression produced by activation of presynaptic $GABA_B$-receptors has not been established (Lambert et al., 1991). Different pharmacological properties of pre- and post-synaptic receptors in the amygdala suggest that two distinct population of $GABA_B$ receptors may exist (Asprodini et al., 1992).

The likelihood that the pre- and post-synaptic receptors are different from one another is supported by Kerr and Ong (1992)

on the basis that these receptors are linked through different G-proteins to Ca^{2+} and K^+ channels. Bowery (1993), however, is uncertain whether the same G-proteins are responsible for coupling K^+ and Ca^{2+} channels.

The postsynaptic K^+ channels modulated by baclofen in hippocampal neurones have been reported to be affected by numerous substances, including the local anaesthetic QX-314 intracellularly, which appears to have no effect on Cl^- channels associated with $GABA_A$-receptors (Nathan et al., 1990; Andrade, 1991), and also quisqualic acid and kainic acid (Rovira et al, 1990).

Late inhibitory postsynaptic potentials (IPSP) which are responses to activation of $GABA_B$-receptors result from activation of K^+ channels (Kerr and Ong, 1992). The late IPSP and baclofen-induced hyperpolarisation can be antagonised by phaclofen, and by the more potent derivative 2-hydroxysaclofen (Turgeon and Albin, 1993), and by CGP35348 which is reported to be as potent as 2-hydroxysaclofen (Turgeon and Albin, 1993), or more potent than it (Fromm et al., 1992). Post- but not pre-synaptic effects of baclofen are reported to be blocked by 2-hydroxysaclofen (100 µM) and pertussis treatment (Asprodini et al., 1992). The fast IPSP mediated via $GABA_A$-receptors through an increase in Cl^- conductance is however reportedly unaffected (Bowery, 1993), supporting the notion that $GABA_B$- but not $GABA_A$- receptors are linked through G-proteins to K^+ channels.

Finally, figure 7.3.g shows phase-plane plots for a control, and a discharge in the presence of 2 μM baclofen. Multiple discharging of control, and a slower rate of rise of the modified discharge are highlighted in the corresponding Phase-plane plots.

Such analysis may prove useful in disclosing influences that affect the rate of rise of the initial response, and modify its rate of decline during the recovery to resting potential.

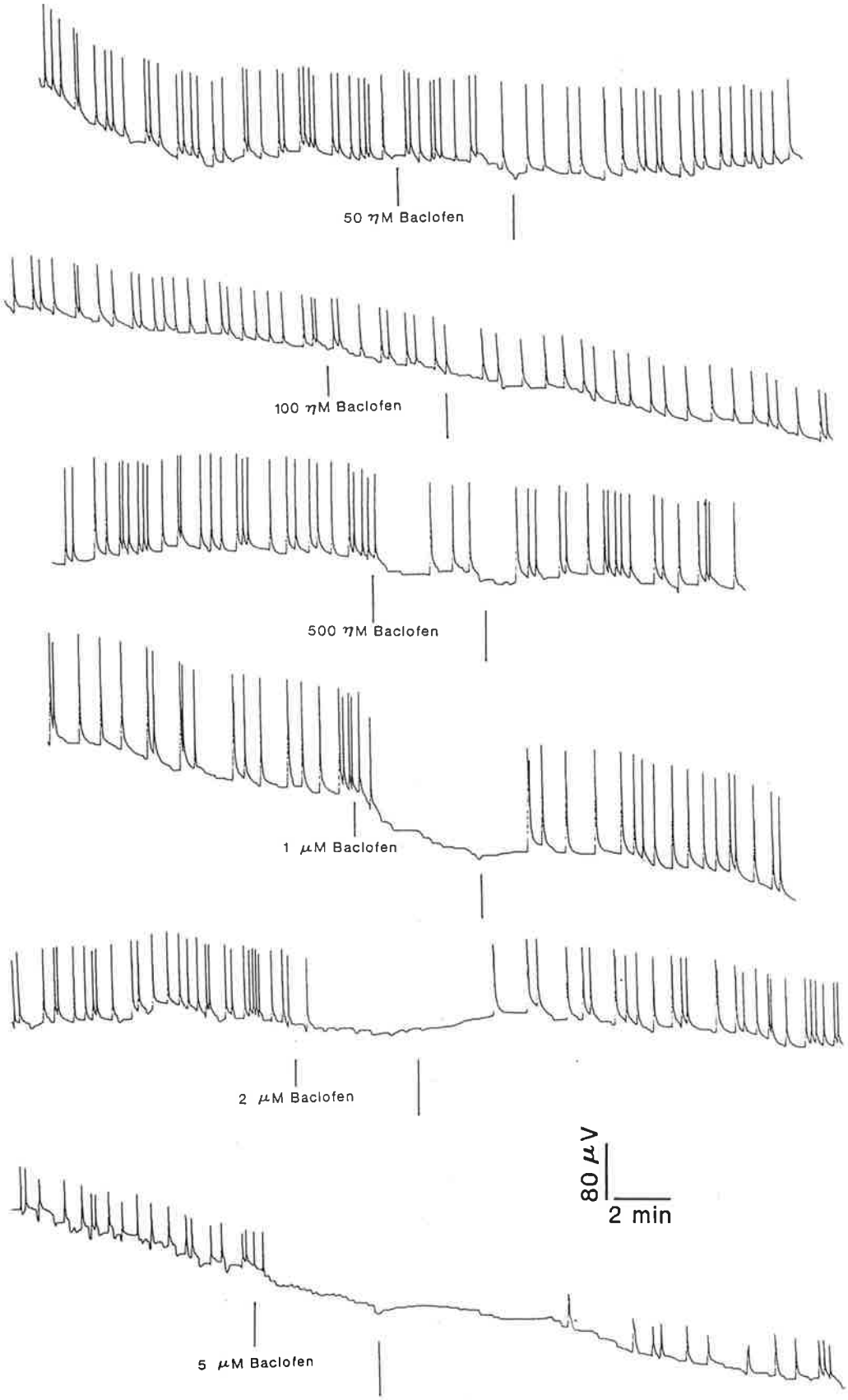

Figure 7.3.a Chart recorder traces showing the effects of 0.05 to 5 μM baclofen on spontaneous discharges recorded from the same neocortical slice. The effect of baclofen in diminishing or abolishing the activity is pronounced with 0.5 μM or higher concentrations.

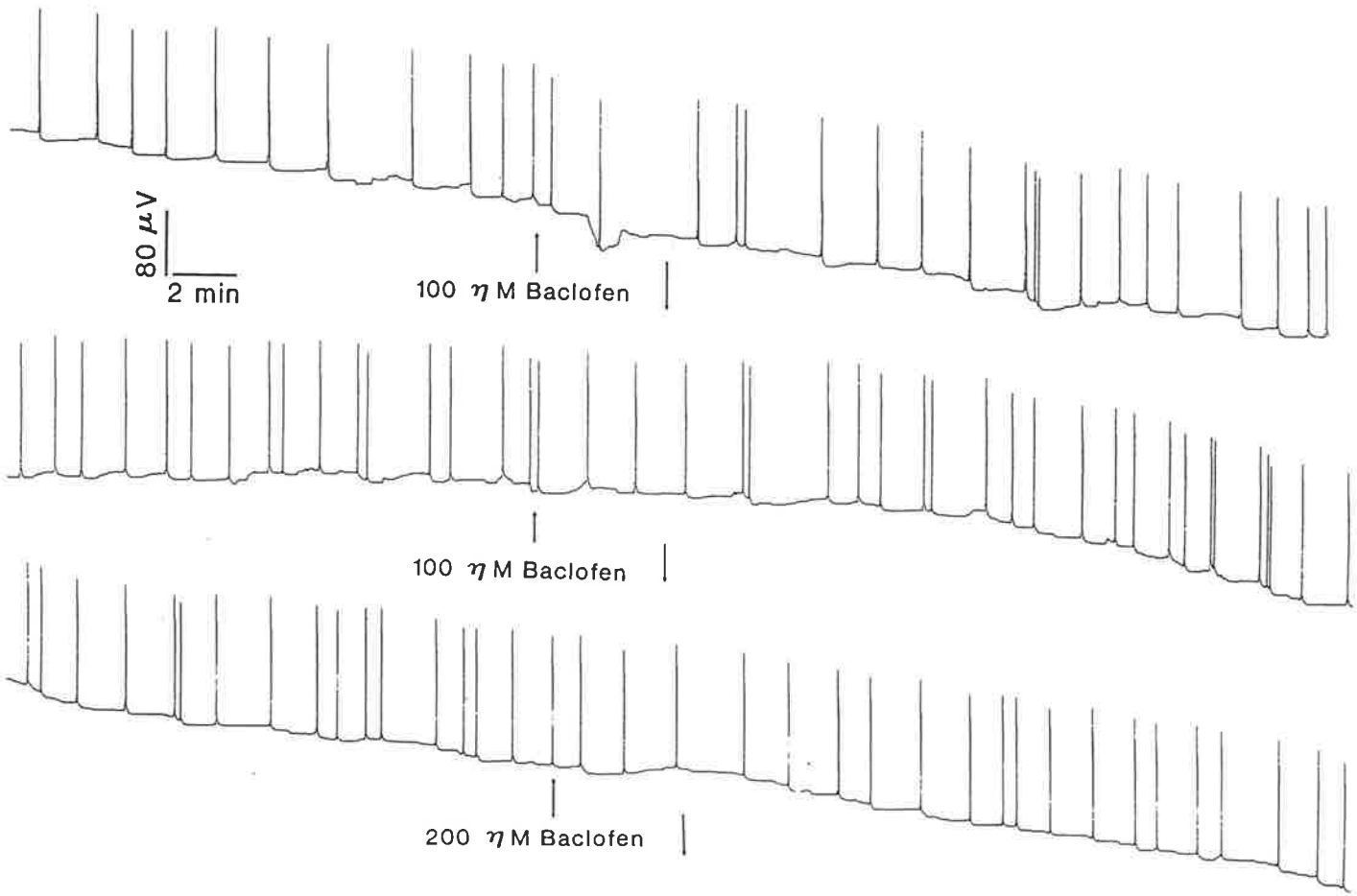

Figure 7.3.b A set of chart recorder data confirming that baclofen concentrations below 0.5 μM do not markedly affect the rate of spontaneous discharges from neocortical slices.

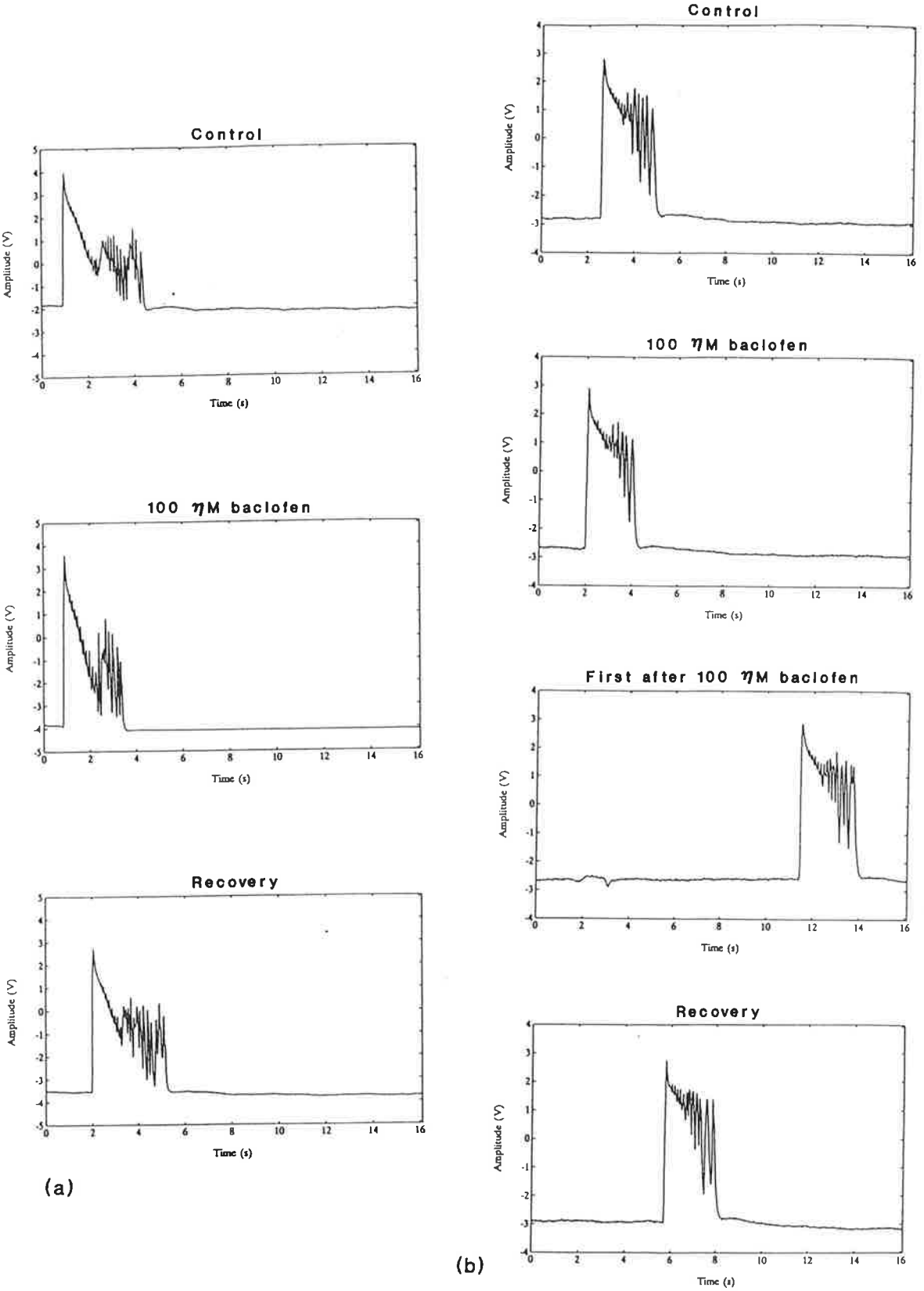

Figure 7.3.c Two sets of computer collected responses showing the effects of 100 ηM baclofen on spontaneous epileptiform discharges recorded from a slice. In both sets (a) and (b), 100 ηM baclofen reduced the after-activity of discharges without significantly affecting their amplitude. Note how the first discharge after baclofen application in (b) is considerably prolonged.

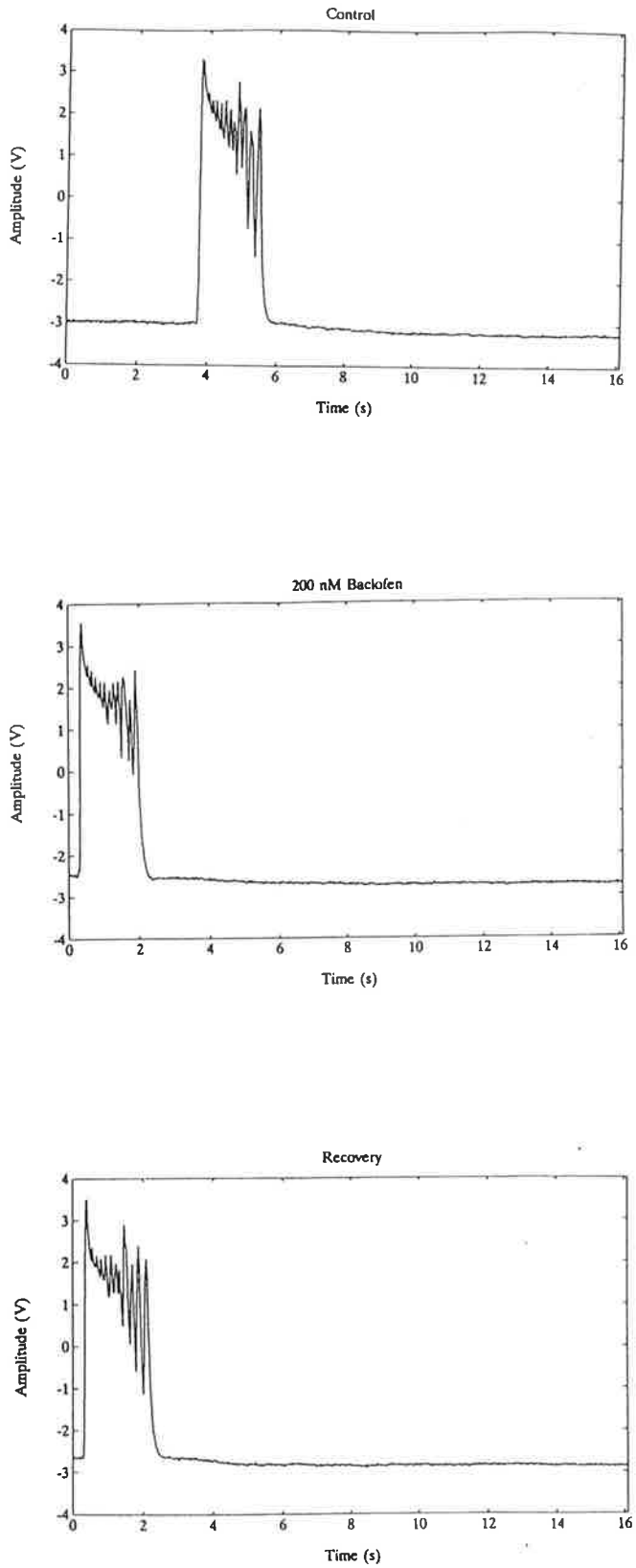

Figure 7.3.d A set of computer collected responses showing control, a discharge in the presence of 200 ηM baclofen, and recovery. The after-potentials are smaller in the middle response.

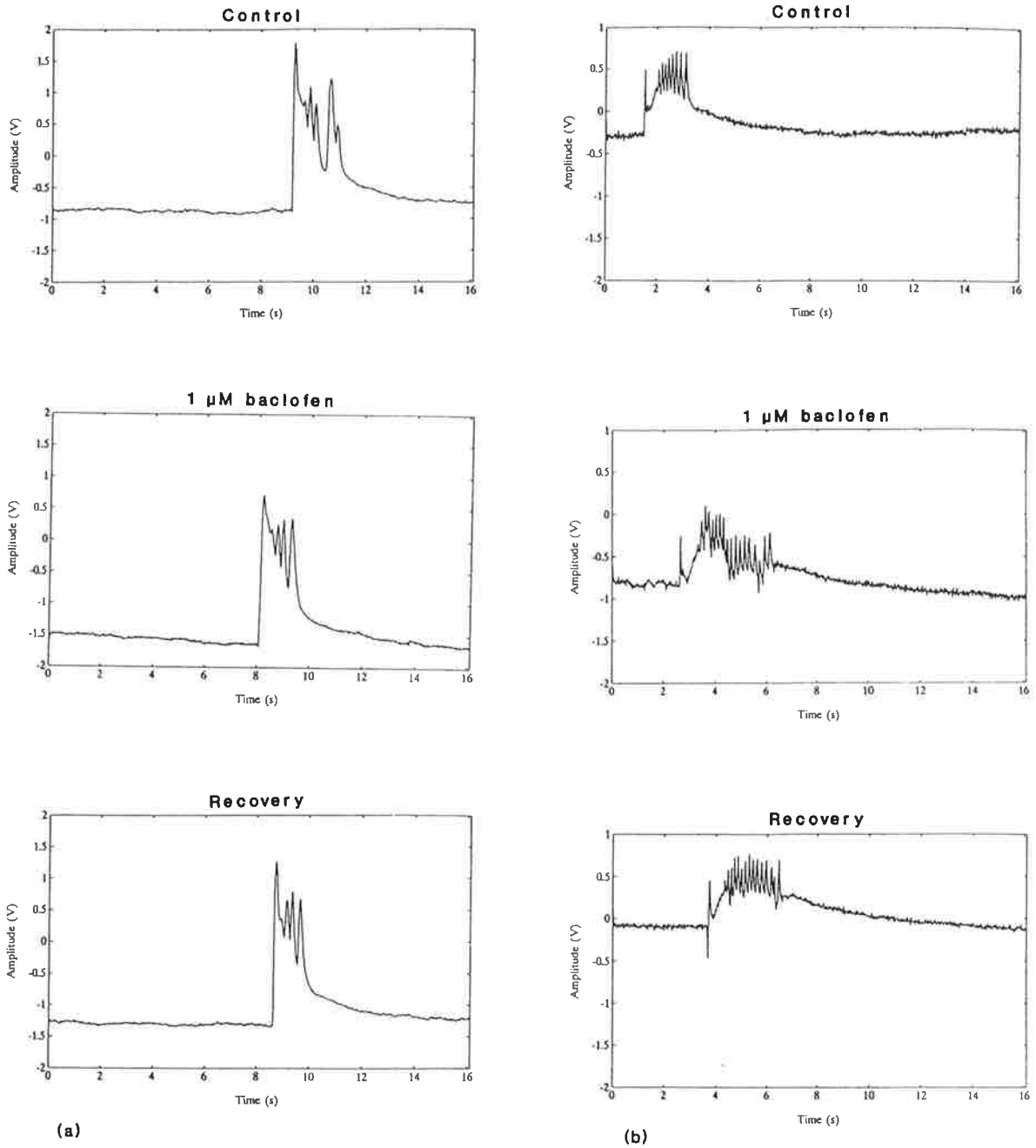

Figure 7.3.e Two sets of computer collected responses showing the effects of 1 μM baclofen on spontaneous discharges recorded from neocortical slices. 1 μM baclofen has reduced both the amplitude and duration of the discharge in set (a). In some experiments as shown in (b), 1 μM baclofen increased the number of after-potentials and moved them down the falling phase of discharges.

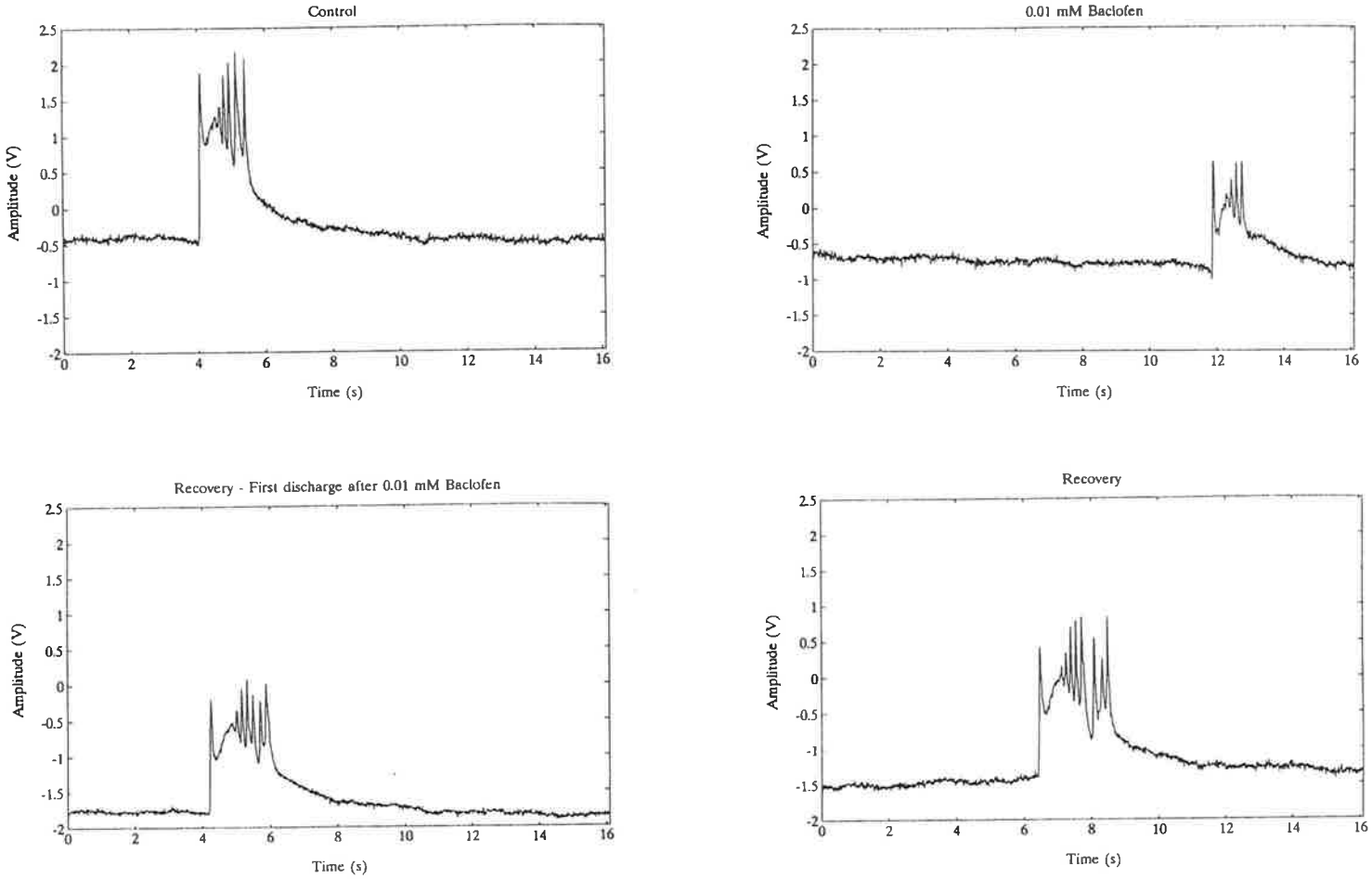

Figure 7.3.1 A set of computer collected responses showing how a discharge was modified by 10 μM baclofen, compared to control. A high baclofen concentration always produced a period of inactivity. Any discharge during this period was smaller, and the first discharge on resumption of activity usually had more after-potentials than control.

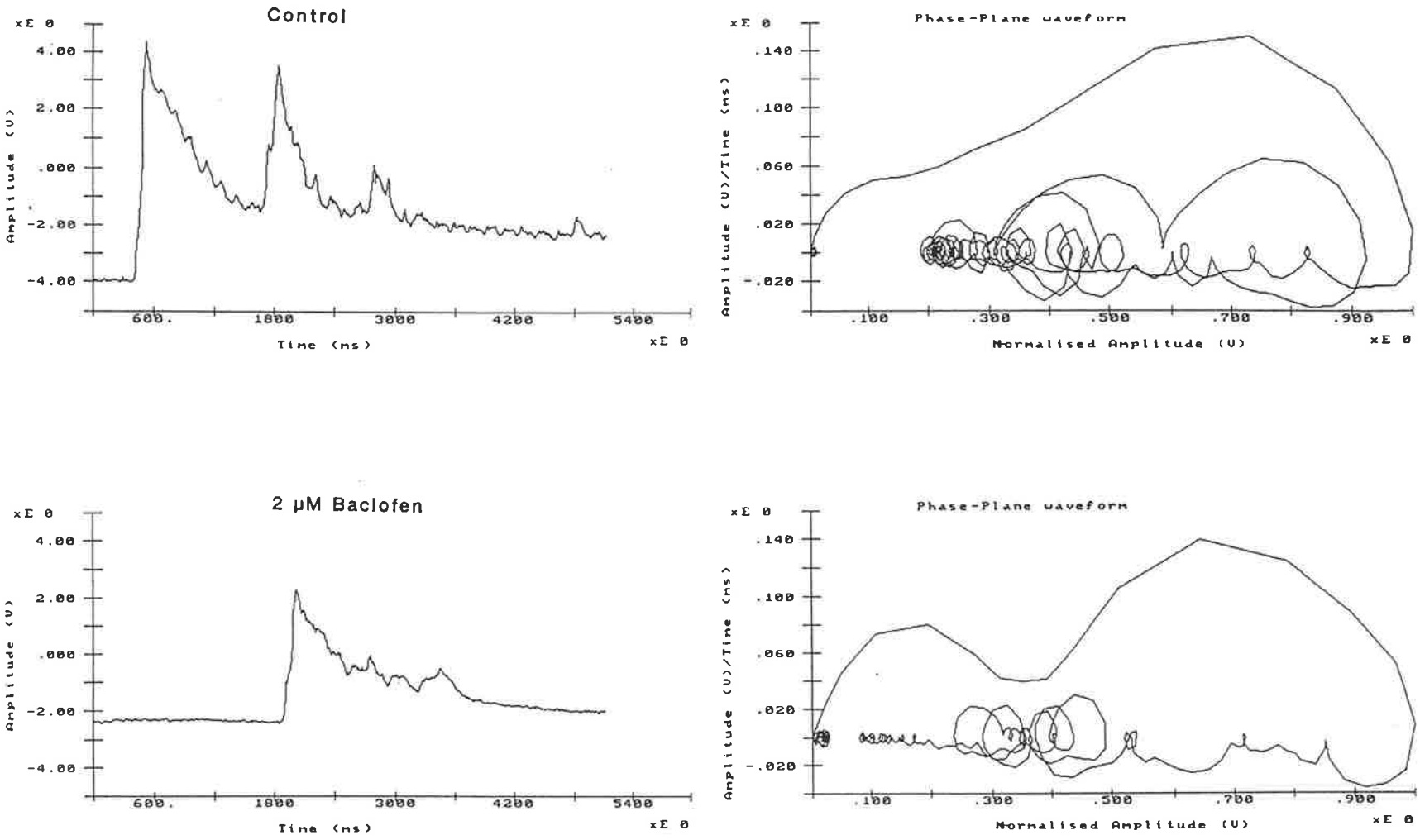

Figure 7.3.g Phase-plane plots comparing a discharge modified by 2 µM baclofen to control. Multiple discharging of control, and a slower rising phase of the modified discharge are highlighted by the phase-plane plots.

7.4 EFFECTS OF A MIXTURE OF BACLOFEN AND 3-APS ON SPONTANEOUS NEOCORTICAL DISCHARGES

Chart recorder traces in figure 7.4.a show the effects of 1 μM baclofen and 1 μM 3-APS on spontaneous neocortical discharges recorded from a slice. This slice appeared to be particularly excitable, since any modification of the amplitude or the rate of occurrence of discharges with 1 μM concentration of either of these agents was not pronounced. However, a mixture of 1 μM baclofen plus 1 μM 3-APS reduced both the frequency and amplitude of discharges, and the effect of a mixture of 5 μM baclofen and 5 μM 3-APS in eliminating regular discharging is clearly seen in the bottom trace. Figure 7.4.b is a set of computer collected responses showing control, discharges modified by the mixture of 1 μM baclofen and 1 μM 3-APS, and recovery. The computer frames clearly show that discharges are smaller in the presence of a mixture of $GABA_A$- and $GABA_B$-receptor agonists, confirming earlier studies that each agonist is effective in inhibiting the activity of neocortical slices. As expected, a mixture of these agents is very effective in abolishing spontaneous discharges, and the effect resembles that of GABA at higher concentrations.

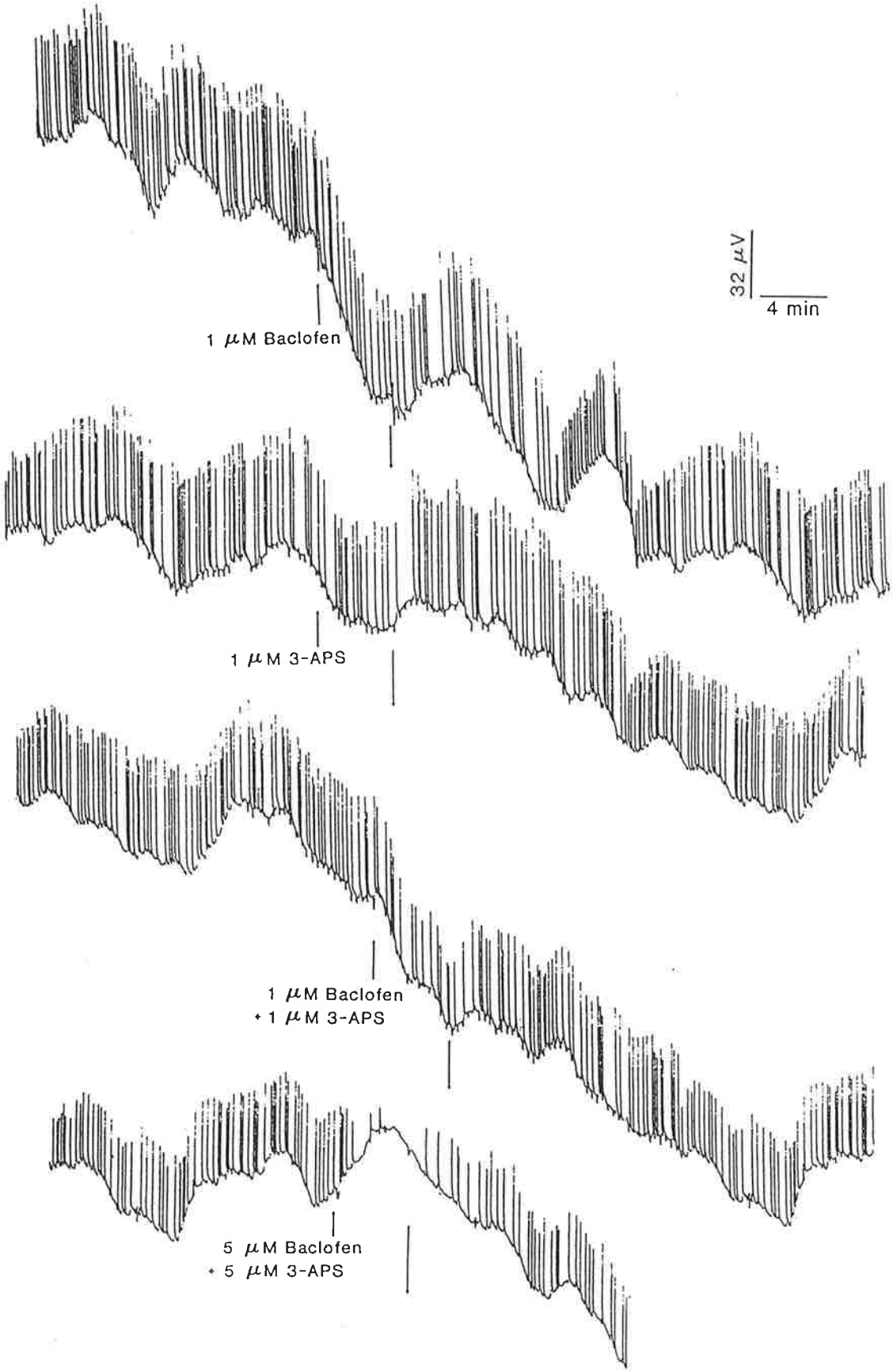

Figure 7.4.a Chart recorder traces showing the effects of 1 μM baclofen, 1 μM 3-APS, and mixtures containing 1 μM or 5 μM of each agonist on spontaneous discharges recorded from a neocortical slice.

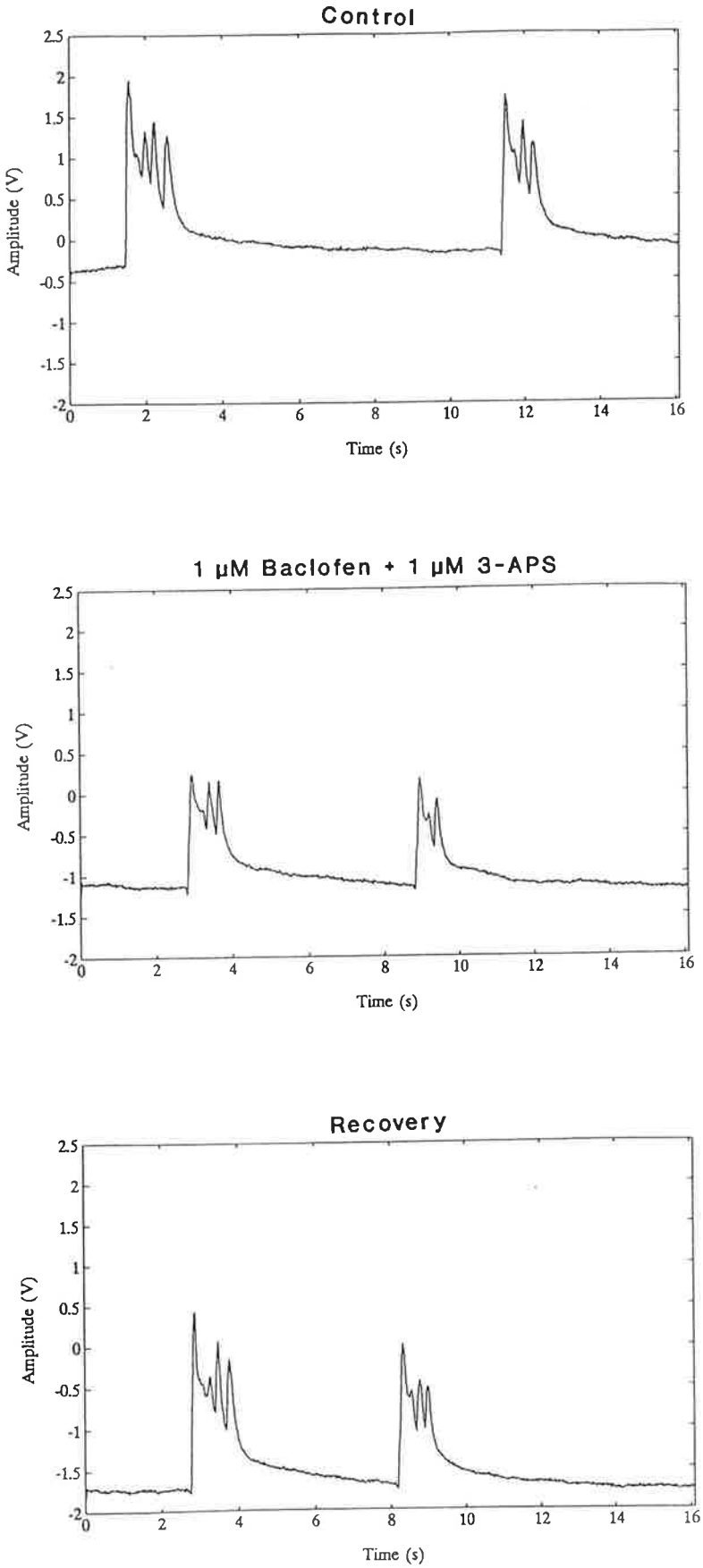

Figure 7.4.b A set of computer collected responses showing control, discharges modified by a mixture of 1 µM baclofen plus 1 µM 3-APS, and recovery. Discharges in presence of the mixture are smaller than control.

7.5 INVESTIGATION OF THE VALIDITY OF THE EQUATION BMI + GABA = BACLOFEN + BMI

As part of the GABA pharmacology studies, a series of experiments were conducted to verify the validity of the pharmacological equation BMI + GABA = BACLOFEN + BMI. BMI was added to the right hand side of the equation to eliminate any residual GABA effects on $GABA_A$-receptors, since each slice was usually superfused with a mixture of GABA plus BMI, followed by a mixture of baclofen and BMI on recovery.

Figure 7.5.a shows chart recorder traces comparing the effects of 50 µM GABA plus 50 µM BMI, and 10 µM baclofen plus 50 µM BMI on spontaneous discharges recorded from a neocortical slice. The mixture containing GABA did not have a notable effect on the frequency or amplitude of discharges, whereas the mixture containing baclofen eliminated discharges for a period of time comparable to duration of its application. Computer collected responses in figure 7.5.d show a discharge modified by the mixture containing 10 µM baclofen is simpler than control, whereas the mixture containing 50 µM GABA did not have a marked effect on discharge complexity.

Chart recorder traces in figure 7.5.b show the effects of 50 µM BMI, a higher concentration of 1 mM GABA, and 10 µM baclofen on discharges from a neocortical slice. 50 µM BMI had no marked effect on the frequency or amplitude of discharges, 1 mM GABA hyperpolarised the tissue, and 10 µM baclofen eliminated discharges for approximately twice the duration of its application. More significantly, a mixture of 1 mM GABA

plus 50 μM BMI reduced the discharge frequency for the duration of its application, with regular activity resuming thereafter, but a mixture of 10 μM baclofen plus 50 μM BMI eliminated discharges for a period longer than the duration of its application. Computer collected data in figure 7.5.e show that 50 μM BMI clearly increased the number of after-potentials, whereas the mixture containing 1 mM GABA somewhat reduced the number of after-potentials, and the mixture containing 10 μM baclofen appeared to have a pro-convulsant effect which may, on this occasion, simply be due to tissue fatigue.

The upper trace in figure 7.5.c shows a chart recording of spontaneous discharges. In this experiment a slice was pre-treated with 50 μM BMI for 2 minutes prior to adding either 10 μM baclofen or 1 mM GABA for 4 minutes, which resulted in mixtures of BMI plus baclofen, and BMI plus GABA reaching the tissue. The mixture containing baclofen reduced both the frequency and amplitude of discharges, whereas no marked change in these characteristics is seen with the mixture containing GABA. All three traces are recorded from the same slice, but a combination of a faster discharge rate and a different amplitude scaling makes the bottom trace appear different. Computer collected responses in figure 7.5.f confirm that 50 μM BMI increased the number of discharge after-potentials, and that significantly smaller discharges were recorded in the presence of both the mixtures of 1 mM GABA plus 50 μM BMI, and 10 μM baclofen plus 50 μM.

The three sets of chart recorder and computer collected responses presented above suggest that 50 μM GABA in the presence of 50 μM BMI is ineffective in greatly modifying the amplitude or frequency of events in Mg^{2+}-free medium. Computer records suggest that in the presence of 50 μM BMI, a high concentration of 1 mM GABA, or 10 μM baclofen, is effective in reducing both the amplitude and the number of after-potentials of discharges. Chart recorder data, however, show that 10 μM baclofen produced quiescent periods during which discharges were absent, whereas although 1 mM GABA reduced the discharge frequency, its action in eliminating events was not as prolonged as that of baclofen.

The results presented in this chapter are only in partial agreement with those reported by Horne et al. (1986) that 1 mM GABA and 10 μM baclofen, each reduced the frequency of events in zero Mg^{2+}, while GABA also reduced the amplitude of events. Furthermore, Horne and colleagues reported that GABA and baclofen were similarly effective against bicuculline-induced events. However, the latter observation on bicuculline-induced events was made in a normal, not a Mg^{2+}-free, medium. In the trigeminal nucleus of rats, iontophoretic administration of GABA is also reported to resemble baclofen in depressing excitatory transmission and facilitating segmental inhibition (Fromm et al., 1992).

As a $GABA_A$-receptor antagonist, BMI, has been shown to increase the number of after-potentials of epileptiform discharges induced in Mg^{2+}-free medium, but it has not greatly modified the frequency of discharges. The present results

indicate that $GABA_B$-receptor mediated effects are more important in the regulation of epileptiform activity. The importance of $GABA_B$-receptors in epileptogenesis is also identified in hippocampal slices with low Mg^{2+} (Lewis et al., 1989).

It was also observed that the effectiveness of 10 μM baclofen in eliminating discharges appeared to have been somewhat diminished in the presence of 50 μM BMI. This phenomenon is not easy to reconcile as bicuculline blocks presynaptic $GABA_A$-receptors, and those $GABA_A$-receptors are on GABA fibres making $GABA_B$ connections. As such bicuculline is expected to enhance the endogenous $GABA_B$ effects. On the other hand, it is known that when $GABA_A$-receptor-mediated synaptic inhibition is gradually blocked by pharmacological agents, the late synaptic hyperpolarisation mediated by $GABA_B$-receptors progressively increases in amplitude (Merlin and Wong, 1993). An explanation would presumably be that the partially disinhibited pyramidal cell population is able to activate a larger population of inhibitory cells through the local connections, and as a result, the amplitude of the $GABA_B$-receptor-mediated events increases.

The results presented in this section confirm that baclofen is a potent agent. A better understanding of any differences between pre- and post-synaptic populations of $GABA_B$-receptors, and of the mechanism of action of baclofen through Ca^{2+} channels pre-synaptically and/or K^+ channels post-synaptically, should help explain why the equation BMI + GABA = baclofen + BMI does not appear to be unquestionably valid.

More importantly, different actions of GABA compared to baclofen probably reflect the susceptibility of GABA to cellular uptake processes. This caveat in the GABA study suggested that the effects of GABA be investigated in the presence of a GABA uptake blocker, namely L-2,4-diamino-n-butyric acid (DABA), which is discussed below.

7.5.1 Effects of GABA on Spontaneous Neocortical Discharges in the Presence of DABA

A major limitation in all GABA studies is the possibility that the observed activity of particular ligands may in fact be greatly influenced by uptake mechanisms. This is especially so if the agents themselves are inhibitors of this process, when their apparent activity is likely to be confounded by accumulation of endogenous GABA in the region of the receptors at GABAergic synapses. Indeed, even GABA itself is considerably more potent in the presence of glial and neuronal uptake inhibitors (Kerr and Ong, 1992).

Inhibition of GABA transport (uptake) mechanisms may represent a flexible way of stimulating GABA-mediated neurotransmission. It has been established that neuronal and glial GABA uptake mechanisms have dissimilar inhibitor/substrate specificities, and the best strategy for pharmacological intervention seems to be:

(i) effective blockade of both neuronal and glial GABA uptake

in order to enhance the inhibitory effect of synaptically released GABA, or

(ii) selective blockade of glial GABA uptake in order to increase the amount of GABA taken up by the neuronal carrier with subsequent elevation of the GABA concentration in nerve terminals.

While substrates/inhibitors of neuronal GABA uptake appear to be proconvulsant or convulsant, compounds acting as selective substrates/inhibitors for the glial uptake system have anticonvulsant effects. There is interest in selective inhibitors of glial uptake, which do not act as substrates for the transport carrier (Krogsgaard-Larsen et al., 1988).

Figure 7.5.g represents chart recording from a slice showing the effects of 500 µM GABA on spontaneous discharges from a neocortical slice, and how the firing pattern was modified by smaller concentrations of GABA in the presence of 500 µM DABA. The effects of DABA on its own, and 5 µM baclofen are also presented. In tests where mixtures were applied, the tissue was pre-treated with 500 µM DABA for 2 minutes before 50 or 100 µM GABA was added for 4 minutes.

It is noted that at smaller concentrations, 50 or 100 µM GABA in the presence of DABA had a similar effect on discharge frequency to 500 µM GABA on its own, confirming the susceptibility of GABA to uptake. 500 µM DABA on its own did not markedly modify the frequency of discharges, with any reduction being due to its action in preventing the uptake of

residual GABA, or its possible anti-epileptic property. Note that 5 μM baclofen eliminated discharges for a period approximately twice the duration its application, and the discharge frequency was lower on return.

Computer collected data in figure 7.5.h show that 500 μM GABA, 50 μM GABA plus 500 μM DABA, and 500 μM DABA, each reduced the number of discharge after-potentials compared to controls. The effect of 500 μM GABA in reducing the discharge amplitude is more pronounced that the other two. Figure 7.5.h shows a good example how a miniaturised discharge is produced in the presence of 500 μM GABA.

Nipecotic acid is an effective inhibitor of neuronal as well as glial uptake, being slightly more potent at the latter system. Furthermore, nipecotic acid is a substrate for both neuronal and glial GABA transport carriers, and appears to provide a retrograde tracer specific to neurones whose terminals exhibit preferential GABA uptake. (R)-Nipecotic acid is more potent than the (S)-isomer in enhancing the depressant action of GABA on spinal neurones (Krogsgaard-Larsen et al., 1988). In rat hippocampal slices, 2-4 mM nipecotic acid is reported to reversibly block occurrence of interictal and ictal epileptiform discharges, while increasing the amplitude of field potentials (Avoli et al., 1993). The BBB effectively prevents nipecotic acid from entering the brain from the bloodstream.

A mixture of 500 μM nipecotic acid plus 500 μM DABA may provide more effective uptake blocker, allowing GABA to

eliminate discharges at smaller concentrations, in a similar fashion to baclofen.

Recent developments in the field of GABA uptake inhibitors have greatly stimulated the therapeutic interest in compounds with effects on GABA transport mechanisms. Since $GABA_A$ agonist THIP has only very weak antiepileptic properties, and in view of the high doses of the GABA prodrug, progabide, required for significant reduction of symptoms in epileptic patients, the potent anticonvulsant effects of new GABA uptake inhibitors, which do not show the same sedative effect as diazepam, is promising. It is likely that compounds with selective effect on glial GABA uptake are of primary interest as anticonvulsants, making the glial-selective uptake inhibitors important in future drug design (Krogsgaard-Larsen et al., 1988).

More detailed studies of the kind illustrated here, with such effective GABA-uptake inhibitors, would therefore be worthwhile in order to test the validity of the equation GABA + BMI = baclofen + BMI, since the experiments reported here question the identity of central responses to exogenous GABA and baclofen. In other words, are the $GABA_B$-receptor-mediated actions of GABA and baclofen identical? GABA uptake evidently almost nullifies any simple attempts to answer this question in the neocortical slices.

It appears that GABA never abolishes discharges, even in the presence of DABA, like baclofen does.

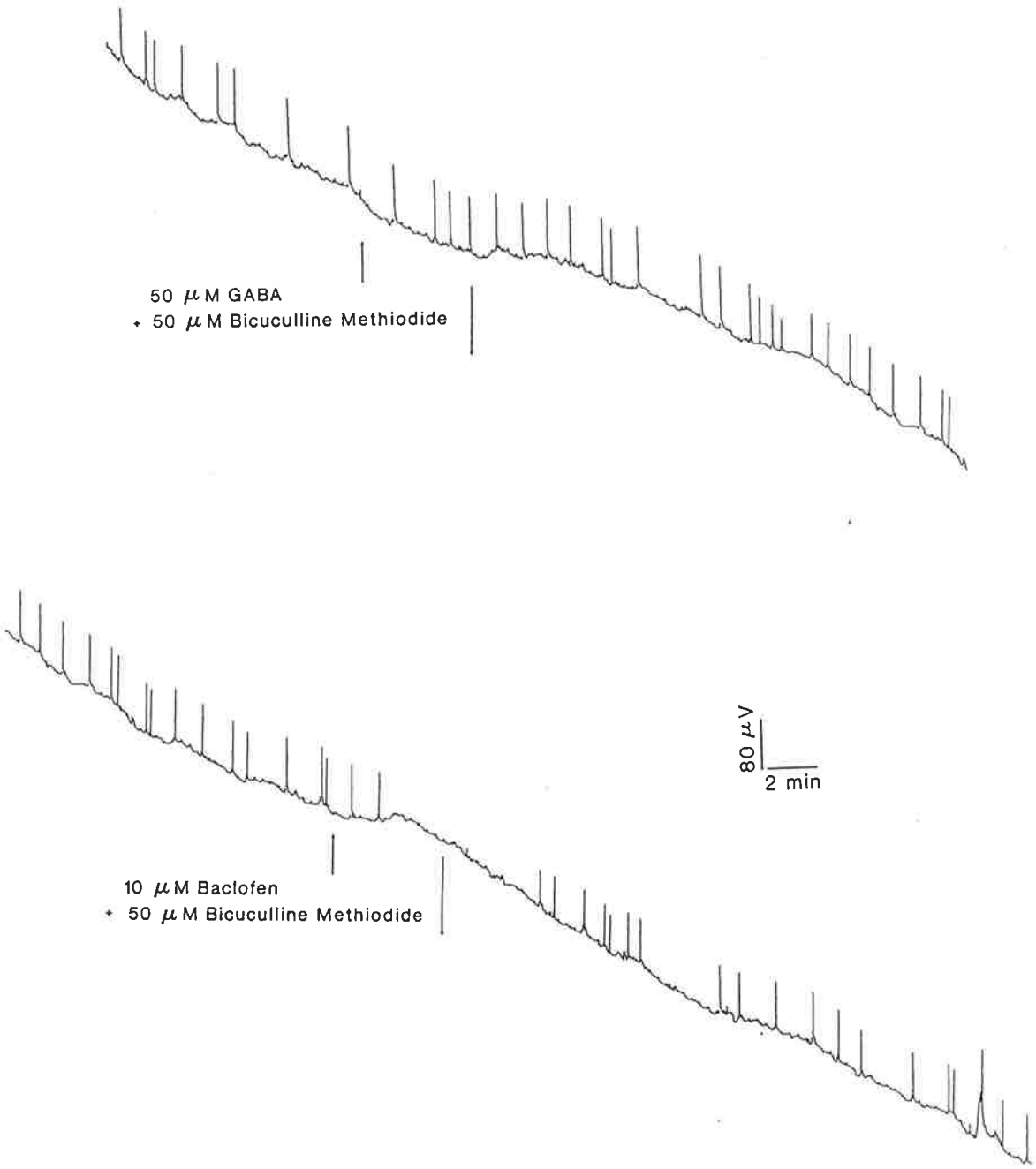

Figure 7.5.a Chart recorder traces comparing the effects of 50 μM GABA plus 50 μM BMI, and 10 μM baclofen plus 50 μM BMI on spontaneous discharges from a neocortical slice. The mixture of GABA plus BMI did not significantly modify discharges, whereas the mixture of baclofen plus BMI eliminated discharges for a period longer than its application.

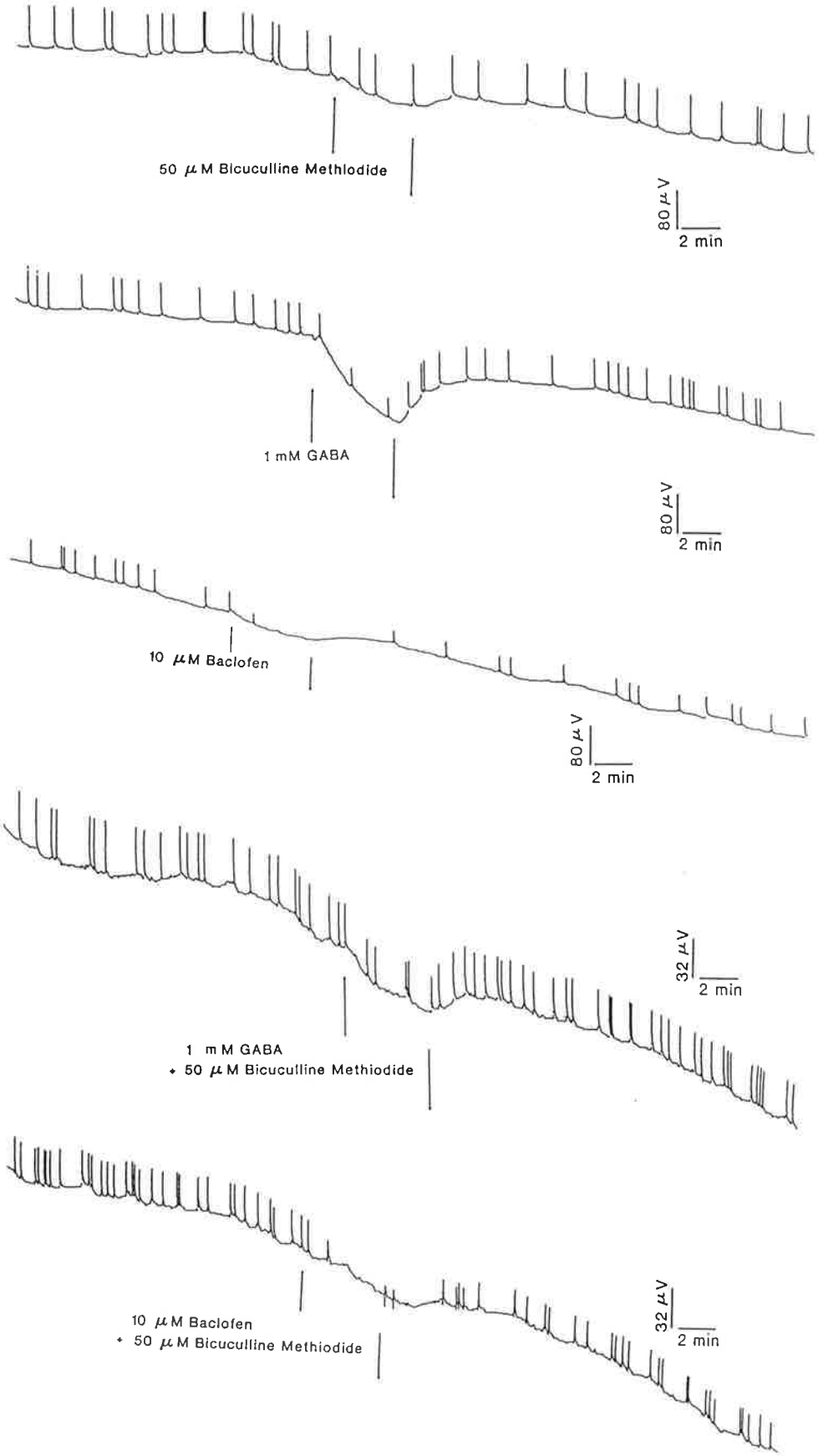

Figure 7.5.b Chart recorder traces showing the effects of 50 μM BMI, 1 mM GABA and 10 μM baclofen as well as mixtures of 1 mM GABA plus 50 μM BMI and 10 μM baclofen plus 50 μM BMI on spontaneous discharges from a slice. It is noted that the mixture containing baclofen has been more effective in reducing the discharge frequency than the mixture containing a high concentration of GABA.

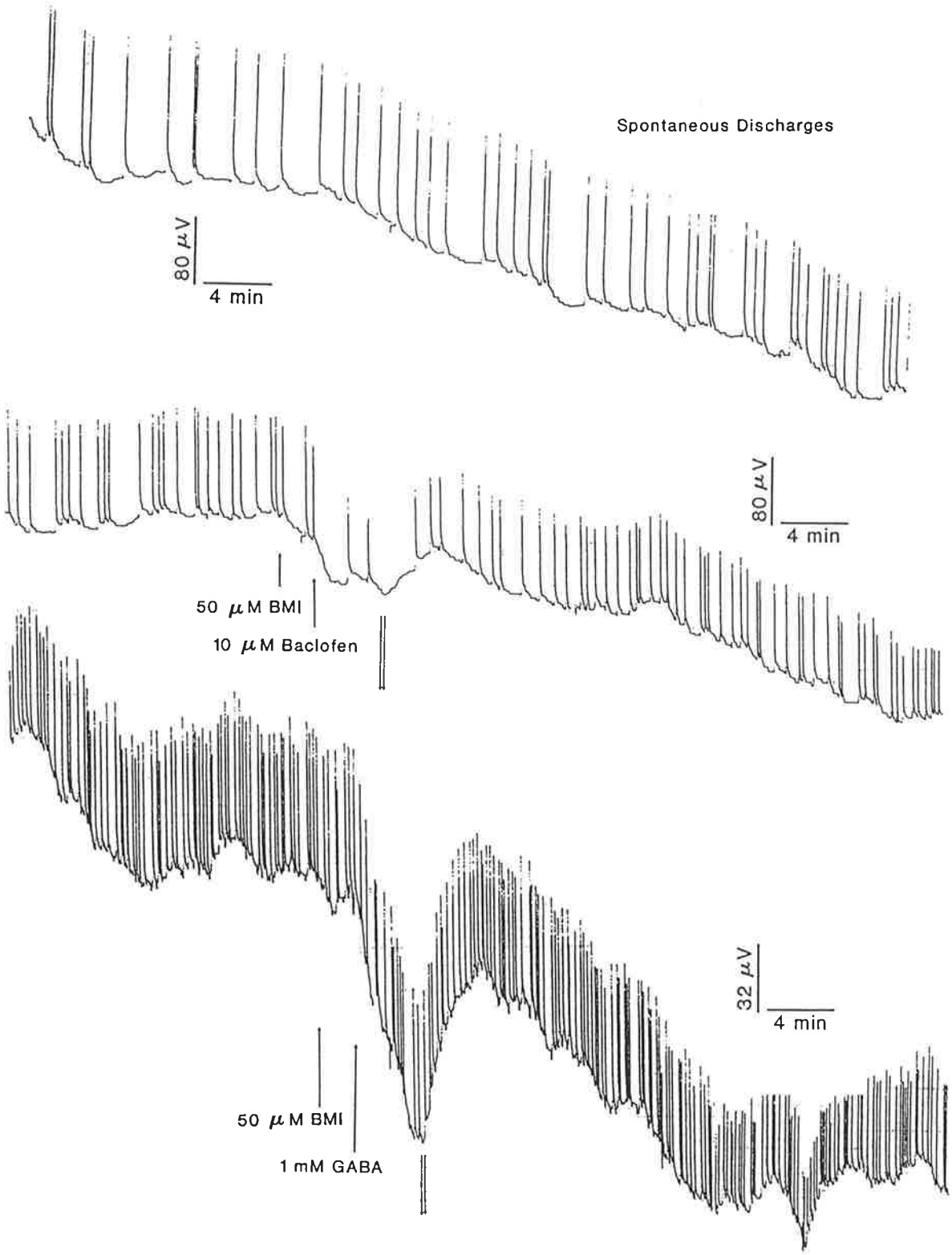

Figure 7.5.c Chart recorder traces showing spontaneous activity from a slice, and how discharges were modified by application of mixtures of 50 μM BMI plus 10 μM baclofen and 50 μM BMI plus 1 mM GABA. In both tests the slice was treated with 50 μM BMI for 2 minutes prior to application of each mixture for 4 minutes. The bottom trace is recorded with a higher amplitude sensitivity.

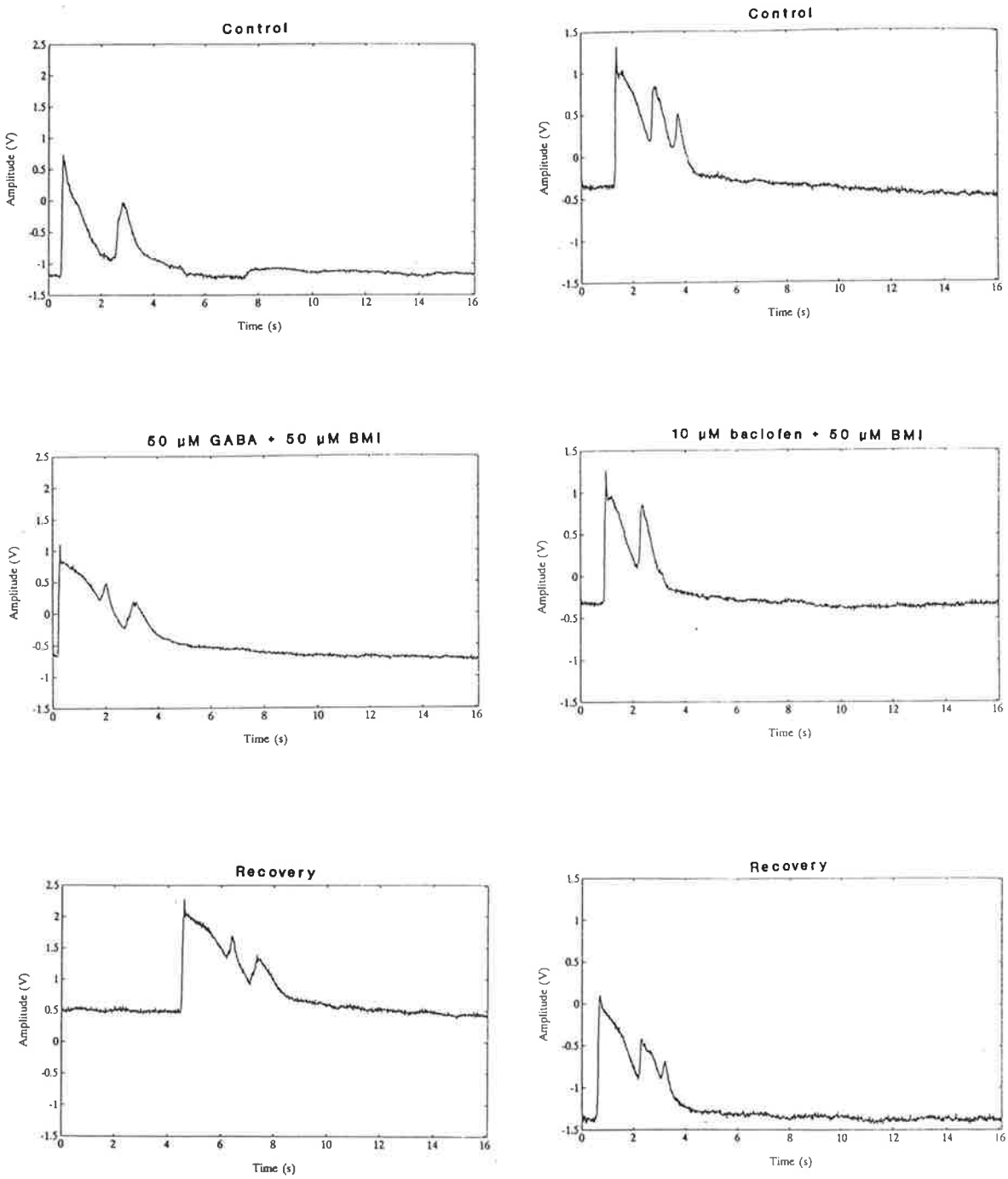

Figure 7.5.d Computer collected data showing how individual discharges were modified by mixtures of 50 µM GABA plus 50 µM BMI, and 10 µM baclofen plus 50 µM BMI. The chart recorder traces showing these discharges are given in figure 7.5.a. Note that the mixture containing baclofen produced a simpler discharge.

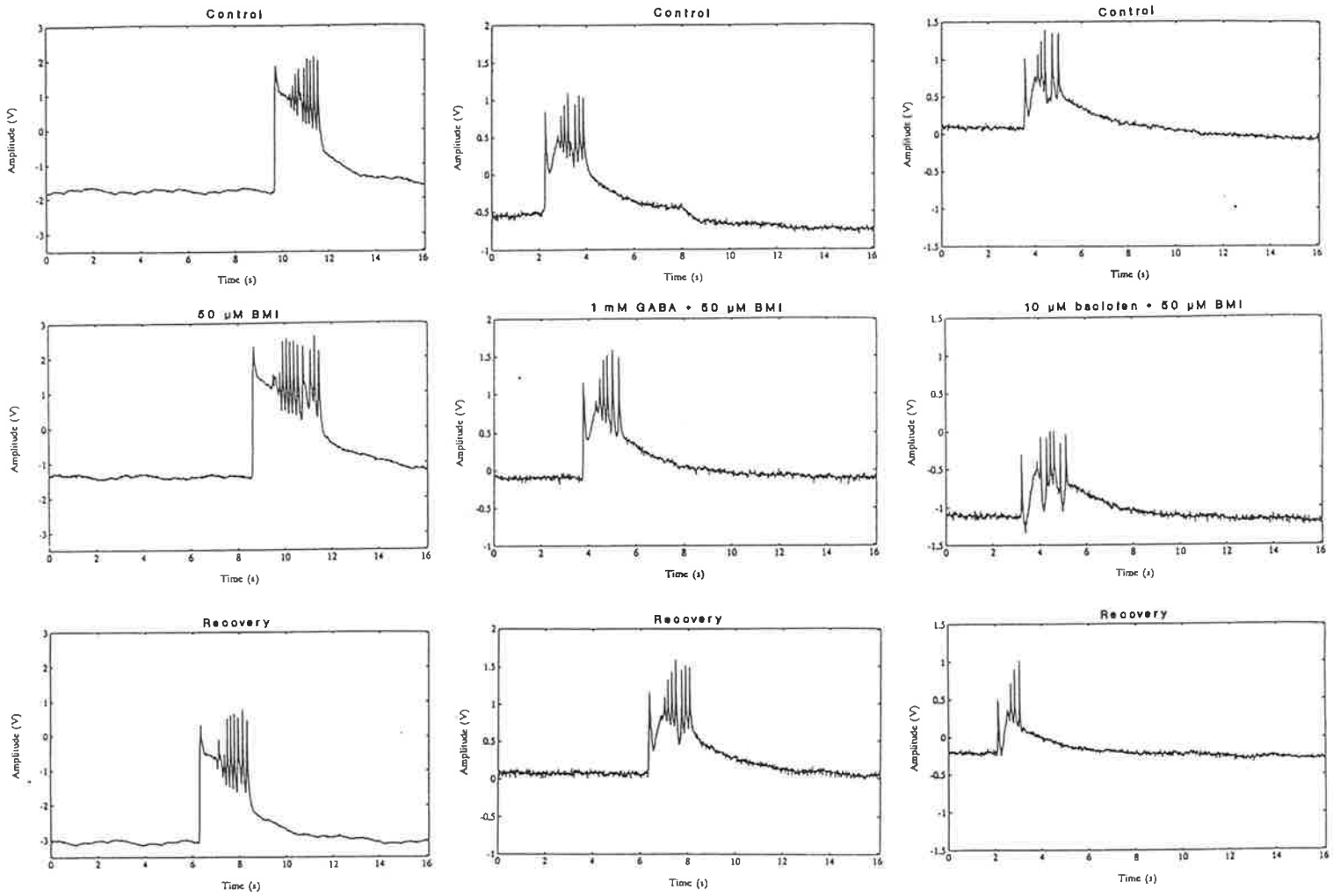

Figure 7.5.e Computer collected responses showing how individual discharges were modified by 50 µM BMI, a mixture of 1 mM GABA plus 50 µM BMI, and a mixture of 10 µM baclofen plus 50 µM BMI. Note how 50 µM BMI increased the number of after-potentials. The chart recorder traces showing these discharges are given in figure 7.5.b.

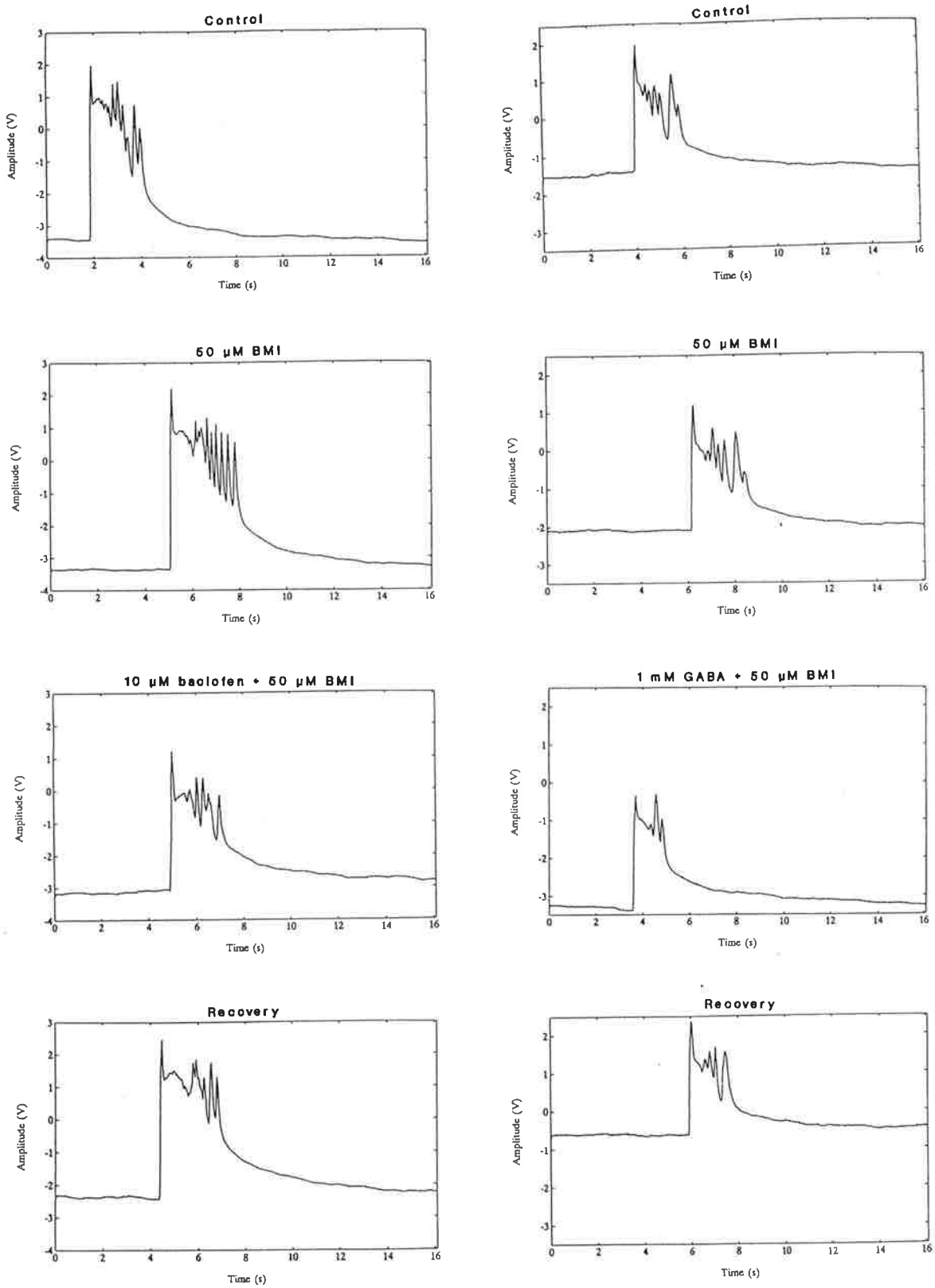

Figure 7.5.1 Computer collected responses showing discharges modified by 50 µM BMI, a mixtures of 10 µM baclofen plus 50 µM BMI, and 1 mM GABA plus 50 µM BMI. The mixtures immediately followed BMI applications. Note how 50 µM BMI increased the number of after-potentials, and how simpler discharges were produced with both mixtures. The chart recorder traces showing these discharges are given in figure 7.5.c.

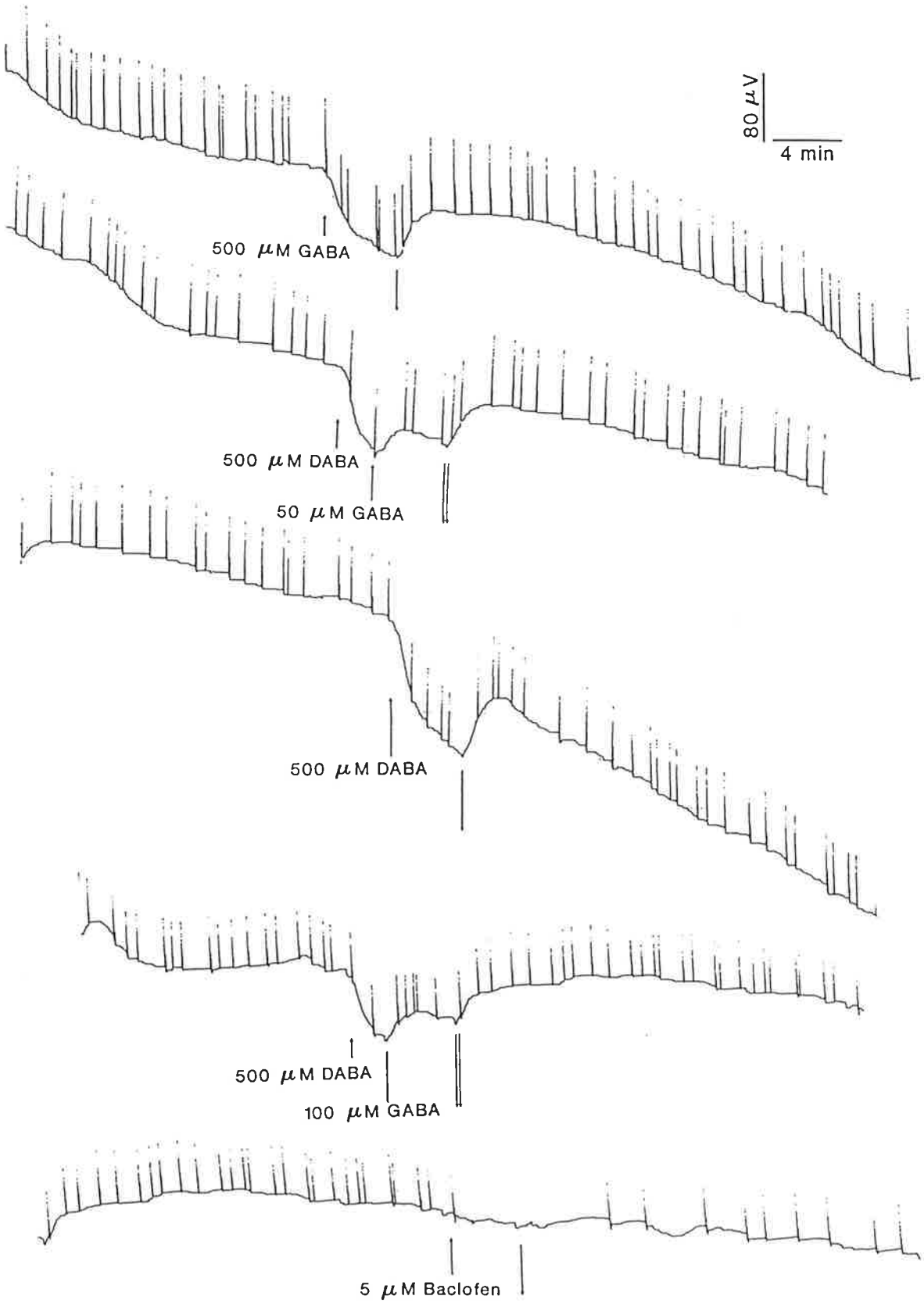

Figure 7.5.g Chart recorder data showing the effects of 500 μM GABA, 50 μM GABA plus 500 μM DABA following a pre-treatment with 500 μM DABA, 500 μM DABA on its own, 100 μM GABA plus 500 μM DABA following a pre-treatment with 500 μM DABA, and 5 μM baclofen on discharges from a neocortical slice. GABA produced a baseline hyperpolarisation, and 5 μM baclofen eliminated discharges for a period approximately twice the duration of its application.

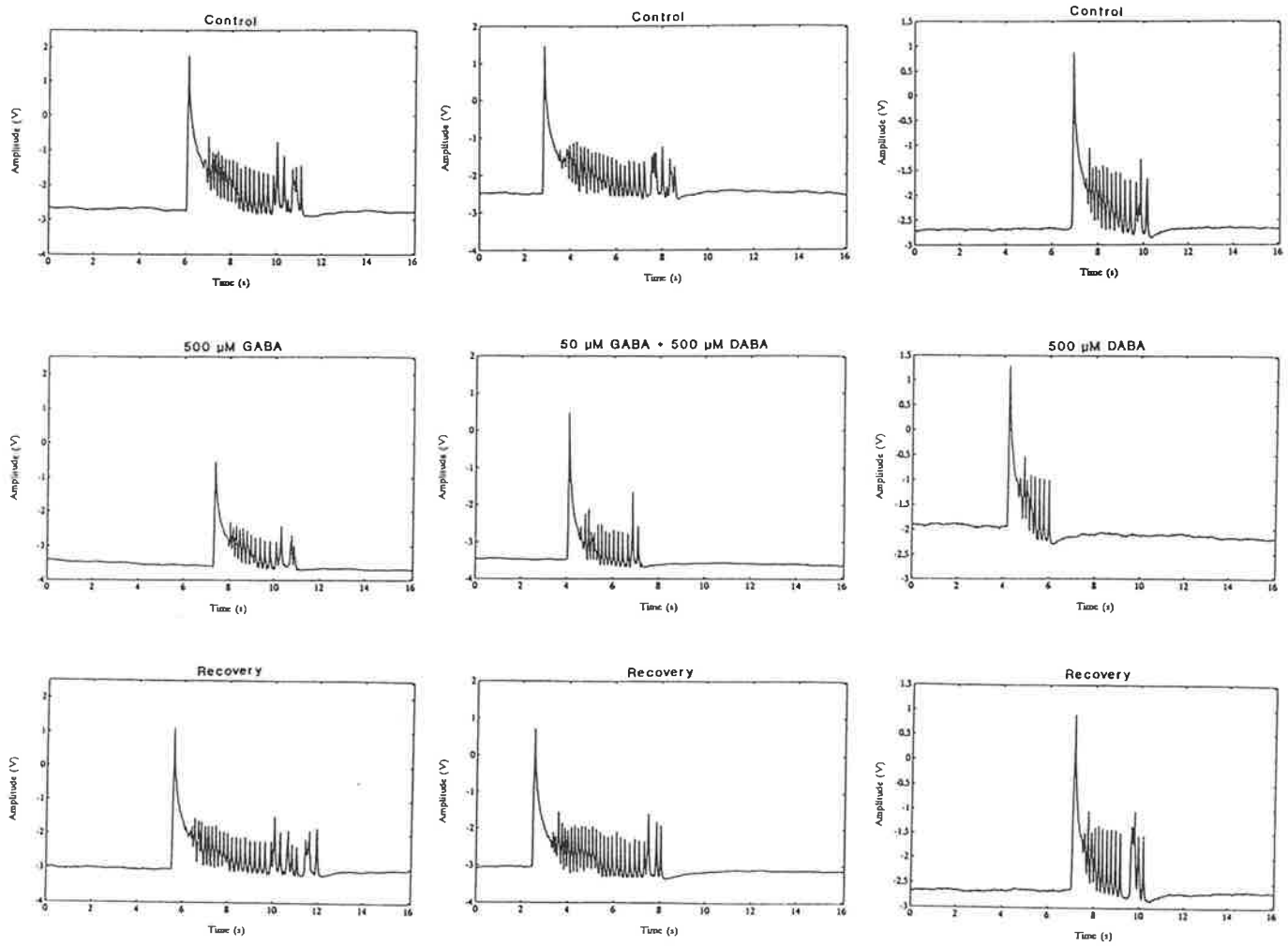

Figure 7.5.h Computer collected responses showing a discharge in the presence of 500 µM GABA being significantly smaller than control. Although a mixture of 50 µM GABA plus 500 µM DABA, and 500 µM DABA on its own reduced the number of after-potentials in discharges, their effect in reducing the amplitude of discharges is not as marked as with 500 µM GABA. Chart recorder traces for these data are shown in figure 7.5.g.

7.6. EFFECTS OF 4-AMINOBUTYLPHOSPHONIC ACID AS A $GABA_B$-RECEPTOR ANTAGONIST ON SPONTANEOUS NEOCORTICAL DISCHARGES

Due to a great specificity of the binding site for agonists or antagonists, no $GABA_A$-antagonists show any significant activity on $GABA_B$-receptors. Kerr et al. (1987) introduced the first specific $GABA_B$ antagonist phaclofen, the phosphonic analog of baclofen, followed by the more potent sulphonic analogs, saclofen and 2-hydroxysaclofen, providing physiological evidence for $GABA_B$-receptor mediated actions in the CNS (Kerr et al., 1990a). Phaclofen is only a weak antagonist, but nevertheless was the first agent able to selectively inhibit neuronal postsynaptic hyperpolarisation induced by baclofen, and antagonise $GABA_B$-receptor mediated late IPSPs (Dutar and Nicoll, 1988a; Dutar and Nicoll, 1988b). In addition, phaclofen antagonises the depression of synaptic transmission by both baclofen and GABA in a range of peripheral tissue (Kerr et al., 1990b). Similar effects have been demonstrated using the more potent derivatives, saclofen and 2-hydroxysaclofen. For example, Lambert et al. (1989) showed blockade of the late IPSP in rat CA_1 hippocampal neurones by 2-hydroxysaclofen. These compounds, however, do not readily penetrate the BBB. CGP35348, which penetrates the BBB, is the first compound in this class to be reported. It acts competitively, but has only low potency (Bittiger et al., 1990; Olpe et al., 1990). The most recent brain-penetrating antagonist to be introduced is CGP 36742, which appears to have a greater potency in vivo than CGP 35348, and reaches the

brain even after oral administration (Bittiger et al., 1993; Bowery, 1993).

4-aminobutanephosphonic acid (4-ABPA) was a compound of interest during development of $GABA_B$-receptor antagonist by Kerr et al. (1990b). Chart recorder traces in figure 7.6.a show the effects of 500 µM and 1 mM 4-ABPA on spontaneous discharges recorded from 5 independent experiments. 4-ABPA has reduced the discharge frequency without having a significant effect on the amplitude of discharges. The variability of baseline potential in these experiments confirms uncertainty about its pure physiological nature in neocortical wedge model, as discussed in chapter 5. Computer collected data in figure 7.6.b, which reveal details of individual discharges, are amongst discharges shown in traces (i) and (ii) of figure 7.6.a. In this experiment, the number of after-potentials and the amplitude of discharges have increased with both 500 µM and 1 mM concentrations of 4-ABPA. Set (a) of computer acquired discharges in figure 7.6.c, which are from those in the chart recorder trace (iv) in figure 7.6.a, confirm that 500 µM 4-ABPA has increased the number of discharge after-potentials. Computer collected discharges in figure 7.6.d, which are from those in the chart recorder trace (vii) in figure 7.6.a, show the effect of 1 mM 4-ABPA in prolonging the after-activity of discharges.

Chart recorder trace (v) in figure 7.6.a shows the effects of a mixture of 25 µM BMI and 500 µM 4-ABPA on neocortical discharges. This mixture of $GABA_A$- and $GABA_B$-receptor antagonists has not shown an effect much different to the

effect of each antagonist separately. Set (b) from computer collected responses in figure 7.6.c shows small increases in the number of after-potentials and the amplitude of a discharge in the presence of the mixture. These results suggest that when synaptic transmission mediated by $GABA_A$-receptors is pharmacologically blocked, additional blockade of $GABA_B$-receptors produces only minor effects on the pattern or form of epileptiform discharges. It is possible, however, that when responses mediated by $GABA_A$-receptors are only partially suppressed, $GABA_B$-receptor mediated events may serve to limit excitation propagation and demarcate the synchronised population (Merlin and Wong, 1993).

It can generally be concluded, from the experiments presented in this chapter, that agents acting on $GABA_A$- and $GABA_B$-receptors can intensely modulate neuronal activity, implicating these receptors as possible sites for the actions of both analgesic and anaesthetic agents.

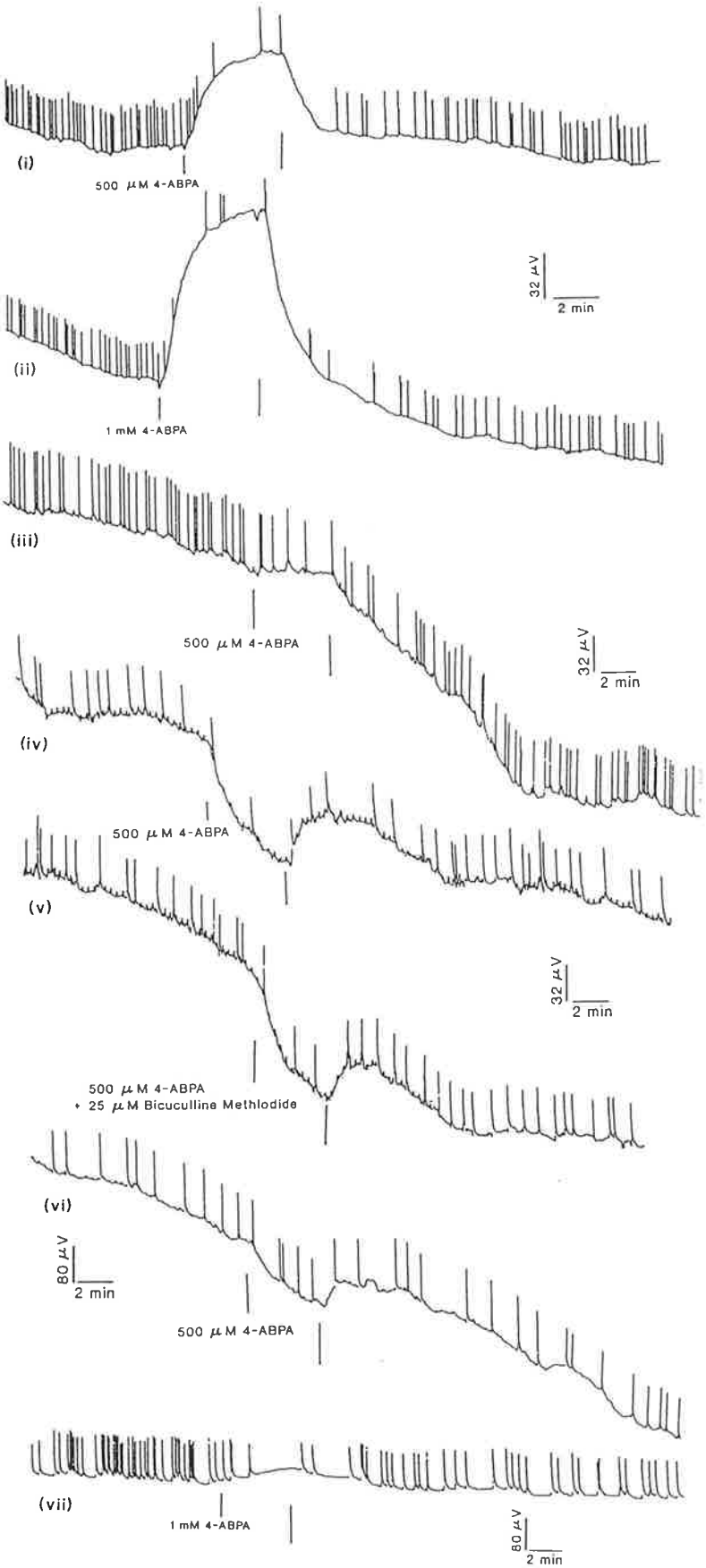

Figure 7.6.a Chart recorder traces from 5 independent experiments showing the effects of 500 μM and 1 mM 4-ABPA, as well as a mixture of 500 μM 4-ABPA plus 25 μM BMI on spontaneous dischargesrecorded from neocortical slices. The baseline potential varies between experiments. Note that traces in each pairs (i) and (ii), and (iv) and (v) share the same axes.

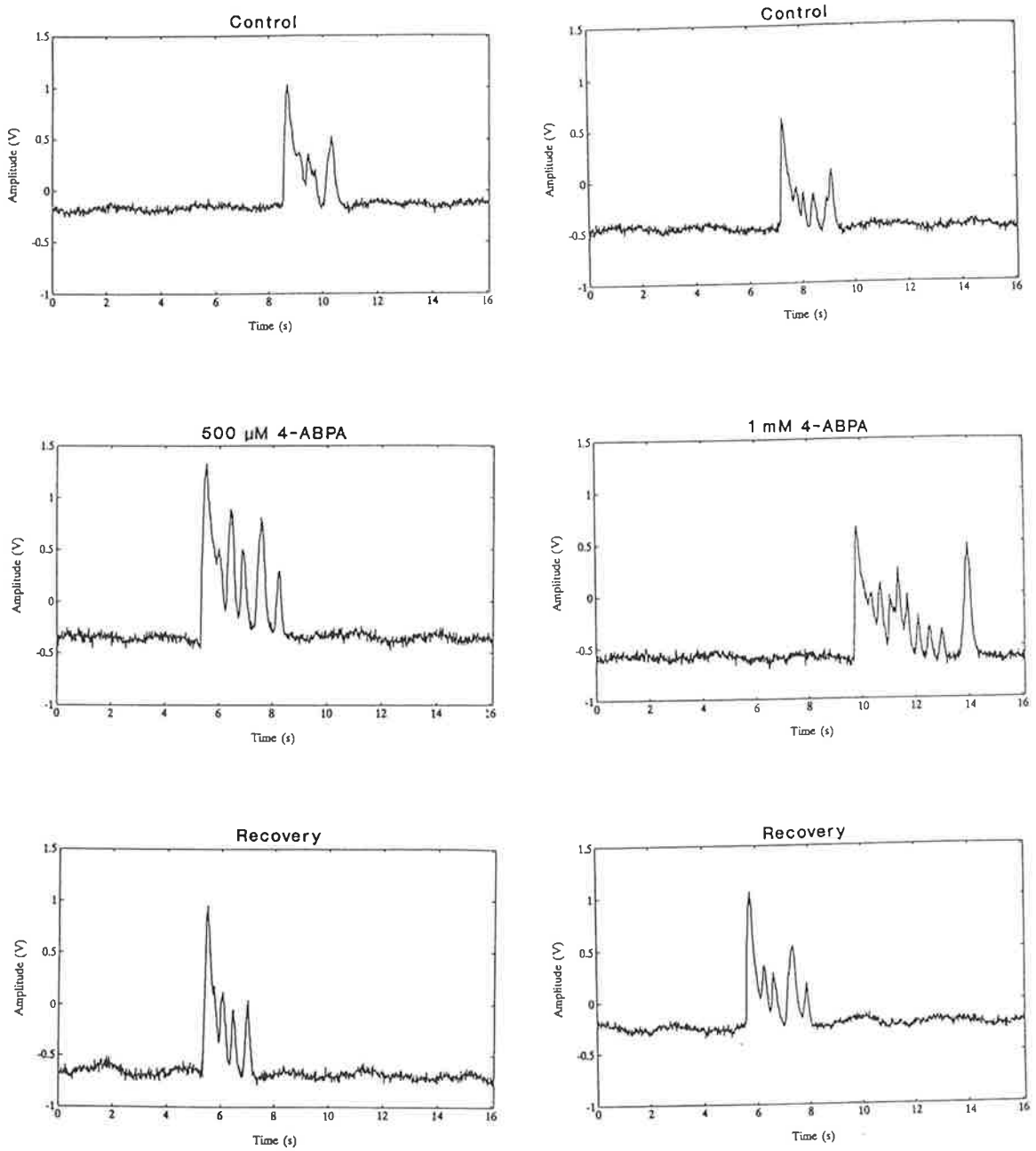

Figure 7.6.b Computer collected responses showing the effects of 500 µM and 1 mM 4-ABPA in prolonging discharges by increasing the number of after-potentials. The amplitude of discharges have also increased. Traces (i) and (ii) in figure 7.6.a, which are from the same slice, represent the chart recording of these discharges.

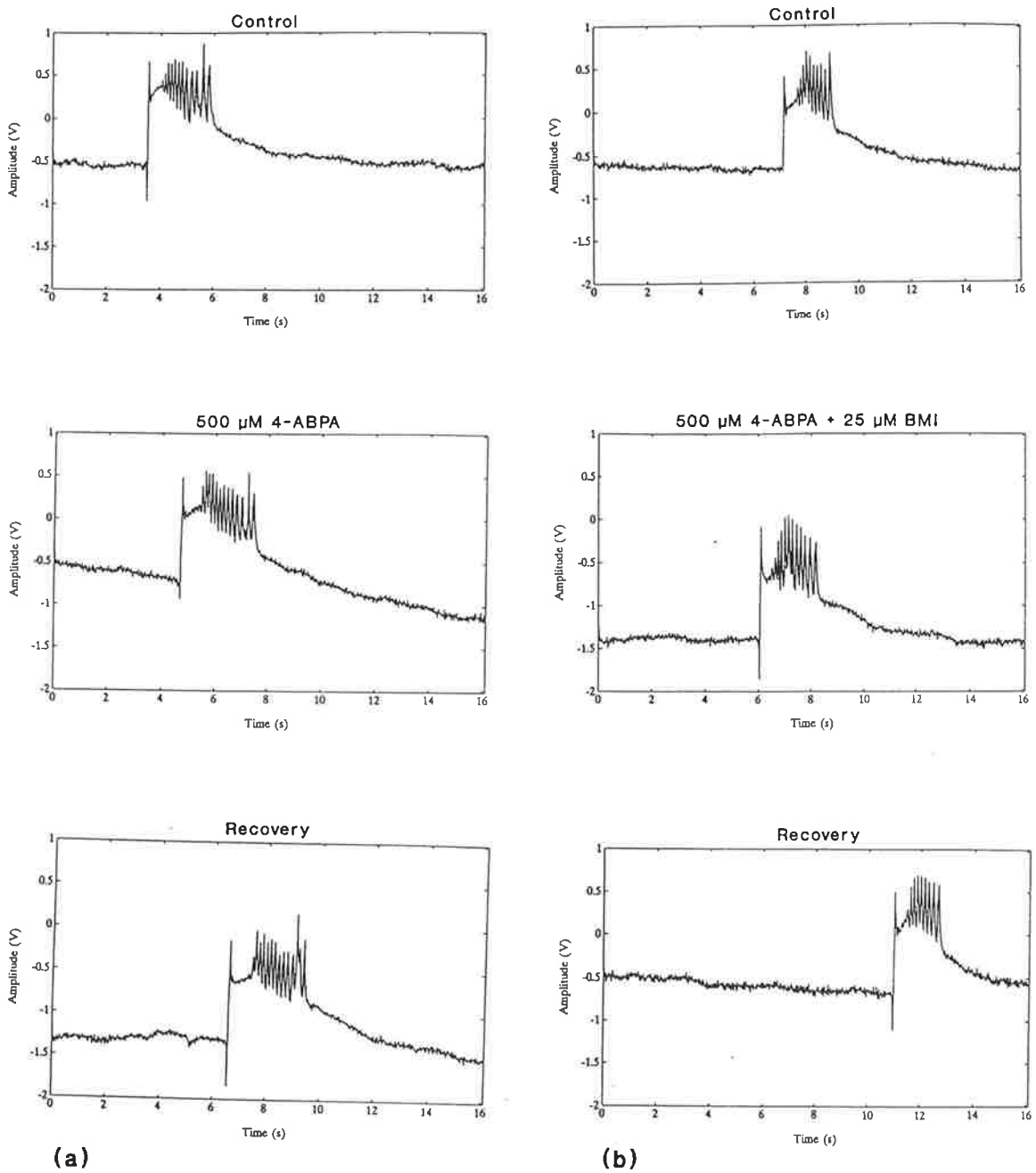

Figure 7.6.c Computer collected responses showing the effects of 500 µM 4-ABPA, and a mixture of 500 µM 4-ABPA plus 25 µM BMI in increasing the number of after-potentials of discharges. Traces (iv) and (v) in figure 7.6.a, which are from the same slice, represent the chart recording of these discharges.

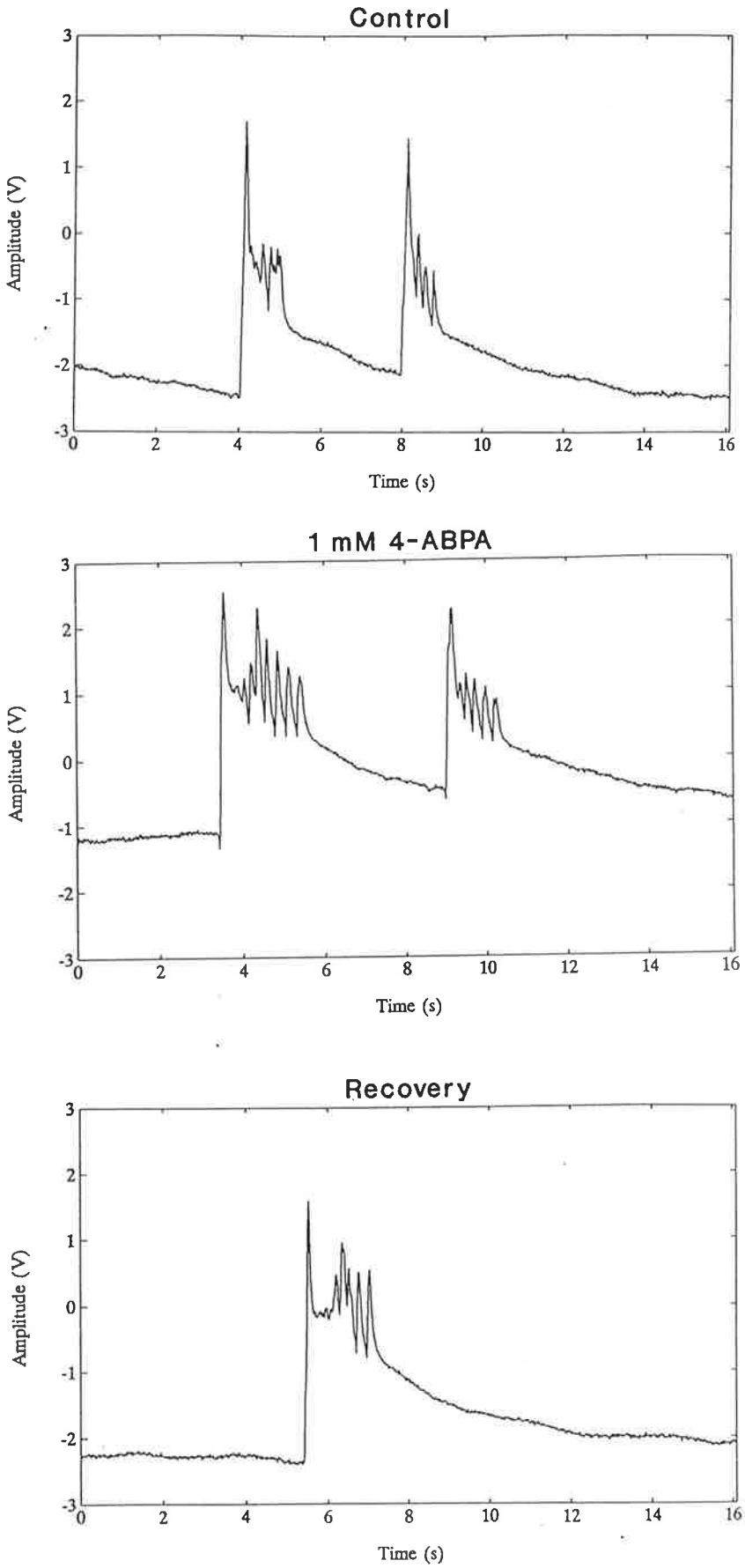

Figure 7.6.d Computer collected responses showing the effect of 1 mM 4-ABPA in prolonging discharges by increasing the number of after-potentials. Trace (vii) in figure 7.6.a represents the chart recording of these discharges.

CHAPTER 8

INTERACTION STUDIES BETWEEN BACLOFEN AND POTASSIUM CHANNEL BLOCKERS

The effects of baclofen, a potent $GABA_B$-receptor agonist, on spontaneous discharges from neocortical slices in Mg^{2+}-free ACSF are discussed in detail in chapter 7. Chart recorder and computer data in section 7.3 show that higher concentrations of baclofen eliminate discharges, and any discharges seen in the presence of baclofen are smaller than control. The effects of higher baclofen concentrations (5 µM or greater) may be related to a G-protein coupled action on presynaptic Ca^{2+}-influx which would abolish discharges due to suppression of neurotransmitter release (Dunlap and Fischbach, 1981; Huston et al., 1990).

Unique effects for each classical K^+ channel blocker are reported in chapter 5. In this chapter, interaction studies between baclofen and K^+ channel blockers will be presented in an attempt to discover to what extent baclofen exerts its actions postsynaptically through the K^+ channels in the neocortical neurones.

In general, the responses with 1 and 5 µM baclofen are to be compared with those already seen in figure 7.3.a. In a more accurate experimental design, control responses to baclofen are firstly established by repeated applications, the effects of baclofen in the presence of a K^+ channel blocker are then

tested, and finally baclofen alone is re-applied to the slice to re-establish control.

As only very limited number of experiments were conducted for each interaction study reported here, and because of difficulty in meaningfully interpreting individual computer-recorded responses, no such single discharges are presented in this chapter.

8.1 BACLOFEN MEDIATION OF THE NEOCORTICAL SLICE RESPONSE TO TEA

Figure 8.1 represents a set of chart recorder traces obtained in sequence from a neocortical slice. As discussed in chapter 5, TEA is believed to block the classical delayed (outward) rectifier potassium current ($I_{K(V)}$), and also a large-conductance calcium-dependent potassium current, known as $I_{BK(Ca)}$. The traces showing the effects of 5 mM TEA on spontaneous discharges are provided in figure 8.1. 5 μM baclofen added to 5 mM TEA is seen to be effective in significantly reducing the discharge frequency. It is unknown if baclofen specifically unblocks $I_{K(V)}$, since an increase in the initial amplitude of chart recorder discharges is seen in the presence of a mixture of 5 mM TEA and 5 μM baclofen. It is notable that the depolarisation induced by TEA blocking K^+ channels is reduced in size by baclofen which is believed to cause hyperpolarisation by increasing the conductance of K^+ channels.

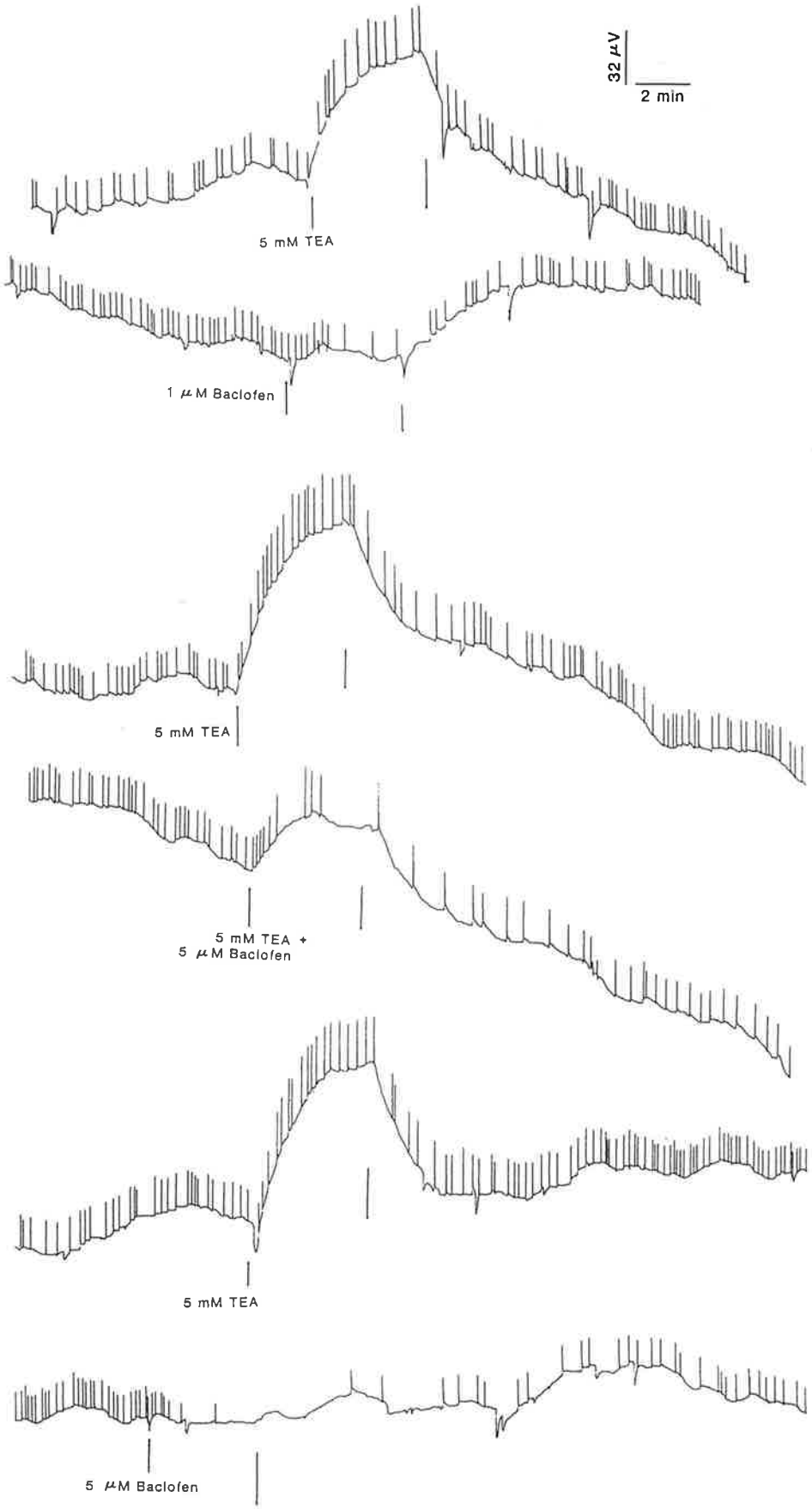

Figure 8.1 Chart recorder traces showing the effects of 5 mM TEA applied to a cortical slice 3 times. 1 μM baclofen, following recovery from the first TEA application, decreased the discharge frequency. Applying a mixture of 5 mM TEA plus 5 μM baclofen, after tissue recovery from the second TEA application, significantly reduced the discharge frequency. 5 μM baclofen after third TEA application was very effective in eliminating discharges.

Additionally, chart recorder traces in figure 8.1 showing the effects of 1 and 5 μM baclofen alone confirm its potency in diminishing or eliminating discharges. Re-establishment of TEA-modified discharge pattern upon baclofen washout provides some evidence that the effects of baclofen are reversible.

8.2 BACLOFEN MEDIATION OF THE NEOCORTICAL SLICE RESPONSE TO CCh

Carbamyl-choline (CCh), also known as carbachol, is a muscarinic agonist. It is reported to block the resting potassium current (I_M). CCh modification of individual discharges is illustrated in chapter 5. Figure 8.2 represents a collection of responses recorded from a neocortical slice in sequence. Although the figure does not show baclofen control, the effects of 20 and 100 μM carbachol alone are presented. It is seen that 1 μM baclofen in the presence of 20 or 100 μM carbachol did not significantly diminish discharges, whereas 10 μM baclofen eliminated discharges for approximately twice the duration of its application, as illustrated in the bottom trace. As signified by the arrows, in each test the slice was pre-treated with carbachol alone before baclofen was co-applied.

These chart recorder data suggest that baclofen at a higher concentration is very effective in opening the K_M channel which was blocked by carbachol, or it acts on some other channels that can counteract the effect of $I_{K(M)}$ block.

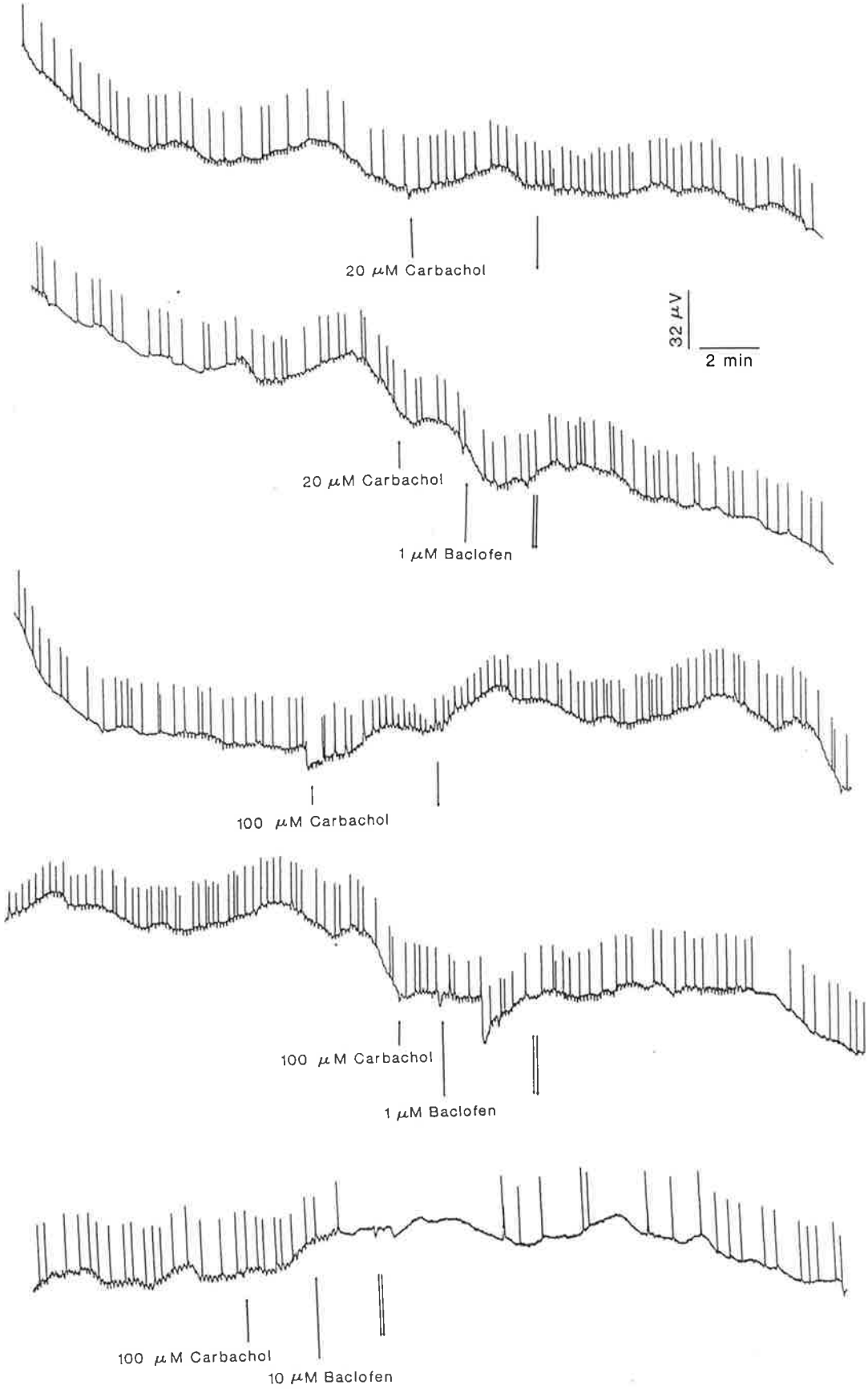

Figure 8.2 chart recorder data showing the effects of 20 and 100 μM carbachol applied to a neocortical slice. 1 μM baclofen in the presence of 20 or 100 μM carbachol did not show marked effects on the amplitude or frequency of discharges, whereas 10 μM baclofen in the presence of 100 μM carbachol eliminated discharges, and a lower discharge frequency is seen on resumption of activity before complete recovery.

Solis and Nicoll (1992) found that 0.3 to 20 μM carbachol had no effect on outward currents evoked by either baclofen or GABA, whereas Peet and Mclennan (1986) found that 20 μM baclofen completely suppressed the late inhibitory post-synaptic potentials (IPSPs) in hippocampal CA_1 neurones. These $GABA_B$-receptor-mediated slow IPSPs are known to result from activation of K^+ channels.

8.3 BACLOFEN MEDIATION OF THE NEOCORTICAL SLICE RESPONSE TO CsCl

CsCl is regarded as a general K^+ channel blocker, and its effects on individual discharges are discussed in chapter 5. The upper trace in figure 8.3 shows the effect of 5 mM CsCl on spontaneous discharges recorded from a neocortical slice. The middle trace shows that 1 μM baclofen in the presence of 5 mM CsCl did not have a marked effect on discharge frequency, whereas the bottom trace shows that 5 μM baclofen in the presence of 5 mM CsCl reduced the discharge frequency. Note how the baseline depolarisation induced by CsCl alone is modified by the mixtures of CsCl and baclofen.

It would have been desirable to establish control for 1 and 5 μM baclofen concentrations before applying 5 mM CsCl. However, the results using CsCl suggest that a variety of K^+ channels may be responsible for mediating the response to baclofen. Further experiments on interaction between CsCl and baclofen are required before firm conclusions can be drawn.

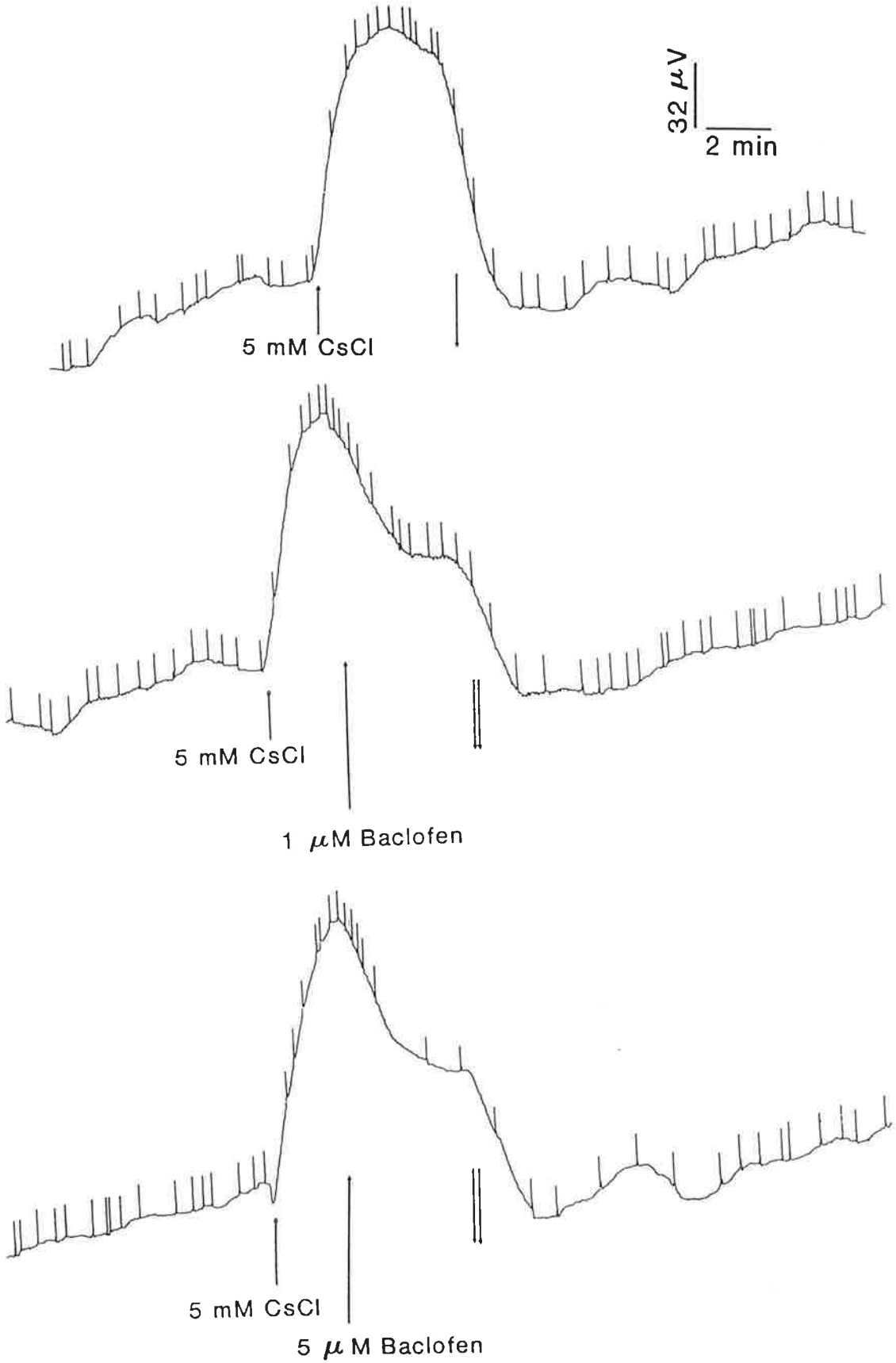

Figure 8.3 Chart recorder data showing the effects of 1 an 5 μM baclofen, each in the presence of 5 mM CsCl, on spontaneous discharges recorded from a neocortical slice. The upper trace shows the effects of 5 mM CsCl alone. Note how the mixture containing 5 μM baclofen was effective in reducing the discharge frequency. Also note the combined effect of CsCl and baclofen on the baseline potential.

8.4 BACLOFEN MEDIATION THE NEOCORTICAL SLICE RESPONSE TO 4-AP

The effects of 4-AP on discharges recorded from neocortical slices are discussed in chapter 5. As reported 4-AP is widely believed to block the transient outward K^+ current, $I_{K(A)}$. This current is voltage sensitive and is virtually inactivated at normal resting membrane potential. 4-AP also induces neurotransmitter release. It is a potent agent in increasing the frequency of neocortical discharges.

The upper trace in figure 8.4 shows that 1 µM baclofen, co-applied to a slice pre-treated with 20 µM 4-AP alone, could not diminish the hyperexcitability induced by 4-AP. The lower trace shows that 5 µM baclofen still diminished discharges in the presence of 20 µM 4-AP, suggesting that baclofen is capable of unblocking the $I_{K(A)}$ current, or baclofen induced effects can over-ride $I_{K(A)}$ current block. Alternatively, the results may be suggesting that baclofen does not act through the potassium conductance. Further experiments on baclofen mediation of the responses to 4-AP are desirable, where control responses to each of baclofen and 4-AP are firstly established.

Solis and Nicoll (1992) report that 5 µM to 1 mM 4-AP did not change baclofen responses, despite causing a large increase in cell excitability; but at a higher 5 mM concentration, 4-AP reduced both baclofen and GABA evoked outward currents to a similar extent.

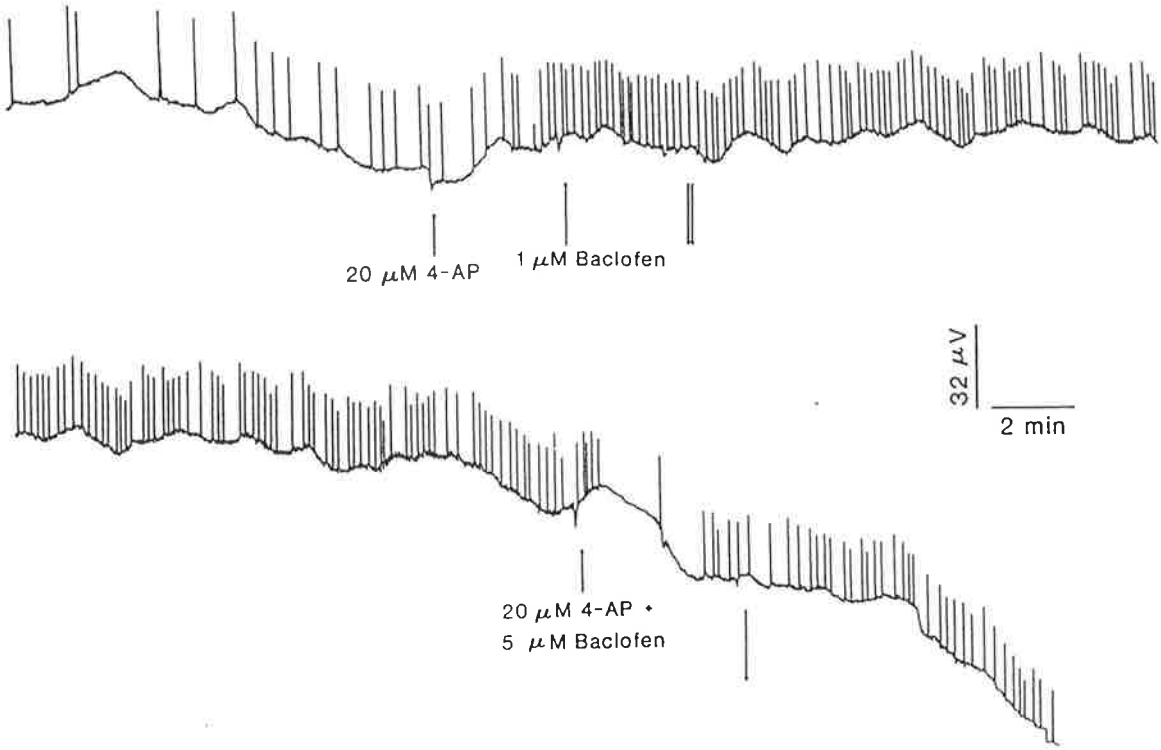

Figure 8.4 Chart recorder data showing how baclofen and 4-AP interact. The upper trace shows that adding 1 μM baclofen after pre-treating the slice with 20 μM 4-AP failed to diminish the hyperexcitability induced by 4-AP. The lower trace shows that 5 μM baclofen mixed with 20 μM 4-AP was effective in diminishing discharges.

$GABA_B$-receptors are reported to potentiate $I_{K(A)}$ current (Saint et al., 1990). It is suggested this current may be responsible for mediating responses to baclofen (Gage, 1992). Since $GABA_B$-receptors are also present on presynaptic terminals, this action may be responsible for modifying transmitter release rather than any direct effect on Ca^{2+} channels, as proposed by Dunlap (1981) and Huston et al. (1990). As $GABA_B$-receptors are G-protein coupled, any activation of the postsynaptic K^+ channels has to be mediated through G-protein and second messengers (Premkumar et al., 1990).

8.5 BACLOFEN MEDIATION OF THE RESPONSES OF NEOCORTICAL SLICES TO $BaCl_2$

The effects of $BaCl_2$ on spontaneous discharges recorded from neocortical slices are discussed in depth in chapter 5. $BaCl_2$ is known to block the anomalous (inward) rectifier K^+ current ($I_{K(IR)}$), and can induce neurotransmitter release. In the neocortical slice preparations reported in this project, 0.5 or 1 mM $BaCl_2$ always increased the discharge frequency very significantly. $BaCl_2$ was proven to be the most potent K^+ channel blocker for increasing the rate of occurrence of discharges.

Two sets, (a) and (b), in figure 8.5 show $BaCl_2$-induced actions on baclofen mediated responses in two independent neocortical slices. In (a), 1 or 5 μM baclofen appeared to

have only marginal effects on the hyperexcitability induced by 500 μM $BaCl_2$. In (b), a higher concentration of 10 μM baclofen failed to eliminate discharges in the presence of 500 μM $BaCl_2$, although a reduction in discharge frequency can be seen. Even 50 μM baclofen could not stop the neocortical discharges in the presence of 500 μM $BaCl_2$, but this concentration of baclofen depressed the amplitude of discharges, with tissue seemingly unable to recover from it. In each experiment the effects of 500 μM $BaCl_2$ alone is shown, but establishing baclofen control first is desirable for such investigations. In these baclofen mediation tests, the slice was pre-treated with 500 μM $BaCl_2$ for approximately 2 minutes before adding a baclofen concentration for up to 4 minutes.

These data show the hyperexcitability induced by $BaCl_2$ could not be overcome by baclofen. This may suggest that baclofen can not unblock the K_{IR} channels. Alternatively, Ba^{2+} may be entering through Ca^{2+} channels prior to its blockade by baclofen, and releasing more transmitter than can be modified by $GABA_B$-receptors on presynaptic terminals.

Although there is agreement between Misgeld et al. (1989) and Lambert et al. (1991) that baclofen induced hyperpolarisation of hippocampal interneurones is blocked by Ba^{2+}, the first group of authors report that baclofen-induced depression of IPSP is blocked by Ba^{2+}, whereas the second group of researchers report that baclofen-induced depression of IPSP is resistant to Ba^{2+}. However, the significance of Ba^{2+} resistance in the present study is unclear.

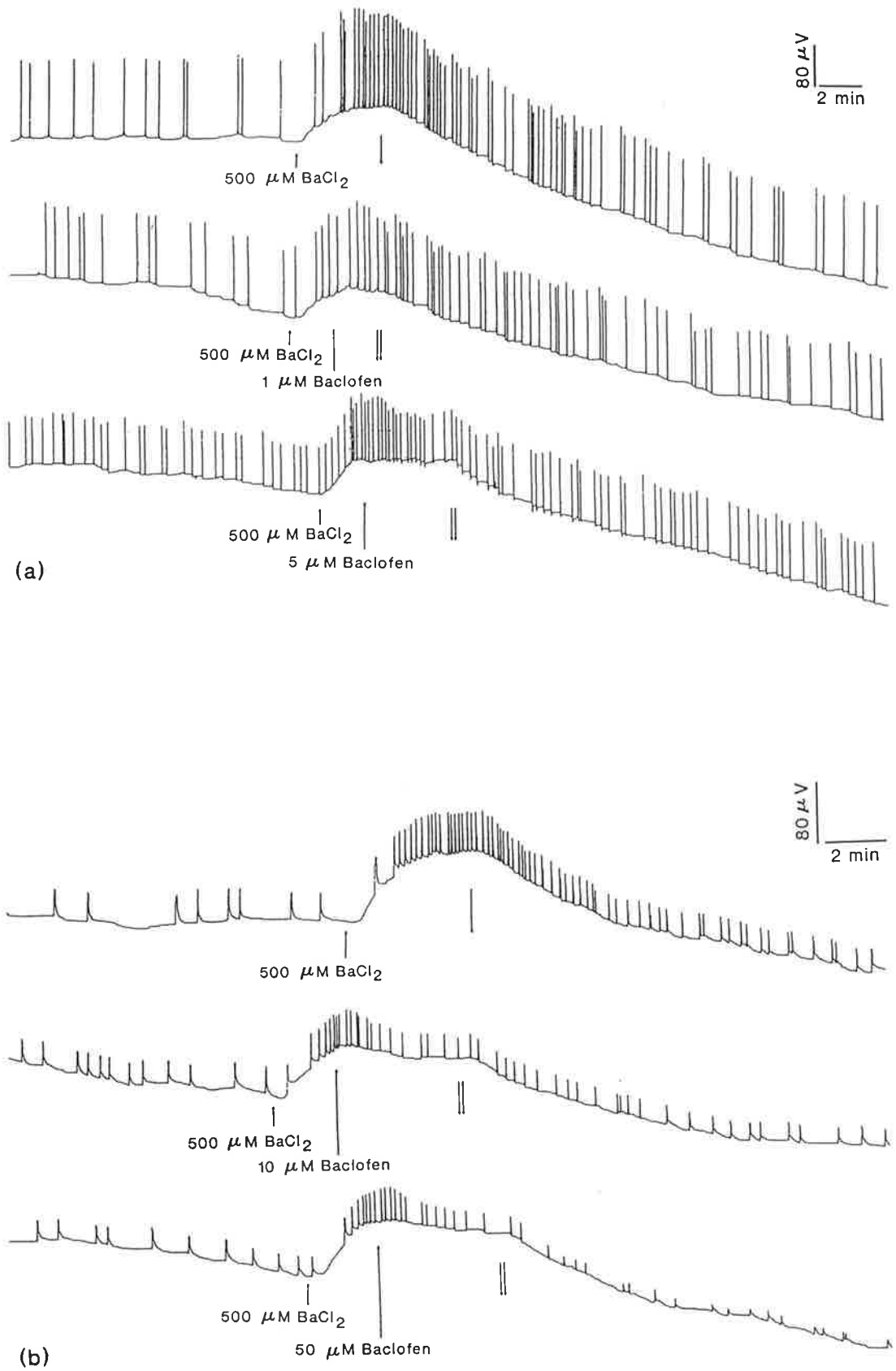

Figure 8.5 Chart recorder data from 2 independent experiments showing interaction between baclofen and $BaCl_2$. Data from (a) show that 1 or 5 μM baclofen were were ineffective in diminishing the hyperexcitability induce by 500 μM $BaCl_2$. In (b), 10 μM baclofen had some effect in reducing the discharge frequency. A high 50 μM baclofen could not eliminate discharges from the second slice, but depressed the discharge amplitude.

Following the above-mentioned observation, Misgeld et al. (1989) suggest that hyperpolarisation of interneurones mediates depression of IPSPs. On the other hand, it is reported that baclofen depresses IPSPs recorded from cultured hippocampal neurones, which are not hyperpolarised by baclofen (Harrison et al., 1988), suggesting that activation of $GABA_B$-receptors on inhibitory terminals, rather than hyperpolarisation of interneurones, mediates baclofen-induced disinhibition, and the hyperpolarisation of interneurones does not affect IPSPs evoked by direct activation of interneurones (Lambert et al., 1991).

Collectively, the results reported in this chapter indicate that baclofen is a potent agent in depressing Mg^{2+}-free induced discharges in neocortical slices. With the exception of Ba^{2+}, baclofen is still capable of diminishing or abolishing the hyperexcitability induced by the other classical K^+ channel blockers. The significance of baclofen mediation of the responses of neocortical slices to the K^+ channel blockers remains to be clearly identified, with the aid of computer-collected data.

SUMMARY AND CONCLUSIONS

Originally, anaesthesia was considered due to a non-specific action of anesthestic agents on neuronal lipid membranes. However, to the contrary, stereospecificity of chiral anaesthetic agents implicates specific membrane proteins, presumably ion channels, in their actions. Ultimately, anaesthesia is due to reduced excitation or increased inhibition, leading to decreased neuronal activity. This thesis explores the possibility that these protein targets are the ionic channels activated by the central inhibitory transmitter GABA, and that potentiation of the inhibitory actions of GABA would lead to general anaesthesia (Chaps 1 & 2).The GABA-receptors that might be affected by anaesthestic agents are $GABA_A$-receptors that open integral Cl^- channels, and/or $GABA_B$-receptors that open G-protein coupled K^+ channels, both of which have been examined here.

Using pharmacological studies of spontaneous neuronal burst discharges, in isolated slices of rat neocortex maintained in Mg^{2+}-free Krebs medium, neural activity has been recorded from a superfused grease gap system with data acquisition and analysis, under computer control utilizing ASYST software (Chaps 3 & 4).Since the particular K^+ channel coupled to $GABA_B$-receptors is presently unknown, various K^+ channels have been investigated as potential anaesthetic targets. The best characterized currents are the delayed rectifier $I_{K(V)}$, the fast transient current $I_{K(A)}$, the calcium activated currents $I_{K(Ca)}$, and muscarinic modulated resting current $I_{K(M)}$. Each of these can be modified by external agents (TEA, 4-aminopyridine, Cs^+, Sr^{2+} and Ba^{2+}).

Here, for the first time, spontaneous neocortical discharges have been examined in the presence of these K^+ channel blockers (Chap 5), each of which produced a characteristic "signature" effect in exaggerating the discharge waveforms. Quantitative descriptions of these effects were undertaken with power-spectrum analysis of discharges using the MatLab package (Chap 6). The Fourier transform (FFT) proved inappropriate so that a routine was developed based on the Yule-Walker parametric method that allowed statistical assessment of

discharge power density and frequency, characteristic for each K^+ channel blocker. Evidently, this method will have general application for analysing non-stationary time series, and is being further developed.

A comparison has been made of the modification of discharges by activation of either $GABA_A$ or $GABA_B$ receptors, to see if these receptors could be distinguished using specific agonists and antagonists (Chap 7). Higher concentrations of agonists activating either $GABA_A$ (3-APS) or $GABA_B$ receptors (baclofen) completely stopped the discharges whilst lower concentrations attenuated the discharges, and in combination the two effects more nearly halted the discharges. Although analysis of these effects was essentially qualitative, nevertheless, the $GABA_A$ antagonist bicuculline distinguished the effects of these two receptor types. In particular, GABA and bicuculline [(GABA(A + B)$_{ag}$ + A_{ant})= B_{ag} + A_{ant}] did not reproduce baclofen + A_{ant}= B_{ag} + A_{ant}], i.e. baclofen and GABA did not appear strictly comparable on $GABA_B$ receptors. This paradox should be explored further, using a wider range of antagonists and test preparations.

Interaction studies of baclofen in the presence of K^+ channel blockers were also made, in an attempt to identify the channel(s) opened by $GABA_B$ receptor agonists (Chap 8). However, except for Ba^{2+}, all such blocking actions could be overcome by baclofen which depressed or abolished the discharges. Moreover, the agents were less specific at particular channels than the literature implies, suggesting that various different anaesthetic agents and specific peptide K^+ channel blockers should be used in future investigations of this problem.

Overall, these studies suggest that the appropriate use of $GABA_A$ and $GABA_B$ receptor antagonists, together with K^+ channel blockers, provides a method for distinguishing which GABA receptor type is responsible for a particular anaesthetic action in isolated, functional neocortex. This aspect of $GABA_A$ and $GABA_B$ receptor pharmacology should be pursued further, in order to gain a better understanding of the cellular mechanisms underlying general anaesthesia, particularly since not all agents appear to affect the same receptor type.

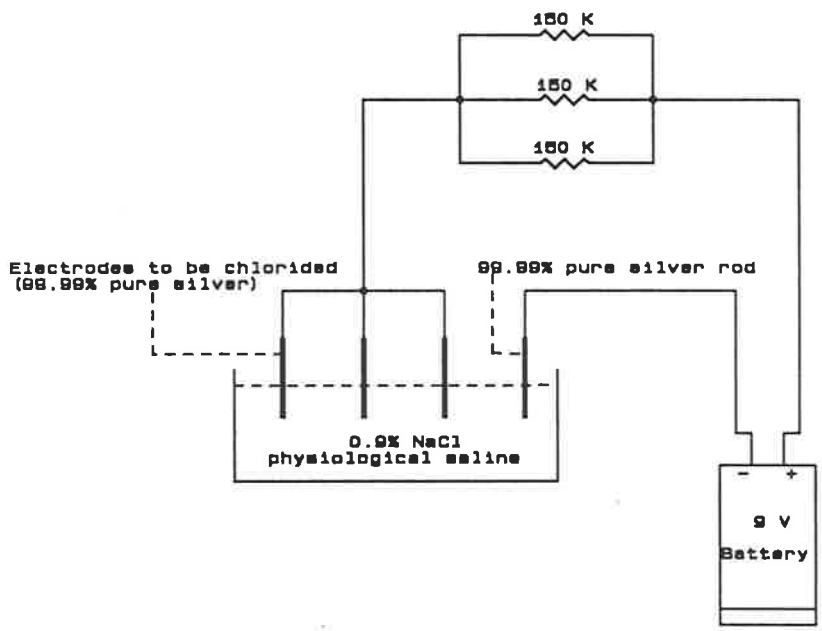

Appendix A.3.1

A Method for Chloriding Silver Electrodes

Silver chloriding		
Size A	Document Number	REV
Date: August 18, 1994	Sheet 1 of 1	

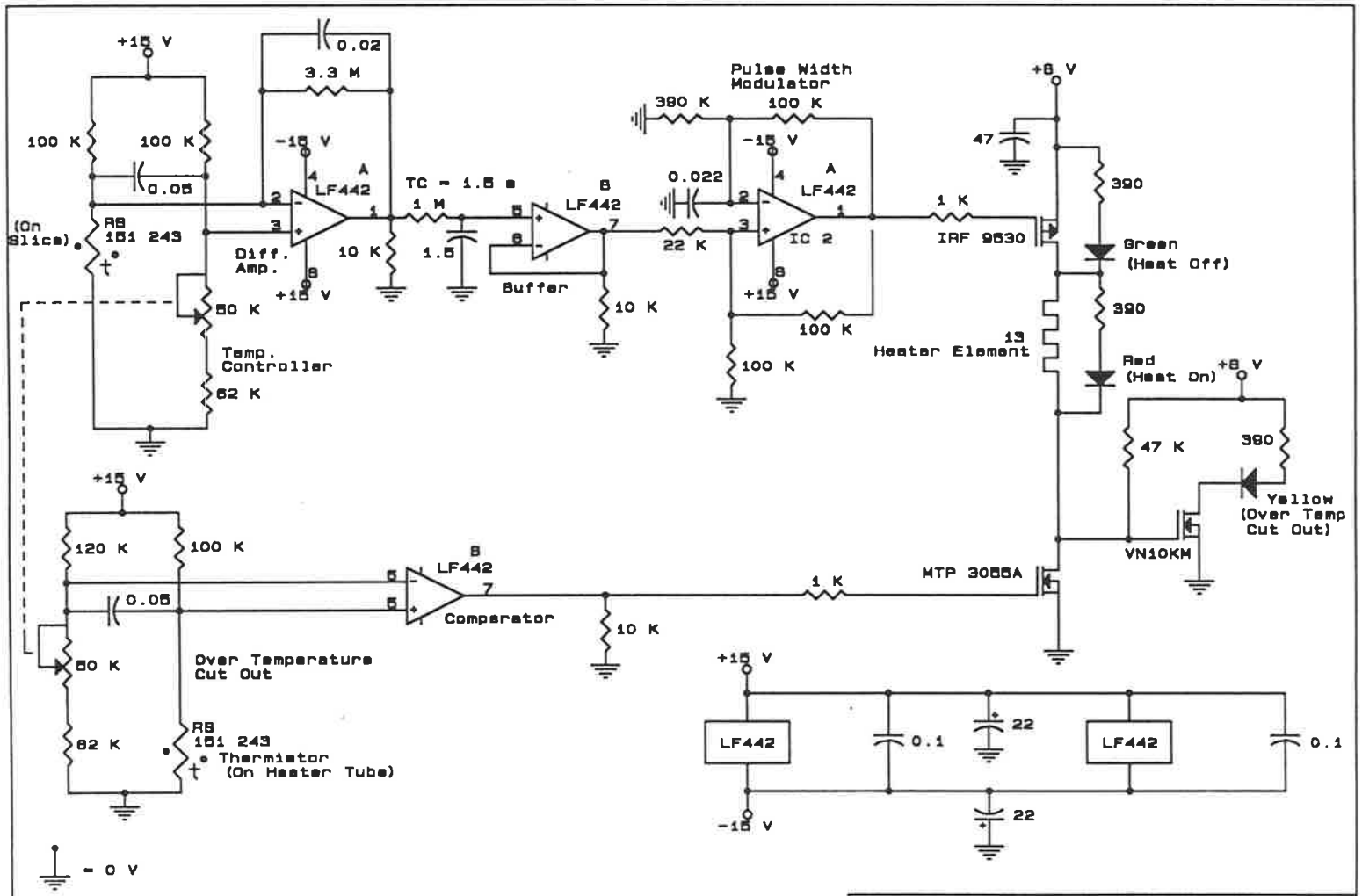

Appendix A.3.2

Temperature Controller

Resistors in Ohm or Kilo Ohm
Capacitors in micro Farad

Temperature Controller		
Size A	Document Number	REV
Date: August 19, 1994	Sheet 1 of 1	

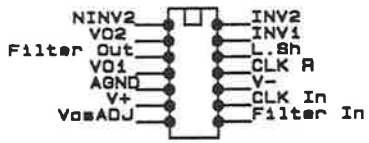

LMF60

8th-order Switched Capacitor Butterworth Lowpass Filter

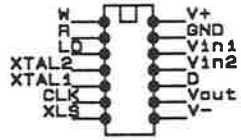

LMF90

4th-order Elliptic Notch Filter

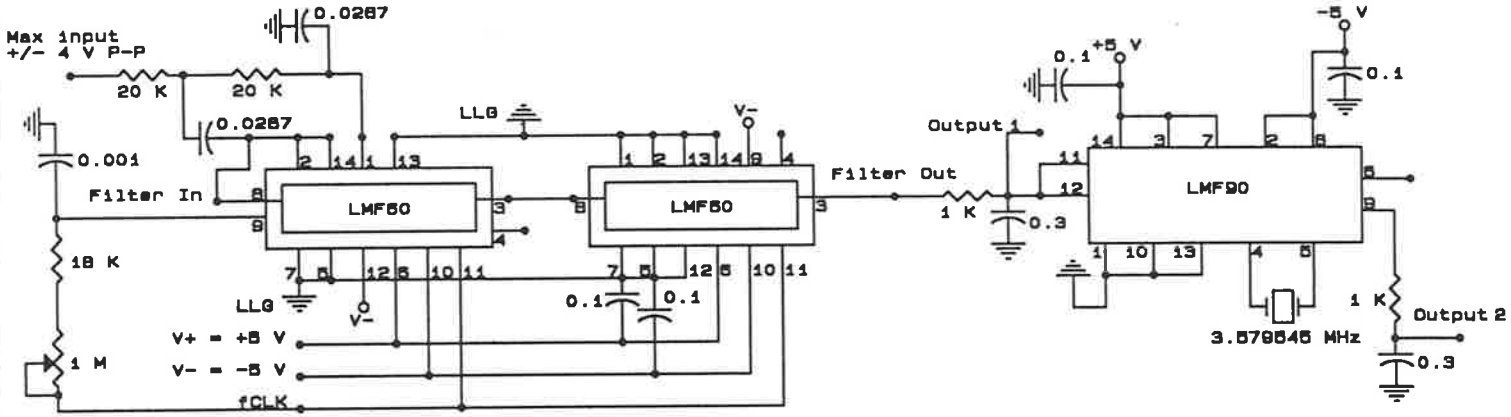

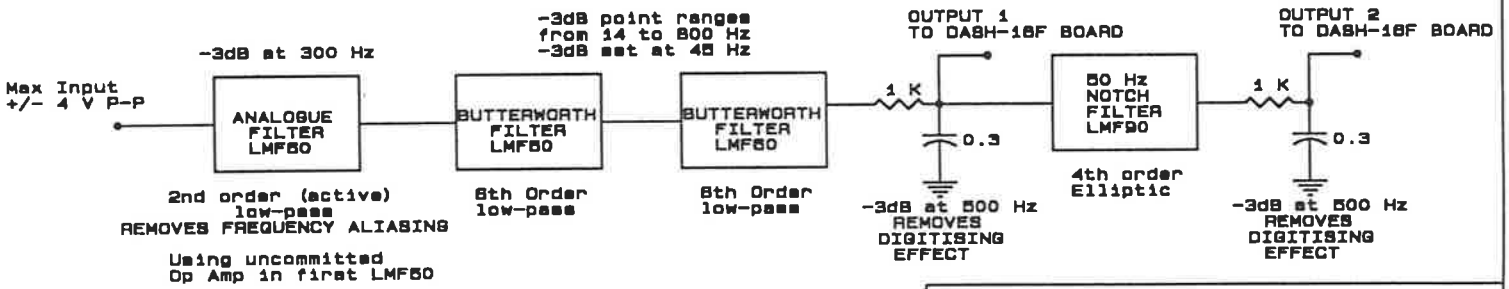

Appendix A.3.3
Low-pass and Notch Filters

Low-pass and Notch Filters		
Size A	Document Number	REV
Date: August 18, 1994	Sheet 1 of 1	

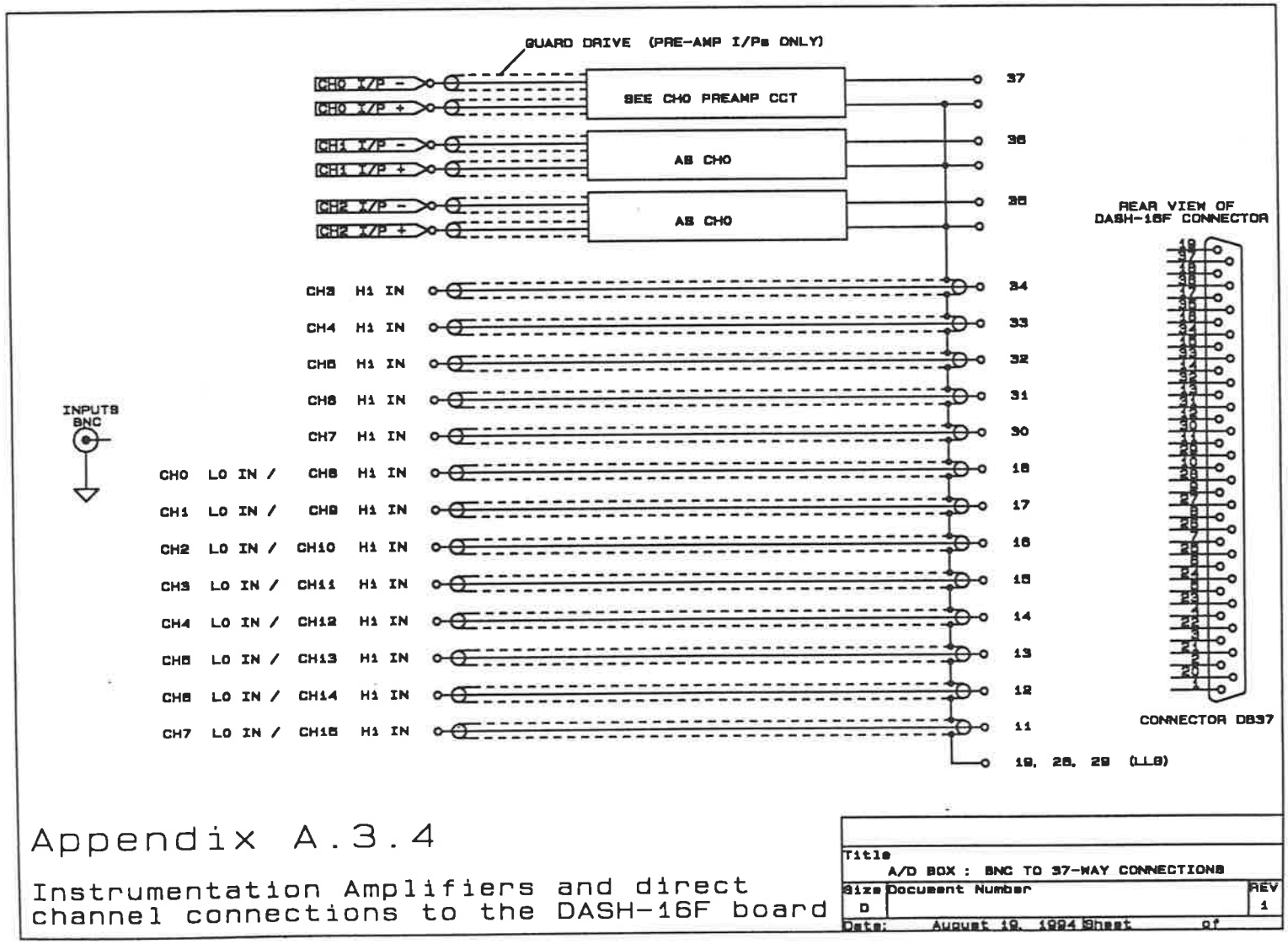

Appendix A.3.4

Instrumentation Amplifiers and direct channel connections to the DASH-16F board

Title: A/D BOX : BNC TO 37-WAY CONNECTIONS		
Size: D	Document Number	REV 1
Date: August 19, 1994	Sheet of	

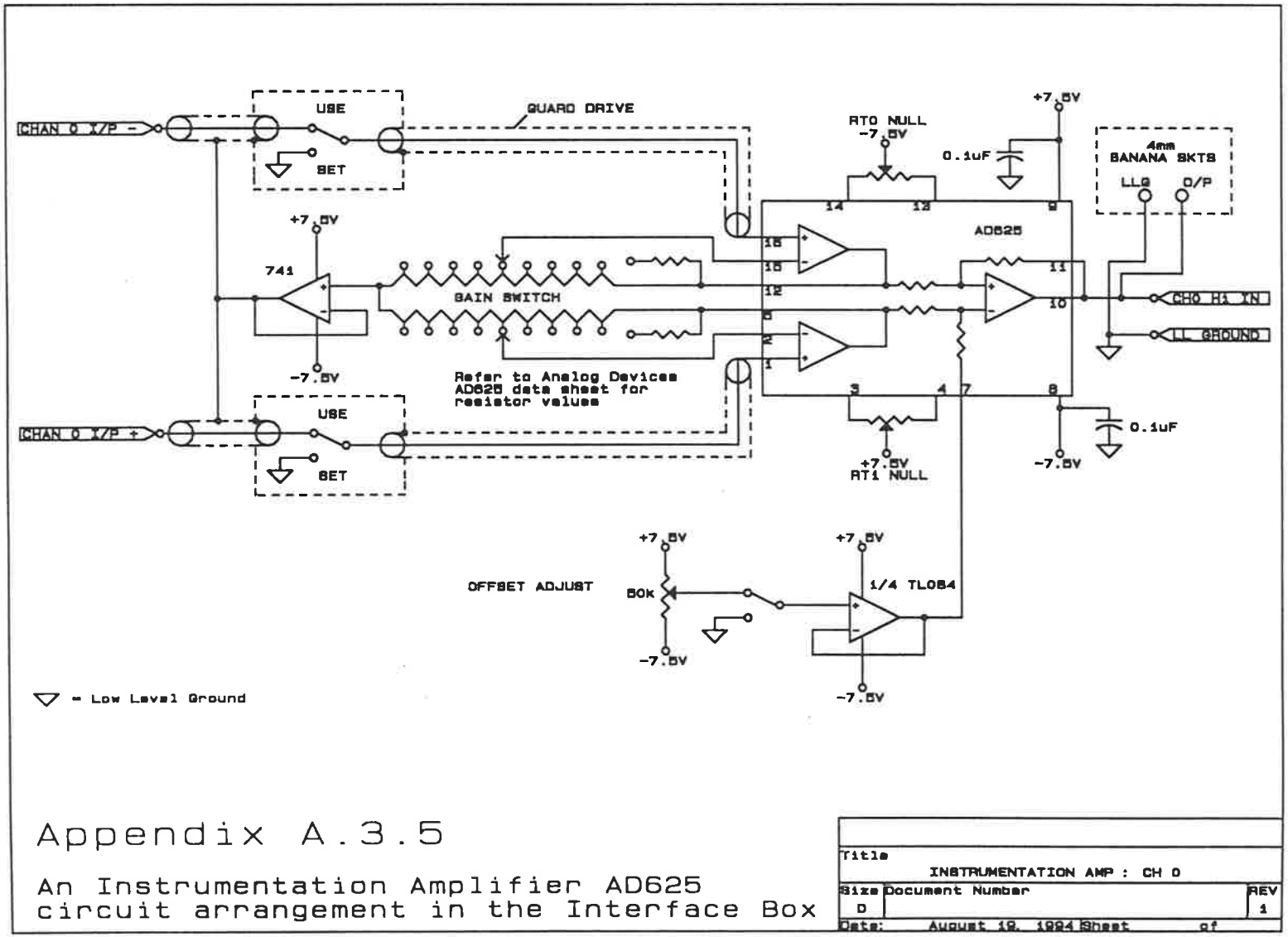

Appendix A.3.5

An Instrumentation Amplifier AD625 circuit arrangement in the Interface Box

Title	INSTRUMENTATION AMP : CH 0	
Size D	Document Number	REV 1
Date: August 19, 1994	Sheet of	

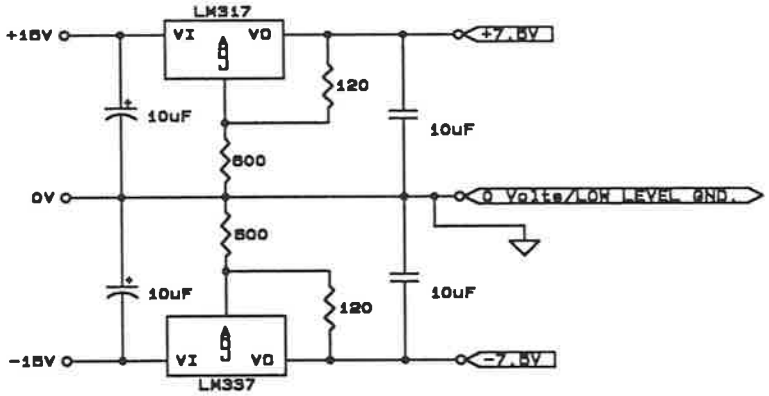

Appendix A.3.6

Voltage Regulators and
Low Level Ground line

Title	VOLTAGE REGULATORS	
Size D	Document Number	REV 1
Date: August 19, 1994	Sheet 8 of 8	

Appendix A.3.7

BSDAAP.GAP

BSDAAP1.GAP

BSDAAP2.GAP

Brain Slice Data Acquisition and Analysis Programme

```
\
\                        *********************
\                  ******   BSDAAP.GAP 8/12/92  ******
\                        LAST MODIFIED ON 28.7.93
\                        *********************
\
\ ********   ELECTROPHYSIOLOGICAL/PHARMACOLOGICAL RESEARCH   **********
\ ******************************************************************
\ DATA ACQUISITION AND ANALYSIS PROGRAM BY AHMAD HASHEMI-SAKHTSARI
\ ******************************************************************
\
\  Acquires data into DATA.ARRAY using A/D.IN>ARRAY, and then allows
\  differentiation, smoothing, zooming, FFT, phase-planing or other
\  mathematical/statistical functions of acquired data using ASYST
\  analysis words. This program is menu driven, and is made suitable
\  for turnkey application.
\
\                                 ***** NOTE *****
\ ******************************                ******************************
\    GAIN TO SPAN FROM -10 TO +10 V. SUITABLE SWITCHES ON DASH16-F BOARD ARE  *
\    ALSO SET TO -10 - +10 (UP TO 16 SINGLE-ENDED, BIPOLAR INPUTS).           *
\ ******************************                ******************************
\                                 ****************

\ Create different arrays e.g. one array for receiving voltages from the A/D.

ECHO.ON

REAL SCALAR ARRAY.SIZE
\ 1610 ARRAY.SIZE  :=
 512 ARRAY.SIZE :=

\   N.B.  Some modules such as the data concatenation do not work properly with
\   the long array size (1610) due to memory limitations. All modules work well
\   with a shorter array.size of 512. Number of modules and, especially, the
\   number of arrays should be kept to a minimum, if array size of 1610 is used
\   for a longer frame collection. In general, try to select just the segments
\   to do the required tasks. As listed here, the programme does not run with
\   array.size of 1610. It runs out of memory trying to allocate memory to too
\   many arrays.

INTEGER DIM[ ARRAY.SIZE ] ARRAY DATA.ARRAY

REAL DIM[ ARRAY.SIZE ] ARRAY DATA1.ARRAY
REAL DIM[ ARRAY.SIZE ] ARRAY DATA2.ARRAY
REAL DIM[ ARRAY.SIZE ] ARRAY DATA3.ARRAY
REAL DIM[ ARRAY.SIZE ] ARRAY CONCAT.ARRAY
REAL DIM[ ARRAY.SIZE ] ARRAY SIGNAL.ARRAY
REAL DIM[ ARRAY.SIZE ] ARRAY DIFFERENTIATE.ARRAY
REAL DIM[ ARRAY.SIZE ] ARRAY FFT.ARRAY
REAL DIM[ ARRAY.SIZE ] ARRAY PSPECTRUM.ARRAY
REAL DIM[ ARRAY.SIZE ] ARRAY SMOOTH.ARRAY
REAL DIM[ ARRAY.SIZE ] ARRAY SMOOTH.ARRAY.OFF
REAL DIM[ ARRAY.SIZE ] ARRAY PHASE.FILTER.ARRAY
```

```
REAL DIM[ ARRAY.SIZE ] ARRAY TIME.AXIS
REAL DIM[ ARRAY.SIZE ] ARRAY TIME1.AXIS
REAL DIM[ ARRAY.SIZE ] ARRAY FREQ.AXIS
REAL DIM[ ARRAY.SIZE ] ARRAY MINMAX.ARRAY          \ For example, remove these
REAL DIM[ ARRAY.SIZE ] ARRAY PHASE.PLANE.ARRAY     \ arrays and related Amplitude
                                                   \ Normalisation Routines for
                                                   \ array.size 1610
REAL DIM[ 20 ] ARRAY EXPANSION.ARRAY

12 STRING FNAME
12 STRING FILENAME
12 STRING FNSAVE1
12 STRING FNSAVE2
80 STRING PRINT.COMMENT
50 STRING DATE.TIME
20 STRING X-AXIS.LABEL
20 STRING Y-AXIS.LABEL
50 STRING CHART.TITLE

DP.INTEGER SCALAR GAIN.FACTOR
INTEGER SCALAR COUNTER

REAL SCALAR DEFAULT.NUMBER
REAL SCALAR DEFAULT.FREQUENCY
REAL SCALAR FILTER.CUTOFF
REAL SCALAR INV.FILTER.CUTOFF
REAL SCALAR PERIOD
REAL SCALAR CUTOFF.FREQ
REAL SCALAR LVL.NUMBER
REAL SCALAR UVL.NUMBER
REAL SCALAR MAX.VALUE
REAL SCALAR MIN.VALUE

REAL DIM[ 5000 ] ARRAY PIXBUF   \ Used for fast erase of lines

VUPORT COLOUR.DISPLAY           \ Configure the graphics display
0 .35 VUPORT.ORIG               \ Save bottom four lines for text
1 .80 VUPORT.SIZE
COLOR.ON
0  BACKGROUND
10 FOREGROUND
INTEN.ON

VUPORT PLOTTER.DISPLAY          \ Configure the graphics display for plotter
0 .35 VUPORT.ORIG
1 .80 VUPORT.SIZE
COLOR.ON
0  BACKGROUND
10 FOREGROUND
INTEN.ON

\ There are a maximum of 16 A/D channels available. We will use channel 3.
\ DATA.ARRAY is the designated array for the key word IN.FROM.BOARD.
\ We use ARRAY.SIZE TEMPLATE.REPEAT to fill the whole array in one pass.
```

```
\ Internal TRIGGER pulse is triggered once for each block of ARRAY.SIZE
\ samples.

DASH16                                  \ Using DAS-16F board
                                        \ One A/D channel number 3

3 3 A/D.TEMPLATE IN.FROM.BOARD
    A/D.INIT

:    DELAY
     5000 MSEC.DELAY                    \ Define a delay period
;

:    INIT.INT.TRIG
     IN.FROM.BOARD
     DATA.ARRAY TEMPLATE.BUFFER
     ARRAY.SIZE TEMPLATE.REPEAT
     INT.TRIG
     A/D.INIT
     ONERR:
     DAS.INIT
     BELL CR ." Error initialising board, attempting reset"
     SCREEN.CLEAR MYSELF
;

: INSTRUCTIONS.1
    SCREEN.CLEAR
    CR ." <F1> ACQUIRE DATA FRAME BY FRAME            <F2> READ DATA FROM DISK "
    CR ." <F3> EXPAND DATA REGIONS                    <F4> PRINT-SCREEN DATA   "
    CR ." <F5> PLOT DATA ON A PEN PLOTTER             <Alt F2> CONCATENATE DATA"
    CR ." <Alt F1> EXIT TO DOS                        <F6> NEXT MENU           "
;

: INSTRUCTIONS.2
    SCREEN.CLEAR
    CR ." <F7> ACQUIRE FILTERED DATA ON-LINE             <F8> FFT DATA OFF-LINE"
    CR ." <F9> DIFFERENTIATE (& PHASE-PLANE) DATA OFF-LINE                      "
    CR ." <F10> SMOOTH DATA OFF-LINE                     <Alt F6> MAIN MENU     "
    CR ." <Alt F1> EXIT TO DOS                           <F4> PRINT-SCREEN DATA"
;

: INSTRUCTIONS.3
    SCREEN.CLEAR
    CR ." <Ctrl F1> READ A STORED WAVEFORM FROM DISK                            "
    CR ." <Ctrl F2> READ ON-LINE FILTERED DATA FROM DISK                        "
    CR ." <Alt F6>  MAIN MENU                                                   "
;

: INSTRUCTIONS.4
    SCREEN.CLEAR
CR ." <Ctrl F3> READ FILES FOR CONCATENATION    <Ctrl F6> FFT CONCAT. DATA      "
CR ." <Ctrl F4> SMOOTH CONCAT. WAVEFORM         <Ctrl F8> PEN-PLOT CONCAT. DATA"
CR ." <Ctrl F5> DIFFERENTIATE (& PHASE-PLANE) CONCAT. WAVEFORM                  "
CR ." <Alt F6>  MAIN MENU                                                       "
;
```

```
: GET.NUMBER
   #INPUT
     IF
        DEFAULT.NUMBER :=
     THEN
;

: GET.GAIN.FACTOR
   #INPUT
     IF
        GAIN.FACTOR :=
     THEN
;

: GET.LVL.VOLTAGE
   #INPUT
     IF
        LVL.NUMBER :=
     THEN
;

: GET.UVL.VOLTAGE
   #INPUT
     IF
        UVL.NUMBER :=
     THEN
;

: GET.FILTER.CUTOFF
   #INPUT
     IF
        FILTER.CUTOFF :=
     THEN
;

:    TIME.GENERATE
     ARRAY.SIZE 1 + ARRAY.SIZE :=
     ARRAY.SIZE 1 DO
        DEFAULT.NUMBER I * TIME.AXIS [ I ] :=
     LOOP
     ARRAY.SIZE 1 - ARRAY.SIZE :=
;

:    FREQUENCY.GENERATE
     DEFAULT.NUMBER
     INV
     DEFAULT.FREQUENCY :=
     ARRAY.SIZE 1 + ARRAY.SIZE :=
     ARRAY.SIZE 1 DO
         DEFAULT.FREQUENCY I * FREQ.AXIS [ I ] :=
     LOOP
     ARRAY.SIZE 1 - ARRAY.SIZE :=
;
```

```
:  MIN.VALUE.FIND
       ARRAY.SIZE 1 + ARRAY.SIZE :=
       SMOOTH.ARRAY.OFF
       MINMAX.ARRAY :=
       MINMAX.ARRAY [ 1 ] MIN.VALUE :=
       ARRAY.SIZE 1 DO
         MIN.VALUE MINMAX.ARRAY [ I ] >
           IF
              MINMAX.ARRAY [ I ] MIN.VALUE :=
           THEN
       LOOP
       ARRAY.SIZE 1 - ARRAY.SIZE :=
;

:  SCALE.ARRAY.ZERO.ONE
       MINMAX.ARRAY MIN.VALUE -
       MINMAX.ARRAY :=
;

:  MAX.VALUE.FIND
       ARRAY.SIZE 1 + ARRAY.SIZE :=
       MINMAX.ARRAY [ 1 ] MAX.VALUE :=
       ARRAY.SIZE 1 DO
         MAX.VALUE MINMAX.ARRAY [ I ] <
           IF
              MINMAX.ARRAY [ I ] MAX.VALUE :=
           THEN
       LOOP
       ARRAY.SIZE 1 - ARRAY.SIZE :=
;

:  NORMALISE.AMPLITUDE
       MINMAX.ARRAY MAX.VALUE /
       MINMAX.ARRAY :=
       MINMAX.ARRAY PHASE.PLANE.ARRAY :=
;

:    SAVE.DATA.FRAME.BY.FRAME
     FILE.TEMPLATE
     9 COMMENTS
     REAL  DIM[ ARRAY.SIZE ] SUBFILE
     REAL  DIM[ ARRAY.SIZE ] SUBFILE
     END
     SCREEN.CLEAR
     CR ." Name of file to create? "
     "INPUT FILENAME ":=
     CR ." Creating - " FILENAME "TYPE
     CR ." Comment on nature of data to be acquired: "
     "INPUT PRINT.COMMENT ":=
     " Time (ms) " X-AXIS.LABEL ":=
     " Amplitude (V) " Y-AXIS.LABEL ":=
     CR ." Enter plot title: "
     "INPUT CHART.TITLE ":=
```

```
    "DATE "  " "CAT "TIME "CAT DATE.TIME ":=
    FILENAME DEFER> FILE.CREATE   \ Create the specified file
    FILENAME DEFER> FILE.OPEN
    1 SUBFILE SIGNAL.ARRAY ARRAY>FILE
    2 SUBFILE TIME.AXIS ARRAY>FILE
    LVL.NUMBER "." 1 >COMMENT
    UVL.NUMBER "." 2 >COMMENT
    PRINT.COMMENT 3 >COMMENT
    DATE.TIME 4 >COMMENT
    GAIN.FACTOR "." 5 >COMMENT
    X-AXIS.LABEL 6 >COMMENT
    Y-AXIS.LABEL 7 >COMMENT
    CHART.TITLE 8 >COMMENT
    DEFAULT.NUMBER "." 9 >COMMENT
    FILE.CLOSE
    BELL
    ONERR:
    BELL CR ." Can not save data to disk "
;

:   SAVE.DATA.FRAME.AGAIN
    FILE.TEMPLATE
    9 COMMENTS
    REAL  DIM[ ARRAY.SIZE ] SUBFILE
    REAL  DIM[ ARRAY.SIZE ] SUBFILE
    END
    SCREEN.CLEAR
    "DATE "  " "CAT "TIME "CAT DATE.TIME ":=
    " Time (ms) " X-AXIS.LABEL ":=
    " Amplitude (V) " Y-AXIS.LABEL ":=
    FILENAME DEFER> FILE.CREATE   \ Create the specified file
    FILENAME DEFER> FILE.OPEN
    1 SUBFILE SIGNAL.ARRAY ARRAY>FILE
    2 SUBFILE TIME.AXIS ARRAY>FILE
    LVL.NUMBER "." 1 >COMMENT
    UVL.NUMBER "." 2 >COMMENT
    PRINT.COMMENT 3 >COMMENT
    DATE.TIME 4 >COMMENT
    GAIN.FACTOR "." 5 >COMMENT
    X-AXIS.LABEL 6 >COMMENT
    Y-AXIS.LABEL 7 >COMMENT
    CHART.TITLE 8 >COMMENT
    DEFAULT.NUMBER "." 9 >COMMENT
    FILE.CLOSE
    BELL
    ONERR:
    BELL CR ." Can not save data to disk "
;

:   READ.DATA.FILE
    STACK.CLEAR
    SCREEN.CLEAR
    CR ." Name of file to read? "
    "INPUT FILENAME ":=
```

```
     CR ." Reading - " FILENAME "TYPE
     FILENAME DEFER> FILE.OPEN
     1 SUBFILE DATA1.ARRAY FILE>ARRAY
     2 SUBFILE TIME1.AXIS FILE>ARRAY
     1 COMMENT> 20 "NUMBER LVL.NUMBER :=
     2 COMMENT> 20 "NUMBER UVL.NUMBER :=
     3 COMMENT> PRINT.COMMENT ":=
     4 COMMENT> DATE.TIME ":=
     5 COMMENT> 20 "NUMBER GAIN.FACTOR :=
     6 COMMENT> X-AXIS.LABEL ":=
     7 COMMENT> Y-AXIS.LABEL ":=
     8 COMMENT> CHART.TITLE ":=
     FILE.CLOSE
     SCREEN.CLEAR
     LVL.NUMBER  UVL.NUMBER          VERTICAL    WORLD.SET
     0.          TIME1.AXIS [ ARRAY.SIZE ]  HORIZONTAL  WORLD.SET
     VUPORT.CLEAR
     XY.AXIS.PLOT
     ERASE.LINES
     DATA1.ARRAY -10 10 A/D.SCALE
     11 COLOR
     CURSOR.OFF
     TIME1.AXIS DATA1.ARRAY -10 10 A/D.SCALE XY.DATA.PLOT
     NORMAL.COORDS
     .300 .960 POSITION                              CHART.TITLE LABEL
     .035 .350 POSITION 90 CHAR.DIR 90 LABEL.DIR     Y-AXIS.LABEL LABEL
     .400 .060 POSITION  0 CHAR.DIR  0 LABEL.DIR     X-AXIS.LABEL LABEL
     SCREEN.CLEAR
CR ." Name of file: " FILENAME "TYPE  ."        Date and time: " DATE.TIME "TYPE
     CR ." Comment:  " PRINT.COMMENT "TYPE
     CR ." Amplifier gain: " GAIN.FACTOR .
     CR ." Press <F4> Print data  or  <Alt F6> Return to Main menu.
     BELL
     LINE.BUFFER.OFF
     ONERR:
     BELL CR ." Can not recall data from disk "
;

\ We will continuously display the collected DATA.ARRAY on the screen.
\ Parameters relating to data acquisition, such as timing delay and
\ sampling rate, are initialised once. A bell sound signifies the start
\ and end of acquisition process. DATA.ARRAY is reinitialised with each
\ pass of the acquisition loop.

:    ACQUIRE.DATA.FRAME.BY.FRAME       \ ACQUIRE DATA
     STACK.CLEAR                       \ with internal trigger
     SCREEN.CLEAR
     0 COUNTER :=
     INIT.INT.TRIG     \ Initialise board
     ." Select the desired acquisition rate in msec --> "
     0.5 DEFAULT.NUMBER :=
     GET.NUMBER                        \ Get timing delay
     DEFAULT.NUMBER
     CONVERSION.DELAY    \ Set sampling rate
```

```
TIME.GENERATE
CR ." Enter amplifier gain --> "
20000 GAIN.FACTOR :=
GET.GAIN.FACTOR
GAIN.FACTOR
CR ." Enter lower voltage limit in Volts (-0.1 to -5) --> "
-1 LVL.NUMBER :=
GET.LVL.VOLTAGE
LVL.NUMBER
CR ." Enter upper voltage limit in Volts (0.1 to 5) --> "
1 UVL.NUMBER :=
GET.UVL.VOLTAGE
UVL.NUMBER
SAVE.DATA.FRAME.BY.FRAME
A/D.INIT
LVL.NUMBER  UVL.NUMBER         VERTICAL    WORLD.SET
0.          TIME.AXIS [ ARRAY.SIZE ]  HORIZONTAL  WORLD.SET
VUPORT.CLEAR
XY.AXIS.PLOT
PIXBUF LINE.BUFFER.ON                       \ Set up auto erase
BEGIN
   STACK.CLEAR                              \ Enter loop and
   FILENAME FNAME ":=
   COUNTER 1 + COUNTER :=                   \ Reset buffer index
   FILENAME COUNTER "." "CAT
   32 "COMPRESS
   FILENAME ":=
   SCREEN.CLEAR
   CR ." COLLECTING DATA  - FRAME"  COUNTER .
   IN.FROM.BOARD
   A/D.INIT
   A/D.IN>ARRAY
   DATA.ARRAY 2048 -
   DUP SIGNAL.ARRAY :=
   SIGNAL.ARRAY -10 10 A/D.SCALE
   ERASE.LINES                              \ Erase previous data
   TIME.AXIS SIGNAL.ARRAY -10 10 A/D.SCALE
   WORLD.COORDS
   11 COLOR
   CURSOR.OFF
   XY.DATA.PLOT
   SAVE.DATA.FRAME.AGAIN
   0 SIGNAL.ARRAY :=
   FNAME FILENAME ":=
   ?KEY
UNTIL                       \ Loop again if not done
NORMAL.COORDS
.300 .960 POSITION                            " Acquired data" LABEL
.035 .350 POSITION 90 CHAR.DIR 90 LABEL.DIR   " Amplitude (V)" LABEL
.400 .060 POSITION  0 CHAR.DIR  0 LABEL.DIR      " Time (ms)" LABEL
BELL
SCREEN.CLEAR
INSTRUCTIONS.1
LINE.BUFFER.OFF
```

```
    ONERR:
    DAS.INIT
    SCREEN.CLEAR
    ." Acquisition rate too fast for signal frequency, try slower rate."
    MYSELF
;

: SAVE.FILTERED.DATA.FRAMES
    FILE.TEMPLATE
    9 COMMENTS
    REAL  DIM[ ARRAY.SIZE ] SUBFILE
    REAL  DIM[ ARRAY.SIZE ] SUBFILE
    END
    SCREEN.CLEAR
    CR ." Name of file to create? "
    "INPUT FILENAME ":=
    CR ." Creating - " FILENAME "TYPE
    CR ." Comment on nature of filtered data to be collected: "
    "INPUT PRINT.COMMENT ":=
    " Time (ms) " X-AXIS.LABEL ":=
    " Amplitude (V) " Y-AXIS.LABEL ":=
    CR ." Enter plot title: "
    "INPUT CHART.TITLE ":=
    "DATE "  " "CAT "TIME "CAT DATE.TIME ":=
    FILENAME DEFER> FILE.CREATE   \ Create the specified file
    FILENAME DEFER> FILE.OPEN
    1 SUBFILE SMOOTH.ARRAY ARRAY>FILE
    2 SUBFILE TIME.AXIS ARRAY>FILE
    LVL.NUMBER "." 1 >COMMENT
    UVL.NUMBER "." 2 >COMMENT
    PRINT.COMMENT 3 >COMMENT
    DATE.TIME 4 >COMMENT
    GAIN.FACTOR "." 5 >COMMENT
    X-AXIS.LABEL 6 >COMMENT
    Y-AXIS.LABEL 7 >COMMENT
    CHART.TITLE 8 >COMMENT
    FILTER.CUTOFF "." 9 >COMMENT
    FILE.CLOSE
    BELL
    ONERR:
    BELL CR ." Can not save filtered data "
;

: SAVE.FILTERED.DATA.AGAIN
    FILE.TEMPLATE
    9 COMMENTS
    REAL  DIM[ ARRAY.SIZE ] SUBFILE
    REAL  DIM[ ARRAY.SIZE ] SUBFILE
    END
    SCREEN.CLEAR
    "DATE "  " "CAT "TIME "CAT DATE.TIME ":=
    " Time (ms) " X-AXIS.LABEL ":=
    " Amplitude (V) " Y-AXIS.LABEL ":=
    FILENAME DEFER> FILE.CREATE   \ Create the specified file
```

```
     FILENAME DEFER> FILE.OPEN
     1 SUBFILE SMOOTH.ARRAY ARRAY>FILE
     2 SUBFILE TIME.AXIS ARRAY>FILE
     LVL.NUMBER "." 1 >COMMENT
     UVL.NUMBER "." 2 >COMMENT
     PRINT.COMMENT 3 >COMMENT
     DATE.TIME 4 >COMMENT
     GAIN.FACTOR "." 5 >COMMENT
     X-AXIS.LABEL 6 >COMMENT
     Y-AXIS.LABEL 7 >COMMENT
     CHART.TITLE 8 >COMMENT
     FILTER.CUTOFF "." 9 >COMMENT
     FILE.CLOSE
     BELL
     ONERR:
     BELL CR ." Can not save filtered data "
;

:  READ.FILTERED.DATA.FILE
     STACK.CLEAR
     SCREEN.CLEAR
     CR ." Name of file to read? "
     "INPUT FILENAME ":=
     CR ." Reading - " FILENAME "TYPE
     FILENAME DEFER> FILE.OPEN
     1 SUBFILE DATA1.ARRAY FILE>ARRAY
     2 SUBFILE TIME1.AXIS FILE>ARRAY
     1 COMMENT> 20 "NUMBER LVL.NUMBER :=
     2 COMMENT> 20 "NUMBER UVL.NUMBER :=
     3 COMMENT> PRINT.COMMENT ":=
     4 COMMENT> DATE.TIME ":=
     5 comment> 20 "NUMBER GAIN.FACTOR :=
     6 COMMENT> X-AXIS.LABEL ":=
     7 COMMENT> Y-AXIS.LABEL ":=
     8 COMMENT> CHART.TITLE ":=
     9 COMMENT> 20 "NUMBER FILTER.CUTOFF :=
     FILE.CLOSE
     SCREEN.CLEAR
     LVL.NUMBER  UVL.NUMBER                  VERTICAL    WORLD.SET
     0.          TIME1.AXIS [ ARRAY.SIZE ]   HORIZONTAL  WORLD.SET
     VUPORT.CLEAR
     XY.AXIS.PLOT
     DATA1.ARRAY -10 10 A/D.SCALE
     ERASE.LINES
     11 COLOR
     CURSOR.OFF
     TIME1.AXIS DATA1.ARRAY -10 10 A/D.SCALE XY.DATA.PLOT
     NORMAL.COORDS
     .300 .960 POSITION                              CHART.TITLE LABEL
     .035 .350 POSITION 90 CHAR.DIR 90 LABEL.DIR    Y-AXIS.LABEL LABEL
     .400 .060 POSITION  0 CHAR.DIR  0 LABEL.DIR    X-AXIS.LABEL LABEL
     SCREEN.CLEAR
CR ." Name of file: " FILENAME "TYPE ."         Date and time: " DATE.TIME "TYPE
     CR ." Comment: " PRINT.COMMENT "TYPE
```

```
CR ." Amplifier gain: " GAIN.FACTOR . ."       Filter cut-off: " FILTER.CUTOFF .
     CR ." Press <F4> Print data  or  <Alt F6> Return to Main menu.
     BELL
     LINE.BUFFER.OFF
     ONERR:
     BELL CR ." Can not recall filtered data "
;

: ACQUIRE.FILTERED.DATA
     STACK.CLEAR                        \ with external trigger
     SCREEN.CLEAR
     0 COUNTER :=
     INIT.INT.TRIG      \ Initialise board
     ." Select the desired acquisition rate in msec --> "
     0.5 DEFAULT.NUMBER :=
     GET.NUMBER
     DEFAULT.NUMBER
     CONVERSION.DELAY     \ Set sampling rate
     TIME.GENERATE
     CR
." Select filtering cutoff frequency in cycles/data point (0.08 to 0.5)--> "
     0.1 FILTER.CUTOFF :=
     GET.FILTER.CUTOFF
     FILTER.CUTOFF
     SCREEN.CLEAR
     CR ." Enter amplifier gain --> "
     20000 GAIN.FACTOR :=
     GET.GAIN.FACTOR
     GAIN.FACTOR
     CR ." Enter lower voltage limit in Volts (-0.1 to -5) --> "
     -1 LVL.NUMBER :=
     GET.LVL.VOLTAGE
     LVL.NUMBER
     CR ." Enter upper voltage limit in Volts (0.1 to 5) --> "
     1 UVL.NUMBER :=
     GET.UVL.VOLTAGE
     UVL.NUMBER
     SAVE.FILTERED.DATA.FRAMES
     A/D.INIT
     LVL.NUMBER  UVL.NUMBER                VERTICAL    WORLD.SET
     0.          TIME.AXIS [ ARRAY.SIZE ]  HORIZONTAL  WORLD.SET
     VUPORT.CLEAR
     XY.AXIS.PLOT
     PIXBUF LINE.BUFFER.ON
     BEGIN
        STACK.CLEAR
        FILENAME FNAME ":=
        COUNTER 1 + COUNTER :=
        FILENAME COUNTER "." "CAT
        32 "COMPRESS
        FILENAME ":=
        SCREEN.CLEAR
        CR ."  Low-pass filter's cut-off frequency is"  FILTER.CUTOFF .
        CR ."  COLLECTING FILTERED DATA  -  FRAME"  COUNTER .
```

```
      IN.FROM.BOARD
      A/D.INIT
      A/D.IN>ARRAY
      DATA.ARRAY 2048 -
      FILTER.CUTOFF SET.CUTOFF.FREQ          \ Set smoothing cutoff width
      SMOOTH                                 \ Smooth array in place
      DUP SMOOTH.ARRAY :=
      SMOOTH.ARRAY -10 10 A/D.SCALE
      ERASE.LINES
      TIME.AXIS SMOOTH.ARRAY -10 10 A/D.SCALE
      WORLD.COORDS
      11 COLOR
      CURSOR.OFF
      XY.DATA.PLOT
      SAVE.FILTERED.DATA.AGAIN
      0 SMOOTH.ARRAY :=
      FNAME FILENAME ":=
      ?KEY
    UNTIL                      \ Loop again if not done
    NORMAL.COORDS
    .300 .960 POSITION                          " Filtered data frame" LABEL
    .035 .350 POSITION 90 CHAR.DIR 90 LABEL.DIR        " Amplitude (V)" LABEL
    .400 .060 POSITION  0 CHAR.DIR  0 LABEL.DIR            " Time (ms)" LABEL
    BELL
    SCREEN.CLEAR
    INSTRUCTIONS.1
    LINE.BUFFER.OFF
    ONERR:
    DAS.INIT
    SCREEN.CLEAR
    ." Acquisition rate too fast for signal frequency, try slower rate."
    ." OR "
    ." Cutoff frequency too narrow, try again "
    MYSELF
;

:   READ.FILES.FOR.CONCAT
    STACK.CLEAR
    SCREEN.CLEAR
    CR ." Name of first file to read? "
    "INPUT FILENAME ":=
    CR ." Reading - " FILENAME "TYPE
    FILENAME DEFER> FILE.OPEN
    1 SUBFILE DATA2.ARRAY FILE>ARRAY
    2 SUBFILE TIME1.AXIS FILE>ARRAY
    1 COMMENT> 20 "NUMBER LVL.NUMBER :=
    2 COMMENT> 20 "NUMBER UVL.NUMBER :=
    3 COMMENT> PRINT.COMMENT ":=
    4 COMMENT> DATE.TIME ":=
    5 COMMENT> 20 "NUMBER GAIN.FACTOR :=
    6 COMMENT> X-AXIS.LABEL ":=
    7 COMMENT> Y-AXIS.LABEL ":=
    8 COMMENT> CHART.TITLE ":=
    FILE.CLOSE
```

```
FILENAME FNSAVE1 ":=
SCREEN.CLEAR
LVL.NUMBER  UVL.NUMBER          VERTICAL    WORLD.SET
0.          TIME1.AXIS [ ARRAY.SIZE ]  HORIZONTAL  WORLD.SET
VUPORT.CLEAR
XY.AXIS.PLOT
ERASE.LINES
DATA2.ARRAY -10 10 A/D.SCALE
11 COLOR
CURSOR.OFF
TIME1.AXIS DATA2.ARRAY -10 10 A/D.SCALE XY.DATA.PLOT
NORMAL.COORDS
.300 .960 POSITION                              CHART.TITLE LABEL
.035 .350 POSITION 90 CHAR.DIR 90 LABEL.DIR     Y-AXIS.LABEL LABEL
.400 .060 POSITION  0 CHAR.DIR  0 LABEL.DIR     X-AXIS.LABEL LABEL
BELL
STACK.CLEAR
SCREEN.CLEAR
CR ." Name of second file to read? "
"INPUT FILENAME ":=
CR ." Reading - " FILENAME "TYPE
FILENAME DEFER> FILE.OPEN
1 SUBFILE DATA3.ARRAY FILE>ARRAY
2 SUBFILE TIME1.AXIS FILE>ARRAY
1 COMMENT> 20 "NUMBER LVL.NUMBER :=
2 COMMENT> 20 "NUMBER UVL.NUMBER :=
3 COMMENT> PRINT.COMMENT ":=
4 COMMENT> DATE.TIME ":=
5 COMMENT> 20 "NUMBER GAIN.FACTOR :=
6 COMMENT> X-AXIS.LABEL ":=
7 COMMENT> Y-AXIS.LABEL ":=
8 COMMENT> CHART.TITLE ":=
9 COMMENT> 20 "NUMBER DEFAULT.NUMBER :=
FILE.CLOSE
FILENAME FNSAVE2 ":=
SCREEN.CLEAR
LVL.NUMBER  UVL.NUMBER          VERTICAL    WORLD.SET
0.          TIME1.AXIS [ ARRAY.SIZE ]  HORIZONTAL  WORLD.SET
VUPORT.CLEAR
XY.AXIS.PLOT
ERASE.LINES
DATA3.ARRAY -10 10 A/D.SCALE
11 COLOR
CURSOR.OFF
TIME1.AXIS DATA3.ARRAY -10 10 A/D.SCALE XY.DATA.PLOT
NORMAL.COORDS
.300 .960 POSITION                              CHART.TITLE LABEL
.035 .350 POSITION 90 CHAR.DIR 90 LABEL.DIR     Y-AXIS.LABEL LABEL
.400 .060 POSITION  0 CHAR.DIR  0 LABEL.DIR     X-AXIS.LABEL LABEL
BELL
\   DATA2.ARRAY SUB[ 512 , 1024 ] DATA3.ARRAY SUB[ 1 , 511 ]  CATENATE
    DATA2.ARRAY SUB[ 805 , 1610 ] DATA3.ARRAY SUB[ 1 , 804 ]  CATENATE
    CONCAT.ARRAY :=
    SCREEN.CLEAR
```

```
     LVL.NUMBER  UVL.NUMBER          VERTICAL    WORLD.SET
     0.          TIME1.AXIS [ ARRAY.SIZE ]  HORIZONTAL  WORLD.SET
     VUPORT.CLEAR
     XY.AXIS.PLOT
     ERASE.LINES
     CONCAT.ARRAY -10 10 A/D.SCALE
     11 COLOR
     CURSOR.OFF
     TIME1.AXIS CONCAT.ARRAY -10 10 A/D.SCALE XY.DATA.PLOT
     NORMAL.COORDS
     .300 .960 POSITION                                CHART.TITLE LABEL
     .035 .350 POSITION 90 CHAR.DIR 90 LABEL.DIR       Y-AXIS.LABEL LABEL
     .400 .060 POSITION  0 CHAR.DIR  0 LABEL.DIR       X-AXIS.LABEL LABEL
     SCREEN.CLEAR
CR ." A Concatenated Waveform of " FNSAVE1 "TYPE ."   &  " FNSAVE2 "TYPE ." "
     CR ." Date and time: " DATE.TIME "TYPE
     CR ." Comment:  " PRINT.COMMENT "TYPE
     CR ." Amplifier gain: " GAIN.FACTOR .
CR ." <F4> Print data   <Alt F6> Main menu  or  <CTRL F9> Save catenated data.
     BELL
     LINE.BUFFER.OFF
     ONERR:
     BELL CR ." Can not recall data from disk "
;

:    SAVE.CATENATED.DATA
     FILE.TEMPLATE
     9 COMMENTS
     REAL  DIM[ ARRAY.SIZE ] SUBFILE
     REAL  DIM[ ARRAY.SIZE ] SUBFILE
     END
     SCREEN.CLEAR
     CR ." Name of file to create? "
     "INPUT FILENAME ":=
     CR ." Creating - " FILENAME "TYPE
     CR ." Comment on the concatenated data: "
     "INPUT PRINT.COMMENT ":=
     " Time (ms) " X-AXIS.LABEL ":=
     " Amplitude (V) " Y-AXIS.LABEL ":=
     CR ." Enter plot title: "
     "INPUT CHART.TITLE ":=
     "DATE "  " "CAT "TIME "CAT DATE.TIME ":=
     FILENAME DEFER> FILE.CREATE   \ Create the specified file
     FILENAME DEFER> FILE.OPEN
     1 SUBFILE CONCAT.ARRAY ARRAY>FILE
     2 SUBFILE TIME1.AXIS ARRAY>FILE
     LVL.NUMBER "." 1 >COMMENT
     UVL.NUMBER "." 2 >COMMENT
     PRINT.COMMENT 3 >COMMENT
     DATE.TIME 4 >COMMENT
     GAIN.FACTOR "." 5 >COMMENT
     X-AXIS.LABEL 6 >COMMENT
     Y-AXIS.LABEL 7 >COMMENT
     CHART.TITLE 8 >COMMENT
```

```
     DEFAULT.NUMBER "." 9 >COMMENT
     FILE.CLOSE
     BELL
     SCREEN.CLEAR
     INSTRUCTIONS.1
     ONERR:
     BELL CR ." Can not save catenated data to disk "
;

:    PRINT.SCREEN.DATA
     STACK.CLEAR
     SCREEN.PRINT
     LINE.BUFFER.OFF
     ONERR:
     SCREEN.CLEAR
     ." Make sure printer is on line"
     MYSELF
     INSTRUCTIONS.1
     BELL
;

LOAD BSDAAP1.GAP

20 0 24 79 WINDOW {BOT}          \ Define graphics window

: GO
    STACK.CLEAR
    SCREEN.CLEAR
    GRAPHICS.DISPLAY
    VUPORT.CLEAR
    18 GRAPHICS.DISPLAY.MODE
    14 SCREEN.COLOR
    {BOT}
    COLOUR.DISPLAY
    DEVICE.INIT
    0 VUPORT.COLOR VUPORT.CLEAR
    LABEL.COLOR 12
    AXIS.COLOR 5
    CURSOR.COLOR 5

    INSTRUCTIONS.1

    \ Function key definition

    F1 FUNCTION.KEY.DOES ACQUIRE.DATA.FRAME.BY.FRAME
    F2 FUNCTION.KEY.DOES INSTRUCTIONS.3
    F3 FUNCTION.KEY.DOES EXPAND.DATA.REGIONS
    F4 FUNCTION.KEY.DOES PRINT.SCREEN.DATA
    F5 FUNCTION.KEY.DOES PEN.PLOT.DATA.FRAME
    F6 FUNCTION.KEY.DOES INSTRUCTIONS.2
    F7 FUNCTION.KEY.DOES ACQUIRE.FILTERED.DATA
    F8 FUNCTION.KEY.DOES FOURIER.TRANSFORM.DATA
    F9 FUNCTION.KEY.DOES DIFFERENTIATE.DATA.OFF.LINE
    F10 FUNCTION.KEY.DOES SMOOTH.DATA.OFF.LINE
```

```
    \ Alt function key definition

    F1 ALT FUNCTION.KEY.DOES BYE
    F2 ALT FUNCTION.KEY.DOES INSTRUCTIONS.4
    F3 ALT FUNCTION.KEY.DOES DIFF.CONCAT.FILTERED.DATA
    F4 ALT FUNCTION.KEY.DOES PHASE.CONCAT.FILTERED.DATA
    F5 ALT FUNCTION.KEY.DOES PHASE.PLANE.CONCAT.DATA
    F6 ALT FUNCTION.KEY.DOES INSTRUCTIONS.1
    F8 ALT FUNCTION.KEY.DOES POWER.SPECTRUM.DATA
    F9 ALT FUNCTION.KEY.DOES PHASE.PLANE.DATA
    F10 ALT FUNCTION.KEY.DOES DIFF.PHASE.FILTERED.DATA

    \ Ctrl function key definition

    F1 CTRL FUNCTION.KEY.DOES READ.DATA.FILE
    F2 CTRL FUNCTION.KEY.DOES READ.FILTERED.DATA.FILE
    F3 CTRL FUNCTION.KEY.DOES READ.FILES.FOR.CONCAT
    F4 CTRL FUNCTION.KEY.DOES SMOOTH.CONCAT.DATA
    F5 CTRL FUNCTION.KEY.DOES DIFFERENTIATE.CONCAT.DATA
    F6 CTRL FUNCTION.KEY.DOES FFT.CONCAT.DATA
    F7 CTRL FUNCTION.KEY.DOES POWER.SPECTRUM.CONCAT.DATA
    F8 CTRL FUNCTION.KEY.DOES PEN.PLOT.CONCAT.DATA.FRAME
    F9 CTRL FUNCTION.KEY.DOES SAVE.CATENATED.DATA
    F10 CTRL FUNCTION.KEY.DOES PHASE.PLANE.FILTERED.DATA

    INTERPRET.KEYS                \ Infinite loop to scan function keys
    ONERR:
    SCREEN.CLEAR BELL
    CR ." Unknown Error: Type Ctrl/Break to Restart"
    CR ." or another key to Exit"
    KEY BYE
;

BELL BELL BELL
CR ." Type GO to start data acquisition and analysis "
```

```
\
\ ***** ElectroPhysiological Data Acquisition and Analysis System *****
\ *                                                                   *
\ *                          BSDAAP1.GAP                              *
\ *        This is a sub-section of the main program BSDAAP.GAP,      *
\ *              compiled by Ahmad Hashemi-Sakhtsari,                 *
\ *                          on 8.12.92                               *
\ *                                                                   *
\ *********************************************************************

: EXPAND.DATA.REGIONS
    SCREEN.CLEAR
    BELL
    ." Keypad cursors will move the position of 2 selection lines. HOME key"
    CR
    ." indicates position, and INS key expands the graph. PG UP proceeded by"
    CR
    ." a number sets the arrow key step size for distance increment of lines."
    CR
    ." END or PG DN keys fix the left or right selection lines."
    CR
    ." DEL key halts this option.   Press any key to continue."

    ARRAY.READOUT                   \ Enable vertical lines.
    NORMAL.COORDS                   \ Switch to normalized coordinates.
    .70 .98 READOUT>POSITION        \ Set position of readout.
    WORLD.COORDS                    \ Return to world coordinates.
    BEGIN                           \ Wait for any key to be pressed.
      EXPANSION.ARRAY READOUT>ARRAY
      ?KEY
    UNTIL
\   NORMAL.COORDS
\   .300 .960 POSITION                                  " Expanded data frame" LABEL
\   .035 .300 POSITION 90 CHAR.DIR 90 LABEL.DIR              " Amplitude (V)" LABEL
\   .400 .060 POSITION  0 CHAR.DIR  0 LABEL.DIR                 " Time (ms)" LABEL
    SCREEN.CLEAR                   \ Relpace above instructions
    STACK.CLEAR
    CR ." Expanded waveform of file: " FILENAME "TYPE  ."
    CR ." "
    CR ." <F4> PRINT-SCREEN DATA "
    CR ." <Alt F6> MAIN MENU "
\   INSTRUCTIONS.1                 \ With default instructions.
    BELL
    ONERR:
    BELL CR ." Can't expand data regions "
;

: SMOOTH.DATA.OFF.LINE
    STACK.CLEAR
    SCREEN.CLEAR
    CR ." Name of file to smooth off-line? "
    "INPUT FILENAME ":=
    CR ." Reading - " FILENAME "TYPE
    FILENAME DEFER> FILE.OPEN
```

```
    1 SUBFILE DATA1.ARRAY FILE>ARRAY
    2 SUBFILE TIME1.AXIS FILE>ARRAY
    1 COMMENT> 20 "NUMBER LVL.NUMBER :=
    2 COMMENT> 20 "NUMBER UVL.NUMBER :=
    3 COMMENT> PRINT.COMMENT ":=
    4 COMMENT> DATE.TIME ":=
    5 COMMENT> 20 "NUMBER GAIN.FACTOR :=
    6 COMMENT> X-AXIS.LABEL ":=
    7 COMMENT> Y-AXIS.LABEL ":=
    8 COMMENT> CHART.TITLE ":=
    9 COMMENT> 20 "NUMBER DEFAULT.NUMBER :=
    FILE.CLOSE
    SCREEN.CLEAR
    LVL.NUMBER UVL.NUMBER                    VERTICAL     WORLD.SET
    0.         TIME1.AXIS [ ARRAY.SIZE ]     HORIZONTAL   WORLD.SET
    VUPORT.CLEAR
    XY.AXIS.PLOT
    DATA1.ARRAY -10 10 A/D.SCALE
    ERASE.LINES
    11 COLOR
    CURSOR.OFF
    TIME1.AXIS DATA1.ARRAY -10 10 A/D.SCALE XY.DATA.PLOT
    NORMAL.COORDS
    .300 .960 POSITION                                CHART.TITLE  LABEL
    .035 .300 POSITION 90 CHAR.DIR 90 LABEL.DIR       Y-AXIS.LABEL LABEL
    .400 .060 POSITION  0 CHAR.DIR  0 LABEL.DIR       X-AXIS.LABEL LABEL
    SCREEN.CLEAR
CR ." Name of file: " FILENAME "TYPE  ."        Date and time: " DATE.TIME "TYPE
    CR ." Comment:  " PRINT.COMMENT "TYPE
    CR ." Amplifier gain: " GAIN.FACTOR .
    2000 MSEC.DELAY
    BELL
    STACK.CLEAR
    SCREEN.CLEAR
    CR
." Select filtering cutoff frequency in cycles/data point (0.08 to 0.5)--> "
     0.1 FILTER.CUTOFF :=
     GET.FILTER.CUTOFF
     FILTER.CUTOFF
     1 FILTER.CUTOFF /
     INV.FILTER.CUTOFF :=
     INV.FILTER.CUTOFF DEFAULT.NUMBER *
     PERIOD :=
     1000 PERIOD /
     CUTOFF.FREQ :=
     SCREEN.CLEAR
     DATA1.ARRAY
     DUP                                     \ Copy the array
     FILTER.CUTOFF SET.CUTOFF.FREQ           \ Set smoothing cutoff width
     SMOOTH                                  \ Smooth array in place
     DUP SMOOTH.ARRAY.OFF :=
     SCREEN.CLEAR
     LVL.NUMBER UVL.NUMBER                   VERTICAL     WORLD.SET
     0.         TIME1.AXIS [ ARRAY.SIZE ]    HORIZONTAL   WORLD.SET
```

```
    VUPORT.CLEAR
    XY.AXIS.PLOT
    SMOOTH.ARRAY.OFF 2048 -
    SMOOTH.ARRAY.OFF -10 10 A/D.SCALE
    ERASE.LINES
    11 COLOR
    CURSOR.OFF
    TIME1.AXIS SMOOTH.ARRAY.OFF -10 10 A/D.SCALE XY.DATA.PLOT
    NORMAL.COORDS
   .300 .960 POSITION                        " Digitally filtered waveform" LABEL
   .035 .300 POSITION 90 CHAR.DIR 90 LABEL.DIR            " Amplitude (V)" LABEL
   .400 .060 POSITION  0 CHAR.DIR  0 LABEL.DIR                 " Time (ms)" LABEL
   BELL
   SCREEN.CLEAR
   CR ." Name of file: " FILENAME "TYPE  ."
   CR ." Low-pass filter's cut-off frequency is"  CUTOFF.FREQ .  ." Hz"
   CR ." <F4> PRINT-SCREEN DATA "
   CR ." <Alt F6> MAIN MENU "
   CR ." <Alt F10> DIFFERENTIATE AND PHASE-PLANE FILTERED DATA "
   BELL
   ONERR:
   BELL CR ." Can't smooth data off-line "
;

: DIFF.PHASE.FILTERED.DATA
   STACK.CLEAR
   SCREEN.CLEAR
   VUPORT.CLEAR
   MIN.VALUE.FIND
   SCALE.ARRAY.ZERO.ONE
   MAX.VALUE.FIND
   NORMALISE.AMPLITUDE
   PHASE.PLANE.ARRAY 2048 -
   DUP                          \ copy the array
   1 SET.ORDER
   2 SET.DEGREE
   DIFFERENTIATE.DATA     \ Differentiate copy of data
   DUP PHASE.FILTER.ARRAY :=
   PHASE.FILTER.ARRAY 2048 -
   ERASE.LINES
   11 COLOR
   CURSOR.OFF
   TIME1.AXIS PHASE.FILTER.ARRAY   \ -10 10 A/D.SCALE XY.AUTO.PLOT
   XY.AUTO.PLOT
   NORMAL.COORDS
   .300 .960 POSITION                          " Differentiated waveform" LABEL
.035 .150 POSITION 90 CHAR.DIR 90 LABEL.DIR     " Amplitude (V)/Time (ms)" LABEL
   .400 .060 POSITION  0 CHAR.DIR  0 LABEL.DIR                 " Time (ms)" LABEL
   BELL
   CR ." Name of file: " FILENAME "TYPE  ."
   CR ." Cut-off frequency is"  CUTOFF.FREQ .  ." Hz"
   CR ." <F4> PRINT-SCREEN DATA "
   CR ." <Alt F6> MAIN MENU "
   CR ." <CTRL F10> PHASE-PLANE FILTERED DATA "
```

```
    ONERR:
    BELL CR ." Can't differentiate data "
;

:  PHASE.PLANE.FILTERED.DATA
    STACK.CLEAR
    SCREEN.CLEAR
    VUPORT.CLEAR
    ERASE.LINES
    11 COLOR
    CURSOR.OFF
    PHASE.PLANE.ARRAY 2048 -
    PHASE.FILTER.ARRAY 2048 -
    PHASE.PLANE.ARRAY PHASE.FILTER.ARRAY    \  -10 10 A/D.SCALE
    XY.AUTO.PLOT
    NORMAL.COORDS
    .300 .960 POSITION                              " Phase-Plane waveform" LABEL
.035 .150 POSITION 90 CHAR.DIR 90 LABEL.DIR     " Amplitude (V)/Time (ms)" LABEL
.400 .060 POSITION  0 CHAR.DIR  0 LABEL.DIR    " Normalised Amplitude (V)" LABEL
    BELL
    SCREEN.CLEAR
    CR ." Name of file: " FILENAME "TYPE  ."
    CR ." Cut-off frequency is"  CUTOFF.FREQ .  ." Hz"
    CR ." <F4> PRINT-SCREEN DATA "
    CR ." <Alt F6> MAIN MENU "
    ONERR:
    BELL CR ." Can't produce a phase-plane "
;

: DIFFERENTIATE.DATA.OFF.LINE
    STACK.CLEAR
    SCREEN.CLEAR
    CR ." Name of file to differentiate? "
    "INPUT FILENAME ":=
    CR ." Reading - " FILENAME "TYPE
    FILENAME DEFER> FILE.OPEN
    1 SUBFILE DATA1.ARRAY FILE>ARRAY
    2 SUBFILE TIME1.AXIS FILE>ARRAY
    1 COMMENT> 20 "NUMBER LVL.NUMBER :=
    2 COMMENT> 20 "NUMBER UVL.NUMBER :=
    3 COMMENT> PRINT.COMMENT ":=
    4 COMMENT> DATE.TIME ":=
    5 COMMENT> 20 "NUMBER GAIN.FACTOR :=
    6 COMMENT> X-AXIS.LABEL ":=
    7 COMMENT> Y-AXIS.LABEL ":=
    8 COMMENT> CHART.TITLE ":=
    FILE.CLOSE
    SCREEN.CLEAR
    LVL.NUMBER UVL.NUMBER                  VERTICAL     WORLD.SET
    0.         TIME1.AXIS [ ARRAY.SIZE ]   HORIZONTAL   WORLD.SET
    VUPORT.CLEAR
    XY.AXIS.PLOT
    DATA1.ARRAY -10 10 A/D.SCALE
    ERASE.LINES
```

```
    11 COLOR
    CURSOR.OFF
    TIME1.AXIS DATA1.ARRAY -10 10 A/D.SCALE XY.DATA.PLOT
    NORMAL.COORDS
    .300 .960 POSITION                                CHART.TITLE  LABEL
    .035 .300 POSITION 90 CHAR.DIR 90 LABEL.DIR       Y-AXIS.LABEL LABEL
    .400 .060 POSITION  0 CHAR.DIR  0 LABEL.DIR       X-AXIS.LABEL LABEL
    SCREEN.CLEAR
CR ." Name of file: " FILENAME "TYPE  ."        Date and time: " DATE.TIME "TYPE
    CR ." Comment:  " PRINT.COMMENT "TYPE
    CR ." Amplifier gain: " GAIN.FACTOR .
CR ." DIFFERENTIATED DATA will be displayed in 3 seconds "
    3000 MSEC.DELAY
    BELL
    STACK.CLEAR
    SCREEN.CLEAR
    VUPORT.CLEAR
    DATA1.ARRAY 2048 -
    DUP                          \ copy the array
    1 SET.ORDER
    2 SET.DEGREE
    DIFFERENTIATE.DATA            \ Differentiate copy of data
    DUP DIFFERENTIATE.ARRAY :=
    DIFFERENTIATE.ARRAY 2048 -
    DIFFERENTIATE.ARRAY -10 10 A/D.SCALE
    ERASE.LINES
    11 COLOR
    CURSOR.OFF
    TIME1.AXIS DIFFERENTIATE.ARRAY -10 10 A/D.SCALE XY.AUTO.PLOT
    NORMAL.COORDS
    .300 .960 POSITION                          " Differentiated waveform" LABEL
.035 .150 POSITION 90 CHAR.DIR 90 LABEL.DIR     " Amplitude (V)/Time (ms)" LABEL
    .400 .060 POSITION  0 CHAR.DIR  0 LABEL.DIR                " Time (ms)" LABEL
    BELL
    SCREEN.CLEAR
    CR ." Name of file: " FILENAME "TYPE  ."
    CR ." "
    CR ." <F4> PRINT-SCREEN DATA "
    CR ." <Alt F6> MAIN MENU "
    CR ." <Alt F9> PHASE-PLANE DATA "
    ONERR:
    BELL CR ." Can't differentiate data "
;

:  PHASE.PLANE.DATA
    STACK.CLEAR
    SCREEN.CLEAR
    VUPORT.CLEAR
    ERASE.LINES
    11 COLOR
    CURSOR.OFF
    DATA1.ARRAY 2048 -
    DIFFERENTIATE.ARRAY 2048 -
    DATA1.ARRAY -10 10 A/D.SCALE
```

```
    DIFFERENTIATE.ARRAY -10 10 A/D.SCALE
    XY.AUTO.PLOT
    NORMAL.COORDS
    .300 .960 POSITION                              " Phase-Plane waveform" LABEL
.035 .150 POSITION 90 CHAR.DIR 90 LABEL.DIR     " Amplitude (V)/Time (ms)" LABEL
    .400 .060 POSITION  0 CHAR.DIR  0 LABEL.DIR           " Amplitude (V)" LABEL
    BELL
    SCREEN.CLEAR
    CR ." Name of file: " FILENAME "TYPE  ."
    CR ." "
    CR ." <F4> PRINT-SCREEN DATA "
    CR ." <Alt F6> MAIN MENU "
    ONERR:
    BELL CR ." Can't produce a phase-plane "
;

: FOURIER.TRANSFORM.DATA
    STACK.CLEAR
    SCREEN.CLEAR
    CR ." Name of file to transform? "
    "INPUT FILENAME ":=
    CR ." Reading - " FILENAME "TYPE
    FILENAME DEFER> FILE.OPEN
    1 SUBFILE DATA1.ARRAY FILE>ARRAY
    2 SUBFILE TIME1.AXIS FILE>ARRAY
    1 COMMENT> 20 "NUMBER LVL.NUMBER :=
    2 COMMENT> 20 "NUMBER UVL.NUMBER :=
    3 COMMENT> PRINT.COMMENT ":=
    4 COMMENT> DATE.TIME ":=
    5 COMMENT> 20 "NUMBER GAIN.FACTOR :=
    6 COMMENT> X-AXIS.LABEL ":=
    7 COMMENT> Y-AXIS.LABEL ":=
    8 COMMENT> CHART.TITLE ":=
    9 COMMENT> 20 "NUMBER DEFAULT.NUMBER :=
    FILE.CLOSE
    STACK.CLEAR
    SCREEN.CLEAR
    LVL.NUMBER UVL.NUMBER         VERTICAL   WORLD.SET
    0.         TIME1.AXIS [ ARRAY.SIZE ] HORIZONTAL WORLD.SET
    VUPORT.CLEAR
    XY.AXIS.PLOT
    DATA1.ARRAY -10 10 A/D.SCALE
    ERASE.LINES
    11 COLOR
    CURSOR.OFF
    TIME1.AXIS DATA1.ARRAY -10 10 A/D.SCALE XY.DATA.PLOT
    NORMAL.COORDS
    .300 .960 POSITION                              CHART.TITLE  LABEL
    .035 .350 POSITION 90 CHAR.DIR 90 LABEL.DIR     Y-AXIS.LABEL LABEL
    .400 .060 POSITION  0 CHAR.DIR  0 LABEL.DIR     X-AXIS.LABEL LABEL
    SCREEN.CLEAR
CR ." Name of file: " FILENAME "TYPE  ."        Date and time: " DATE.TIME "TYPE
    CR ." Comment:  " PRINT.COMMENT "TYPE
    CR ." Amplifier gain: " GAIN.FACTOR .
```

```
CR ." TRANSFORMED DATA will be displayed in 3 seconds "
    3000 MSEC.DELAY
    BELL
    STACK.CLEAR
    SCREEN.CLEAR
    VUPORT.CLEAR
    FREQUENCY.GENERATE
    DATA1.ARRAY 2048 -          \ Bias offset for bipolar jumpers
    DUP                         \ Copy the array
\   Z=X+I0                      \ Convert real array to complex
\   IFFT                        \ Inverse Fourier transform
\   ZREAL                       \ Throw away imaginary part
    FFT                         \ Fourier transform data
    ZMAG                        \ Obtain the real magnitude part
    DUP FFT.ARRAY :=
    FFT.ARRAY PSPECTRUM.ARRAY :=

    FFT.ARRAY 2 *
    FFT.ARRAY :=
    FFT.ARRAY ARRAY.SIZE /
    FFT.ARRAY :=
\    FFT.ARRAY LN
\    FFT.ARRAY :=
\    FFT.ARRAY 100 *
\    FFT.ARRAY :=
    FREQ.AXIS
    []DIMS []DIM 2 / SWAP SUB[ 2 , ? ]
    FFT.ARRAY -10 10 A/D.SCALE
    []DIMS []DIM 2 / SWAP SUB[ 2 , ? ]
    ERASE.LINES
    11 COLOR
    CURSOR.OFF
    XY.AUTO.PLOT
    NORMAL.COORDS
    .300 .960 POSITION                    " Fourier transformed waveform" LABEL
    .035 .250 POSITION 90 CHAR.DIR 90 LABEL.DIR    " Normalised amplitude" LABEL
\ .035 .250 POSITION 90 CHAR.DIR 90 LABEL.DIR " Ln (Normalised amplitude)" LABEL
    .400 .060 POSITION  0 CHAR.DIR  0 LABEL.DIR          " Frequency (Hz)" LABEL
    SCREEN.CLEAR
    CR ." Name of file: " FILENAME "TYPE  ."
    CR ." "
    CR ." <F4> PRINT-SCREEN DATA "
    CR ." <Alt F6> MAIN MENU "
    CR ." <Alt F8> POWER SPECTRUM DATA "
    BELL
    ONERR:
    BELL CR ." Can't Fourier Transform Data "
;

:  POWER.SPECTRUM.DATA
     PSPECTRUM.ARRAY DUP *
     PSPECTRUM.ARRAY :=
     PSPECTRUM.ARRAY 2 *
     PSPECTRUM.ARRAY :=
```

```
     PSPECTRUM.ARRAY ARRAY.SIZE /
     PSPECTRUM.ARRAY :=
\     PSPECTRUM.ARRAY LN
\     PSPECTRUM.ARRAY :=
\     PSPECTRUM.ARRAY 100 *
\     PSPECTRUM.ARRAY :=
     FREQ.AXIS
     []DIMS []DIM 2 / SWAP SUB[ 2 , ? ]
     PSPECTRUM.ARRAY -10 10 A/D.SCALE
     []DIMS []DIM 2 / SWAP SUB[ 2 , ? ]
     ERASE.LINES
     11 COLOR
     CURSOR.OFF
     XY.AUTO.PLOT
     NORMAL.COORDS
     .300 .960 POSITION                          " Power spectrum waveform" LABEL
.035 .150 POSITION 90 CHAR.DIR 90 LABEL.DIR     " Normalised power density" LABEL
\  .035 .150 POSITION 90 CHAR.DIR 90 LABEL.DIR " Ln (Norm. power density)" LABEL
    .400 .060 POSITION  0 CHAR.DIR  0 LABEL.DIR          " Frequency (Hz)" LABEL
     SCREEN.CLEAR
     CR ." Name of file: " FILENAME "TYPE  ."
     CR ." "
     CR ." <F4> PRINT-SCREEN DATA "
     CR ." <Alt F6> MAIN MENU "
     BELL
     ONERR:
     BELL CR ." Can't Produce the Power Spectrum "
;

20 0 24 79 WINDOW {BOT}

:  PEN.PLOT.DATA.FRAME
    STACK.CLEAR
    SCREEN.CLEAR
    CR ." Name of file to plot? "
    "INPUT FILENAME ":=
    CR ." Reading - " FILENAME "TYPE
    FILENAME DEFER> FILE.OPEN
    1 SUBFILE DATA1.ARRAY FILE>ARRAY
    2 SUBFILE TIME1.AXIS FILE>ARRAY
    1 COMMENT> 20 "NUMBER LVL.NUMBER :=
    2 COMMENT> 20 "NUMBER UVL.NUMBER :=
    3 COMMENT> PRINT.COMMENT ":=
    4 COMMENT> DATE.TIME ":=
    5 COMMENT> 20 "NUMBER GAIN.FACTOR :=
    6 COMMENT> X-AXIS.LABEL ":=
    7 COMMENT> Y-AXIS.LABEL ":=
    8 COMMENT> CHART.TITLE ":=
    FILE.CLOSE
    STACK.CLEAR
    SCREEN.CLEAR
    LVL.NUMBER UVL.NUMBER         VERTICAL   WORLD.SET
    0.         TIME1.AXIS [ ARRAY.SIZE ] HORIZONTAL WORLD.SET
    VUPORT.CLEAR
```

```
    XY.AXIS.PLOT
    DATA1.ARRAY -10 10 A/D.SCALE
    ERASE.LINES
    11 COLOR
    CURSOR.OFF
    TIME1.AXIS DATA1.ARRAY -10 10 A/D.SCALE XY.DATA.PLOT
    NORMAL.COORDS
    .300 .960 POSITION                              CHART.TITLE  LABEL
    .035 .350 POSITION 90 CHAR.DIR 90 LABEL.DIR     Y-AXIS.LABEL LABEL
    .400 .060 POSITION  0 CHAR.DIR  0 LABEL.DIR     X-AXIS.LABEL LABEL
    SCREEN.CLEAR
CR ." Name of file: " FILENAME "TYPE  ."        Date and time: " DATE.TIME "TYPE
    CR ." Comment:  " PRINT.COMMENT "TYPE
    CR ." Amplifier gain: " GAIN.FACTOR .
    PLOTTER.DISPLAY
    HP7440
    PLOTTER.DEFAULTS
    DEVICE.INIT
    CR ." PLOTTING displayed data "
    LVL.NUMBER  UVL.NUMBER    VERTICAL    WORLD.SET
    0.  TIME1.AXIS [ ARRAY.SIZE ]   HORIZONTAL  WORLD.SET
    2 AXIS.COLOR
    3 LABEL.COLOR
    XY.AXIS.PLOT
    DATA1.ARRAY -10 10 A/D.SCALE
    ERASE.LINES
    1 COLOR
    CURSOR.OFF
    TIME1.AXIS DATA1.ARRAY -10 10 A/D.SCALE XY.DATA.PLOT
    NORMAL.COORDS
    .300 .960 POSITION                              CHART.TITLE  LABEL
    .035 .350 POSITION 90 CHAR.DIR 90 LABEL.DIR     Y-AXIS.LABEL LABEL
    .400 .060 POSITION  0 CHAR.DIR  0 LABEL.DIR     X-AXIS.LABEL LABEL
    BELL
    AXIS.DEFAULTS
    IBM.GRAPHICS
    GRAPHICS.DISPLAY
    18 GRAPHICS.DISPLAY.MODE
    14 SCREEN.COLOR
    SCREEN.CLEAR
    {BOT}
    COLOUR.DISPLAY
    0 VUPORT.COLOR VUPORT.CLEAR
    LABEL.COLOR 12
    AXIS.COLOR 5
    CURSOR.COLOR 5
    11 COLOR
    INSTRUCTIONS.1
    BELL
    LINE.BUFFER.OFF
    ONERR:
    BELL CR ." Can not pen-plot data "
;
```

```
LOAD BSDAAP2.GAP

\ ******************** THE END OF SUB-SECTION BSDAAP1.GAP **********************
```

```
\
\ ***** ElectroPhysiological Data Acquisition and Analysis System *****
\ *                                                                   *
\ *                          BSDAAP2.GAP                              *
\ *        This is a sub-section of the main program BSDAAP.GAP       *
\ *              compiled by Ahmad Hashemi-Sakhtsari,                 *
\ *                          on 8.12.92                               *
\ *                                                                   *
\ *********************************************************************

: SMOOTH.CONCAT.DATA
    STACK.CLEAR
    SCREEN.CLEAR
    LVL.NUMBER UVL.NUMBER                    VERTICAL     WORLD.SET
    0.         TIME1.AXIS [ ARRAY.SIZE ]     HORIZONTAL   WORLD.SET
    VUPORT.CLEAR
    XY.AXIS.PLOT
    CONCAT.ARRAY -10 10 A/D.SCALE
    ERASE.LINES
    11 COLOR
    CURSOR.OFF
    TIME1.AXIS CONCAT.ARRAY -10 10 A/D.SCALE XY.DATA.PLOT
    NORMAL.COORDS
    .300 .960 POSITION                                CHART.TITLE  LABEL
    .035 .300 POSITION 90 CHAR.DIR 90 LABEL.DIR       Y-AXIS.LABEL LABEL
    .400 .060 POSITION  0 CHAR.DIR  0 LABEL.DIR       X-AXIS.LABEL LABEL
    SCREEN.CLEAR
CR ." A Concatenated Waveform of " FNSAVE1 "TYPE ."   &  " FNSAVE2 "TYPE ." "
    CR ." Date and time: " DATE.TIME "TYPE
    CR ." Comment:  " PRINT.COMMENT "TYPE
    CR ." Amplifier gain: " GAIN.FACTOR .
    2000 MSEC.DELAY
    BELL
    STACK.CLEAR
    SCREEN.CLEAR
    CR
." Select filtering cutoff frequency in cycles/data point (0.08 to 0.5)--> "
     0.1 FILTER.CUTOFF :=
     GET.FILTER.CUTOFF
     FILTER.CUTOFF
     1 FILTER.CUTOFF /
     INV.FILTER.CUTOFF :=
     INV.FILTER.CUTOFF DEFAULT.NUMBER *
     PERIOD :=
     1000 PERIOD /
     CUTOFF.FREQ :=
     SCREEN.CLEAR
     CONCAT.ARRAY
     DUP                                  \ Copy the array
     FILTER.CUTOFF SET.CUTOFF.FREQ        \ Set smoothing cutoff width
     SMOOTH                               \ Smooth array in place
     DUP SMOOTH.ARRAY.OFF :=
     SCREEN.CLEAR
     LVL.NUMBER UVL.NUMBER                VERTICAL     WORLD.SET
```

```
     0.         TIME1.AXIS [ ARRAY.SIZE ]   HORIZONTAL   WORLD.SET
     VUPORT.CLEAR
     XY.AXIS.PLOT
     SMOOTH.ARRAY.OFF 2048 -
     SMOOTH.ARRAY.OFF -10 10 A/D.SCALE
     ERASE.LINES
     11 COLOR
     CURSOR.OFF
     TIME1.AXIS SMOOTH.ARRAY.OFF -10 10 A/D.SCALE XY.DATA.PLOT
     NORMAL.COORDS
    .300 .960 POSITION                      " Digitally filtered waveform" LABEL
    .035 .300 POSITION 90 CHAR.DIR 90 LABEL.DIR           " Amplitude (V)" LABEL
    .400 .060 POSITION  0 CHAR.DIR  0 LABEL.DIR               " Time (ms)" LABEL
    BELL
    SCREEN.CLEAR
CR ." A Concatenated Waveform of " FNSAVE1 "TYPE ."   &  " FNSAVE2 "TYPE ." "
    CR ." Low-pass filter's cut-off frequency is"  CUTOFF.FREQ .  ." Hz"
    CR ." <F4> PRINT-SCREEN DATA "
    CR ." <Alt F6> MAIN MENU "
    CR ." <Alt F3> DIFFERENTIATE (AND PHASE-PLANE) CONCATENATED FILTERED DATA "
    BELL
    ONERR:
    BELL CR ." Can't smooth data off-line "
;

: DIFF.CONCAT.FILTERED.DATA
    STACK.CLEAR
    SCREEN.CLEAR
    VUPORT.CLEAR
    SMOOTH.ARRAY.OFF 2048 -
    DUP                         \ copy the array
    1 SET.ORDER
    2 SET.DEGREE
    DIFFERENTIATE.DATA           \ Differentiate copy of data
    DUP PHASE.FILTER.ARRAY :=
    PHASE.FILTER.ARRAY 2048 -
    PHASE.FILTER.ARRAY -10 10 A/D.SCALE
    ERASE.LINES
    11 COLOR
    CURSOR.OFF
    TIME1.AXIS PHASE.FILTER.ARRAY -10 10 A/D.SCALE XY.AUTO.PLOT
    NORMAL.COORDS
    .300 .960 POSITION                          " Differentiated waveform" LABEL
.035 .150 POSITION 90 CHAR.DIR 90 LABEL.DIR     " Amplitude (V)/Time (ms)" LABEL
    .400 .060 POSITION  0 CHAR.DIR  0 LABEL.DIR               " Time (ms)" LABEL
    BELL
CR ." A Concatenated Waveform of " FNSAVE1 "TYPE ."   &  " FNSAVE2 "TYPE ." "
    CR ." Cut-off frequency is"  CUTOFF.FREQ .  ." Hz"
    CR ." <F4> PRINT-SCREEN DATA "
    CR ." <Alt F6> MAIN MENU "
    CR ." <Alt F4> PHASE-PLANE CONCATENATED FILTERED DATA "
    ONERR:
    BELL CR ." Can't differentiate data "
;
```

```
:  PHASE.CONCAT.FILTERED.DATA
    STACK.CLEAR
    SCREEN.CLEAR
    VUPORT.CLEAR
    ERASE.LINES
    11 COLOR
    CURSOR.OFF
    SMOOTH.ARRAY.OFF 2048 -
    PHASE.FILTER.ARRAY 2048 -
    SMOOTH.ARRAY.OFF -10 10 A/D.SCALE
    PHASE.FILTER.ARRAY -10 10 A/D.SCALE
    XY.AUTO.PLOT
    NORMAL.COORDS
    .300 .960 POSITION                                  " Phase-Plane waveform" LABEL
.035 .150 POSITION 90 CHAR.DIR 90 LABEL.DIR      " Amplitude (V)/Time (ms)" LABEL
    .400 .060 POSITION  0 CHAR.DIR  0 LABEL.DIR            " Amplitude (V)" LABEL
    BELL
    SCREEN.CLEAR
CR ." A Concatenated Waveform of " FNSAVE1 "TYPE ."   &  " FNSAVE2 "TYPE ." "
    CR ." Cut-off frequency is"  CUTOFF.FREQ .  ." Hz"
    CR ." "
    CR ." <F4> PRINT-SCREEN DATA "
    CR ." <Alt F6> MAIN MENU "
    ONERR:
    BELL CR ." Can't produce a phase-plane "
;

: DIFFERENTIATE.CONCAT.DATA
    STACK.CLEAR
    SCREEN.CLEAR
    LVL.NUMBER UVL.NUMBER                    VERTICAL     WORLD.SET
    0.         TIME1.AXIS [ ARRAY.SIZE ]     HORIZONTAL   WORLD.SET
    VUPORT.CLEAR
    XY.AXIS.PLOT
    CONCAT.ARRAY -10 10 A/D.SCALE
    ERASE.LINES
    11 COLOR
    CURSOR.OFF
    TIME1.AXIS CONCAT.ARRAY -10 10 A/D.SCALE XY.DATA.PLOT
    NORMAL.COORDS
    .300 .960 POSITION                                CHART.TITLE  LABEL
    .035 .300 POSITION 90 CHAR.DIR 90 LABEL.DIR       Y-AXIS.LABEL LABEL
    .400 .060 POSITION  0 CHAR.DIR  0 LABEL.DIR       X-AXIS.LABEL LABEL
    SCREEN.CLEAR
CR ." A Concatenated Waveform of " FNSAVE1 "TYPE ."   &  " FNSAVE2 "TYPE ." "
    CR ." Date and time: " DATE.TIME "TYPE
    CR ." Comment:  " PRINT.COMMENT "TYPE
    CR ." Amplifier gain: " GAIN.FACTOR .
CR ." DIFFERENTIATED DATA will be displayed in 3 seconds "
    3000 MSEC.DELAY
    BELL
    STACK.CLEAR
    SCREEN.CLEAR
```

```
    VUPORT.CLEAR
    CONCAT.ARRAY 2048 -
    DUP                          \ copy the array
    1 SET.ORDER
    2 SET.DEGREE
    DIFFERENTIATE.DATA            \ Differentiate copy of data
    DUP DIFFERENTIATE.ARRAY :=
    DIFFERENTIATE.ARRAY 2048 -
    DIFFERENTIATE.ARRAY -10 10 A/D.SCALE
    ERASE.LINES
    11 COLOR
    CURSOR.OFF
    TIME1.AXIS DIFFERENTIATE.ARRAY -10 10 A/D.SCALE XY.AUTO.PLOT
    NORMAL.COORDS
    .300 .960 POSITION                          " Differentiated waveform" LABEL
.035 .150 POSITION 90 CHAR.DIR 90 LABEL.DIR     " Amplitude (V)/Time (ms)" LABEL
    .400 .060 POSITION  0 CHAR.DIR  0 LABEL.DIR                " Time (ms)" LABEL
    BELL
    SCREEN.CLEAR
CR ." A Concatenated Waveform of " FNSAVE1 "TYPE ."   &  " FNSAVE2 "TYPE ." "
    CR ." "
    CR ." <F4> PRINT-SCREEN DATA "
    CR ." <Alt F6> MAIN MENU "
    CR ." <Alt F5> PHASE-PLANE CONCATENATED DATA "
    ONERR:
    BELL CR ." Can't differentiate data "
;

:  PHASE.PLANE.CONCAT.DATA
    STACK.CLEAR
    SCREEN.CLEAR
    VUPORT.CLEAR
    ERASE.LINES
    11 COLOR
    CURSOR.OFF
    CONCAT.ARRAY 2048 -
    DIFFERENTIATE.ARRAY 2048 -
    CONCAT.ARRAY -10 10 A/D.SCALE
    DIFFERENTIATE.ARRAY -10 10 A/D.SCALE
    XY.AUTO.PLOT
    NORMAL.COORDS
    .300 .960 POSITION                           " Phase-Plane waveform" LABEL
.035 .150 POSITION 90 CHAR.DIR 90 LABEL.DIR     " Amplitude (V)/Time (ms)" LABEL
    .400 .060 POSITION  0 CHAR.DIR  0 LABEL.DIR            " Amplitude (V)" LABEL
    BELL
    SCREEN.CLEAR
CR ." A Concatenated Waveform of " FNSAVE1 "TYPE ."   &  " FNSAVE2 "TYPE ." "
    CR ." "
    CR ." <F4> PRINT-SCREEN DATA "
    CR ." <Alt F6> MAIN MENU "
    ONERR:
    BELL CR ." Can't produce a phase-plane "
;
```

```
: FFT.CONCAT.DATA
    STACK.CLEAR
    SCREEN.CLEAR
    LVL.NUMBER UVL.NUMBER                    VERTICAL    WORLD.SET
    0.         TIME1.AXIS [ ARRAY.SIZE ]  HORIZONTAL  WORLD.SET
    VUPORT.CLEAR
    XY.AXIS.PLOT
    CONCAT.ARRAY -10 10 A/D.SCALE
    ERASE.LINES
    11 COLOR
    CURSOR.OFF
    TIME1.AXIS CONCAT.ARRAY -10 10 A/D.SCALE XY.DATA.PLOT
    NORMAL.COORDS
    .300 .960 POSITION                                CHART.TITLE  LABEL
    .035 .350 POSITION 90 CHAR.DIR 90 LABEL.DIR       Y-AXIS.LABEL LABEL
    .400 .060 POSITION  0 CHAR.DIR  0 LABEL.DIR       X-AXIS.LABEL LABEL
    SCREEN.CLEAR
CR ." A Concatenated Waveform of " FNSAVE1 "TYPE ."   &  " FNSAVE2 "TYPE ." "
    CR ." Date and time: " DATE.TIME "TYPE
    CR ." Comment:  " PRINT.COMMENT "TYPE
    CR ." Amplifier gain: " GAIN.FACTOR .
    CR ." TRANSFORMED DATA will be displayed in 3 seconds "
    3000 MSEC.DELAY
    BELL
    STACK.CLEAR
    SCREEN.CLEAR
    VUPORT.CLEAR
    FREQUENCY.GENERATE
    CONCAT.ARRAY 2048 -            \ Bias offset for bipolar jumpers
    DUP                            \ Copy the array
\   Z=X+I0                         \ Convert real array to complex
\   IFFT                           \ Inverse Fourier transform
\   ZREAL                          \ Throw away imaginary part
    FFT                            \ Fourier transform data
    ZMAG                           \ Obtain the real magnitude part
    DUP FFT.ARRAY :=
    FFT.ARRAY PSPECTRUM.ARRAY :=

    FFT.ARRAY 2 *
    FFT.ARRAY :=
    FFT.ARRAY ARRAY.SIZE /
    FFT.ARRAY :=
\    FFT.ARRAY LN
\    FFT.ARRAY :=
\    FFT.ARRAY 100 *
\    FFT.ARRAY :=
    FREQ.AXIS
    []DIMS []DIM 2 / SWAP SUB[ 2 , ? ]
    FFT.ARRAY -10 10 A/D.SCALE
    []DIMS []DIM 2 / SWAP SUB[ 2 , ? ]
    ERASE.LINES
    11 COLOR
    CURSOR.OFF
    XY.AUTO.PLOT
```

```
    NORMAL.COORDS
    .300 .960 POSITION                          " Fourier transformed waveform" LABEL
    .035 .250 POSITION 90 CHAR.DIR 90 LABEL.DIR     " Normalised amplitude" LABEL
\ .035 .250 POSITION 90 CHAR.DIR 90 LABEL.DIR " Ln (Normalised amplitude)" LABEL
    .400 .060 POSITION  0 CHAR.DIR  0 LABEL.DIR          " Frequency (Hz)" LABEL
    SCREEN.CLEAR
CR ." A Concatenated Waveform of " FNSAVE1 "TYPE ."   &  " FNSAVE2 "TYPE ." "
    CR ." "
    CR ." <F4> PRINT-SCREEN DATA "
    CR ." <Alt F6> MAIN MENU "
    CR ." <CTRL F7> POWER SPECTRUM CONCATENATED DATA "
    BELL
    ONERR:
    BELL CR ." Can't Fourier Transform Data "
;

:  POWER.SPECTRUM.CONCAT.DATA
    PSPECTRUM.ARRAY DUP *
    PSPECTRUM.ARRAY :=
    PSPECTRUM.ARRAY 2 *
    PSPECTRUM.ARRAY :=
    PSPECTRUM.ARRAY ARRAY.SIZE /
    PSPECTRUM.ARRAY :=
\    PSPECTRUM.ARRAY LN
\    PSPECTRUM.ARRAY :=
\    PSPECTRUM.ARRAY 100 *
\    PSPECTRUM.ARRAY :=
    FREQ.AXIS
    []DIMS []DIM 2 / SWAP SUB[ 2 , ? ]
    PSPECTRUM.ARRAY -10 10 A/D.SCALE
    []DIMS []DIM 2 / SWAP SUB[ 2 , ? ]
    ERASE.LINES
    11 COLOR
    CURSOR.OFF
    XY.AUTO.PLOT
    NORMAL.COORDS
    .300 .960 POSITION                           " Power spectrum waveform" LABEL
.035 .150 POSITION 90 CHAR.DIR 90 LABEL.DIR    " Normalised power density" LABEL
\  .035 .150 POSITION 90 CHAR.DIR 90 LABEL.DIR  " Ln (Norm. power density" LABEL
    .400 .060 POSITION  0 CHAR.DIR  0 LABEL.DIR          " Frequency (Hz)" LABEL
    SCREEN.CLEAR
CR ." A Concatenated Waveform of " FNSAVE1 "TYPE ."   &  " FNSAVE2 "TYPE ." "
    CR ." "
    CR ." <F4> PRINT-SCREEN DATA "
    CR ." <Alt F6> MAIN MENU "
    BELL
    ONERR:
    BELL CR ." Can't Produce the Power Spectrum "
;

20 0 24 79 WINDOW {BOT}

:   PEN.PLOT.CONCAT.DATA.FRAME
    STACK.CLEAR
```

```
    SCREEN.CLEAR
    LVL.NUMBER UVL.NUMBER          VERTICAL   WORLD.SET
    0.         TIME1.AXIS [ ARRAY.SIZE ] HORIZONTAL WORLD.SET
    VUPORT.CLEAR
    XY.AXIS.PLOT
    CONCAT.ARRAY -10 10 A/D.SCALE
    ERASE.LINES
    11 COLOR
    CURSOR.OFF
    TIME1.AXIS CONCAT.ARRAY -10 10 A/D.SCALE XY.DATA.PLOT
    NORMAL.COORDS
    .300 .960 POSITION                                CHART.TITLE  LABEL
    .035 .350 POSITION 90 CHAR.DIR 90 LABEL.DIR       Y-AXIS.LABEL LABEL
    .400 .060 POSITION  0 CHAR.DIR  0 LABEL.DIR       X-AXIS.LABEL LABEL
    SCREEN.CLEAR
CR ." A Concatenated Waveform of " FNSAVE1 "TYPE ."   &  " FNSAVE2 "TYPE ." "
    CR ." Date and time: " DATE.TIME "TYPE
    CR ." Comment:  " PRINT.COMMENT "TYPE
    CR ." Amplifier gain: " GAIN.FACTOR .
    PLOTTER.DISPLAY
    HP7440
    PLOTTER.DEFAULTS
    DEVICE.INIT
    CR ." PLOTTING displayed data "
    LVL.NUMBER  UVL.NUMBER    VERTICAL    WORLD.SET
    0.  TIME1.AXIS [ ARRAY.SIZE ]   HORIZONTAL  WORLD.SET
    2 AXIS.COLOR
    3 LABEL.COLOR
    XY.AXIS.PLOT
    CONCAT.ARRAY -10 10 A/D.SCALE
    ERASE.LINES
    1 COLOR
    CURSOR.OFF
    TIME1.AXIS CONCAT.ARRAY -10 10 A/D.SCALE XY.DATA.PLOT
    NORMAL.COORDS
    .300 .960 POSITION                                CHART.TITLE  LABEL
    .035 .350 POSITION 90 CHAR.DIR 90 LABEL.DIR       Y-AXIS.LABEL LABEL
    .400 .060 POSITION  0 CHAR.DIR  0 LABEL.DIR       X-AXIS.LABEL LABEL
    BELL
    AXIS.DEFAULTS
    IBM.GRAPHICS
    GRAPHICS.DISPLAY
    18 GRAPHICS.DISPLAY.MODE
    14 SCREEN.COLOR
    SCREEN.CLEAR
    {BOT}
    COLOUR.DISPLAY
    0 VUPORT.COLOR VUPORT.CLEAR
    LABEL.COLOR 12
    AXIS.COLOR 5
    CURSOR.COLOR 5
    11 COLOR
    INSTRUCTIONS.1
    BELL
```

```
    LINE.BUFFER.OFF
    ONERR:
    BELL CR ." Can not pen-plot data "
;

\ ******************** THE END OF SUB-SECTION BSDAAP2.GAP **********************
```

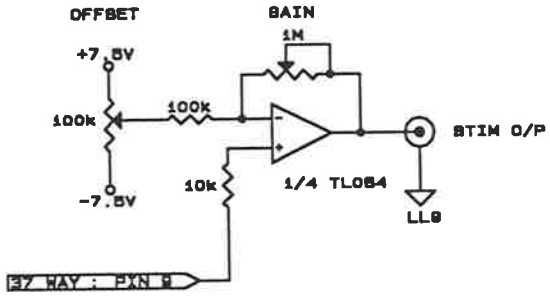

Appendix A.4.1

STIMULUS TRIGGER OUTPUT

Title	Stimulus Trigger Output	
Size D	Document Number	REV 1
Date: August 25, 1994	Sheet 1 of 1	

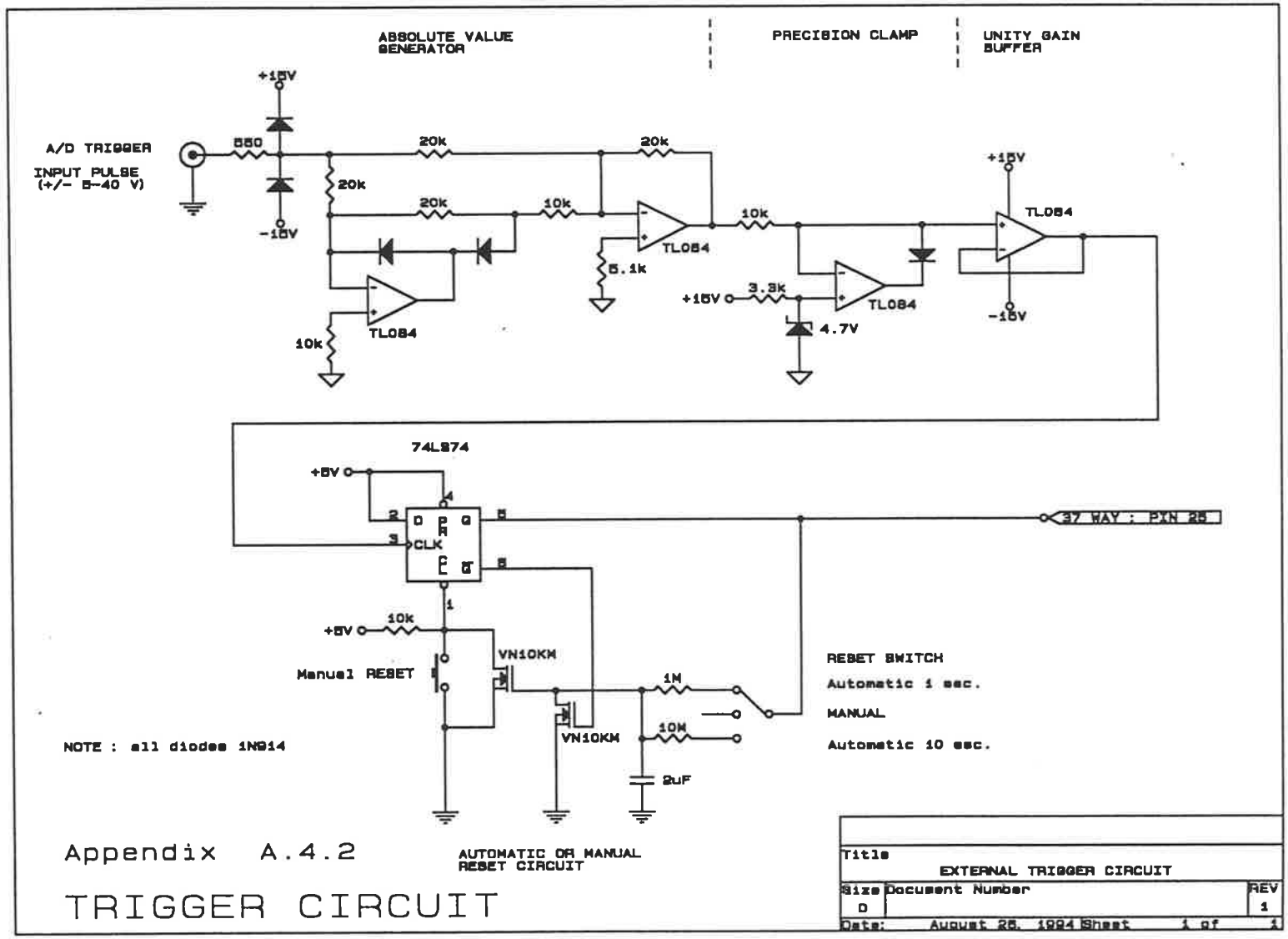

Appendix A.4.2

TRIGGER CIRCUIT

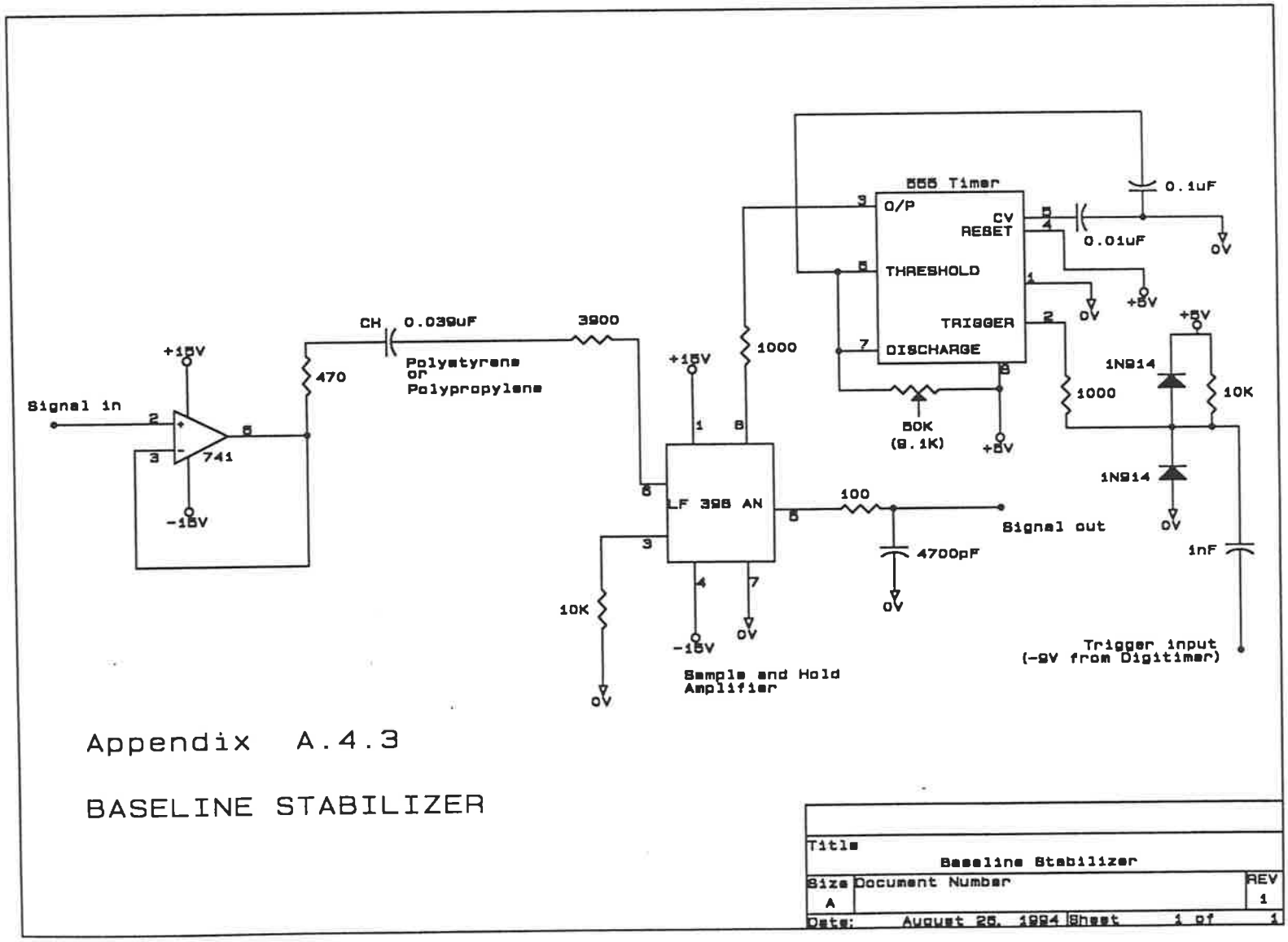

Appendix A.4.3

BASELINE STABILIZER

Appendix A.4.4

EPDAAP.WHL

EPDAAP1.WHL

Evoked Potential Data Acquisition and Analysis Programme

```
\
\                         *********************
\                  ****** EPDAAP.WHL  30/5/91 ******
\                         *********************
\
\ ********   ELECTROPHYSIOLOGICAL/NEUROPHYSIOLOGICAL RESEARCH   *******
\ ******************************************************************
\ DATA ACQUISITION AND ANALYSIS PROGRAM BY AHMAD HASHEMI-SAKHTSARI
\ ******************************************************************

\ Acquires data into DATA.ARRAY using A/D.IN>ARRAY, and then allows
\ averaging & subtraction, differentiation, smoothing, zooming, FFT,
\ or other mathematical/statistical functions of acquired data using
\ ASYST analysis words. This program may be menu driven, and can be
\ made suitable for turnkey application.

\ Create different arrays e.g. one array for receiving voltages from the A/D.

ECHO.ON

INTEGER DIM[ 512 ] ARRAY DATA.ARRAY
INTEGER DIM[ 512 ] ARRAY LAST.ARRAY

REAL DIM[ 512 ] ARRAY DATA1.ARRAY
REAL DIM[ 512 ] ARRAY LAST1.ARRAY
REAL DIM[ 512 ] ARRAY AVERAGE
REAL DIM[ 512 ] ARRAY CONDITION.TEST
REAL DIM[ 512 ] ARRAY TEST.ONLY
REAL DIM[ 512 ] ARRAY DIFFERENCE
REAL DIM[ 512 ] ARRAY SUPERIMPOSED1.ARRAY
REAL DIM[ 512 ] ARRAY SUPERIMPOSED2.ARRAY
REAL DIM[ 512 ] ARRAY SUPERIMPOSED3.ARRAY
REAL DIM[ 512 ] ARRAY DIFFERENTIATE.ARRAY
REAL DIM[ 512 ] ARRAY INTEGRATE.ARRAY
REAL DIM[ 512 ] ARRAY FFT.ARRAY
REAL DIM[ 512 ] ARRAY SMOOTH.ARRAY
REAL DIM[ 512 ] ARRAY AVERAGED.FILTERED.ARRAY
REAL DIM[ 512 ] ARRAY TIME.AXIS
REAL DIM[ 512 ] ARRAY TIME1.AXIS
REAL DIM[ 512 ] ARRAY FREQ.AXIS

20 STRING FILENAME
80 STRING PRINT.COMMENT
50 STRING DATE.TIME
50 STRING X-AXIS.LABEL
50 STRING Y-AXIS.LABEL
50 STRING CHART.TITLE

DP.INTEGER SCALAR GAIN.FACTOR
INTEGER SCALAR COUNTER
INTEGER SCALAR PRINT.AVERAGE.NUMBER
INTEGER SCALAR AVERAGE.NUMBER

REAL SCALAR DEFAULT.NUMBER
```

```
REAL SCALAR FILTER.CUTOFF
REAL SCALAR LVL.NUMBER
REAL SCALAR UVL.NUMBER

REAL DIM[ 5000 ] ARRAY PIXBUF    \ Used for fast erase of lines

VUPORT COLOUR.DISPLAY            \ Configure the graphics display
0 .35 VUPORT.ORIG                \ Save bottom four lines for text
1 .80 VUPORT.SIZE
COLOR.ON
0  BACKGROUND
10 FOREGROUND
INTEN.ON

VUPORT PLOTTER.DISPLAY           \ Configure the graphics display for plotter
0 .35 VUPORT.ORIG
1 .80 VUPORT.SIZE
COLOR.ON
0  BACKGROUND
10 FOREGROUND
INTEN.ON

\ There are a maximum of 16 A/D channels available. We will use channel 3.
\ DATA.ARRAY is the designated array for the key word IN.FROM.BOARD.
\ We use 512 TEMPLATE.REPEAT to fill the whole array in one pass.
\ TRIGGER pulse waits for a sync. pulse to trigger once for each block
\ of 512 samples.

DASH16                              \ Using DAS-16F board
                                    \ One A/D channel number 3
3 3 A/D.TEMPLATE IN.FROM.BOARD
    A/D.INIT

:    DELAY
     5000 MSEC.DELAY                \ Define a delay period
;

 6 DIGITAL.TEMPLATE DIG.OUT  \ Define a template for digital I/O. Mode 6 means
   DIGITAL.INIT              \ write to digital ports 0 & 1; no reading allowed.
                             \ Initialise template (template name = DIG.OUT).
:    PULSE
     DIG.OUT
     0 DIGITAL.OUT       \ Output 0 and then all 1s to DIG.OUT
     255 DIGITAL.OUT     \ Provides positive trigger pulse for the stimulator
     DELAY               \ Wait for a while
     0 DIGITAL.OUT       \ Output 0 again, so that a square pulse is generated
;

:    INIT.EXT.TRIG      \ Data acquisition with external trigger
     IN.FROM.BOARD
     DATA.ARRAY TEMPLATE.BUFFER
     512 TEMPLATE.REPEAT
     EXT.TRIG
     A/D.INIT
```

```
    ONERR:
    DAS.INIT
    BELL CR ." Error initialising board, attempting reset"
    SCREEN.CLEAR MYSELF
;

:   INIT.INT.TRIG      \ Data acquisition with internal trigger
    IN.FROM.BOARD
    DATA.ARRAY TEMPLATE.BUFFER
    512 TEMPLATE.REPEAT
    INT.TRIG
    A/D.INIT
    ONERR:
    DAS.INIT
    BELL CR ." Error initialising board, attempting reset"
    SCREEN.CLEAR MYSELF
;

: INSTRUCTIONS.1
   SCREEN.CLEAR
   CR ." <F1> AVERAGE DATA                          <F2> INTERACT DATA          "
   CR ." <F3> READ DATA FROM DISK                   <F4> EXPAND DATA REGIONS    "
   CR ." <F5> PRINT-SCREEN DATA                     <F6> PLOTTER FOR COLOUR DATA"
   CR ." <F7> NEXT MENU                                                         "
;

: INSTRUCTIONS.2
   SCREEN.CLEAR
   CR ." <F8> AVERAGE FILTERED DATA ON-LINE              <F9> FFT DATA OFF-LINE"
   CR ." <F10> DIFFERENTIATE DATA OFF-LINE               <F5> PRINT-SCREEN DATA"
   CR ." <Alt F1> INTEGRATE DATA OFF-LINE                <Alt F2> EXIT TO DOS  "
   CR ." <Alt F7> MAIN MENU                                                     "
;

: INSTRUCTIONS.3
   SCREEN.CLEAR
   CR ." <Ctrl F1> EXTERNAL TRIGGER TO START ACQUISITION                        "
   CR ." <Ctrl F2> FREE RUN ACQUISITION MODE                                    "
   CR ." <Ctrl F3> GENERATE TRIGGER PULSE FOR ACQUISITION                       "
   CR ." <Alt F7>  MAIN MENU
;

: INSTRUCTIONS.4
   SCREEN.CLEAR
   CR ." <Ctrl F4> INTERACTIVE AVERAGING:  To perform averaging of conditioner"
   CR ." and test interacted complex followed by test only. The test signal is"
   CR ." subsequently taken off the complex to show the effect of conditioner."
   CR ." External trigger synchronises the operation.                          "
   CR ." <Alt F7>  MAIN MENU
;

: INSTRUCTIONS.5
   SCREEN.CLEAR
   CR ." <Ctrl F5> READ A WAVEFORM FROM DISK                                   "
```

```
    CR ." <Ctrl F6> READ SUPERIMPOSED (INTERACTED) DATA                    "
    CR ." <Ctrl F7> READ AVERAGED FILTERED DATA                            "
    CR ." <Alt F7>  MAIN MENU                                              "
;

: INSTRUCTIONS.6
    SCREEN.CLEAR
    CR ." <Ctrl F8> PEN-PLOT DATA                                          "
    CR ." <Ctrl F9> PEN-PLOT SUPERIMPOSED (INTERACTED) DATA                "
    CR ." <Alt F7>  MAIN MENU                                              "
;

: GET.NUMBER
   #INPUT
     IF
        DEFAULT.NUMBER :=
     THEN
;

: GET.GAIN.FACTOR
   #INPUT
     IF
        GAIN.FACTOR :=
     THEN
;

: GET.LVL.VOLTAGE
   #INPUT
     IF
        LVL.NUMBER :=
     THEN
;

: GET.UVL.VOLTAGE
   #INPUT
     IF
        UVL.NUMBER :=
     THEN
;

: GET.AVERAGE.NUMBER
   #INPUT
     IF
        AVERAGE.NUMBER :=
     THEN
;

: GET.FILTER.CUTOFF
   #INPUT
     IF
        FILTER.CUTOFF :=
     THEN
;
```

```
:    TIME.GENERATE
     513 1 DO
       DEFAULT.NUMBER I * TIME.AXIS [ I ] :=
     LOOP
;

:    FREQUENCY.GENERATE
     513 1 DO
        DEFAULT.NUMBER I / FREQ.AXIS [ I ] :=
     LOOP
;

:    SAVE.CONDITION.TEST
     FILE.TEMPLATE
     9 COMMENTS
     REAL  DIM[ 512 ] SUBFILE
     REAL  DIM[ 512 ] SUBFILE
     END
     SCREEN.CLEAR
     CR ." Name of file to create? "
     "INPUT FILENAME ":=
     CR ." Creating - " FILENAME "TYPE
     CR ." Comment on nature of interacted data: "
     "INPUT PRINT.COMMENT ":=
     CR ." Enter date and time: "
     "INPUT DATE.TIME ":=
     SCREEN.CLEAR
     CR ." Enter X-axis label: "
     "INPUT X-AXIS.LABEL ":=
     CR ." Enter Y-axis label: "
     "INPUT Y-AXIS.LABEL ":=
     CR ." Enter plot title: "
     "INPUT CHART.TITLE ":=
     FILENAME DEFER> FILE.CREATE   \ Create the specified file
     FILENAME DEFER> FILE.OPEN
     1 SUBFILE CONDITION.TEST ARRAY>FILE
     2 SUBFILE TIME.AXIS ARRAY>FILE
     LVL.NUMBER "." 1 >COMMENT
     UVL.NUMBER "." 2 >COMMENT
     PRINT.COMMENT 3 >COMMENT
     DATE.TIME 4 >COMMENT
     PRINT.AVERAGE.NUMBER "." 5 >COMMENT
     GAIN.FACTOR "." 6 >COMMENT
     X-AXIS.LABEL 7 >COMMENT
     Y-AXIS.LABEL 8 >COMMENT
     CHART.TITLE 9 >COMMENT
     FILE.CLOSE
     BELL
     LINE.BUFFER.OFF
     ONERR:
     BELL CR ." Can not save condition-test signal "
;

:    AVERAGE.TEST.ONLY
```

```
    SCREEN.CLEAR
    STACK.CLEAR
    0 AVERAGE :=
    0 COUNTER :=
    PRINT.AVERAGE.NUMBER AVERAGE.NUMBER :=
    LVL.NUMBER  UVL.NUMBER         VERTICAL    WORLD.SET
    0.          TIME.AXIS [ 512 ]  HORIZONTAL  WORLD.SET
    VUPORT.CLEAR
    XY.AXIS.PLOT
    PIXBUF LINE.BUFFER.ON
    BEGIN
       STACK.CLEAR
       COUNTER 1 + COUNTER :=
       AVERAGE.NUMBER 1 - AVERAGE.NUMBER :=
       SCREEN.CLEAR
       CR ."  WAITING FOR EXTERNAL TRIGGER"
       CR ."  AVERAGING DATA  -  PASS"  COUNTER .
       IN.FROM.BOARD
       A/D.INIT
       A/D.IN>ARRAY
       DATA.ARRAY 2048 -
       DUP LAST.ARRAY :=
       LAST.ARRAY AVERAGE + AVERAGE :=
       AVERAGE COUNTER / TEST.ONLY :=
       TEST.ONLY -10 10 A/D.SCALE
       ERASE.LINES
       TIME.AXIS TEST.ONLY -10 10 A/D.SCALE
       WORLD.COORDS
       11 COLOR
       CURSOR.OFF
       XY.DATA.PLOT
    AVERAGE.NUMBER 0. =
    UNTIL                       \ Loop again if not done
    NORMAL.COORDS
    .300 .960 POSITION                        " Averaged test data" LABEL
    .035 .350 POSITION 90 CHAR.DIR 90 LABEL.DIR    " Amplitude (V)" LABEL
    .400 .060 POSITION  0 CHAR.DIR  0 LABEL.DIR    " Duration (ms)" LABEL
    BELL
    LINE.BUFFER.OFF
    ONERR:
    DAS.INIT
    SCREEN.CLEAR
    ." Acquisition rate too fast for signal frequency, try slower rate."
    MYSELF
;

:   SAVE.TEST.ONLY
    FILE.TEMPLATE
    9 COMMENTS
    REAL  DIM[ 512 ] SUBFILE
    REAL  DIM[ 512 ] SUBFILE
    END
    SCREEN.CLEAR
    CR ." Name of file to create? "
```

```
    "INPUT FILENAME ":=
    CR ." Creating - " FILENAME "TYPE
    CR ." Comment on nature of test data: "
    "INPUT PRINT.COMMENT ":=
    CR ." Enter date and time: "
    "INPUT DATE.TIME ":=
    SCREEN.CLEAR
    CR ." Enter X-axis label: "
    "INPUT X-AXIS.LABEL ":=
    CR ." Enter Y-axis label: "
    "INPUT Y-AXIS.LABEL ":=
    CR ." Enter plot title: "
    "INPUT CHART.TITLE ":=
    FILENAME DEFER> FILE.CREATE   \ Create the specified file
    FILENAME DEFER> FILE.OPEN
    1 SUBFILE TEST.ONLY ARRAY>FILE
    2 SUBFILE TIME.AXIS ARRAY>FILE
    LVL.NUMBER "." 1 >COMMENT
    UVL.NUMBER "." 2 >COMMENT
    PRINT.COMMENT 3 >COMMENT
    DATE.TIME 4 >COMMENT
    PRINT.AVERAGE.NUMBER "." 5 >COMMENT
    GAIN.FACTOR "." 6 >COMMENT
    X-AXIS.LABEL 7 >COMMENT
    Y-AXIS.LABEL 8 >COMMENT
    CHART.TITLE 9 >COMMENT
    FILE.CLOSE
    BELL
    LINE.BUFFER.OFF
    ONERR:
    BELL CR ." Can not save data to disk "
;

:   SUBTRACT.CONDITION.TEST
    STACK.CLEAR
    PIXBUF LINE.BUFFER.ON
    SCREEN.CLEAR
    LVL.NUMBER  UVL.NUMBER         VERTICAL    WORLD.SET
    0.          TIME.AXIS [ 512 ]  HORIZONTAL  WORLD.SET
    VUPORT.CLEAR
    XY.AXIS.PLOT
    CR ."  SUBTRACTING TEST WAVEFORM FROM CONDITIONER-TEST COMPLEX AND "
    CR ."  PLOTTING THE DIFFERENCE "
    CONDITION.TEST TEST.ONLY - DIFFERENCE :=
    DIFFERENCE -10 10 A/D.SCALE
    ERASE.LINES
    11 COLOR
    CURSOR.OFF
    TIME.AXIS DIFFERENCE -10 10 A/D.SCALE XY.DATA.PLOT
    NORMAL.COORDS
    .300 .960 POSITION                            " Difference waveform" LABEL
    .035 .350 POSITION 90 CHAR.DIR 90 LABEL.DIR   " Amplitude (V)" LABEL
    .400 .060 position  0 CHAR.DIR  0 LABEL.DIR   " Duration (ms)" LABEL
    BELL
```

```
      LINE.BUFFER.OFF
      ONERR:
      BELL CR ." Can not produce difference waveform "
;

:     SAVE.DIFFERENCE
      FILE.TEMPLATE
      9 COMMENTS
      REAL  DIM[ 512 ] SUBFILE
      REAL  DIM[ 512 ] SUBFILE
      END
      SCREEN.CLEAR
      CR ." Name of file to create? "
      "INPUT FILENAME ":=
      CR ." Creating - " FILENAME "TYPE
      CR ." Comment on nature of resultant data: "
      "INPUT PRINT.COMMENT ":=
      CR ." Enter date and time: "
      "INPUT DATE.TIME ":=
      SCREEN.CLEAR
      CR ." Enter X-axis label: "
      "INPUT X-AXIS.LABEL ":=
      CR ." Enter Y-axis label: "
      "INPUT Y-AXIS.LABEL ":=
      CR ." Enter plot title: "
      "INPUT CHART.TITLE ":=
      FILENAME DEFER> FILE.CREATE   \ Create the specified file
      FILENAME DEFER> FILE.OPEN
      1 SUBFILE DIFFERENCE ARRAY>FILE
      2 SUBFILE TIME.AXIS ARRAY>FILE
      LVL.NUMBER "." 1 >COMMENT
      UVL.NUMBER "." 2 >COMMENT
      PRINT.COMMENT 3 >COMMENT
      DATE.TIME 4 >COMMENT
      PRINT.AVERAGE.NUMBER "." 5 >COMMENT
      GAIN.FACTOR "." 6 >COMMENT
      X-AXIS.LABEL 7 >COMMENT
      Y-AXIS.LABEL 8 >COMMENT
      CHART.TITLE 9 >COMMENT
      FILE.CLOSE
      BELL
      LINE.BUFFER.OFF
      ONERR:
      BELL CR ." Can not save difference waveform "
;

:     SAVE.SUPERIMPOSED.DATA
      FILE.TEMPLATE
      9 COMMENTS
      REAL  DIM[ 512 ] SUBFILE
      REAL  DIM[ 512 ] SUBFILE
      REAL  DIM[ 512 ] SUBFILE
      REAL  DIM[ 512 ] SUBFILE
      END
```

```
      SCREEN.CLEAR
      CR ." Name of file to create? "
      "INPUT FILENAME ":=
      CR ." Creating - " FILENAME "TYPE
      CR ." Comment on nature of superimposed data: "
      "INPUT PRINT.COMMENT ":=
      CR ." Enter date and time: "
      "INPUT DATE.TIME ":=
      SCREEN.CLEAR
      CR ." Enter X-axis label: "
      "INPUT X-AXIS.LABEL ":=
      CR ." Enter Y-axis label: "
      "INPUT Y-AXIS.LABEL ":=
      CR ." Enter plot title: "
      "INPUT CHART.TITLE ":=
      FILENAME DEFER> FILE.CREATE   \ Create the specified file
      FILENAME DEFER> FILE.OPEN
      1 SUBFILE CONDITION.TEST ARRAY>FILE
      2 SUBFILE TEST.ONLY ARRAY>FILE
      3 SUBFILE DIFFERENCE ARRAY>FILE
      4 SUBFILE TIME.AXIS ARRAY>FILE
      LVL.NUMBER "." 1 >COMMENT
      UVL.NUMBER "." 2 >COMMENT
      PRINT.COMMENT 3 >COMMENT
      DATE.TIME 4 >COMMENT
      PRINT.AVERAGE.NUMBER "." 5 >COMMENT
      GAIN.FACTOR "." 6 >COMMENT
      X-AXIS.LABEL 7 >COMMENT
      Y-AXIS.LABEL 8 >COMMENT
      CHART.TITLE 9 >COMMENT
      FILE.CLOSE
      BELL
      LINE.BUFFER.OFF
      ONERR:
      BELL CR ." Can not save superimposed waveforms "
;

:     READ.DATA.FILE
      STACK.CLEAR
      SCREEN.CLEAR
      CR ." Name of file to read? "
      "INPUT FILENAME ":=
      CR ." Reading - " FILENAME "TYPE
      FILENAME DEFER> FILE.OPEN
      1 SUBFILE LAST1.ARRAY FILE>ARRAY
      2 SUBFILE TIME1.AXIS FILE>ARRAY
      1 COMMENT> 20 "NUMBER LVL.NUMBER :=
      2 COMMENT> 20 "NUMBER UVL.NUMBER :=
      3 COMMENT> PRINT.COMMENT ":=
      4 COMMENT> DATE.TIME ":=
      5 comment> 20 "NUMBER PRINT.AVERAGE.NUMBER :=
      6 comment> 20 "NUMBER GAIN.FACTOR :=
      7 COMMENT> X-AXIS.LABEL ":=
      8 COMMENT> Y-AXIS.LABEL ":=
```

```
     9 COMMENT> CHART.TITLE ":=
     FILE.CLOSE
     SCREEN.CLEAR
     LVL.NUMBER  UVL.NUMBER          VERTICAL    WORLD.SET
     0.          TIME1.AXIS [ 512 ]  HORIZONTAL  WORLD.SET
     VUPORT.CLEAR
     XY.AXIS.PLOT
     ERASE.LINES
     LAST1.ARRAY -10 10 A/D.SCALE
     11 COLOR
     CURSOR.OFF
     TIME1.AXIS LAST1.ARRAY -10 10 A/D.SCALE XY.DATA.PLOT
     NORMAL.COORDS
     .300 .960 POSITION                              CHART.TITLE LABEL
     .035 .350 POSITION 90 CHAR.DIR 90 LABEL.DIR     Y-AXIS.LABEL LABEL
     .400 .060 POSITION  0 CHAR.DIR  0 LABEL.DIR     X-AXIS.LABEL LABEL
     SCREEN.CLEAR
CR ." Name of file: " FILENAME "TYPE  ."        Date and time: " DATE.TIME "TYPE
     CR ." Comment:  " PRINT.COMMENT "TYPE
     CR ." Number of averages: " PRINT.AVERAGE.NUMBER .
     CR ." Amplifier gain: " GAIN.FACTOR .
     CR ." Press <F5> Print data  or  <Alt F7> Return to Main menu.
     BELL
     LINE.BUFFER.OFF
     ONERR:
     BELL CR ." Can not recall data from disk "
;

:    READ.SUPERIMPOSED.DATA
     STACK.CLEAR
     SCREEN.CLEAR
     CR ." Name of file to read? "
     "INPUT FILENAME ":=
     CR ." Reading - " FILENAME "TYPE
     FILENAME DEFER> FILE.OPEN
     1 SUBFILE SUPERIMPOSED1.ARRAY FILE>ARRAY
     2 SUBFILE SUPERIMPOSED2.ARRAY FILE>ARRAY
     3 SUBFILE SUPERIMPOSED3.ARRAY FILE>ARRAY
     4 SUBFILE TIME1.AXIS FILE>ARRAY
     1 COMMENT> 20 "NUMBER LVL.NUMBER :=
     2 COMMENT> 20 "NUMBER UVL.NUMBER :=
     3 COMMENT> PRINT.COMMENT ":=
     4 COMMENT> DATE.TIME ":=
     5 comment> 20 "NUMBER PRINT.AVERAGE.NUMBER :=
     6 comment> 20 "NUMBER GAIN.FACTOR :=
     7 COMMENT> X-AXIS.LABEL ":=
     8 COMMENT> Y-AXIS.LABEL ":=
     9 COMMENT> CHART.TITLE ":=
     FILE.CLOSE
     SCREEN.CLEAR
     LVL.NUMBER  UVL.NUMBER          VERTICAL    WORLD.SET
     0.          TIME1.AXIS [ 512 ]  HORIZONTAL  WORLD.SET
     VUPORT.CLEAR
     XY.AXIS.PLOT
```

```
     ERASE.LINES
     SUPERIMPOSED1.ARRAY -10 10 A/D.SCALE
     11 COLOR
     CURSOR.OFF
     TIME1.AXIS SUPERIMPOSED1.ARRAY -10 10 A/D.SCALE XY.DATA.PLOT
     SUPERIMPOSED2.ARRAY -10 10 A/D.SCALE
     13 COLOR
     TIME1.AXIS SUPERIMPOSED2.ARRAY -10 10 A/D.SCALE XY.DATA.PLOT
     SUPERIMPOSED3.ARRAY -10 10 A/D.scale
     10 COLOR
     TIME1.AXIS SUPERIMPOSED3.ARRAY -10 10 A/D.SCALE XY.DATA.PLOT
     NORMAL.COORDS
     .200 .960 POSITION                              CHART.TITLE LABEL
     .035 .350 POSITION 90 CHAR.DIR 90 LABEL.DIR    Y-AXIS.LABEL LABEL
     .400 .060 POSITION  0 CHAR.DIR  0 LABEL.DIR    X-AXIS.LABEL LABEL
     SCREEN.CLEAR
CR ." Name of file: " FILENAME "TYPE  ."        Date and time: " DATE.TIME "TYPE
     CR ." Comment:  " PRINT.COMMENT "TYPE
     CR ." Number of averages: " PRINT.AVERAGE.NUMBER .
     CR ." Amplifier gain: " GAIN.FACTOR .
     CR ." Press <F5> Print data  or  <Alt F7> Return to Main menu.
     BELL
     LINE.BUFFER.OFF
     ONERR:
     BELL CR ." Can not recall superimposed data "
;

\ We will continuously display the collected DATA.ARRAY on the screen.
\ Parameters relating to data acquisition, such as timing delay and
\ sampling rate, are initialised once. A bell sound signifies the start
\ and end of acquisition process. DATA.ARRAY is reinitialised with each
\ pass of the acquisition loop.
\ N.B. THE ABOVE STATMENTS APPLY TO ALL DATA ACQUISITION SUB_ROUTINES
\      IN THE PROGRAMME.

:    DATA.AVERAGE.EXT.TRIG              \ Averaging data
     STACK.CLEAR                        \ with external trigger
     SCREEN.CLEAR
     0 AVERAGE :=
     0 COUNTER :=
     INIT.EXT.TRIG     \ Initialise board
     SCREEN.CLEAR
     ." Select the desired acquisition rate in msec (0.02 to 5.0) --> "
     0.5 DEFAULT.NUMBER :=
     GET.NUMBER                       \ Get timing delay
     DEFAULT.NUMBER
     CONVERSION.DELAY    \ Set sampling rate
     TIME.GENERATE
     SCREEN.CLEAR
     CR ." Enter amplifier gain --> "
     20000 GAIN.FACTOR :=
     GET.GAIN.FACTOR
     GAIN.FACTOR
     CR ." Enter lower voltage limit in Volts (-0.1 to -5) --> "
```

```
-1 LVL.NUMBER :=
GET.LVL.VOLTAGE
LVL.NUMBER
CR ." Enter upper voltage limit in Volts (0.1 to 5) --> "
1 UVL.NUMBER :=
GET.UVL.VOLTAGE
UVL.NUMBER
CR ." Enter number of times you wish to average --> "
20 AVERAGE.NUMBER :=
GET.AVERAGE.NUMBER
AVERAGE.NUMBER
AVERAGE.NUMBER PRINT.AVERAGE.NUMBER :=
A/D.INIT
LVL.NUMBER  UVL.NUMBER         VERTICAL    WORLD.SET
0.          TIME.AXIS [ 512 ]  HORIZONTAL  WORLD.SET
VUPORT.CLEAR
XY.AXIS.PLOT
PIXBUF LINE.BUFFER.ON                \ Set up auto erase
BEGIN
   STACK.CLEAR                               \ Enter loop and
   COUNTER 1 + COUNTER :=                    \ Reset buffer index
   AVERAGE.NUMBER 1 - AVERAGE.NUMBER :=      \ with each pass of
   SCREEN.CLEAR                              \ the loop.
   CR ."  WAITING FOR EXTERNAL TRIGGER"
   CR ."  AVERAGING DATA  -  PASS"  COUNTER .
   IN.FROM.BOARD
   A/D.INIT
   A/D.IN>ARRAY
   DATA.ARRAY 2048 -
   DUP LAST.ARRAY :=
   LAST.ARRAY AVERAGE + AVERAGE :=
   AVERAGE COUNTER / TEST.ONLY :=
   TEST.ONLY -10 10 A/D.SCALE
   ERASE.LINES                               \ Erase previous data
   TIME.AXIS TEST.ONLY -10 10 A/D.SCALE
   WORLD.COORDS
   11 COLOR
   CURSOR.OFF
   XY.DATA.PLOT
AVERAGE.NUMBER 0. =
UNTIL                        \ Loop again if not done
NORMAL.COORDS
.300 .960 POSITION                                  " Averaged data" LABEL
.035 .350 POSITION 90 CHAR.DIR 90 LABEL.DIR         " Amplitude (V)" LABEL
.400 .060 POSITION  0 CHAR.DIR  0 LABEL.DIR         " Duration (ms)" LABEL
BELL
SAVE.TEST.ONLY
SCREEN.CLEAR
INSTRUCTIONS.1
LINE.BUFFER.OFF
ONERR:
DAS.INIT
SCREEN.CLEAR
." Acquisition rate too fast for signal frequency, try slower rate."
```

```
    MYSELF
;

:   DATA.AVERAGE.INT.TRIG            \ Averaging data
    STACK.CLEAR                      \ with internal trigger
    SCREEN.CLEAR
    0 AVERAGE :=
    0 COUNTER :=
    INIT.INT.TRIG     \ Initialise board
    SCREEN.CLEAR
    ." Select the desired acquisition rate in msec (0.02 to 5.0) --> "
    0.5 DEFAULT.NUMBER :=
    GET.NUMBER
    DEFAULT.NUMBER
    CONVERSION.DELAY    \ Set sampling rate
    TIME.GENERATE
    SCREEN.CLEAR
    CR ." Enter amplifier gain --> "
    20000 GAIN.FACTOR :=
    GET.GAIN.FACTOR
    GAIN.FACTOR
    CR ." Enter lower voltage limit in Volts (-0.1 to -5) --> "
    -1 LVL.NUMBER :=
    GET.LVL.VOLTAGE
    LVL.NUMBER
    CR ." Enter upper voltage limit in Volts (0.1 to 5) --> "
    1 UVL.NUMBER :=
    GET.UVL.VOLTAGE
    UVL.NUMBER
    CR ." Enter number of times you wish to average --> "
    20 AVERAGE.NUMBER :=
    GET.AVERAGE.NUMBER
    AVERAGE.NUMBER
    AVERAGE.NUMBER PRINT.AVERAGE.NUMBER :=
    A/D.INIT
    LVL.NUMBER  UVL.NUMBER         VERTICAL    WORLD.SET
    0.          TIME.AXIS [ 512 ]  HORIZONTAL  WORLD.SET
    VUPORT.CLEAR
    XY.AXIS.PLOT
    PIXBUF LINE.BUFFER.ON
    BEGIN
       STACK.CLEAR
       COUNTER 1 + COUNTER :=
       AVERAGE.NUMBER 1 - AVERAGE.NUMBER :=
       SCREEN.CLEAR
       CR ."  WAITING FOR INTERNAL TRIGGER"
       CR ."  AVERAGING DATA  -  PASS"  COUNTER .
       IN.FROM.BOARD
       A/D.INIT
       A/D.IN>ARRAY
       DATA.ARRAY 2048 -
       DUP LAST.ARRAY :=
       LAST.ARRAY AVERAGE + AVERAGE :=
       AVERAGE COUNTER / TEST.ONLY :=
```

```
        TEST.ONLY -10 10 A/D.SCALE
        ERASE.LINES
        TIME.AXIS TEST.ONLY -10 10 A/D.SCALE
        WORLD.COORDS
        11 COLOR
        CURSOR.OFF
        XY.DATA.PLOT
     AVERAGE.NUMBER 0. =
     UNTIL                        \ Loop again if not done
     NORMAL.COORDS
     .300 .960 POSITION                              " Averaged data" LABEL
     .035 .350 POSITION 90 CHAR.DIR 90 LABEL.DIR     " Amplitude (V)" LABEL
     .400 .060 POSITION  0 CHAR.DIR  0 LABEL.DIR     " Duration (ms)" LABEL
     BELL
     SAVE.TEST.ONLY
     SCREEN.CLEAR
     INSTRUCTIONS.1
     LINE.BUFFER.OFF
     ONERR:
     DAS.INIT
     SCREEN.CLEAR
     ." Acquisition rate too fast for signal frequency, try slower rate."
     MYSELF
;

:    DATA.AVERAGE.PULSE.TRIG          \ Averaging data
     STACK.CLEAR                      \ with computer generated pulse
     SCREEN.CLEAR
     0 AVERAGE :=
     0 COUNTER :=
     INIT.INT.TRIG
     SCREEN.CLEAR
     ." Select the desired acquisition rate in msec (0.02 to 5.0) --> "
     0.5 DEFAULT.NUMBER :=
     GET.NUMBER
     DEFAULT.NUMBER
     CONVERSION.DELAY     \ Set sampling rate
     TIME.GENERATE
     SCREEN.CLEAR
     CR ." ENTER AMPLIFIER GAIN -->"
     20000 GAIN.FACTOR :=
     GET.GAIN.FACTOR
     GAIN.FACTOR
     CR ." Enter lower voltage limit in Volts (-0.1 to -5) --> "
     -1 LVL.NUMBER :=
     GET.LVL.VOLTAGE
     LVL.NUMBER
     CR ." Enter upper voltage limit in Volts (0.1 to 5) --> "
     1 UVL.NUMBER :=
     GET.UVL.VOLTAGE
     UVL.NUMBER
     CR ." Enter number of times you wish to average --> "
     20 AVERAGE.NUMBER :=
     GET.AVERAGE.NUMBER
```

```
      AVERAGE.NUMBER
      AVERAGE.NUMBER PRINT.AVERAGE.NUMBER :=
      A/D.INIT
      LVL.NUMBER  UVL.NUMBER         VERTICAL    WORLD.SET
      0.          TIME.AXIS [ 512 ]  HORIZONTAL  WORLD.SET
      VUPORT.CLEAR
      XY.AXIS.PLOT
      PIXBUF LINE.BUFFER.ON
      BEGIN
         STACK.CLEAR
         COUNTER 1 + COUNTER :=
         AVERAGE.NUMBER 1 - AVERAGE.NUMBER :=
         SCREEN.CLEAR
         CR ."  WAITING FOR A TRIGGER PULSE TO BE GENERATED "
         CR ."  AVERAGING DATA  -  PASS"  COUNTER .
         IN.FROM.BOARD
         A/D.INIT
         PULSE
         A/D.IN>ARRAY
         DATA.ARRAY 2048 -
         DUP LAST.ARRAY :=
         LAST.ARRAY AVERAGE + AVERAGE :=
         AVERAGE COUNTER / TEST.ONLY :=
         TEST.ONLY -10 10 A/D.SCALE
         ERASE.LINES
         TIME.AXIS TEST.ONLY -10 10 A/D.SCALE
         WORLD.COORDS
         11 COLOR
         CURSOR.OFF
         XY.DATA.PLOT
      AVERAGE.NUMBER 0. =
      UNTIL                       \ Loop again if not done
      NORMAL.COORDS
      .300 .960 POSITION                            " Averaged data" LABEL
      .035 .350 POSITION 90 CHAR.DIR 90 LABEL.DIR   " Amplitude (V)" LABEL
      .400 .060 POSITION  0 CHAR.DIR  0 LABEL.DIR   " Duration (ms)" LABEL
      BELL
      SAVE.TEST.ONLY
      SCREEN.CLEAR
      INSTRUCTIONS.1
      LINE.BUFFER.OFF
      ONERR:
      DAS.INIT
      SCREEN.CLEAR
      ." Acquisition rate too fast for signal frequency, try slower rate."
      MYSELF
;

:     INTERACT.DATA.EXT.TRIG          \ Averaging and subtracting data
      STACK.CLEAR                     \ with external trigger
      0 AVERAGE :=
      0 COUNTER :=
      INIT.EXT.TRIG     \ Initialise board
      SCREEN.CLEAR
```

```
    ." Select the desired acquisition rate in msec (0.02-5.0) --> "
    0.5 DEFAULT.NUMBER :=
    GET.NUMBER
    DEFAULT.NUMBER
    CONVERSION.DELAY     \ Set sampling rate
    TIME.GENERATE
    SCREEN.CLEAR
    CR ." Enter amplifier gain --> "
    20000 GAIN.FACTOR :=
    GET.GAIN.FACTOR
    GAIN.FACTOR
    CR ." Enter lower voltage limit in Volts (-0.1 TO -5) --> "
    -1 LVL.NUMBER :=
    GET.LVL.VOLTAGE
    LVL.NUMBER
    CR ." Enter upper voltage limit in Volts (0.1 TO 5) --> "
    1 UVL.NUMBER :=
    GET.UVL.VOLTAGE
    UVL.NUMBER
    CR ." Enter number of times you wish to average --> "
    20 AVERAGE.NUMBER :=
    GET.AVERAGE.NUMBER
    AVERAGE.NUMBER
    AVERAGE.NUMBER PRINT.AVERAGE.NUMBER :=
    A/D.INIT
    LVL.NUMBER  UVL.NUMBER         VERTICAL    WORLD.SET
    0.          TIME.AXIS [ 512 ]  HORIZONTAL  WORLD.SET
    VUPORT.CLEAR
    XY.AXIS.PLOT
    PIXBUF LINE.BUFFER.ON
    BEGIN
       STACK.CLEAR
       COUNTER 1 + COUNTER :=
       AVERAGE.NUMBER 1 - AVERAGE.NUMBER :=
       SCREEN.CLEAR
       CR ."  WAITING FOR EXTERNAL TRIGGER "
       CR ."  AVERAGING DATA  -  PASS"  COUNTER .
       IN.FROM.BOARD
       A/D.INIT
       A/D.IN>ARRAY
       DATA.ARRAY 2048 -
       DUP LAST.ARRAY :=
       LAST.ARRAY AVERAGE + AVERAGE :=
       AVERAGE COUNTER / CONDITION.TEST :=
       CONDITION.TEST -10 10 A/D.SCALE
       ERASE.LINES
       TIME.AXIS CONDITION.TEST -10 10 A/D.SCALE
       WORLD.COORDS
       11 COLOR
       CURSOR.OFF
       XY.DATA.PLOT
    AVERAGE.NUMBER 0. =
    UNTIL                          \ Loop again if not done
    NORMAL.COORDS
```

```
    .300 .960 POSITION            " Averaged Conditioner-Test data" LABEL
    .035 .350 POSITION 90 CHAR.DIR 90 LABEL.DIR    " Amplitude (V)" LABEL
    .400 .060 POSITION  0 CHAR.DIR  0 LABEL.DIR    " Duration (ms)" LABEL
    BELL
    SAVE.CONDITION.TEST
    AVERAGE.TEST.ONLY
    SAVE.TEST.ONLY
    SUBTRACT.CONDITION.TEST
    SAVE.DIFFERENCE
    SCREEN.CLEAR
    LVL.NUMBER  UVL.NUMBER         VERTICAL    WORLD.SET
    0.          TIME.AXIS [ 512 ]  HORIZONTAL  WORLD.SET
    VUPORT.CLEAR
    XY.AXIS.PLOT
    CONDITION.TEST -10 10 A/D.SCALE
    ERASE.LINES
    11 COLOR
    CURSOR.OFF
    TIME.AXIS CONDITION.TEST -10 10 A/D.SCALE XY.DATA.PLOT
    TEST.ONLY -10 10 A/D.SCALE
    13 COLOR
    TIME.AXIS TEST.ONLY -10 10 A/D.SCALE XY.DATA.PLOT
    DIFFERENCE -10 10 A/D.SCALE
    10 COLOR
    TIME.AXIS DIFFERENCE -10 10 A/D.SCALE XY.DATA.PLOT
    NORMAL.COORDS
    .200 .960 POSITION " Conditioner-Test, Test, Difference superimposed" LABEL
    .035 .350 POSITION 90 CHAR.DIR 90 LABEL.DIR    " Amplitude (V)" LABEL
    .400 .060 POSITION  0 CHAR.DIR  0 LABEL.DIR    " Duration (ms)" LABEL
    SAVE.SUPERIMPOSED.DATA
    BELL
    INSTRUCTIONS.1
    LINE.BUFFER.OFF
    ONERR:
    DAS.INIT
    SCREEN.CLEAR
    ." Acquisition rate too fast for signal frequency, try slower rate."
    MYSELF
;

:   PRINT.SCREEN.DATA
    STACK.CLEAR
    SCREEN.PRINT
    LINE.BUFFER.OFF
    ONERR:
    SCREEN.CLEAR
    ." Make sure printer is on line"
    MYSELF
    INSTRUCTIONS.1
    BELL
;

LOAD EPDAAP1.WHL
```

```
20 0 24 79 WINDOW {BOT}          \ Define graphics window

: GO
    STACK.CLEAR
    SCREEN.CLEAR
    GRAPHICS.DISPLAY
    VUPORT.CLEAR
    18 GRAPHICS.DISPLAY.MODE
    14 SCREEN.COLOR
    SCREEN.CLEAR
    {BOT}
    COLOUR.DISPLAY
    DEVICE.INIT
    0 VUPORT.COLOR VUPORT.CLEAR
    LABEL.COLOR 12
    AXIS.COLOR 5
    CURSOR.COLOR 5

    INSTRUCTIONS.1

    \ Function key definition

    F1 FUNCTION.KEY.DOES INSTRUCTIONS.3
    F2 FUNCTION.KEY.DOES INSTRUCTIONS.4
    F3 FUNCTION.KEY.DOES INSTRUCTIONS.5
    F4 FUNCTION.KEY.DOES EXPAND.DATA.REGIONS
    F5 FUNCTION.KEY.DOES PRINT.SCREEN.DATA
    F6 FUNCTION.KEY.DOES INSTRUCTIONS.6
    F7 FUNCTION.KEY.DOES INSTRUCTIONS.2
    F8 FUNCTION.KEY.DOES AVERAGE.FILTER.DATA
    F9 FUNCTION.KEY.DOES FOURIER.TRANSFORM.DATA
    F10 FUNCTION.KEY.DOES DIFFERENTIATE.DATA
    \ Alt function key definition

    F1 ALT FUNCTION.KEY.DOES INTEGRATE.DATA
    F2 ALT FUNCTION.KEY.DOES BYE
    F7 ALT FUNCTION.KEY.DOES INSTRUCTIONS.1

    \ Ctrl function key definition

    F1 CTRL FUNCTION.KEY.DOES DATA.AVERAGE.EXT.TRIG
    F2 CTRL FUNCTION.KEY.DOES DATA.AVERAGE.INT.TRIG
    F3 CTRL FUNCTION.KEY.DOES DATA.AVERAGE.PULSE.TRIG
    F4 CTRL FUNCTION.KEY.DOES INTERACT.DATA.EXT.TRIG
    F5 CTRL FUNCTION.KEY.DOES READ.DATA.FILE
    F6 CTRL FUNCTION.KEY.DOES READ.SUPERIMPOSED.DATA
    F7 CTRL FUNCTION.KEY.DOES READ.AVERAGED.FILTERED.DATA
    F8 CTRL FUNCTION.KEY.DOES PEN.PLOT.DATA
    F9 CTRL FUNCTION.KEY.DOES PEN.PLOT.SUPERIMPOSED.DATA

    INTERPRET.KEYS               \ Infinite loop to scan function keys
    ONERR:
    SCREEN.CLEAR BELL
    CR ." Unknown Error: Type Ctrl/Break to Restart"
```

```
    CR ." or another key to Exit"
    KEY BYE
;

BELL BELL BELL
CR ." Type GO to start data acquisition and analysis "
```

```
\
\ ***** ElectroPhysiological Data Acquisition and Analysis System *****
\ *                                                                   *
\ *       This is a sub-section of the main program EPDAAP.WHL,       *
\ *              compiled by Ahmad Hashemi-Sakhtsari,                 *
\ *                      on 13th June 1991                            *
\ *                                                                   *
\ *********************************************************************

: EXPAND.DATA.REGIONS
    SCREEN.CLEAR
    BELL
    ." Keypad cursors will move the position of selection lines. HOME key"
    CR
    ." indicates position, and INS key expands the graph. PG UP proceeded by"
    CR
    ." a number sets the arrow key step size for distance increment of lines."
    CR
    ." END or PG DN key fixes the left or right selection line."
    CR
    ." DEL key halts this option. Press any key to continue."

    ARRAY.READOUT                    \ Enable vertical lines.
    NORMAL.COORDS                    \ Switch to normalized coordinates.
    .70 .98 READOUT>POSITION         \ Set position of readout.
    WORLD.COORDS                     \ Return to world coordinates.
    BEGIN                            \ Wait for any key to be pressed.
     ?KEY
    UNTIL
    SCREEN.CLEAR                    \ Relpace above instructions
    INSTRUCTIONS.1                  \ With default instructions.
    BELL
    ONERR:
    BELL CR ." Can't expand data regions "
;

:  SAVE.AVERAGED.FILTERED.DATA
     FILE.TEMPLATE
     10 COMMENTS
     REAL  DIM[ 512 ] SUBFILE
     REAL  DIM[ 512 ] SUBFILE
     END
     SCREEN.CLEAR
     CR ." Name of file to create? "
     "INPUT FILENAME ":=
     CR ." Creating - " FILENAME "TYPE
     CR ." Comment on nature of filtered data: "
     "INPUT PRINT.COMMENT ":=
     CR ." Enter date and time: "
     "INPUT DATE.TIME ":=
     SCREEN.CLEAR
     CR ." Enter X-axis label: "
     "INPUT X-AXIS.LABEL ":=
     CR ." Enter Y-axis label: "
```

```
    "INPUT Y-AXIS.LABEL ":=
    CR ." Enter plot title: "
    "INPUT CHART.TITLE ":=
    FILENAME DEFER> FILE.CREATE   \ Create the specified file
    FILENAME DEFER> FILE.OPEN
    1 SUBFILE AVERAGED.FILTERED.ARRAY ARRAY>FILE
    2 SUBFILE TIME.AXIS ARRAY>FILE
    LVL.NUMBER "." 1 >COMMENT
    UVL.NUMBER "." 2 >COMMENT
    PRINT.COMMENT 3 >COMMENT
    DATE.TIME 4 >COMMENT
    PRINT.AVERAGE.NUMBER "." 5 >COMMENT
    GAIN.FACTOR "." 6 >COMMENT
    X-AXIS.LABEL 7 >COMMENT
    Y-AXIS.LABEL 8 >COMMENT
    CHART.TITLE 9 >COMMENT
    FILTER.CUTOFF "." 10 >COMMENT
    FILE.CLOSE
    BELL
    LINE.BUFFER.OFF
    ONERR:
    BELL CR ." Can not save averaged filtered data "
;

: READ.AVERAGED.FILTERED.DATA
    STACK.CLEAR
    SCREEN.CLEAR
    CR ." Name of file to read? "
    "INPUT FILENAME ":=
    CR ." Reading - " FILENAME "TYPE
    FILENAME DEFER> FILE.OPEN
    1 SUBFILE LAST1.ARRAY FILE>ARRAY
    2 SUBFILE TIME1.AXIS FILE>ARRAY
    1 COMMENT> 20 "NUMBER LVL.NUMBER :=
    2 COMMENT> 20 "NUMBER UVL.NUMBER :=
    3 COMMENT> PRINT.COMMENT ":=
    4 COMMENT> DATE.TIME ":=
    5 comment> 20 "NUMBER PRINT.AVERAGE.NUMBER :=
    6 comment> 20 "NUMBER GAIN.FACTOR :=
    7 COMMENT> X-AXIS.LABEL ":=
    8 COMMENT> Y-AXIS.LABEL ":=
    9 COMMENT> CHART.TITLE ":=
    10 COMMENT> 20 "NUMBER FILTER.CUTOFF :=
    FILE.CLOSE
    SCREEN.CLEAR
    LVL.NUMBER  UVL.NUMBER          VERTICAL    WORLD.SET
    0.          TIME1.AXIS [ 512 ]  HORIZONTAL  WORLD.SET
    VUPORT.CLEAR
    XY.AXIS.PLOT
    LAST1.ARRAY -10 10 A/D.SCALE
    ERASE.LINES
    11 COLOR
    CURSOR.OFF
    TIME1.AXIS LAST1.ARRAY -10 10 A/D.SCALE XY.DATA.PLOT
```

```
     NORMAL.COORDS
     .300 .960 POSITION                                CHART.TITLE LABEL
     .035 .350 POSITION 90 CHAR.DIR 90 LABEL.DIR    Y-AXIS.LABEL LABEL
     .400 .060 POSITION  0 CHAR.DIR  0 LABEL.DIR    X-AXIS.LABEL LABEL
     SCREEN.CLEAR
CR ." Name of file: " FILENAME "TYPE ."         Date and time: " DATE.TIME "TYPE
     CR ." Comment: " PRINT.COMMENT "TYPE
     CR ." Number of averages: " PRINT.AVERAGE.NUMBER .
CR ." Amplifier gain: " GAIN.FACTOR . ."       Filter cut-off: " FILTER.CUTOFF .
     CR ." Press <F5> Print data  or  <Alt F7> Return to Main menu.
     BELL
     LINE.BUFFER.OFF
     ONERR:
     BELL CR ." Can not recall averaged filtered data "
;

: AVERAGE.FILTER.DATA
     STACK.CLEAR                        \ with external trigger
     SCREEN.CLEAR
     0 AVERAGE :=
     0 COUNTER :=
     INIT.EXT.TRIG     \ Initialise board
     SCREEN.CLEAR
     ." Select the desired acquisition rate in msec (0.02 to 5.0) --> "
     0.5 DEFAULT.NUMBER :=
     GET.NUMBER
     DEFAULT.NUMBER
     CONVERSION.DELAY    \ Set sampling rate
     TIME.GENERATE
     CR
." Select filtering cutoff frequency in cycles/data point (0.08 to 0.5)--> "
     0.1 FILTER.CUTOFF :=
     GET.FILTER.CUTOFF
     FILTER.CUTOFF
     SCREEN.CLEAR
     CR ." Enter amplifier gain --> "
     20000 GAIN.FACTOR :=
     GET.GAIN.FACTOR
     GAIN.FACTOR
     CR ." Enter lower voltage limit in Volts (-0.1 to -5) --> "
     -1 LVL.NUMBER :=
     GET.LVL.VOLTAGE
     LVL.NUMBER
     CR ." Enter upper voltage limit in Volts (0.1 to 5) --> "
     1 UVL.NUMBER :=
     GET.UVL.VOLTAGE
     UVL.NUMBER
     CR ." Enter number of times you wish to average --> "
     20 AVERAGE.NUMBER :=
     GET.AVERAGE.NUMBER
     AVERAGE.NUMBER
     AVERAGE.NUMBER PRINT.AVERAGE.NUMBER :=
     A/D.INIT
     LVL.NUMBER  UVL.NUMBER         VERTICAL    WORLD.SET
```

```
    0.          TIME.AXIS [ 512 ]  HORIZONTAL  WORLD.SET
    VUPORT.CLEAR
    XY.AXIS.PLOT
    PIXBUF LINE.BUFFER.ON
    BEGIN
       STACK.CLEAR
       COUNTER 1 + COUNTER :=
       AVERAGE.NUMBER 1 - AVERAGE.NUMBER :=
       SCREEN.CLEAR
       CR ."  LOW-PASS FILTER'S CUT-OFF FREQUENCY IS"  FILTER.CUTOFF .
       CR ."  WAITING FOR EXTERNAL TRIGGER"
       CR ."  AVERAGING FILTERED DATA  -  PASS"  COUNTER .
       IN.FROM.BOARD
       A/D.INIT
       A/D.IN>ARRAY
       DATA.ARRAY 2048 -
       FILTER.CUTOFF SET.CUTOFF.FREQ          \ Set smoothing cutoff width
       SMOOTH                                 \ Smooth array in place
       DUP SMOOTH.ARRAY :=
       SMOOTH.ARRAY AVERAGE + AVERAGE :=
       AVERAGE COUNTER / AVERAGED.FILTERED.ARRAY :=
       AVERAGED.FILTERED.ARRAY -10 10 A/D.SCALE
       ERASE.LINES
       TIME.AXIS AVERAGED.FILTERED.ARRAY -10 10 A/D.SCALE
       WORLD.COORDS
       11 COLOR
       CURSOR.OFF
       XY.DATA.PLOT
    AVERAGE.NUMBER 0. =
    UNTIL                       \ Loop again if not done
    NORMAL.COORDS
    .300 .960 POSITION                    " Averaged filtered data" LABEL
    .035 .350 POSITION 90 CHAR.DIR 90 LABEL.DIR    " Amplitude (V)" LABEL
    .400 .060 POSITION  0 CHAR.DIR  0 LABEL.DIR    " Duration (ms)" LABEL
    BELL
    SAVE.AVERAGED.FILTERED.DATA
    SCREEN.CLEAR
    INSTRUCTIONS.1
    LINE.BUFFER.OFF
    ONERR:
    DAS.INIT
    SCREEN.CLEAR
    ." Acquisition rate too fast for signal frequency, try slower rate."
    ." OR "
    ." Cutoff frequency too narrow, try again "
    MYSELF
;

: DIFFERENTIATE.DATA
   STACK.CLEAR
   SCREEN.CLEAR
   CR ." Name of file to differentiate? "
   "INPUT FILENAME ":=
   CR ." Reading - " FILENAME "TYPE
```

```
    FILENAME DEFER> FILE.OPEN
    1 SUBFILE LAST1.ARRAY FILE>ARRAY
    2 SUBFILE TIME1.AXIS FILE>ARRAY
    1 COMMENT> 20 "NUMBER LVL.NUMBER :=
    2 COMMENT> 20 "NUMBER UVL.NUMBER :=
    3 COMMENT> PRINT.COMMENT ":=
    4 COMMENT> DATE.TIME ":=
    5 COMMENT> 20 "NUMBER PRINT.AVERAGE.NUMBER :=
    6 COMMENT> 20 "NUMBER GAIN.FACTOR :=
    7 COMMENT> X-AXIS.LABEL ":=
    8 COMMENT> Y-AXIS.LABEL ":=
    9 COMMENT> CHART.TITLE ":=
    FILE.CLOSE
    SCREEN.CLEAR
    LVL.NUMBER UVL.NUMBER         VERTICAL   WORLD.SET
    0.         TIME1.AXIS [ 512 ] HORIZONTAL WORLD.SET
    VUPORT.CLEAR
    XY.AXIS.PLOT
    LAST1.ARRAY -10 10 A/D.SCALE
    ERASE.LINES
    11 COLOR
    CURSOR.OFF
    TIME1.AXIS LAST1.ARRAY -10 10 A/D.SCALE XY.DATA.PLOT
    NORMAL.COORDS
    .300 .960 POSITION                              CHART.TITLE  LABEL
    .035 .300 POSITION 90 CHAR.DIR 90 LABEL.DIR     Y-AXIS.LABEL LABEL
    .400 .060 POSITION  0 CHAR.DIR  0 LABEL.DIR     X-AXIS.LABEL LABEL
    SCREEN.CLEAR
CR ." Name of file: " FILENAME "TYPE  ."        Date and time: " DATE.TIME "TYPE
    CR ." Comment:  " PRINT.COMMENT "TYPE
    cr ." Number of averages: " PRINT.AVERAGE.NUMBER .
    cr ." Amplifier gain: " GAIN.FACTOR .
CR ." DIFFERENTIATED DATA WILL BE DISPLAYED IN 3 SECONDS "
    3000 MSEC.DELAY
    BELL
    STACK.CLEAR
    SCREEN.CLEAR
    VUPORT.CLEAR
    LAST1.ARRAY 2048 -
    DUP                          \ copy the array
    1 SET.ORDER
    2 SET.DEGREE
    DIFFERENTIATE.DATA            \ Differentiate copy of data
    DUP DIFFERENTIATE.ARRAY :=
    DIFFERENTIATE.ARRAY -10 10 A/D.SCALE
    ERASE.LINES
    11 COLOR
    TIME1.AXIS DIFFERENTIATE.ARRAY -10 10 A/D.SCALE XY.AUTO.PLOT
    NORMAL.COORDS
    .300 .960 POSITION                          " Differentiated waveform" LABEL
.035 .150 POSITION 90 CHAR.DIR 90 LABEL.DIR " Amplitude (V)/Duration (ms)" LABEL
    .400 .060 POSITION  0 CHAR.DIR  0 LABEL.DIR           " Duration (ms)" LABEL
    SCREEN.CLEAR
    CR ." <F5> PRINT-SCREEN DATA "
```

```
    CR ." <Alt F7> MAIN MENU "
    BELL
    ONERR:
    BELL CR ." Can't differentiate data "
;

: INTEGRATE.DATA
    STACK.CLEAR
    SCREEN.CLEAR
    CR ." Name of file to integrate? "
    "INPUT FILENAME ":=
    CR ." Reading - " FILENAME "TYPE
    FILENAME DEFER> FILE.OPEN
    1 SUBFILE LAST1.ARRAY FILE>ARRAY
    2 SUBFILE TIME1.AXIS FILE>ARRAY
    1 COMMENT> 20 "NUMBER LVL.NUMBER :=
    2 COMMENT> 20 "NUMBER UVL.NUMBER :=
    3 COMMENT> PRINT.COMMENT ":=
    4 COMMENT> DATE.TIME ":=
    5 COMMENT> 20 "NUMBER PRINT.AVERAGE.NUMBER :=
    6 COMMENT> 20 "NUMBER GAIN.FACTOR :=
    7 COMMENT> X-AXIS.LABEL ":=
    8 COMMENT> Y-AXIS.LABEL ":=
    9 COMMENT> CHART.TITLE ":=
    FILE.CLOSE
    SCREEN.CLEAR
    LVL.NUMBER UVL.NUMBER         VERTICAL   WORLD.SET
    0.         TIME1.AXIS [ 512 ] HORIZONTAL WORLD.SET
    VUPORT.CLEAR
    XY.AXIS.PLOT
    LAST1.ARRAY -10 10 A/D.SCALE
    ERASE.LINES
    11 COLOR
    CURSOR.OFF
    TIME1.AXIS LAST1.ARRAY -10 10 A/D.SCALE XY.DATA.PLOT
    NORMAL.COORDS
    .300 .960 POSITION                              CHART.TITLE  LABEL
    .035 .350 POSITION 90 CHAR.DIR 90 LABEL.DIR     Y-AXIS.LABEL LABEL
    .400 .060 POSITION  0 CHAR.DIR  0 LABEL.DIR     X-AXIS.LABEL LABEL
    SCREEN.CLEAR
CR ." Name of file: " FILENAME "TYPE  ."        Date and time: " DATE.TIME "TYPE
    CR ." Comment:  " PRINT.COMMENT "TYPE
    cr ." Number of averages: " PRINT.AVERAGE.NUMBER .
    cr ." Amplifier gain: " GAIN.FACTOR .
CR ." INTEGRATED DATA WILL BE DISPLAYED IN 3 SECONDS "
    3000 MSEC.DELAY
    BELL
    STACK.CLEAR
    SCREEN.CLEAR
    VUPORT.CLEAR
    LAST1.ARRAY 2048 -
    DUP                          \ Copy the array
    INTEGRATE.DATA               \ Integrate the copy of data
    DUP INTEGRATE.ARRAY :=
```

```
    INTEGRATE.ARRAY -10 10 A/D.SCALE
    ERASE.LINES
    11 COLOR
    TIME1.AXIS INTEGRATE.ARRAY -10 10 A/D.SCALE XY.AUTO.PLOT
    NORMAL.COORDS
    .300 .960 POSITION                                " Integrated waveform" LABEL
    .035 .350 POSITION 90 CHAR.DIR 90 LABEL.DIR      " Running integral" LABEL
    .400 .060 POSITION  0 CHAR.DIR  0 LABEL.DIR      " Duration (ms)" LABEL
    SCREEN.CLEAR
    CR ." <F5> PRINT-SCREEN DATA "
    CR ." <Alt F7> MAIN MENU "
    BELL
    ONERR:
    BELL CR ." Can't integrate data "
;

: FOURIER.TRANSFORM.DATA
    STACK.CLEAR
    SCREEN.CLEAR
    CR ." Name of file to transform? "
    "INPUT FILENAME ":=
    CR ." Reading - " FILENAME "TYPE
    FILENAME DEFER> FILE.OPEN
    1 SUBFILE LAST1.ARRAY FILE>ARRAY
    2 SUBFILE TIME1.AXIS FILE>ARRAY
    1 COMMENT> 20 "NUMBER LVL.NUMBER :=
    2 COMMENT> 20 "NUMBER UVL.NUMBER :=
    3 COMMENT> PRINT.COMMENT ":=
    4 COMMENT> DATE.TIME ":=
    5 COMMENT> 20 "NUMBER PRINT.AVERAGE.NUMBER :=
    6 COMMENT> 20 "NUMBER GAIN.FACTOR :=
    7 COMMENT> X-AXIS.LABEL ":=
    8 COMMENT> Y-AXIS.LABEL ":=
    9 COMMENT> CHART.TITLE ":=
    FILE.CLOSE
    SCREEN.CLEAR
    LVL.NUMBER UVL.NUMBER         VERTICAL   WORLD.SET
    0.         TIME1.AXIS [ 512 ] HORIZONTAL WORLD.SET
    VUPORT.CLEAR
    XY.AXIS.PLOT
    LAST1.ARRAY -10 10 A/D.SCALE
    ERASE.LINES
    11 COLOR
    CURSOR.OFF
    TIME1.AXIS LAST1.ARRAY -10 10 A/D.SCALE XY.DATA.PLOT
    NORMAL.COORDS
    .300 .960 POSITION                              CHART.TITLE  LABEL
    .035 .350 POSITION 90 CHAR.DIR 90 LABEL.DIR    Y-AXIS.LABEL LABEL
    .400 .060 POSITION  0 CHAR.DIR  0 LABEL.DIR    X-AXIS.LABEL LABEL
    SCREEN.CLEAR
CR ." Name of file: " FILENAME "TYPE  ."        Date and time: " DATE.TIME "TYPE
    CR ." Comment:  " PRINT.COMMENT "TYPE
    cr ." Number of averages: " PRINT.AVERAGE.NUMBER .
    cr ." Amplifier gain: " GAIN.FACTOR .
```

```
CR ." TRANSFORMED DATA WILL BE DISPLAYED IN 3 SECONDS "
    3000 MSEC.DELAY
    BELL
    STACK.CLEAR
    SCREEN.CLEAR
    VUPORT.CLEAR
    LAST1.ARRAY 2048 -          \ Bias offset for bipolar jumpers
    DUP                         \ Copy the array
\   Z=X+I0                      \ Convert real array to complex
\   IFFT                        \ Inverse Fourier transform
\   ZREAL                       \ Throw away imaginary part
    FFT                         \ Fourier transform data
    ZMAG                        \ Obtain the real magnitude part
    DUP FFT.ARRAY :=
    FFT.ARRAY -10 10 A/D.SCALE
    ERASE.LINES
    FREQUENCY.GENERATE
    11 COLOR
    CURSOR.OFF
    FREQ.AXIS FFT.ARRAY -10 10 A/D.SCALE XY.AUTO.PLOT       \ Plot data
    NORMAL.COORDS
    .300 .960 POSITION                    " Fourier transformed waveform" LABEL
    .035 .250 POSITION 90 CHAR.DIR 90 LABEL.DIR     " Relative amplitudes" LABEL
    .400 .060 POSITION  0 CHAR.DIR  0 LABEL.DIR         " Frequency (KHz)" LABEL
    SCREEN.CLEAR
    CR ." <F5> PRINT-SCREEN DATA "
    CR ." <Alt F7> MAIN MENU "
    BELL
    ONERR:
    BELL CR ." Can't Fourier transform data "
;

20 0 24 79 WINDOW {BOT}

:   PEN.PLOT.DATA
    STACK.CLEAR
    SCREEN.CLEAR
    CR ." Name of file to plot? "
    "INPUT FILENAME ":=
    CR ." Reading - " FILENAME "TYPE
    FILENAME DEFER> FILE.OPEN
    1 SUBFILE LAST1.ARRAY FILE>ARRAY
    2 SUBFILE TIME1.AXIS FILE>ARRAY
    1 COMMENT> 20 "NUMBER LVL.NUMBER :=
    2 COMMENT> 20 "NUMBER UVL.NUMBER :=
    3 COMMENT> PRINT.COMMENT ":=
    4 COMMENT> DATE.TIME ":=
    5 COMMENT> 20 "NUMBER PRINT.AVERAGE.NUMBER :=
    6 COMMENT> 20 "NUMBER GAIN.FACTOR :=
    7 COMMENT> X-AXIS.LABEL ":=
    8 COMMENT> Y-AXIS.LABEL ":=
    9 COMMENT> CHART.TITLE ":=
    FILE.CLOSE
    STACK.CLEAR
```

```
    SCREEN.CLEAR
    LVL.NUMBER UVL.NUMBER          VERTICAL   WORLD.SET
    0.         TIME1.AXIS [ 512 ] HORIZONTAL WORLD.SET
    VUPORT.CLEAR
    XY.AXIS.PLOT
    LAST1.ARRAY -10 10 A/D.SCALE
    ERASE.LINES
    11 COLOR
    CURSOR.OFF
    TIME1.AXIS LAST1.ARRAY -10 10 A/D.SCALE XY.DATA.PLOT
    NORMAL.COORDS
    .300 .960 POSITION                              CHART.TITLE  LABEL
    .035 .350 POSITION 90 CHAR.DIR 90 LABEL.DIR     Y-AXIS.LABEL LABEL
    .400 .060 POSITION  0 CHAR.DIR  0 LABEL.DIR     X-AXIS.LABEL LABEL
    SCREEN.CLEAR
CR ." Name of file: " FILENAME "TYPE  ."        Date and time: " DATE.TIME "TYPE
    CR ." Comment:  " PRINT.COMMENT "TYPE
    cr ." Number of averages: " PRINT.AVERAGE.NUMBER .
    cr ." Amplifier gain: " GAIN.FACTOR .
    PLOTTER.DISPLAY
    HP7440
    PLOTTER.DEFAULTS
    DEVICE.INIT
    CR ." PLOTTING DISPLAYED DATA "
    LVL.NUMBER  UVL.NUMBER    VERTICAL    WORLD.SET
    0.  TIME1.AXIS [ 512 ]   HORIZONTAL  WORLD.SET
    2 AXIS.COLOR
    3 LABEL.COLOR
    XY.AXIS.PLOT
    LAST1.ARRAY -10 10 A/D.SCALE
    ERASE.LINES
    1 COLOR
    CURSOR.OFF
    TIME1.AXIS LAST1.ARRAY -10 10 A/D.SCALE XY.DATA.PLOT
    NORMAL.COORDS
    .300 .960 POSITION                              CHART.TITLE  LABEL
    .035 .350 POSITION 90 CHAR.DIR 90 LABEL.DIR     Y-AXIS.LABEL LABEL
    .400 .060 POSITION  0 CHAR.DIR  0 LABEL.DIR     X-AXIS.LABEL LABEL
    BELL
    AXIS.DEFAULTS
    IBM.GRAPHICS
    GRAPHICS.DISPLAY
    18 GRAPHICS.DISPLAY.MODE
    14 SCREEN.COLOR
    SCREEN.CLEAR
    {BOT}
    COLOUR.DISPLAY
    0 VUPORT.COLOR VUPORT.CLEAR
    LABEL.COLOR 12
    AXIS.COLOR 5
    CURSOR.COLOR 5
    11 COLOR
    INSTRUCTIONS.1
    BELL
```

```
    LINE.BUFFER.OFF
    ONERR:
    BELL CR ." Can not pen-plot data "
;

:   PEN.PLOT.SUPERIMPOSED.DATA
    STACK.CLEAR
    SCREEN.CLEAR
    CR ." Name of file to plot? "
    "INPUT FILENAME ":=
    CR ." Reading - " FILENAME "TYPE
    FILENAME DEFER> FILE.OPEN
    1 SUBFILE SUPERIMPOSED1.ARRAY FILE>ARRAY
    2 SUBFILE SUPERIMPOSED2.ARRAY FILE>ARRAY
    3 SUBFILE SUPERIMPOSED3.ARRAY FILE>ARRAY
    4 SUBFILE TIME1.AXIS FILE>ARRAY
    1 COMMENT> 20 "NUMBER LVL.NUMBER :=
    2 COMMENT> 20 "NUMBER UVL.NUMBER :=
    3 COMMENT> PRINT.COMMENT ":=
    4 COMMENT> DATE.TIME ":=
    5 COMMENT> 20 "NUMBER PRINT.AVERAGE.NUMBER :=
    6 COMMENT> 20 "NUMBER GAIN.FACTOR :=
    7 COMMENT> X-AXIS.LABEL ":=
    8 COMMENT> Y-AXIS.LABEL ":=
    9 COMMENT> CHART.TITLE ":=
    FILE.CLOSE
    STACK.CLEAR
    SCREEN.CLEAR
    LVL.NUMBER UVL.NUMBER         VERTICAL   WORLD.SET
    0.         TIME1.AXIS [ 512 ] HORIZONTAL WORLD.SET
    VUPORT.CLEAR
    XY.AXIS.PLOT
    ERASE.LINES
    SUPERIMPOSED1.ARRAY -10 10 A/D.SCALE
    11 COLOR
    CURSOR.OFF
    TIME1.AXIS SUPERIMPOSED1.ARRAY -10 10 A/D.SCALE XY.DATA.PLOT
    SUPERIMPOSED2.ARRAY -10 10 A/D.SCALE
    13 COLOR
    TIME1.AXIS SUPERIMPOSED2.ARRAY -10 10 A/D.SCALE XY.DATA.PLOT
    SUPERIMPOSED3.ARRAY -10 10 A/D.SCALE
    10 COLOR
    TIME1.AXIS SUPERIMPOSED3.ARRAY -10 10 A/D.SCALE XY.DATA.PLOT
    NORMAL.COORDS
    .200 .960 POSITION                              CHART.TITLE  LABEL
    .035 .350 POSITION 90 CHAR.DIR 90 LABEL.DIR     Y-AXIS.LABEL LABEL
    .400 .060 POSITION  0 CHAR.DIR  0 LABEL.DIR     X-AXIS.LABEL LABEL
    SCREEN.CLEAR
CR ." Name of file: " FILENAME "TYPE  ."        Date and time: " DATE.TIME "TYPE
    CR ." Comment:  " PRINT.COMMENT "TYPE
    cr ." Number of averages: " PRINT.AVERAGE.NUMBER .
    cr ." Amplifier gain: " GAIN.FACTOR .
    PLOTTER.DISPLAY
    HP7440
```

```
    PLOTTER.DEFAULTS
    DEVICE.INIT
    LVL.NUMBER UVL.NUMBER          VERTICAL    WORLD.SET
    0.         TIME1.AXIS [ 512 ]  HORIZONTAL  WORLD.SET
    2 AXIS.COLOR
    3 LABEL.COLOR
    XY.AXIS.PLOT
    SUPERIMPOSED1.ARRAY -10 10 A/D.SCALE
    ERASE.LINES
    CR ." PLOTTING CONDITIONER-TEST COMPLEX "
    1 COLOR
    CURSOR.OFF
    TIME1.AXIS SUPERIMPOSED1.ARRAY -10 10 A/D.SCALE XY.DATA.PLOT
    AXIS.DEFAULTS
    IBM.GRAPHICS
    GRAPHICS.DISPLAY
    18 GRAPHICS.DISPLAY.MODE
    14 SCREEN.COLOR
    SCREEN.CLEAR
    {BOT}
    COLOUR.DISPLAY
    0 VUPORT.COLOR VUPORT.CLEAR
    LABEL.COLOR 12
    AXIS.COLOR 5
    CURSOR.COLOR 5
    11 COLOR
    STACK.CLEAR
    SCREEN.CLEAR
    LVL.NUMBER UVL.NUMBER         VERTICAL   WORLD.SET
    0.         TIME1.AXIS [ 512 ] HORIZONTAL WORLD.SET
    VUPORT.CLEAR
    XY.AXIS.PLOT
    ERASE.LINES
    SUPERIMPOSED1.ARRAY -10 10 A/D.SCALE
    11 COLOR
    CURSOR.OFF
    TIME1.AXIS SUPERIMPOSED1.ARRAY -10 10 A/D.SCALE XY.DATA.PLOT
    SUPERIMPOSED2.ARRAY -10 10 A/D.SCALE
    13 COLOR
    TIME1.AXIS SUPERIMPOSED2.ARRAY -10 10 A/D.SCALE XY.DATA.PLOT
    SUPERIMPOSED3.ARRAY -10 10 A/D.SCALE
    10 COLOR
    TIME1.AXIS SUPERIMPOSED3.ARRAY -10 10 A/D.SCALE XY.DATA.PLOT
    NORMAL.COORDS
    .200 .960 POSITION                          CHART.TITLE  LABEL
    .035 .350 POSITION 90 CHAR.DIR 90 LABEL.DIR  Y-AXIS.LABEL LABEL
    .400 .060 POSITION  0 CHAR.DIR  0 LABEL.DIR  X-AXIS.LABEL LABEL
    SCREEN.CLEAR
CR ." Name of file: " FILENAME "TYPE  ."        Date and time: " DATE.TIME "TYPE
    CR ." Comment:  " PRINT.COMMENT "TYPE
    cr ." Number of averages: " PRINT.AVERAGE.NUMBER .
    cr ." Amplifier gain: " GAIN.FACTOR .
    PLOTTER.DISPLAY
    HP7440
```

```
    PLOTTER.DEFAULTS
    DEVICE.INIT
    SUPERIMPOSED2.ARRAY -10 10 A/D.SCALE
    CR ." PLOTTING TEST ONLY DATA "
    4 COLOR
    CURSOR.OFF
    TIME1.AXIS SUPERIMPOSED2.ARRAY -10 10 A/D.SCALE XY.DATA.PLOT
    AXIS.DEFAULTS
    IBM.GRAPHICS
    GRAPHICS.DISPLAY
    18 GRAPHICS.DISPLAY.MODE
    14 SCREEN.COLOR
    SCREEN.CLEAR
    {BOT}
    COLOUR.DISPLAY
    0 VUPORT.COLOR VUPORT.CLEAR
    LABEL.COLOR 12
    AXIS.COLOR 5
    CURSOR.COLOR 5
    11 COLOR
    STACK.CLEAR
    SCREEN.CLEAR
    LVL.NUMBER UVL.NUMBER          VERTICAL   WORLD.SET
    0.         TIME1.AXIS [ 512 ] HORIZONTAL WORLD.SET
    VUPORT.CLEAR
    XY.AXIS.PLOT
    ERASE.LINES
    SUPERIMPOSED1.ARRAY -10 10 A/D.SCALE
    11 COLOR
    CURSOR.OFF
    TIME1.AXIS SUPERIMPOSED1.ARRAY -10 10 A/D.SCALE XY.DATA.PLOT
    SUPERIMPOSED2.ARRAY -10 10 A/D.SCALE
    13 COLOR
    TIME1.AXIS SUPERIMPOSED2.ARRAY -10 10 A/D.SCALE XY.DATA.PLOT
    SUPERIMPOSED3.ARRAY -10 10 A/D.SCALE
    10 COLOR
    TIME1.AXIS SUPERIMPOSED3.ARRAY -10 10 A/D.SCALE XY.DATA.PLOT
    NORMAL.COORDS
    .200 .960 POSITION                              CHART.TITLE  LABEL
    .035 .350 POSITION 90 CHAR.DIR 90 LABEL.DIR     Y-AXIS.LABEL LABEL
    .400 .060 POSITION  0 CHAR.DIR  0 LABEL.DIR     X-AXIS.LABEL LABEL
    SCREEN.CLEAR
CR ." Name of file: " FILENAME "TYPE  ."        Date and time: " DATE.TIME "TYPE
    CR ." Comment:  " PRINT.COMMENT "TYPE
    cr ." Number of averages: " PRINT.AVERAGE.NUMBER .
    cr ." Amplifier gain: " GAIN.FACTOR .
    PLOTTER.DISPLAY
    HP7440
    PLOTTER.DEFAULTS
    DEVICE.INIT
    SUPERIMPOSED3.ARRAY -10 10 A/D.SCALE
    CR ." PLOTTING DIFFERENCE DATA "
    5 COLOR
    CURSOR.OFF
```

```
    TIME1.AXIS SUPERIMPOSED3.ARRAY -10 10 A/D.SCALE XY.DATA.PLOT
    NORMAL.COORDS
    .200 .960 POSITION                                CHART.TITLE  LABEL
    .035 .350 POSITION 90 CHAR.DIR 90 LABEL.DIR       Y-AXIS.LABEL LABEL
    .400 .060 POSITION  0 CHAR.DIR  0 LABEL.DIR       X-AXIS.LABEL LABEL
    BELL
    AXIS.DEFAULTS
    IBM.GRAPHICS
    GRAPHICS.DISPLAY
    18 GRAPHICS.DISPLAY.MODE
    14 SCREEN.COLOR
    SCREEN.CLEAR
    {BOT}
    COLOUR.DISPLAY
    0 VUPORT.COLOR VUPORT.CLEAR
    LABEL.COLOR 12
    AXIS.COLOR 5
    CURSOR.COLOR 5
    11 COLOR
    INSTRUCTIONS.1
    BELL
    LINE.BUFFER.OFF
    ONERR:
    BELL CR ." Can not pen-plot superimposed data "
;

\ ************************** THE END OF THIS SUB-SECTION ************************
```

REFERENCES

Adams, D.J., Gillespie, J.I. (1988) The action of l-glutamate at the postsynaptic membrane of the squid giant synapse, J. exp. Biol., 140: 535-548

Akaishi, T., Jiang, Z.-Y. and Sakuma, Y. (1988) Ascending fiber projections from the midbrain central gray to the ventromedial hypothalamus in the rat, Exp. neurol., 99: 247-258.

Akins, P.T. and McCleskey, E.W. (1993) Characterization of potassium currents in adult rat sensory neurons and modulation by opioids and cyclic AMP, Neurosci., 56: 759-769.

Alarcon, G., Guy, C.N., Walker, R. (1991) An assembler routine for on-line graphic display and averaging of data acquired on a personal microcomputer, J. Neurosci. Meth., 38: 1-14.

Alger, B.E. and Nicoll, R.A. (1980) Epileptiform burst afterhyperploarization: calcium-dependent potassium potential in hippocampal CA1 pyramidal cells, Sci., 210: 1122-1124.

Alger, B.E. and Nicoll, R.A. (1982) Feed-forward dendritic inhibition in rat hippocampal pyramidal cells studied in vitro, J. Physiol., 328: 105-123.

Amri, M., Car, A. and Roman, C. (1990) Axonal branching of medullary swallowing neurons projecting on the trigeminal and hypoglossal motor nuclei: demonstration by electrophysiological and fluorescent double labelling techniques, Exp. Brain Res., 81: 384-390.

Andrade, R. (1991) Blockade of neurotransmitter-activated K^+ conductance by QX-314 in the rat hippocampus, Eur. J. Pharmacol., 199: 259-262.

Aram, J.A. and Lodge, D. (1985) N-Methylaspartate antagonists block epileptiform discharges in rat cortical slices maintained in magnesium free medium, Br. J. Pharmacol., 86: 528P.

Aram, J.A. and Lodge, D. (1988) Validation of a neocortical slice preparation for the study of epileptiform activity, J. Neurosci. Meth., 23: 211-224.

Aram, J.A., Martin, D., Tomczyk, M., Zeman, S. Millar, J., Pohler, G. and Lodge, D. (1989) Neocortical epileptogenesis in vitro: studies with N-methyl-D-aspartate, phencyclidine, sigma and dextromethorphan receptor ligands, J. Pharmacol. Exp. Ther., 248: 320-328.

Armestrang-James, M., Caan, A.W. and Fox, K. (1985) Threshold effects of N-methyl-D-aspartate (NMDA) and 2-amino-5-phosphonovaleric acid (2 APV) on the spontaneous activity of neocortical single neurones in the urethane anaesthetised rat, Exp. Brain Res., 60: 209-213.

Aronson, J.K. (1992) Potassium channels in nervous tissue, Biochem. Pharmacol., 43: 11-14.

Asprodini, E.K., Rainnie, D.G. and Shinnick-Gallagher, P. (1992) Epileptogenesis reduces the sensitivity of presynaptic gamma-aminobutyric $acid_B$ receptors on glutamatergic afferents in the amygdala, J. Pharmacol. Exp. Ther., 262: 1011-21.

Asyst (1987) Up and Running with ASYST 2, Macmillan Software, New York, USA.

ASYST (1987) ASYST 2 Modules 1 to 4, Macmillan Software, New York, USA.

Avoli, M., Psarropoulou, C., Tancredi, V. and Fueta, Y. (1993) On the synchronous activity induced by 4-aminopyridine in the CA3 subfield of juvenile rat hippocampus, J. Neurophysiol., 70: 1018- 1029.

Awapara, J., Landua, A.J., Fuerst, R. and Searle, B. (1950) Free gamma-aminobutyric acid in brain, J. Neurochem., 187: 35-39.

Banerjee, P.K., Hirsch, E. and Snead III, O.C. (1993) Gamma-hydroxybutyric acid induced spike and wave discharges in rats: relation to high-affinity [^{3}H]gamma-hydroxybutyric acid binding sites in the thalamus and cortex, Neurosci., 56: 11-21.

Barton, D. (1991) A PC user's guide to data acquisition, Physics World (J. Br. Institute of Physics), Feb. 1991, 56-60.

Bartschad, D.K. and Blaustein, M.P. (1985a) Potassium channels in isolated presynaptic nerve terminals from rat brain, J. Physiol., 361: 419-440.

Bartschad, D.K. and Blaustein, M.P.[2] (1985b) Calcium-activated potassium channels in isolated presynaptic nerve terminals from rat brain, J. Physiol., 361: 441-457.

Bean, B.P. (1989) Neurotransmitter inhibition of neuronal calcium currents by changes in channel voltage dependence, Nature, 340: 153-156.

Belhage, B., Hansen, G.H. and Schousboe, A. (1993) Depolarisation by K^+ and glutamate activates different neurotransmitter release mechanisms in GABAergic neurons: vesicular versus non-vesicular release of GABA, Neurosci., 54: 1019-1034.

Bernasconi, R., Lauber, J., Marescaux, C., Vergnes, M., Martin, P., Rubio, V., Leonhardt, T., Reymann, N. and Bittiger, H. (1992) Experimental absence seizures: potential role of gamma-hydroxybutyric acid and $GABA_B$ receptors, J. Neural. Transm. Suppl., 35: 155-177.

Besson, J.-M., Rivot, J.-P. and Aleonard P. (1971) Action of picrotoxin on presynaptic inhibition of various origins in the cat's spinal cord, Brain Res., 26: 212-216.

Birch, B.D., Kocsis, J.D., Di-gregorio, F., Bhisitkul, R.B. and Waxman, S.G. (1991) A voltage and time-dependent rectification in rat dorsal spinal root axons, J. Neurophysiol., 66: 719:728.

Birnstiel, S., Gerber, U. and Greene, R.W. (1992) Adenosine-mediated synaptic inhibition: partial blockade by barium does not prevent anti-epileptiform activity, synapse, 11: 191-196.

Bittiger, H., Froestl, W., Hall, R. Karlsson, G., Klebs, K., et al. (1990) Biochemistry, electrophysiology and pharmacology of a new GABAB antagonist: CGP 35348. In N.G. Bowery, H. Bittiger, and H-R. Olpe (Eds.), $GABA_B$ Receptors in Mammalian Function, Wiley, Chichester, pp. 47-60.

Bittiger, H., Froestl, W., Mickel, S.J. and Olpe, H.-R. (1993) $GABA_B$ receptor antagonists: from synthesis to therapeutic applications, Trends Pharmacol. Sci. 14: 391-394.

Blake, J.F., Brown, M.W. and Collingridge, G.L. (1988) A quantitative study of the actions of excitatory amino acids and antagonists in rat hippocampal slices, Br. J. Pharmacol., 95: 291-299.

Bonanno, G. and Raiteri, M. (1993) Multiple $GABA_B$ receptors, Trends Pharmacol. Sci., 14: 259-261.

Boulton, C.L. and O'Saughnessy, C.T. (1991) The effect of calcium channel antagonists on spontaneous and evoked epileptiform activity in the rat neocortex in vitro, Eur. J. Neurosci., 3: 992-1000.

Boulton, C.L., McCrohan, C.R. and O'Saughnessy, C.T. (1993) Cyclic AMP analogues increase excitability and enhance epileptiform activity in rat neocortex in vitro, Eur. J. Pharmacol., 236: 131-136

Bowery, N.G., Doble, A., Hill, D.R., Hudson, A.L., Shaw, J.S., et al. (1981) Bicuculline-insensitive GABA receptors on peripheral autonomic nerve terminals, Eur. J. Pharmacol., 71: 53-70.

Bowery N.G. (1993) $GABA_B$ receptor pharmacology, Annu. Rev. Pharmacol. Toxicol., 33: 109-147.

Burgard, E.C. and Sarvey, J.M. (1991) Long-lasting potentiation and epileptiform activity produced by $GABA_B$ receptor activation in the dentate gyrus of rat hippocampal slice, Neurosci., 11: 1198-11209

Burton, N.R., Smith, D.A.S. and Stone, T.W. (1988) A quantitative analysis of some excitatory amino acid receptors in the mouse neocortex *in vitro*, Br. J. Pharmacol., 93: 693-701.

Carla, V. and Moroni, F. (1992) General anaesthetics inhibit the responses induced by glutamate receptor agonists in the mouse cortex, Neurosci. Lett., 146: 21-24.

Chad, J.E. and Eckert, R. (1986) An enzymatic mechanism for calcium current inactivation in dialysed *Helix* neurones, J. Physiol., 378: 31-51.

Chamberlin, N.L. and Dingledine, R. (1988) GABAergic inhibition and the induction of spontaneous epileptiform activity by low chloride and high potassium in the hippocampal slice, Brain res., 445: 12-18.

Connor J.A. and Stevens C.F. (1971) Voltage clamp studies of a transient outward membrane current in gastropod neural somata, J. Physiol., 213: 21-30.

Connors, B.W. (1984) Initiation of synchronized neuronal bursting in neocortex, Nature (Lond.), 310: 685-687.

Connors, B.W. and Gutnick, M.J. (1984) Cellular mechanisms of neocortical epileptogenesis in an acute experimental model. In P.A. Schwarzkroin and H.V. Wheal (Eds.), Electrophysiology of Epilepsy, Academic, Lond., pp. 79-105.

Constanti, A., Adams, P.R. and Brown, D.A. (1981) Why do barium ions imitate acetylcholine?, Brain Res., 206: 244-250.

Cook, N.S. (1988) The pharmacology of potassium channels and their therapeutic potential, Trends Pharmacol. Sci., 9: 21-28.

Courtney, M.J. and Nicholls, D.G. (1992) Interaction between phospholipase C-coupled and N-methyl-D-aspartate receptors in cultured cerebellar granule cells: protein kinase C mediated inhibition of N-methyl-D-aspartate responses, J. Neurochem. 59: 983-992.

Curtis, D.R., Duggan, A.W., Felix, D., and Johnston, G.A.R. (1970) GABA, bicuculline and central inhibition, Nature (Lond.), 226: 1222-1224.

Curtis, D.R. and Johnston G.A.R. (1974) Amino acid transmitters in the mammalian central nervous system, Ergeb. Physiol., 69: 97-188.

Das, B., Libri, V. and Constanti, A. (1992) Carbachol-evoked suppression of excitatory neurotransmission in guinea-pig olfactory cortex slices is unlikely to involve an M_4-muscarinic receptor subtype, Funct. Neurol., 7: 135-140.

Davies, C.H., Starkey, S.J., Pozza, M.F. and Collingridge, G.L. (1991) $GABA_B$ autoreceptors regulate the induction of LTP, Nature, 349: 609-611.

Devices sales limited, Digitimer, Welwyn Garden City, Hertfordshire, UK.

Devices sales limited, Gated Pulse Generator, Welwyn Garden City, Hertfordshire, UK.

Devices sales limited, Isolated Stimulator (Mk. IV), Welwyn Garden City, Hertfordshire, UK.

Dingledine, R. (1983) N-Methyl-D-aspartate activates voltage-dependent calcium conductance in rat hippocampal pyramidal cells, J. Physiol., 343: 385-405.

Dunlap, K. (1981) Two types of gamma-aminobutyric acid receptor on embryonic sensory neurones, Br. J. Pharmacol., 74: 579-585

Dunlap, K. and Fischbach, G.D. (1981) Neurotransmitters decrease the calcium conductance activated by depolarisation of embryonic chick sensory neurones, J. Physiol., 317: 519-535.

Dutar, P. and Nicoll, R.A. (1988a) A Physiological role for $GABA_B$ receptors in the central nervous system, Nature, 332: 156-158.

Dutar, P. and Nicoll, R.A.[2] (1988b) Pre- and post-synaptic $GABA_B$ receptors in the hippocampus have different pharmacological properties, Neuron 1: 585-598.

Fatatis, A., Bassi, A., Monsurro, M.R., Sorrentino, G., Mita, G.D., Di-Renzo, G.F. and Annunziato, L. (1992) LAN-1: a human neuroblastoma cell line with M_1 and M_3 muscarinic receptor subtypes coupled to intracellular Ca^{2+} elevation and lacking Ca^{2+} channels activated by membrane depolarization, J. Neurochem. 59: 1-9.

Flatman, J.A., Schwindt, P.C., Crill, W.E. and Stafstorm, C.E. (1983) Multiple actions of N-methyl-D-aspartate on cat neocortical neurons in vitro, Brain Res., 266: 169-173.

Flint, A.C. and Connors, B.W. (1993) Two distinct forms of synchronous rhythms mediated by different glutamate receptors and separate populations of neurons in neocortex, Society for Neurosci. abstracts, 19: 16.1.

Flower, D.C. (1993) FFT analysis of brain slice discharges, final year undergraduate project A, Department of Electrical and Electronic Engineering, The University of Adelaide, Adelaide, Adelaide 5005, Australia.

Foehring, R.C. and Surmeier, D.J. (1993) Voltage-gated potassium currents in acutely dissociated rat cortical neurons, J. Neurophysiol., 70: 51-63.

Formenti, A. and Sansone, V. (1991) Inhibitory action of acetylcholine, baclofen and GTP-gamma-S on calcium channels in adult rat sensory neurons, Neurosci. Lett., 131: 267-272.

Franks, N.P. and Lieb, W.R. (1982) Molecular mechanisms of general anaesthesia, Nature, 300: 487-493.

Franks, N. P. and Lieb, W.R. (1988) Volatile general anaesthetics activate a novel neuronal K^+ current, Nature, 333: 662-664.

Franks, N.P. and Lieb, W.R. (1991) Stereospecific effects of inhalational general anaesthetic optical isomers on nerve ion channels, Science, 254: 426-430.

Franks, N.P. and Lieb, W.R. (1994) Molecular and cellular mechansims of general anaesthesia, Nature, 367: 607-614.

Fromm, G.H., Sato, K. and Nakata, M. (1992) The action of $GABA_B$ antagonists in the trigeminal nucleus of the rat, Neuropharmacol., 31: 475-480.

Fujiwara, N., Higashi, H., Nishi, S., Shimoji, K., Sugita, S. and Yoshimura, M. (1988) Changes in spontaneous firing patterns of rat hippocampal neurons induced by volatile anaesthetics, J. Physiol., 402: 155-175.

Gage, P.W. and Robertson, B. (1985) Prolongation of inhibitory postsynaptic currents by pentobarbitone, halothane and ketamine in CA1 pyramidal cells in rat hippocampus, Br. J. Pharmac., 85: 675-681.

Gage, P.W. (1992) Activation and modulation of neuronal K^+ channels by GABA, Trends Neurosci., 15: 46-51.

Gahwiler, B.H. and Brown, D.A. (1985) $GABA_B$-receptor-activated K^+ current in voltage-clamped CA3 pyramidal cells in hippocampal cultures, Proc. Natl. Acad. Sci. USA, 82: 1558-1562.

Girgis, M., and Shin-Chang, W. (1981) A new stereotaxic atlas of the rabbit brain, Warren H. Green, USA.

Glaum, S.R. and Miller, R.J. (1992) Metabotropic glutamate receptors mediate excitatory transmission in the nucleus of the solitary tract, J. Neurosci. 12: 2251-2258.

Gorman, A.L.F. and Hermann, A. (1979) Internal effects of divalent cations on potassium permeability in molluscan neurones, J. Physiol., 296: 393-410.

Grant, P.M. (1993) Digital signal processing. part 1: Digital filters and the DFT. In Electronics & Communication Engineering Journal, Vol. 5, IEE, Lond., pp. 13-21.

Grant, P.M. and J.T.E. McDonnell (1993) Digital signal processing. part 2: Spectral analysis. In Electronics & Communication Engineering Journal, Vol. 5, IEE, Lond., pp. 212-220.

Grass Instrument Company (1964) P511 AC Preamplifier, Quincy, Mass., USA.

Guilbaud, G., Peschanski, M. and Gautron, M. (1981) Functional changes in the ventrobasal thalamic neurons responsive to noxious and non-noxious cutaneous stimuli after chloralose treatment: new evidence for the presence of pre-existing "silent connections" in the adult nervous system?, Pain, 11: 9-19.

Gutnic, M.J., Connors, B.W. and Prince, D.A. (1982) Mechanisms of neocortical epileptogenesis *in vitro*, J. Neurophysiol., 48: 1321-1335.

Hagiwara, S. and Ohmori, H. (1982) Studies of calcium channels in rat clonal pituitary cells with patch electrode voltage clamp, J. Physiol., 331: 231-252.

Hamba, M., Hisamitsu, H. and Muro, M. (1990) Nociceptive projection from tooth pulp to the lateral hypothalamus in Rats, Brain Res. Bulletin, 25: 355-364.

Hales, T.G. and Lambert, J.J. (1991) The action of propofol on inhibitory amino acid receptors of bovine adrenomedullary chromaffin cells and rodent central neurones, Br. J. Pharmacol., 104: 619-628.

Halsey, M.J. (1989) Molecular mechanisms of anaesthesia. In Nunn, J.F., Utting, J.E. and Brown jr, B.R. (Eds.) General Anaesthesia, part 1 - Fundamentals of anaesthesia, 5th Ed., Butterworth Int., pp. 19-29.

Harris, N.C., Webb, C. and Greenfield, S.A. (1989) The effects of gamma-hydroxybutyrate on the membrane properties of guinea-pig pars compacta neurons in the substantial nigra in vitro, Neurosci., 31: 363-370.

Harris, B.D., Moody, E.J., Basile, A.S. and Skolnick, P. (1994) Volatile anesthetics bidirectionally and stereospecifically modulate ligand binding to GABA receptors, Eur. J. Pharmacol., Molecular Pharmacology Section, 267: 269-274.

Harrison, N.L. and Simmonds, M.A. (1985) Quantative studies on some antagonists of N-methyl-D-aspartate in slices of rat cerebral cortex, Br. J. Pharmacol., 84: 381-391.

Harrison, N.L., Lange, G.D. and Barker, J.L. (1988) (-)-Baclofen activates presynaptic $GABA_B$ receptors on GABAergic inhibitory neurons from embryonic rat hippocampus, Neurosci. Lett., 85: 105-109.

Hasselmo, M. E. and Bower, J. M. (1990) Afferent and association fiber differences in short-term potentiation in piriform (olfactory) cortex of the rat, J. Neurophysiol., 64: 179-190.

Heemskerk, F.M.J., Schrama, L.H., Ghijsen, W.E.J.M., De Graan, P.N.E., Lopes da silva, F.H., and Gispen, W.H. (1991) pre-synaptic mechanism of action of 4-aminopyridine: changes in intracellular free Ca^{2+} concentration and its relationship to B-50 (GAP-43) phosphorylation, J. Neurochem., 56: 1827-1835.

Hill, D.R. and Bowery, N.G. (1981) ^{3}H-baclofen and ^{3}H-GABA bind to bicuculline-insensitive $GABA_B$ sites in rat brain, Nature, 290: 149-152.

Hill, R.C., Maurer, R., Buescher, H-H. and Roemer, D. (1981) Analgesic properties of the GABA-mimetic THIP, Eur. J. Pharmacol., 69: 221-224.

Hille, B. (1968) Charges and potentials at the nerve surface. Divalent ions and pH, J. Gen. Physiol., 51: 221-236.

Hille, B. (1992) Ionic Channels of Excitable Membranes, 2nd Ed., Sinauer, Sunderland, MA.

Hirata, K., Sawada, S. and Yamamoto, C. (1992) Quantal analysis of suppressing action of baclofen on mossy fibre synapses in guinea pig hippocampus, Brain Res., 578: 33-40.

Hodgkin, A.L. and Huxley, A.F. (1952) A quantitative description of membrane currents and its application to conduction and excitation in nerve, J. Physiol., 117: 500-544.

Horne, A.L., Harrison, N.L., Turner, J.P. and Simmonds, M.A. (1986) Spontaneous paroxysmal activity induced by zero magnesium and bicuculline: suppression by NMDA antagonists and GABA mimetics, Eur. J. Phramacol., 122: 231-238.

Hosford, D.A., Clark, S., Cao, Z., Wilson, W.A., Lin, F.-H., Morrisett, R.A. and Huin, A. (1992) The role of $GABA_B$ receptor activation in absence seizures of lethargic (lh/lh) mice, Science, 257: 398-401.

Hubbard, J.I., Jones, S.F. and Landau, E.M. (1971) The effect of temperature change upon transmitter release, facilitation and post-tetanic potentiation, J. Physiol., 216: 591-609.

Huleux, C., Dreux, C., Lemullios, M. and Rossignol, B. (1991) Process of re-establishment of beta-adrenergic induced protein secretion after cytochalasin D inhibition in rat parotid gland. Effect of cholinergic agonist, phorbol ester and calcium, Biol. Cell., 73: 57-62.

Huston, E., Scott, R.H. and Dolphin, A.C. (1990) A comparison of the effect of calcium channel ligands and $GABA_B$ agonist and antagonists on transmitter release and somatic calcium channel currents in cultured neurons, Neurosci., 38: 721-729.

Irwin, R.P., Maragakis, N.J., Rogawski, M.A., Purdy, R.H., Farb, D.H. and Paul, S.M. (1992) Pregnenolone sulfate augments NMDA receptor mediated increases in intracellular Ca^{2+} in cultured rat hippocampal neurons, Neurosci. Lett., 141: 30-34.

Jessop, J. and Jones, J.G. (1992) Evaluation of the actions of general anaesthetics in the human brain, Gen. Pharmac., 23: 927-935.

Jinu, J. D. (1993) Power spectrum density estimation of brain discharges, final year undergraduate project B, Department of Electrical and Electronic Engineering, The University of Adelaide, Adelaide 5005, Australia.

Johnston, G.A.R., Hailstone, M.H. and Freeman, C.G. (1980) Baclofen: stereoselective inhibition of excitant amino acid release, J. Pharmacol., 32: 230-231.

Jones, M.V., Brooks, P.A. and Harrison, N.L. (1992) Enhancement of gamma-aminobutyric acid-activated Cl^- currents in cultured rat hippocampal neurones by three volatile anesthetics, J. Physiol., 449: 279-293.

Jones, M.V. and Harrison, N.L. (1993) Effects of volatile anesthetics on the kinetics of inhibitory postsynaptic currents in cultured rat hippocampal neurons, J. Neurophysiol., 70: 1339-1349.

K^+ channels (1994) Receptor and ion channel nomenclature supplement, Trends pharmacol. sci., 5th ed., pp. 44-47.

Karnup, S.V. (1992) Background firing activity in guinea-pig neocortex in vitro, Neurosci., 48: 915-924.

Keane, P.E. and Biziere, K. (1987) The effects of general anaesthetics on GABAergic synaptic transmission, Life Sci., 41: 1437-1448.

Kendig, J.J. (1989) Neuronal basis of the anaesthetic state. In Nunn, J.F., Utting, J.E. and Brown jr, B.R. (Eds.) General Anaesthesia, part 1 - Fundamentals of anaesthesia, 5th Ed., Butterworth Int., pp. 30-43.

Kerr, D.I.B., Ong, J., Prager, R.H., Gynther, B.D. and Curtis, D.R. (1987) Phaclofen: a peripheral and central baclofen antagonist, Brain Res., 405: 150-154.

Kerr, D.I.B., Ong, J. and Prager, R.H. (1990a) $GABA_B$ receptor agonists and antagonists. In N.G. Bowery, H. Bittiger, and H-R. Olpe (Eds.), $GABA_B$ Receptors in Mammalian Function, Wiley, Chichester, pp. 29-45.

Kerr, D.I.B., Ong, J. and Prager, R.H. (1990b) Antagonism of $GABA_B$-receptor-mediated responses in the guinea-pig isolated ileum and vas deferens by phosphono-analogues of GABA, Br. J. Pharmacol., 99: 422-426.

Kerr, D.I.B. and Ong, J. (1992) GABA agonists and antagonists, Medicinal Res. Rev., 12: 593-636.

Kirzinger, A. and Jurgens, U. (1990) Chemical brain stimulation as a means to circumvent electrical stimulation artefacts in single-unit recording studies of evoked vocalization, J. Neurosci. Meth., 33: 165-170.

Krnjevicacute, K. and Schwartz, S. (1967) The action of gamma-aminobutyric acid on cortical neurones, Exp. Brain Res., 3: 320-326.

Krnjevic, K. (1974) Chemical nature of synaptic transmission in vertebrates, Physiol. Rev., 54: 418-540.

Krnjevic, K. (1992) Cellular and synaptic actions of general anaesthetics, Gen. Pharmac., 23: 965-975.

Krogsgaard-Larsen, P., Hjeds, H., Falch, E., Jorgensen, F.S. and Nielsen, L. (1988) Recent advances in GABA agonists, antagonists and uptake inhibitors: structure-activity relationships and therapeutic potential, Advances Drug Res., 17: 381-456.

LaBella, F.S. and Queen, G. (1993) General anaesthetics inhibit cytochrome P450 monooxygenases and arachidonic acid metabolism, Can. J. Physiol. Pharmacol., 71: 48-53.

Lambert, N.A., Harrison, N.L., Kerr, D.I.B., Ong, J., Prager, R.H. and Teyler, T.J. (1989) Blockade of the late IPSP in rat CA1 hippocampal neurons by 2-hydroxy saclofen, Neurosci. Lett., 107: 125-128.

Lambert, N.A., Harrison, N.L. and Teyler, T.J. (1991) Baclofen-induced disinhibition in area CA1 of rat hippocampus is resistant to extracellular Ba^{2+}, Brain Res., 547: 349-352.

Lambert, D.G., Wojcikiewicz, R.J., safrany, S.T., Whitam, E.M. and Nahorski, S.R. (1992) Muscarinic receptors, phosphoinositide metabolism and intracelluar calcium in neuronal cells, Prog. Neuropsychopharmacol. Biol. psychiatry., 16: 253-270.

Latorre, R. (1993) The intimacies of K^+ channels revealed, NIPS, 8: 1-2.

Legoratti-Sanchez, M.O., Guevara-Guzman R. and Solano-Flores L.P. (1989) Electrophysiological evidences of a bidirectional communication between the locus coeruleus and the supra chiasmatic nucleus, Brain Res. Bulletin, 23: 283-288.

Lemos, J.R. and Nowycky, C. (1989) Two types of calcium coexist in peptide-releasing vertebrate nerve terminals, Neuron, 2: 1419-1426.

Lewis, D.V., Jones, L.S. and Swartzwelder, H.S. (1989) The effects of baclofen and pertussis toxin on epileptiform activity induced in the hippocampal slice by magnesium depletion, Epilepsy Res., 4: 109-118.

Liebeskind, J. and Mayer, D. (1971) Somatosensory evoked responses in the mesencephalic central gray matter of the rat, Brain Res., 27: 133-151.

Lin, L-H, Leonard, S. and Harris, R.A.[1] (1993) Enflurane inhibits the function of mouse and human brain phosphatidylinositol-linked acetylcholine and serotonin receptors expressed in xenopus oocytes, Molecular Pharmacol., 43: 941-948.

Lin, L-H, Whiting, P. and Harris, R.A.[2] (1993) Molecular determinants of general anesthetic action: role of $GABA_A$ receptor structure, J. Neurochem., 60: 1548-1553.

Llinas, R. and Walton, K. (1980) Voltage-dependent calcium conductances in neurons. In C.W. Cotman, G. Poste and G.L. Nicholson (Eds.), The cell surface and neuronal function, Elsevier/North-Holland, Amesterdam, pp. 87-118.

Lodge, D., Anis, N.A. and Buron N.R. (1982) Effect of optical isomers of ketamine on excitation of cat and rat spinal neurones by amino acids and acetylcholine, Neurosci. Lett., 29: 281-286.

Marescaux, C., Vergnes, M. and Bernasconi, R. (1992) $GABA_B$ receptor antagonists: potential new anti-absence drugs, J. Neural. Transm. (suppl.), 35: 179-188.

Marion-Poll, F., and Tobin, T.R. (1991) Software filter for detecting spikes superimposed on a fluctuating baseline, J. Neurosci. Meth., 37: 1-6.

Martin, D., Bowe, M.A. and Nadler, J.V. (1989) A grease-gap method for studying the excitatory amino acid pharmacology of CA1 hippocampal pyramidal cells, J. Neurosci. Meth., 29: 107-114.

Mathworks (1993) Matlab 4.0, Cambridge Control, Cambridge, UK.

Mayer, M.L. and Westbrook, G.L. (1987) The physiology of excitatory amino acids in the vertebrate central nervous system, Prog. Neurobiol., 28: 197-276.

McLarnon, J.G. and Sawyer, D. (1993) Effect of divalent cations on the activation of a calcium-dependent potassium channel in hippocampal neurons, Eur. J. Physiol., 424: 1-8.

Meldrum, B. and Garthwaite, J. (1991) Excitatory amino acid neurotoxicity and neurodegenerative disease, Trends Pharmacol. Sci., special report, pp. 54-62.

Meller, S.T. (1985) A stereotaxic atlas of the rabbit brain, Department of Physiology, The University of Adelaide, Adelaide 5005, Australia, unpublished material.

Meller, S.T., and Dennis, B.J. (1986) Afferent connections of the periaqueductal gray in the rabbit, Neurosci., 5: 444-445.

Meller, S.T., and Dennis, B.J. (1990a) A multiple golgi analysis of the periaqueductal gray in the rabbit, J. Comp. Neurol., 302: 66-86.

Meller, S.T., and Dennis, B.J. (1990b) Quantitative Nissl study of the neuronal types, and recognition of cytoarchitectural subdivisions, within the rabbit periaqueductal gray, J. Comp. Neurol., 302: 87-99.

Meller, S.T., and Dennis, B.J. (1991) Efferent connections of the periaqueductal gray in the rabbit, Neurosci., 40: 191-216

Merlin, L.R. and Wong, R.K.S. (1993) Synaptic modifications accompanying epileptogenesis in vitro: long-term depression of GABA-mediated inhibition, Brain Res., 627: 330-340.

Metrabyte Corporation (1986) DASH-16/16F Manual, Taunton, MA, USA.

Miljkovic, Z. and MacDonald, J.F. (1986) Voltage-dependent block of excitatory amino acid currents by pentobarbital, Brain Res., 376: 396-399.

Miles, R., Wong, R.K.S. and Traub, R.D. (1984) Synchronized afterdischarges in the hippocampus: contribution of local synaptic interactions, Neurosci., 12: 1179-1189.

Miller, K.W. (1985) The nature of the site of general anesthesia, Int. Rev. Neurobiol., 27: 1-61.

Miller, R.J. (1987) Multiple calcium channels and neuronal function, Science, 235: 46-52.

Misgeld, U., Muller, W. and Brunner, H. (1989) Effects of (-)-baclofen on inhibitory neurons in the guinea pig hippocampal slice, Pflugers Arch., 414: 139-144.

Mody, E., Tanelian, D.L. and MacIver, M.B. (1991) Halothane enhances tonic neuronal inhibition by elevating intracellular calcium, Brain Res., 538: 319-323.

Mody, I., Lambert, J.D.C. and Heinemann, U. (1987) Low extracellular magnesium induces epileptiform activity and spreading depression in rat hippocampal slices, J. Neurophysiol., 57: 869-888.

Monaghan, D.T., Holets, V.R., Toy, D.W. and Cotman, C.W. (1983) Anatomical distributions of four pharmacologically distinct ^{3}H-L- glutamate binding sites, Nature (Lond.), 306: 176-179.

Moody, E.J., Suzdak, P.D., Paul, S.M. and Skolnick, P. (1988) Modulation of the benzodiazepine/gamma-aminobutyric acid receptor complex by inhalation anesthetics, J. Neurochem., 51: 1386-1393.

Moody, E.J., Harris, B.D. and Skolnick, P. (1993) Stereospecific actions of the inhalation anesthetic isoflurane at the $GABA_A$ receptor complex, Brain Res., 615: 101-106.

Mott, D.D. and Lewis, D.V. (1991) Facilitation of the induction of long-term potentiation by $GABA_B$ receptors, Science, 252: 1718-1720.

Mulle, C., Lena, C. and Changeux, J.P. (1992) Potentiation of nicotinic receptor response by external calcium in rat central neurons, Neuron., 8: 937-945.

Nathan, T., Jensen, M.S. and Lambert, J.D. (1990) The slow inhibitory post-synaptic potential in rat hippocampal CA1 neurones is blocked by intracelluar injection of QX-314, Neurosci. Lett., 110: 309-313.

Newland, C.F., Adelman, J.P., Tempel, B.L. and Almers, W. (1992) Repulsion between tetraethylammonium ions in cloned voltage-gated potassium channels, Neuron, 8: 975-982.

Nunn, J.F., Utting, J.E. and Brown jr, B.R. (1989) Introduction. In Nunn, J.F., Utting, J.E. and Brown jr, B.R. (Eds.), General Anaesthesia, 5th ed., Butterworth Int. pp. 1-6.

Ochs, S. and Booker, H (1961) Spatial and temporal interactions of direct cortical responses, Exp. Neurol., 4: 70-82.

Ochs, S. and Clark, F.J. (1968) Interaction of direct cortical responses - a possible dendritic site of inhibition, Electroencephalography and Clinical Neurophysiol., 24: 108-115

Olpe, H-R, Karlsson, G., Pozza, M.F., Brugger, F., Steinmann, M., et al. (1990) CGP 35348: a centrally active blocker of $GABA_B$ receptors, Eur. J. Pharmacol., 187: 27-28.

Ong, J., Kerr, D.I.B., and Johnston, G.A.R. (1990) Effect of potassium channel blockers on baclofen induced suppression of paroxysmal discharges in rat neo-cortical slices, Neurosci. Lett., 112: 216-222.

O'Shaughnessy, C.T., Aram, J.A., and Lodge, D. (1988) A_1 adenosine receptor-mediated block of epileptiform activity induced in zero magnesium in rat neocortex in vitro, Epilepsy Res., 2: 294:301.

Oyama, Y., Harata, N. and Akaike, N. (1991) Rapid interaction of tetraethylammonium with delayed K^+ channel in mammalian brain neuron, Neurosci. Lett., 131: 153-155.

Pearce, R.A., Stringer, J.L. and Lothman E.W. (1989) Effect of volatile anaesthetics on synaptic transmission in the rat hippocampus, Anaesthesiology, 71: 591-598.

Peet, M.J. and McLennan, H. (1986) Pre- and postsynaptic actions of baclofen: blockade of the synaptically evoked hyperpolarization of CA1 hippocampal neurones, Exp. Brain Res., 61: 567-574.

Pennington, N.J., Kelly, J.S. and Fox, A.P. (1991) A study of the mechanism of Ca^{2+} current inhibition produced by serotonin in rat dorsal raphe neurones, J. Neurosci., 11: 3594-3609.

Premkumar, L.S., Gage, P.W. and Chung, S.H. (1990) Coupled potassium channels induced by arachidonic acid in cultured neurons, Proc. R. Soc., Lond., Ser. B, 242: 17-22.

Proakis, J.G. and Manolakis, D.G. (1992) Digital Signal Processing, Principles, Algorithms and Applications, 2nd edn., Macmillan, New York.

Rang, H.P. and Dale, M.M. (1987) Chemical transmission and drug action in the central nervous system. In Rang, H.P. and Dale, M.M. (Eds.), Pharmacology, Churchill Livingstone, pp. 447-470.

Rang, H.P. and Dale, M.M. (1987) General anaesthetic agents. In Rang, H.P. and Dale, M.M. (Eds.), Pharmacology, Churchill Livingstone, pp. 471-485.

Ratzlaff, E.H. and Siegel, R. M. (1990) A workstation interface for measuring interspike intervals, J. Neurosci. Meth., 35: 195-201.

Rhoades, B.K. and Gross, G.W. (1994) Potassium and calcium channel dependence of bursting in cultured neuronal networks, Brain Res., 643: 310-318.

Robichaud, L.J. and Boxer, P.A. (1993) Polyamine modulation of excitatory amino acid responses in the rat cortical wedge, Neuropharmacol., 32: 1025-1035.

Robichaud, L.J., Wurster, S. and Boxer, P.A. (1994) The voltage-sensitive Ca^{2+} channel (VSCC) antagonists w-Aga-IVA and w-CTX-MVIIC inhibit spontaneous epileptiform discharges in the rat cortical wedge, Brain Res., 643: 352-356.

Roeper, J., Hainsworth, A.H. and Ashcroft, F.M. (1990) Tolbutamide reverses membrane hyperpolarisation induced by activation of D2 receptors and $GABA_B$ receptors in isolated substantial nigra neurones, Pfluegers Arch., 416: 473-475.

Rose, G. (1983) A temperature controller for in vitro recording chambers, Brain Res. Bulletin, 10: 713-714.

Rovira, C., Gho, M. and Ben-Ari, Y. (1990) Block of $GABA_B$-activated K_+ conductance by kainate and quisqualate in rat CA3 hippocampal pyramidal neurones, Pfluegers Arch., 415: 471-478.

Rudy, B. (1988) Diversity and ubiquity of K channels, Neurosci., 25: 729-749.

Saint, D.A., Thomas, T. and Gage, P.W. (1990) $GABA_B$ agonists modulate a transient potassium current in cultured mammalian hippocampal neurons, Neurosci. Lett., 118: 9-13.

Sanchez, D., Ganfornina, M.D., Ribas, J. (1988) Periaqueductal gray neurons, activity in a mesencephalic slice preparation, Brain Res., 455: 166-169.

Sander, G., Schmitt, P. and Karli, P. (1986) Unit activity alterations induced in the mesencephalic periaqueductal gray by local electrical stimulation, Brain Res., 386: 53-63.

Sanders, K.H., Klein, C.E., Mayer, T.E., Heym, Ch. and Handwerker, H.O. (1980) Differential effects of noxious and non-noxious inputs on neurons according to location in ventral periaqueductal grey or dorsal raphe nucleus, Brain Res., 186: 83-97.

Scholz, K.P. and Miller, R.J. (1991) $GABA_B$ receptor-mediated inhibition of Ca^{2+} currents and synaptic transmission in cultured rat hippocampal neurones, J. Physiol., 444: 669-686.

Sihra, T.S., Piomelli, D. and Nichols, R.A. (1993) Barium evokes glutamate release from rat brain synaptosomes by membrane depolarisation: involvement of K^+, Na^+, and Ca^{2+} channels, J. Neurochem., 61: 1220-1230.

Simmonds, M.A. and Horne, A.L. (1987) Barbiturates and excitatory amino acid interactions. In D. Lodge (ed.), Excitatory Amino Acids in Health and Disease, Wiley, Lond., pp. 219-236.

Slater, S.J., Cox, K.J.A., Lombardi, J.V., Ho, C., Kelly, M.B., Rubin, E. and Stubbs, C.D. (1993) Inhibition of protein kinase C by alchohols and anaesthetics, Nature, 364: 82-84.

Smith, H.J. (1988) Introduction to the principles of drug design, Butterworth, Lond., pp. 249-263.

Solis, J.M. and Nicoll, R.A. (1992) Pharmacological characterisation of $GABA_B$-mediated responses in the CA1 region of the rat hippocampal slice, J. Neurosci., 12: 3466-3472.

Soltesz, I., Haby, M., Leresche, N. and Crunelli, V. (1988) The $GABA_B$ antagonist phaclofen inhibits the late K^+-dependent IPSP in cat and rat thalamic and hippocampal neurones, Brain Res., 448: 351-354.

Stanton, P.K., Jones, R.S.G., Mody, I. and Heinemann, U. (1987) Epileptiform activity induced by lowering extracellular [Mg^{2+}] in combined hippocampal-entorhinal cortex slices: modulation by receptors for norepinephrine and N-methyl-D-aspartate, Epilepsy Res., 1: 53-62.

Stromquist, B.R., Pavlides, C. and Zelano, J.A. (1990) On-line acquisition, analysis and presentation of neurophysiological data based on a personal microcomputer system, J. Neurosci. Meth., 35: 215-222.

Suszkiw, M., Murawsky, M. and Shi, M. (1989) Further characterization of phasic calcium influx in rat cerebrocortical synaptosomes: inferences regarding calcium channel types(s) in nerve endings, J. Neurochem., 52: 1260-1269.

Sutor, B. and Hablitz, J.J. (1993) Influence of barium on rectification in rat neocortical neurons, Neurosci. Lett., 157: 62-66.

Tallan, H.H., Moore, S. and Stein, W.H. (1954) Studies on free amino acids and related compounds in the tissues of the cat., J. Biol. Chem., 211: 927-939.

Tatebayashi, H. and Ogata, N. (1992) $GABA_B$-mediated modulation of the voltage-gated Ca^{2+} channels, Gen. Pharmacol., 23: 309-316.

Tibbs, G.R., Barrie, A.P., VanMieghem, F., McMahon H.T., and Nicholls, D.G. (1989) Repetitive action potentials in isolated nerve terminals in the presence of 4-aminopyridine: effects on cytosolic free Ca^{2+} and glutamate release, J. Neurochem., 53: 1693-1699.

Thomson, A.M. and West, D.C. (1990) Factors affecting slow regular firing in the suprachiasmatic nucleus in vitro, J. Biol. Rhythms, 5: 59-75.

Tortora, G.J. and Anagnostakos, N.P. (1981) Principles of Anatomy and Physiology, 3rd ed., Harper int. ed., Harper & Row, New York, USA.

Traub, R.D. and Wong, R.K.S. (1983) Synchronized burst discharge in disinhibited hippocampal slice. II. Model of cellular mechanisms, J. Neurophysiol., 49: 459-471.

Traub, R.D., Jefferys, J.G.R. and Whittington, M.A. (1994) Enhanced NMDA conductance can account for epileptiform activity induced by low Mg^{2+} in the rat hippocampal slice, J. Physiol., 478.3: 379-393.

Tsuruoka, M. Li, Q-J., Matsui, A. and Matsui, Y. (1990) Inhibition of nociceptive responses of wide-dynamic-range neurons by peripheral nerve stimulation, Brain Res. Bulletin, 25: 387-392.

Tunnicliff, G. (1992) Significance of gamma-hydroxybutyric acid in the brain, Gen. Pharmac., 23: 1027-1034.

Turgeon, S.M. and Albin, R.L. (1993) Pharmacology, distribution, cellular localization, and development of $GABA_B$ binding in rodent cerebellum, Neurosci., 55: 311-323.

Turner, D.A., Schliechert, M. (1990) Data acquisition and analysis system for intercellular neuronal signals, J Neurosci. Meth., 35: 241-251.

Vidal, C. and Changeux, J.-P. (1993) Nicotinic and muscarinic modulations of excitatory synaptic transmission in the rat prefrontal cortex in vitro, Neurosci., 56: 23-32.

Waldmeier, P.C., Stocklin, K. and Feldtrauer, J-J. (1992) Systemic administration of baclofen and the $GABA_B$ antagonist, CGP 35348, does not affect GABA, glutamate or aspartate in microdialysates of the striatum of conscious rats, Naunyn-Schmiedebergs Arch. Pharmacol., 345: 548-552.

Weinberg, R.J., Tribble, III G.L., Schwindth, P.C. (1985) A baseline stabilizer for electrophysiology, J. Neurosci. Meth., 14: 117-120.

West, C.H.K. and Michael, R.P. (1990) Responses of units in the mesolimbic system to olfactory and somatosensory stimuli: modulation of sensory input by ventral tegmental stimulation, Brain Res., 532: 307-316.

Wheatley, P.L. (1986) A simple method for recording excitatory amino acid-evoked depolarisations of rat cortex in vitro, Br. J. Pharmacol., 87: 159P.

Williams, T.L., Smith, D.A.S., Burton, N.R. and Stone, T.W. (1988) Amino acid pharmacology in neocortical slices: evidence for bimolecular actions from an extension of the Hill and Gaddum-Schild equations, Br. J. Pharmacol., 95: 805-810.

Wong, S. (1994) Power density spectrum estimation in MATLAB, final year undergraduate project A, Department of Electrical and Electronic Engineering, The University of Adelaide, Adelaide 5005, Australia.

Yamaguchi, K. and Ohmori, H. (1993) Suppression of the slow K^+ current by cholinergic agonists in cultured chick cochlear ganglion neurones, J. Physiol., 464: 213:228.

Yoshida, A., Oda, M. and Ikemoto, Y. (1991) Kinetics of the Ca^{2+}-activated K^+ channel in rat hippocampal neurons, Jpn. J. Physiol., 41: 297-315.

Zorn, L., Kulkarni, R., Anantharam, V., Bayley, H. and Treistman, S.N. (1993) Halothane acts on many potassium channels, including a minimal potassium channel, Neurosci. Lett., 161: 81-84.